Metals in urban dust: Potentials of spider web biomonitoring and statistical approaches to identify anthropogenic sources of urban particulate matter

FRIEDRICH-SCHILLER-
UNIVERSITÄT
JENA

Dissertation

zur Erlangung des akademischen Grades

doctor rerum naturalium (Dr. rer. nat.)

vorgelegt dem Rat der Chemisch-Geowissenschaftlichen Fakultät der

Friedrich-Schiller-Universität Jena

von M.Sc. Neele Birte van Laaten

geboren am 11.11.1990 in Bremen

Gutachter:

1. **Prof. Dr. Thorsten Schäfer (Friedrich-Schiller-Universität Jena)**
2. **PD Dr. Wolf von Tümpling (Helmholtz-Zentrum für Umweltforschung UFZ, Magdeburg)**

Tag der Verteidigung: 08.07.2020

Contents

List of Figures

List of Tables

Abbreviations

CF	Conversion factor
C_{org}	Organic carbon
C_{total}	Total carbon
EF	Enrichment factor
e.g.	Example given
E-PRTR	European Pollutant Release and Transfer Register
EU	European Union
FA	Factor analysis
HDPE	High-density polyethylene
ICP-MS	Inductively coupled plasma-mass spectrometry
ICP-OES	Inductively coupled plasma-optical emission spectroscopy
IQR	Interquartile range (75% quantile minus 25% quantile)
kNN	k-nearest neighbours classification
LDA	Linear discriminant analysis
LDF	Linear discriminant function
LOD	Limit of detection
n	Number of samples (in a data set)
PA	Polyamide
PC	Principal component
PCA	Principal component analysis
PE	Polyethylene
PETG	Polyethylene terephthalate glycol
PFA	Perfluoroalkoxy alkane
PLS-DA	Partial least squares-discriminant analysis
PM	Particulate matter
PMP	Polymethylpentene
POM	Polyoxymethylene
PP	Polypropylene
PTFE	Polytetrafluoroethylene
PVC	Polyvinyl chloride
REE	Rare earth elements

r_s	Spearman rank correlations coefficient
SD	Standard deviation
SEM	Scanning electron microscope
SIMCA	Soft independent method of class analogy
SRM	Standard reference material
UBA	Umweltbundesamt (German Environment Agency)
UCC	Upper continental crust
UFP	Ultra-fine particles
USGS	United States Geological Survey
WHO	World Health Organization

Abstract

Elevated levels of particulate matter can be observed in the atmosphere of many urban areas today. This is caused by a combination of various anthropogenic sources, whose emissions add to the naturally induced levels. To lower effectively the amount of dust particles in urban atmospheres, actual sources of particulate matter have to be identified.

For this purpose, four different, rather novel methods to characterize dust were tested in this work. Contents of up to 52 elements, mainly trace metals, were determined in the samples and subjected to a statistical evaluation, aiming at an identification of sources. Sampling materials that were investigated are spider webs (biomonitoring), moss bags (biomonitoring), dust from windows and long-term deposition samples. Sampling of all of these materials is comparatively cost-effective and space-saving. Therefore, a great number of both sampling locations and total amount of samples, which are needed for the statistical evaluation, could be realized. Most of those samples were taken in the city of Jena (Central Germany), which serves as a model environment for medium-sized cities located in valleys.

An adaption of methods, described in general in the literature, that are suited for both monitoring of particulate matter as well as the identification of dust sources has been one main aim of this work. By repeated sampling, temporal and spatial variation could be checked. The individual sampling locations were chosen with regard to evident dust sources, since emissions of them should be found in the samples. Possible identifications of sources as well as a comparison of the different methods shall provide guidance for future users.

Of the four materials, the focus has been on spider webs, for which the biggest data set was recorded. Spider webs entrapping dust particles can be found in almost all kinds of environments. In addition, their sampling is easy and inexpensive. In case of the sampling of wheel webs, that are renewed almost every day, a high temporal resolution is possible. The main part of the evaluation has been a (multivariate) statistical evaluation, aiming at the identification of dust sources. By initially calculating enrichment factors, a rather geogenic or anthropogenic origin could be allocated to every single element. By means of a combination of correlation coefficients, cluster analysis and factor analysis of the element contents in spider webs altogether it could be demonstrated that sampling and evaluation of spider webs is an effective method for the identification of dust sources. For the city of Jena, three sources could be geochemically identified: resuspended natural/geogenic dust (characterized by high contents of Al, Ca, Co, Cs, La, Li, Mg, Sr, Th, Ti, Y, Zr), brake wear from car traffic (Cu, Sb, Sn, Zn) and abrasion of tram/train tracks (Ba, Cr, Fe, Mn, Ni). This shows that emissions from the transport sector are to be subdivided and can be regarded individually. Furthermore, it could be demonstrated that resuspension and associated higher contents of natural dust are mainly caused by driving cars.

A clear identification of sources, as it could be done with the spider web data, could not be performed with data from the other materials, even when using the same statistical approach.

The latter reveals other differences in the data sets of the three methods, for example differences between the sampling campaigns. Especially moss bags and long-term deposit samples are rather suited for the display of seasonal/annual differences or a general burden of particulate matter as well as for the identification of highly polluted locations. Methods should therefore be chosen according to the individual problem to be tackled as well as the requirements that have to be met for this.

Overall, the sampling, analysis and subsequent evaluation of spider webs has been proven a promising method for the identification of sources of particulate matter. The simple operability allows for an application not only in scientific studies but also in routine monitoring. In contrast to theoretical calculations or calculations based on emission inventories, sources can be identified on the basis of real measurements in urban areas with this method. This yields new information both in a scientific as well as in a sociopolitical framework. Many studies on urban air quality performed so far are based on data acquired with classical methods (using samples from e.g. impactor samplers) and seldomly focus on source identification. Spider web biomonitoring itself has only been performed at a few other locations so far and rarely with the aim of source identification. To the author's knowledge, the work presented here is therefore the most extensive data basis for spider web biomonitoring so far.

Zusammenfassung

Erhöhte Gehalte an Feinstaub (*engl. particulate matter*) lassen sich heutzutage in der Atmosphäre vieler Städte feststellen. Dies ist bedingt durch eine Kombination verschiedener anthropogener Quellen, deren Emissionen zu der natürlichen Staubbelastung hinzukommen. Um die Feinstaubgehalte in der Atmosphäre nachhaltig zu reduzieren, müssen zunächst die Feinstaubquellen in der jeweiligen Umgebung identifiziert werden.

Vor diesem Hintergrund wurden in der vorliegenden Arbeit vier verschiedene, nicht klassische Methoden zur Charakterisierung von Feinstaub erprobt und die Gehalte von bis zu 52 Elementen, vorwiegend Spurenmetalle, in den Proben bestimmt. Diese wurden einer statistischen Auswertung mit dem Ziel der Quellidentifikation unterworfen. Bei den untersuchten Probenmaterialien handelte es sich um Spinnweben (Biomonitoring), Moossäckchen (Biomonitoring), Staub auf Fensterscheiben und Staub aus Depositionssammlern. Deren Beprobung ist vergleichsweise kostengünstig und platzsparend, so dass eine große Anzahl an Probennahmestellen sowie an Einzelproben, wie sie für die statistische Auswertung benötigt werden, realisiert werden konnten. Die meisten Proben wurden dabei im Stadtgebiet Jenas (Mitteldeutschland) genommen, welches als Modellumgebung für mittelgroße Städte in Talsenken betrachtet wurde.

Ziel der Arbeit war es, Methoden herauszuarbeiten, die für das Monitoring von Feinstaub sowie die Identifikation von Feinstaubquellen geeignet sind. Über Mehrfachbeprobungen konnten zeitliche und räumliche Variationen getestet werden. Dabei wurden die Standorte der Probennahme so gewählt, dass offensichtliche Feinstaubquellen in den Proben identifizierbar sein sollten. Mögliche Quellidentifikationen sowie ein Vergleich der verschiedenen Methoden sollen hinterher als Orientierung für andere Anwender dienen.

Bevorzugt wurden Spinnweben untersucht, für welche auch der größte Datensatz erhoben wurde. Spinnweben fangen und akkumulieren Staubpartikel. Sie lassen sich in fast jeder Umgebung finden und ihre Beprobung lässt sich einfach und kostengünstig durchführen. Werden Radnetze beprobt, die nahezu täglich erneuert werden, ist zudem eine hohe zeitliche Auflösung möglich. Bei der Auswertung lag das Augenmerk auf der (multivariat) statistischen Auswertung mit dem Ziel der Identifikation von Feinstaubquellen. Über die Berechnung von Anreicherungsfaktoren konnte zunächst für einzelne Elementgehalte eine Zuordnung zu geogenem oder anthropogenem partikulärem Material vorgenommen werden. Mit Hilfe des Datensatzes der Elementgehalte in Spinnweben und einer Kombination aus Korrelationskoeffizienten, Clusteranalyse und Faktorenanalyse konnte gezeigt werden, dass die Beprobung und Auswertung von Spinnweben eine effektive Methode zur Quellidentifikation darstellt. Im Stadtgebiet von Jena konnten damit drei Feinstaubquellen geochemisch identifiziert werden: aufgewirbelter natürlicher/geogener Feinstaub (gekennzeichnet durch hohe Gehalte an Al, Ca, Co, Cs, La, Li, Mg, Sr, Th, Ti, Y, Zr), Bremsabrieb vom Autoverkehr (Cu, Sb, Sn, Zn) und Abrieb von Straßenbahn- und Zugschienen (Ba, Cr, Fe, Mn, Ni). Dies zeigt,

dass die Emissionen des Verkehrssektors räumlich weiter zu unterteilen sind und sich getrennt betrachten lassen. Weiterhin konnte demonstriert werden, dass die Aufwirbelung und dadurch bedingte erhöhte Gehalte an natürlichem Staub vorwiegend durch fahrende Autos verursacht werden.

Eine ähnlich eindeutige Identifikation von Feinstaubquellen wie mit den Daten der Spinnweben ließ sich mit den anderen drei Methoden bei analoger statistischer Betrachtung nicht realisieren. Die statistische Auswertung führte vielmehr zur Herausstellung anderer Unterschiede, zum Beispiel zwischen unterschiedlichen Beprobungskampagnen. Insbesondere Moossäckchen und Depositionssammler eignen sich deshalb eher für die Herausstellung saisonaler/jährlicher Unterschiede oder einer allgemeinen Feinstaubbelastung sowie die Identifikation besonders belasteter Probennahmestellen. Die Auswahl einer Methode sollte somit je nach Fragestellung und den jeweils damit verbundenen Anforderungen erfolgen.

Für die Identifikation von Feinstaubquellen konnte insgesamt die Beprobung und Analyse von Spinnweben als besonders gut geeignete Methode herausgestellt werden. Die einfache Durchführbarkeit ermöglicht einen Einsatz über wissenschaftliche Studien hinaus im Routine-Monitoring. Im Gegensatz zu theoretischen Berechnungen oder solchen auf der Basis von Emissionen können mit dieser Methode Quellen auf der Grundlage realer Messungen in urbanen Räumen identifiziert werden. Dies bedeutet sowohl einen wissenschaftlichen, als auch einen gesellschaftspolitischen Informationsgewinn, da viele bisherige Studien auf mit klassischen Methoden (z.B. Impaktor-Sammler) erhobenen Daten beruhen. Nur selten liegt bei diesen der Fokus auf der Quelldetektion. Auch Spinnweben wurden erst an einigen wenigen Lokationen und selten zur Identifikation von Feinstaubquellen beprobt. Die vorliegende Arbeit stellt, nach Wissen der Autorin, daher die bisher umfassendste Datengrundlage für Spinnweben zum Feinstaub-Monitoring dar.

1 Aim of the thesis

Dust or particulate matter (PM) suspended in the atmosphere is regarded as one of the major environmental problems of the Anthropocene, especially in urban areas (LANDRIGAN et al. 2018). With increasing urbanisation, the problem becomes even more pressing (SALMOND and MCKENDRY 2009). As a result, air quality standards including threshold values have been set in many countries, e.g. 2008/50/EC (European Union), 39. BImSchV (Germany), 78 FR 3085 (USA) and GB 3095-2012 (China). To check compliance with those threshold values and quantify selected constituents of PM, mainly high-volume samplers are used. They suck in air and collect particles either on a filter or in subdivided size ranges with a cascade impactor (GIERÉ and QUEROL 2010; STERNBECK et al. 2002). Other typical samplers are commercial devices that collect dust during deposition, like the Bergerhoff sampler or the Sigma-2 passive sampler (GUÉGUEN et al. 2012; VDI 2119 Part 4: 2013-06). Collection of PM with those typically used samplers is regarded in this work as classical monitoring.

Those classical methods are often expensive, need supervision and, in case of high-volume samplers, power supply (URBAT et al. 2004). In contrast to that, the Lancet Commission on pollution and health has pointed out a great need for low-cost air pollution monitors (LANDRIGAN et al. 2018). Urban air pollution can vary over short distances of less than a kilometer, thus single, expensive stations cannot be considered as representative for all parts of a city (APTE et al. 2017). In addition, urban air pollution has been increasing mainly in developing and newly industrialized countries like India or China within the last decades (HERTEL and GOODSITE 2009; SUVARAPU and BAEK 2017; YADAV and RAJAMANI 2006). Due to their big national territory and/or low budget for environmental monitoring, applications of classical methods are likely limited in those countries. Overall, alternative or additional non-classical methods are needed. Those are often methods that have been used seldomly in research so far.

In the course of this work, four non-classical methods were regarded: spider web biomonitoring, moss bag biomonitoring, the collection of dust from windows and the collection of long-term deposit. The focus, including the majority of the samples taken, has been on collection and analysis of spider webs to whose adhesive surface dust particles can attach. To the knowledge of the author, this method of biomonitoring has only been studied a few times so far (e.g. RACHOLD et al. 1992; RYBAK 2015; XIAO-LI et al. 2006). It seems promising as web weaving spiders can be found almost worldwide, they can tolerate high pollution levels and the sampling is easy and cost-effective (RYBAK et al. 2012; YANG et al. 2016). One aim of this thesis has been to test spider web biomonitoring in another exemplary environment in Europe and to a greater extent, as so far it has only been performed at selected locations in Hamburg, Germany (RACHOLD et al. 1992), and Wrocław, Poland (e.g. RYBAK 2015; RYBAK et al. 2012).

To lower levels of PM and promote legislation, an identification of relevant sources is needed (GU et al. 2011). Still, detailed knowledge of the sources of urban PM is often missing (e.g.

JOHANSSON et al. 2009). The main aim of the thesis has thus been to use spider web biomonitoring to detect sources of urban PM and to quantify their relative influences on total urban PM. For this purpose, element contents were determined in the samples and subjected to a multivariate statistical evaluation. Mainly trace metals and metalloids were determined, as anthropogenic emissions are often enriched in heavy metals (HOVMAND et al. 2008). Furthermore, the metal composition of dust is source specific and does not change during transportation and deposition (FURUSJÖ et al. 2007).

Smaller sampling campaigns of three other non-classical methods were performed to assess if they lead to the same conclusions on PM with regard to anthropogenic influences and identification of sources. In case of differences, this comparison shall also give guidance to which method might be applied promisingly in which case. Another biomonitoring technique that was applied is moss bag biomonitoring, in which moss from a remote area is exposed to ambient air in small mesh bags (ARES et al. 2012). Locations of the moss bag biomonitoring can be chosen quite freely as it is not dependent on naturally occurring material. Due to an increased interest in the last decades, it is more commonly used than spider web biomonitoring and likely closer to application in non-research monitoring (e.g. ARES et al. 2012; CAPOZZI et al. 2016a; TRETIACH et al. 2011). Spider web and moss bag biomonitoring have therefore been compared in more detail in this work compared to the two other methods (collection of dust from windows and collection of long-term deposit). In addition to the comparison named above, another purpose of this has been to test if different biomonitoring methods for PM can be combined or replaced by each other.

A non-classical, non-biomonitoring method to sample PM is the collection of dust deposit rinsed off from surfaces. ŚWIETLIK et al. (2013) for example described the analysis of heavy metals in PM rinsed off from acoustic noise barriers next to busy roads. In the present work, dust particles have been sampled from windows with a window vacuum cleaner. Windows are present in almost all urban areas and ground floor windows are normally in the same height as respiratory organs of standing people.

Spider web and moss bag biomonitoring as well as the collection of dust from windows have been performed mainly in the city of Jena as an exemplary urban environment. For comparison with a more classical method and to get samples from locations with other than typical urban land-uses, dustfall has been collected in plastic vessels at several locations in Central Germany over longer periods (one year). This sampling is rather similar to the one with Bergerhoff samplers. Similar approaches have been done so far, but mainly for shorter timescales and in arid areas (e.g. AL-KHASHMAN 2004). Overall, this comparison shall point out the potentials of the different methods and give indications to where they can be applied and/or which information can be gained.

2 Introduction

The term particulate matter (PM) describes particles suspended in the atmosphere that do not immediately fall to the ground (UMWELTBUNDESAMT 2009). This definition covers particles with an aerodynamic diameter of approximately 2 nm to more than 100 µm and a variability in shape and composition (ENAMORADO-BÁEZ et al. 2015; RUSSELL and BRUNEKREEF 2009): A single particle can be formed from a single component or contain hundreds of different components. Due to its small size and large variability in components, PM has several adverse effects on human health, ecosystems and the atmosphere, that will be discussed in the course of this chapter (e.g. FANG et al. 2005; GIERÉ and QUEROL 2010; LANDRIGAN et al. 2018).

To prevent mainly the effects on human health, threshold values have been set by the European Union (EU, 2008/50/EC) and transformed into national laws and regulations (e.g. 39. BImSchV in Germany). Different size ranges of PM have been defined in those regulations: PM_{10} sums particles that pass through a size-selective inlet (e.g. in a cascade impactor) with a 50% cut-off for an aerodynamic diameter of 10 µm, while for $PM_{2.5}$ the 50% cut-off is set for an aerodynamic diameter of 2.5 µm (39. BImSchV). Particles with an aerodynamic diameter of 2.5–10 µm are also often referred to as coarse particles while $PM_{2.5}$ is called fine PM and the term ultra-fine particles (UFP) refers to particles smaller than 100 nm (FANG et al. 2005; GRANTZ et al. 2003). Especially in urban areas, a large amount of PM is in the lower coarse and fine size range. ZHENG et al. (2004) for example found 97% of the particles in dust samples from Shanghai, China, being smaller than 10 µm and 70% smaller than 3 µm.

The threshold for the annual mean content in air in the EU is 40 µg/m³ for PM_{10} and 25 µg/m³ for $PM_{2.5}$; in addition, the threshold value of 50 µg/m³ for PM_{10} shall only be exceeded at 35 days of a year (2008/50/EC). As there is no threshold under which no harmful effects can happen, the World Health Organization (WHO) has recommended lower thresholds in its air quality guidelines (WHO 2006): For PM_{10} an annual mean of maximum 20 µg/m³ and a daily mean of maximum 50 µg/m³ are recommended while the thresholds are 10 µg/m³ and 25 µg/m³ respectively for $PM_{2.5}$. Only for selected heavy metals/metalloids thresholds or so-called target values have been set by law. For Pb the mean annual threshold value is 0.5 µg/m³ (2008/50/EC) and for As, Cd and Ni mean annual target values of 6 ng/m³, 5 ng/m³ and 20 ng/m³ respectively in PM_{10} have been defined (2004/107/EC).

In Germany, compliance with these limits is checked by federal environment agencies as well as by the German Environment Agency (Umweltbundesamt – UBA), who have set up monitoring stations for that purpose. Only at the station "Lünen Frydagstraße" (North Rhine-Westphalia) the daily mean of 50 µg/m³ for PM_{10} has been exceeded at more than 35 days (36 days) in 2018 (this and all further numbers in this paragraph are taken from UMWELTBUNDESAMT 2019). The station is located in an urban industrial area with several recycling facilities and a coal-fired power plant. In the city of Jena, where most of the samples regarded in this work have been taken, the threshold of 50 µg/m³ for PM_{10} has been exceeded at five days

in 2018. At none of the 368 monitoring stations in Germany the annual mean of 40 µg/m³ for PM_{10} has been exceeded in 2018, but the threshold of 20 µg/m³ named by the WHO has been exceeded at 119 stations. Those are mainly stations with urban traffic and a few urban industrial sites while only one of them is located in a rural area. The annual mean in 2018 for PM_{10} in Thuringia ranged between 11 µg/m³ ("Neuhaus", rural area) and 23 µg/m³ ("Mühlhausen, Wanfrieder Straße", urban traffic), with 18 µg/m³ at the only station in Jena ("Jena, Dammstr."), located at an urban background site.

2.1 Potential sources of particulate matter and metals in the urban atmosphere

Urban areas often show highest contents of PM in the atmosphere compared to residential and even industrial zones (FANG et al. 2005). This is mainly due to a combination of natural (background) sources and various anthropogenic ones accumulating in cities. Besides, most of the surfaces in urban areas are sealed and thus less capable to fix dust than e.g. meadows or forests (NORRA and STÜBEN 2004). Therefore, resuspension of dust particles is also an important factor influencing PM contents in cities.

The source probably most often discussed is road traffic, producing both exhaust (from fuel combustion) and non-exhaust emissions (all other emissions). Examples for non-exhaust emissions are brake abrasion and tyre wear (GIERÉ and QUEROL 2010; JOHANSSON et al. 2009). Besides, resuspension of particles is mainly induced by driving vehicles. Related to exhaust emissions are emissions from other fossil fuel burnings, e.g. in power plants or private households (BLISSETT et al. 2014; BLUNDELL et al. 2009; STERNBECK et al. 2002). The latter do also contribute to PM loadings in the urban atmosphere by residential heating with solid fuels, especially in colder periods (FURUSJÖ et al. 2007; UMWELTBUNDESAMT 2009). This does also include biomass burning. In Germany, burning of wood and wooden pellets for heating is fairly popular with an estimated number of 14 million fire places in 2006 (UMWELTBUNDESAMT 2007). Fourteen years ago, LAHL et al. (2005) even stated that the emissions from wood burning have the same magnitude than the emissions from traffic in Germany. Another source of PM is waste incineration, which is often done in or in the vicinity of cities (JOHANSSON et al. 2009). In addition, small businesses like auto repair shops can be sources of PM (QIANG et al. 2015). Compared to big industrial facilities, small businesses are a rather diffuse source of PM, comparable to private households, as they may be distributed over the whole urban area. A temporal but often significantly influential source of dust are construction areas (GIERÉ and QUEROL 2010). Models of LI et al. (2016) for example point out urban construction activities as the major source of urban PM in the Guanzhong Basin, China, in 2013.

Additional sources of dust can frequently be found in the outskirts and vicinity of cities. Industrial plants are often located there, emitting PM both with exhaust streams of own power plants or from the processes themselves (ORDÓÑEZ et al. 2003; UMWELTBUNDESAMT 2009). Typical processes emitting dust are metallurgical processes, glass production and handling

and sorting in stone and earth industries (AL-KHASHMAN 2004; LUMPP et al. 2012; RAMPAZZO et al. 2008). Airports are also often located in the vicinity of larger cities. In addition to emissions from aircrafts, HERTEL et al. (2009) also stressed the influence of traffic going to and from the airports. Many cities are surrounded by agricultural areas. For Europe, agriculture has been stated the leading source of PM, contributing up to 40% to total PM (LELIEVELD et al. 2015). Aerosols like NH_3, that are transformed into particles in the atmosphere (so-called secondary PM) are emitted in large amounts by e.g. livestock farming (UMWELTBUNDESAMT 2009). Besides, open/bare fields as well as activities like harrowing and ploughing allow for erosion and suspension of soils to an enhanced extent (LI et al. 2016).

Erosion is strongly connected with and cannot always be separated from natural dust sources. Wind erosion of weathered rocks and soils is a natural process introducing dust particles into the atmosphere (e.g. MORENO et al. 2008). Soil particles introduced into the atmosphere by both natural and anthropogenic processes have been stated a major contributor to PM on a global scale by MEGIDO et al. (2017). Dust storms are another natural source. Especially in arid regions desert dust is a significant part of PM (SANTACATALINA et al. 2010). Desert dust from dust storms can undergo long-distance transport, thus reaching more distant regions (ANSMANN et al. 2003). Some of the highest contents of PM_{10} in Palermo, Italy, were for example related to long-range transport of Saharan dust by DONGARRÀ et al. (2007) and Saharan dust can even reach (southern) Germany (FLENTJE et al. 2015). Besides from minerogenic particles, natural dust can be composed of a variety of organic substances. These include pollen, spores, bacteria, plant debris and algae (GIERÉ and QUEROL 2010). Some natural sources of PM, that only have an influence in selected regions, are volcanic eruptions, forest and peat fires and marine aerosols (GRANTZ et al. 2003; GUÉGUEN et al. 2012; HERTEL and GOODSITE 2009).

Compared to the natural abundance of metals in the earth crust or in pristine soils, anthropogenic dust emissions are enriched in metals (HOVMAND et al. 2008). Fly-ash, emissions from burning of fossil fuels and from steel industry can for example be enriched in Fe (BLUNDELL et al. 2009; OLDFIELD et al. 1985). Another example are non-exhaust emissions of automobile traffic with enhanced contents of e.g. Ba, Cu, Fe and Sb (VUKOVIC et al. 2016). Therefore, urban populations are exposed to enhanced levels of metals in the atmosphere (FANG et al. 2005). Many of the studies on metals in PM performed so far have focused on heavy metals like Cd, Cr, Ni, Pb and Sn (e.g. ENAMORADO-BÁEZ et al. 2015; SUVARAPU and BAEK 2017). DAI et al. (2016) stated that this is due to the fact that those elements have been found to widely pollute also other compartments of the environment. Heavy metals are non-degradable (as all metals), bioaccumulative and often toxic (CHAND and PRASAD 2013). They are primarily emitted as oxides, sulfates or silicates and with regard to PM are often associated with the more fine fraction (GUÉGUEN et al. 2012; YADAV and RAJAMANI 2006). As a broad range of heavy metals is only seldomly monitored in studies on PM, reliable data on contents and atmospheric transport of several elements (e.g. La, Rb) is still missing.

2.2 Effects of particulate matter on human health, atmosphere and ecosystems

PM has a variety of adverse effects on human health, the atmosphere itself and different ecosystems. Air pollution in general has been stated a major cause of global disease burden and has been attributed to 7.6% of the total global mortality in 2015 in recent publications (COHEN et al. 2017; LANDRIGAN et al. 2018). In this context, PM is regarded as the most harmful of all ambient air pollutants with negative effects of both short- and long-term exposure (FANG et al. 2005; HERTEL and GOODSITE 2009). The smaller the particles are, the deeper they can enter into the body (see Fig. 2-1): While coarse particles remain in the upper respiratory tract, fine particles reach the pulmonary alveoli and UFP can enter the bloodstream within whom they can be transported through the whole body. Therefore, a variety of diseases can be induced by the exposure to PM.

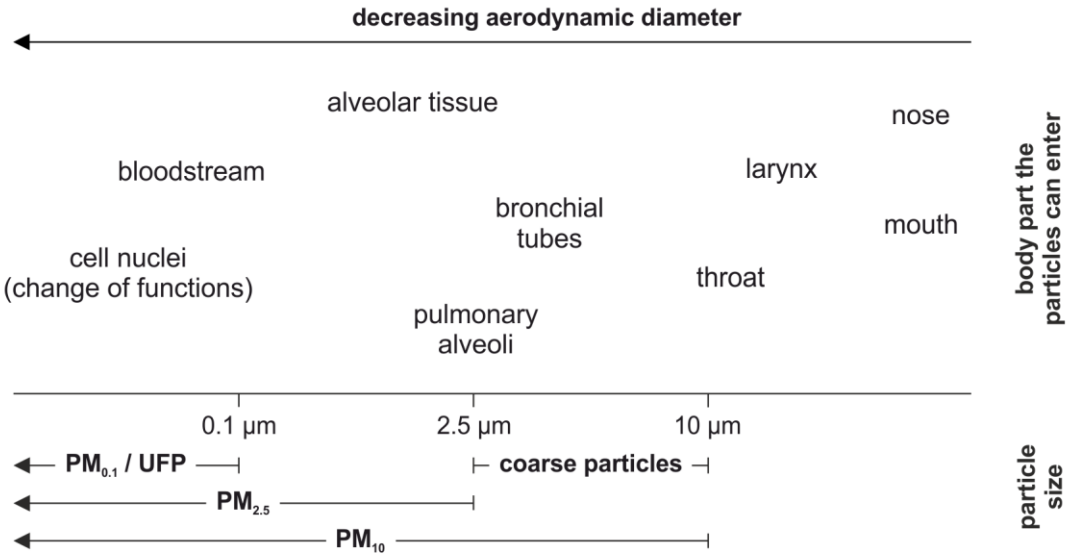

Fig. 2-1: Parts of the human body dust particles can reach depending on their aerodynamic diameter (information collected from LAHL and STEVEN 2005; UMWELTBUNDESAMT 2009; WHO 2013).

Inhalation of dust is for example linked to premature mortality with estimations ranging from 811,000 to 4.2 million annual deaths worldwide (COHEN et al. 2017; LELIEVELD et al. 2015; RUSSELL and BRUNEKREEF 2009). Common respiratory symptoms that can be induced by PM are acute lower respiratory infections, chronic obstructive pulmonary disease, allergies and asthma (DONGARRÀ et al. 2007; LELIEVELD et al. 2019). Besides, also cardiovascular diseases like myocardial infarction, arterial hypertension and stroke as well as lung cancer can be caused (LANDRIGAN et al. 2018; LELIEVELD et al. 2019). The WHO names an additional amount of diseases like artherosclerosis, osteoporosis and altered neurodevelopment which have not been proven but are expected to be inducible by PM (WHO 2013). All of these lead to a reduced life expectancy which is estimated to be 9 months in Europe, and 10 months in Germany (LAHL and STEVEN 2005; RUSSELL and BRUNEKREEF 2009).

While those health effects are attributable to PM in general, very little is kown about health effects of different particle types or substances attached to them (LELIEVELD et al. 2015). Especially heavy metals, which are a majority of the elements regarded in this work, are often known to be toxic and/or carcinogen, but this data is often only valid for ingestion or dermal intake (WHO 2013). Even though the health aspects of inhaled particles are expected to be different for different metals, detailed information on the health aspects of metals in/attached to particles is missing (LAHL and STEVEN 2005; WHO 2013). Some few records show for example that the inhalation of Pb attached to particles can lead to neurological damages and within pregnant women to a reduced growth of the foetus and premature birth (LAHD GEAGEA et al. 2007; SUVARAPU and BAEK 2017). Other heavy metals/metalloids for which an adverse effect on human health by inhalation is known are As, Mn and Ni. Ni dust is toxic and carcinogen, Mn in high amounts leads to respiratory tract irritation and damages to the nervous system, and inhaled As can lead to liver and kidney damages (HOLLEMAN et al. 2007).

Even though legislation and research are often driven by the health effects of PM, GRANTZ et al. (2003) stated that the most severe effects are the long-term impacts on ecosystems. Especially for metals, transport through the atmosphere and the following deposition can be a significant part of their biogeochemical cycles (FANG et al. 2005). Input of dust particles from desert dust and combustion sources is for example a key component for the supply with Fe in open ocean regions (MAHOWALD et al. 2009). Besides, aerosols play an important role in depositioning metals into forest ecosystems and onto soils (GRANTZ et al. 2003; ZHU et al. 2015). HOVMAND et al. (2008) found for top soils in remote areas that 50–90% of the heavy metal contents are due to dust deposition.

Effects of PM can also be found directly in the atmosphere. Effects caused by scattering and absorption of radiation, called direct effects, influence the radiative balance (GIERÉ and QUEROL 2010; LI et al. 2016): While most particles scatter sunlight, leading to a cooling effect, black carbon absorbs radiation and therefore warms the atmosphere. This warming contributes to global warming, leading to e.g. enhanced melting of glaciers and thawing permafrost soils (IPCC 2013). As these effects cannot easily be estimated, aerosols make up for the largest uncertainties in models estimating the energy imbalance of the climate system, the radiative forcing (EALO et al. 2016). An example of the radiative forcing of the global climate by combined model simulations and observations can be found in Fig. 2-2, which has been taken from the Fifth Assessment Report of the Intergovernmental Panel on Climate Change (IPCC 2013): Greatest uncertainties of all forcing agents are inherent in the aerosol-radiation interactions and the aerosol-cloud interactions.

In the lower part of the atmosphere, regional haze due to PM can diminish visible solar radiation, which in extreme cases can reduce plant growth and crop yield in agricultural regions (GRANTZ et al. 2003). Indirect effects on the atmosphere are those resulting from the fact that particles can act as cloud condensation nuclei (GIERÉ and QUEROL 2010). Aerosols lead to a

smaller cloud droplet size, influencing both the cloud's microphysical properties and lifetime (CATTANI et al. 2006). Besides, particles can influence atmospheric chemistry, mainly photochemical and heterogeneous reactions (EALO et al. 2016; LI et al. 2016). BIAN et al. (2003) for example calculated a global mean decrease of tropospheric content of 0.7% for O_3, 11.1% for OH-radicals, 5.2% for HO_2-radicals and 3.5% for HNO_3 due to mineral dust influencing atmospheric chemistry.

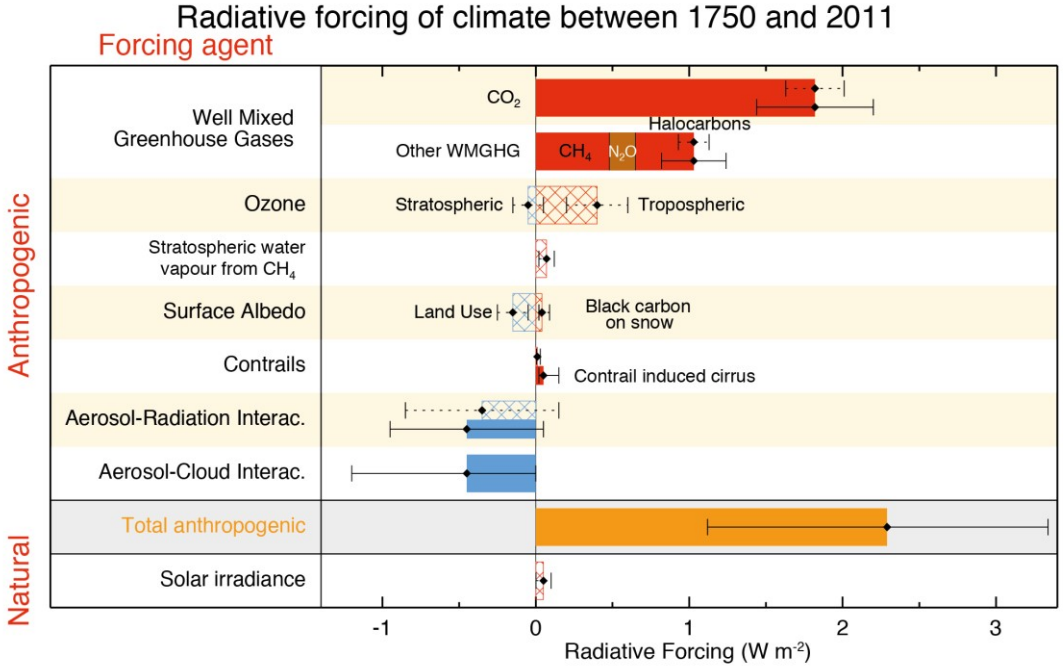

Fig. 2-2: Radiative forcing (energy imbalance in the earth and troposphere, hatched bars) and effective radiative forcing (including rapid tropospheric adjustments, solid bars) with uncertainties (5 to 95% confidence range) for the period 1750–2011 (MYHRE et al. 2013).

2.3 Non-classical monitoring approaches

Due to the legislation and threshold values discussed, PM is monitored constantly. For this purpose, gravimetric (high-volume) samplers are installed in containers monitoring PM, NO_2 and O_3 (UMWELTBUNDESAMT 2012; VIANA et al. 2008). In 2018, 368 stations in Germany were detecting PM amounts with some of them also measuring contents of As, Cd, Ni, Pb and benzo[a]pyrene (UMWELTBUNDESAMT 2019). In addition, dust deposits are collected for example at selected weather stations and for long-term studies, using vessels to catch dustfall. This is typically done with Bergerhoff samplers (open glass collecting pots), simple poylethylene (PE) cylinders with or without a cover for precipitation events or cylinders with a protected adhesive surface (e.g. AL-KHASHMAN 2004; GUÉGUEN et al. 2012; NORRA and STÜBEN 2004). Those classical approaches are important for monitoring PM contents, examining compliance with threshold values and generating data on a long-term scale.

Nevertheless, they cannot be applied for all scientific questions. As monitoring containers require an area of several square meters (see Fig. 2-3) as well as expensive constant supervision and power supply, they exhibit a poor spatial coverage (CAPOZZI et al. 2016a): Contain-

ers are often only installed in urban areas, with one or a few stations in a single city (KARDEL et al. 2011). In comparison, collection of dustfall in vessels is less expensive and space-consuming, but each sample represents bulk deposition of a longer sampling period. Information on short time periods (e.g. a day or week) is not available with this method (GUÉGUEN et al. 2012). In contrast, PM contents and composition can vary sharply over short distances (tens or hundreds of meters) and times (single days) (e.g. DONGARRÀ et al. 2007; SALMOND and MCKENDRY 2009). A few fixed-site monitoring stations do not cover all of the variation in urban PM, which might be needed to characterize local hotspots and detect sources of PM (APTE et al. 2017; SALMOND and MCKENDRY 2009). To do the latter, based on a statistical evaluation, a broader amount of data is necessary, including both more sampling locations as well as more parameters being determined.

Fig. 2-3: Examples of classical air quality monitoring stations in Thuringia. a) "Greiz, Mollbergstr." (urban background), b) "Suhl, F.-König-Str." (urban traffic).

A possible approach to this is the collection and analysis of biological materials, which is called biomonitoring in this context (RACHWAŁ et al. 2018). Biomonitoring is simple and cost-effective, as nearly no equipment has to be bought and no power supply and maintenance are needed for the sampling (VUKOVIC et al. 2016). Most of the studies to assess PM use mosses and lichen, as they exhibit a large surface area and a high efficiency to adsorb heavy metals (BERISHA et al. 2017; GONZÁLEZ and POKROVSKY 2014; TRETIACH et al. 2011). Other materials that have been used so far are tree leaves and needles as well as tree bark (NOROUZI et al. 2015; URBAT et al. 2004).

Moss bag biomonitoring is a modification of these methods: Bags of plastic mesh are filled with moss of a selected species from a remote place and exposed to ambient air at selected locations (ARES et al. 2012). It has been shown, that contents of PM and heavy metals in the moss bags correlate with their atmospheric levels (DMUCHOWSKI and BYTNEROWICZ 2009). Being first published in 1971, there has been a growing interest in this method which, up to

now, is limited to scientific research (ARES et al. 2012; CAPOZZI et al. 2016b; GOODMAN and ROBERTS 1971). RYBAK (2015) even stated the moss bag technique as more relevant for urban areas than the collection of naturally occurring mosses, mainly as the use of moss of the same species prevents some of the variation inherent in classical moss monitoring (ARES et al. 2012). Besides, a moss bag biomonitoring campaign can be repeated and large, dense and flexible monitoring networks can be designed (CAPOZZI et al. 2016b; DMUCHOWSKI and BYTNEROWICZ 2009; TRETIACH et al. 2011).

Another seldomly applied method is the collection of spider webs. Being first published in 1992 (RACHOLD et al. 1992), only a few studies have dealt with this method so far (e.g. HOSE et al. 2002; RYBAK and OLEJNICZAK 2014; RYBAK et al. 2015). Spider silk is a fibrous biopolymer consisting of peptides and proteins which can adsorb dust particles (RYBAK et al. 2012; VOLLRATH 1999). The method has been stated to be suitable to evaluate air pollution and RYBAK et al. (2012) found similar results for the analysis of heavy metals in spider webs and with classical monitoring methods (RYBAK et al. 2015). In cities, webs can be collected easily e.g. from fences, walls or handrails. Spider webs are widespread in urban areas and can even be found in adverse surroundings (AYEDUN et al. 2013; YANG et al. 2016). Besides, the sampling is cheap and non-invasive, if webs are not collected too often at the same place (RYBAK et al. 2015; XIAO-LI et al. 2006). As spiders can be found in most of the earth's climate zones, this method might be applied in many regions worldwide, including developing countries (AYEDUN et al. 2013).

2.4 Study area: Jena as a typical medium-sized city in Central Germany

Most of the sampling has been performed in the city of Jena. The city is situated in Central Germany, in the central eastern part of the federal state of Thuringia. With a number of approximately 111,000 inhabitants it can be called a medium-sized city (THÜRINGER LANDESAMT FÜR STATISTIK 2019). Located in the eastern part of the Thuringian Basin, an area of particularly low precipitation, the local climate is rather arid for a German city (KOCH 1953). Within the last ten years (2009–2018), the mean annual precipitation was 489 mm, ranging from 299 mm to 669 mm (MAX PLANCK INSTITUTE FOR BIOGEOCHEMISTRY 2019). A particular geographical feature of the city is its location in a valley, formed by the river Saale, with distinct north-south elongation. Likely due to the sheltered location in the valley and the heat-island effect of the city (HERTEL and GOODSITE 2009), mean annual temperatures are comparably warm, ranging from 7.5 °C to 10.8 °C (mean: 9.6 °C) within the last ten years (2009–2018, MAX PLANCK INSTITUTE FOR BIOGEOCHEMISTRY 2019). The main wind direction is south to southwest, as the wind is channelled by the valley (KOCH 1953). Nevertheless the wind might not be very important for PM distribution throughout the whole year, as the city is extremely sheltered from wind (KOCH 1953).

Various local businesses and small industries, but no big industrial plants, are resident in the city and its direct surroundings. To get information on the pollutants emitted to the air from industrial facilities, the European Pollutant Release and Transfer Register (E-PRTR) can be

used. Latest entries for Jena (from 2016) name only two facilities in the city emitting air pollutants: Schott Technical Glass Solutions GmbH and the thermal power station Jena Süd (EUROPEAN ENVIRONMENT AGENCY 2019). Both emit nitrogen oxides (NO_x/NO_2) and the latter emits also CO_2. Documented emissions of PM_{10} or heavy metals by industrial point sources according to the E–PRTR are several kilometers away from Jena (see Tab. 2-1). If particles from there are not very small and thus can be transported on a long-range distance, the anthropogenic influence on PM in Jena can be expected to be mainly due to diffuse sources like traffic, small businesses and emissions from households.

Tab. 2-1: Industrial facilities in the surroundings of Jena emitting PM_{10} and/or heavy metals according to the European Pollutant Release and Transfer Register (E-PRTR, EUROPEAN ENVIRONMENT AGENCY 2019).

Facility	**Coordinates [°] (ETRS 1989)**		**Distance to the city center of Jena**	**Industrial activity**	**Pollutant(s) emitted (per year)**
	Longitude	**Latitude**			
Silbitz Guss GmbH	11.98854	50.95735	28 km Direction: E	Production of pig iron or steel including continuous casting	PM_{10} (210 t)
Stahlwerk Thüringen GmbH	11.43429	50.65350	32 km Direction: SW	Manufacture of basic iron and steel and of ferro-alloys	Cu (305 kg) Ni (87 kg) Zn (2.20 t)
OPTERRA Zement GmbH Karsdorf	11.66034	51.27022	39 km Direction: N	Cement clinker in rotary kilns	Hg (22 kg)
Mitteldeutsche Braunkohlengesellschaft mbH (MIBRAG) Deuben, Teuchern	12.07678	51.11207	40 km Direction: NE	Thermal power stations and other combustion installations	Hg (31.2 kg)
Mitteldeutsche Braunkohlengesellschaft mbH (MIBRAG) Wählitz, Hohenmölsen	12.07640	51.16633	43 km Direction: NE	Thermal power stations and other combustion installations	Hg (17.1 kg)
Uniper Kraftwerk GmbH Schkopau	11.95040	51.39846	58 km Direction: NE	Thermal power stations and other combustion installations	Hg (288 kg) Ni (126 kg) PM_{10} (68.7 t)
Stahl- und Hartgusswerk Bösdorf GmbH	12.26722	51.24591	59 km Direction: NE	Casting of metals	Cu (106 kg)
ROMONTA GmbH Amsdorf	11.71791	51.46161	60 km Direction: N	Mineral oil and gas refineries	Hg (27.5 kg)
LEAG Lausitz Energie Kraftwerke AG Kraftwerk Lippendorf	12.37164	51.18414	62 km Direction: NE	Electric power generation, transmission and distribution	As (31.9 kg) Cu (120 kg) Hg (538 kg) Ni (64.8 kg) PM_{10} (95.8 t)

PM in Jena is also expected to be influenced by the local geology, for example by erosion. The valley mentioned before has been formed by the river Saale carving into the surface of the eastern Thuringian Basin since the Tertiary. This process has brought up various Triassic sedimentary rocks that characterize the geology of the study area (VOIGT et al. 2000). The

lower layers are formed of sandstones (Buntsandstein), which are mainly continental deposits (MÄGDEFRAU 1929). They contain high amounts of quartz and quartzite as well as feldspars and carbonates as cement (SEIDEL 1993; SEIDEL 2003). Above the Buntsandstein, shell limestones (Muschelkalk) can be found (MÄGDEFRAU 1929). Those marine deposits contain mainly limestone (calciumcarbonate), dolomite and gypsum (SEIDEL 2003). During the Quaternary glacial periods, loess has been deposited with a low thickness on the plateau area and thicknesses of several meters in some parts of the valley (ELLENBERG 2012). This eolian transported, fine-grained sediment contains mainly quartz particles enclosed by calciumcarbonate. Further Quaternary sediments like alluvial loams can be found at the valley bottom around the river (SEIDEL 1993). Soils and also the land use are influenced by this host rock geology (ELLENBERG 2012): The Upper Buntsandstein causes a shallow slope and is mainly used for settlement areas and agriculture. A steep slope, covered to a large extent by forests, is typical for the Lower Muschelkalk, whereas the Middle and Upper Muschelkalk are again used for agriculture due to the undulating terrain with shallow slopes. Fig. 2-4 shows a superposition of the geological formation and the land use to illustrate the connection described. This connection should be kept in mind as agricultural fields are more prone to erosion than forests and (resuspended) surface dust largely contributes to natural emissions of trace metals (ALLEN et al. 2001).

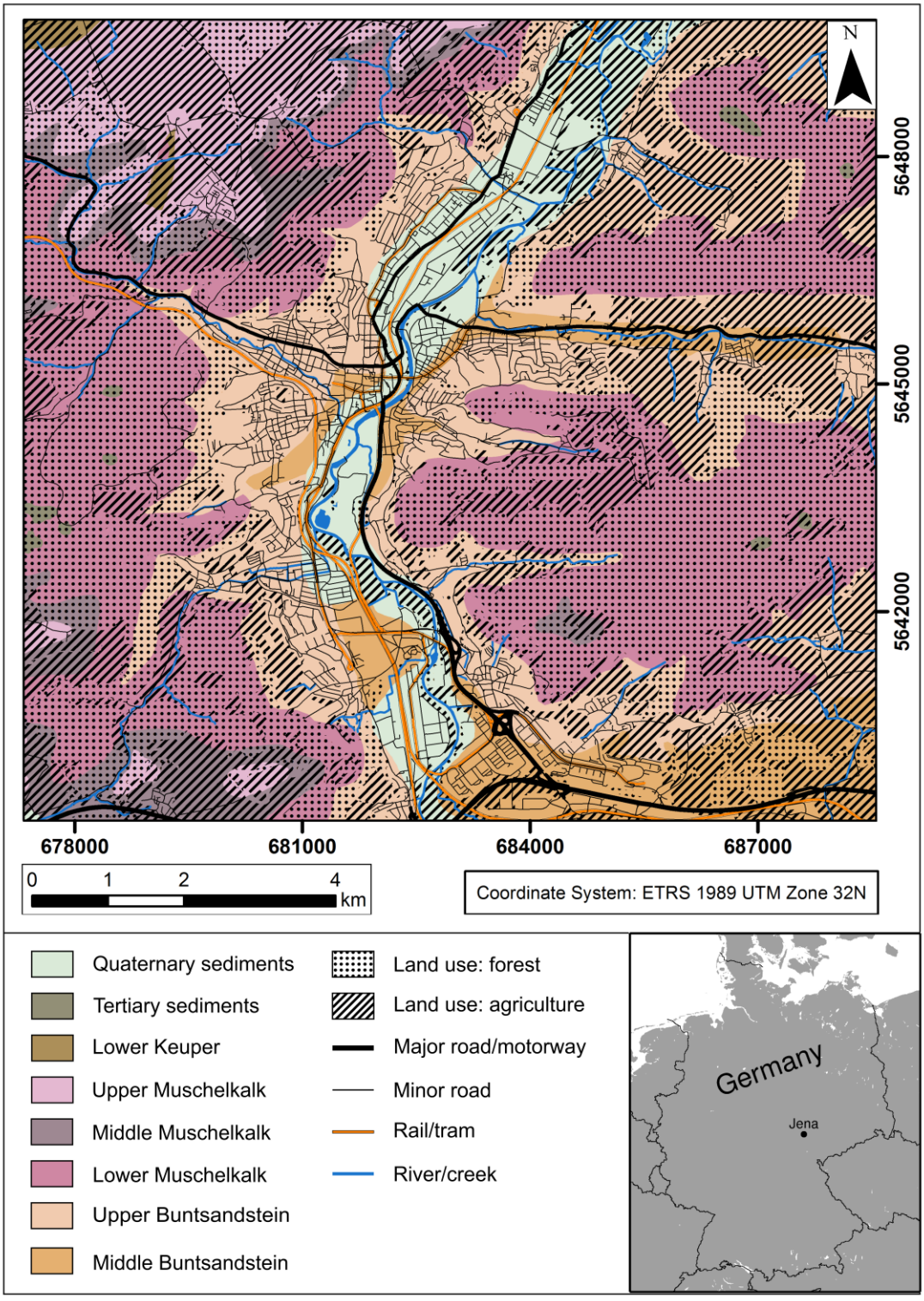

Fig. 2-4: Geology and land use in the city of Jena and its direct surrounding. The superposition shows, that for agriculture mainly Upper Buntsandstein as well as Middle and Upper Muschelkalk areas are used while the Lower Muschelkalk is mainly covered with forests. Geological formations have been taken from SEIDEL (1993, p. 3) and information on land use, traffic routes and water bodies has been derived from the Thuringian open geodata program (THÜRINGER LANDESAMT FÜR BODENMANAGEMENT UND GEOINFORMATION 2019).

3 Material and methods

Approximately 470 samples have been taken in this work, mainly for performing non-classical monitoring of PM. The main part of the samples has been taken in the city of Jena, Germany. Prior to determining the contents of 52 elements, all samples were digested using aqua regia. The analytical data was used for statistical evaluation, including multivariate chemometric tools to identify element patterns and sources of PM. A flow chart illustrating the steps of the analytical process for four sample materials sampled to assess PM can be found in Fig. 3-1. To get more information on the different sample materials/matrices, total digestions with HF, determination of the total and organic carbon content and microscopic imaging were performed for selected samples. All steps will be described in this chapter, following the course of the method of analysis.

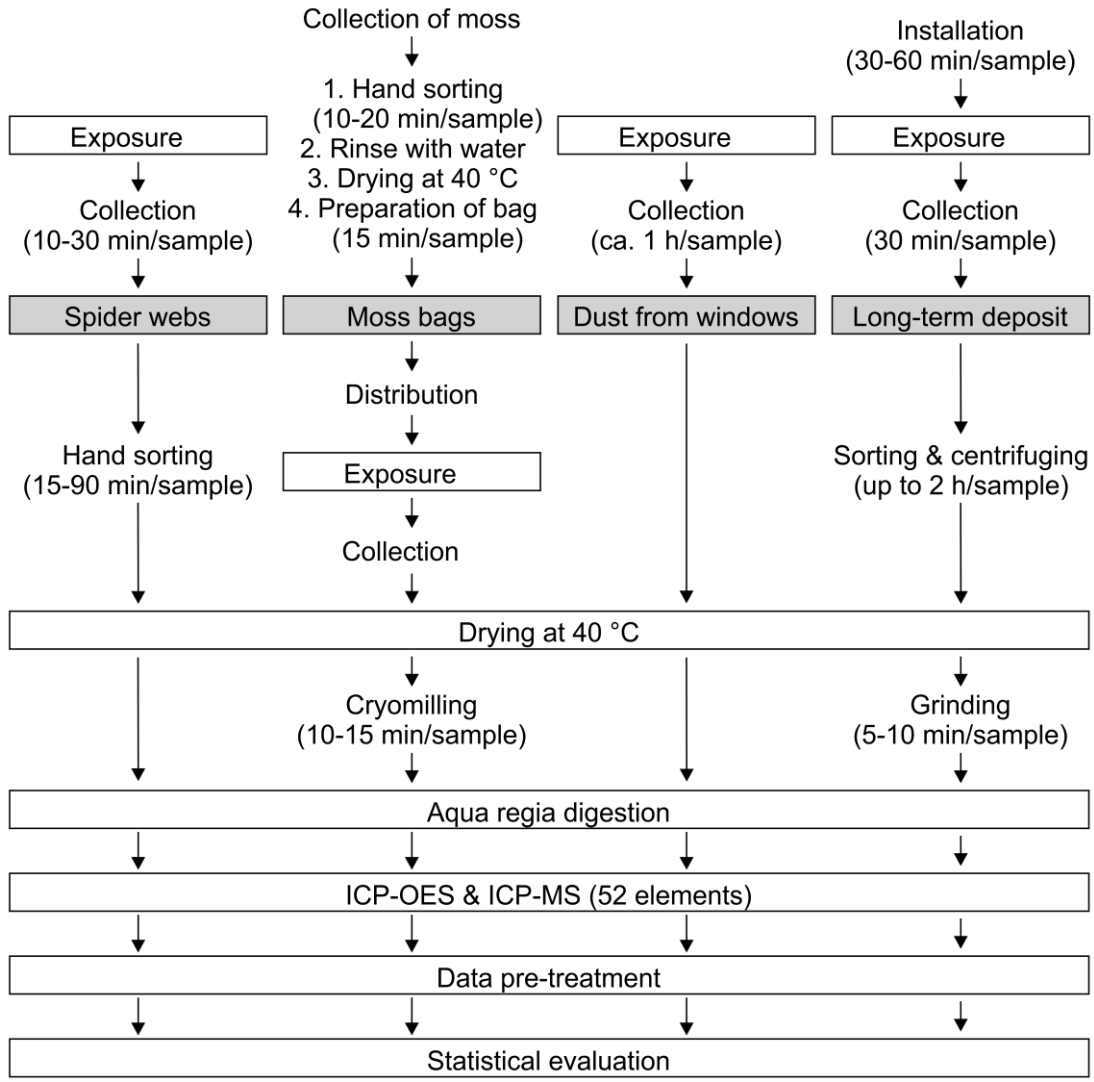

Fig. 3-1: Flow chart of the steps of the analytical method for the four different sample materials regarded to assess PM. For time-consuming steps of the sampling and sample preparation approximate durations per sample are added.

3.1 Sampling and sample preparation

A large part of the samples are spider webs that have mainly been sampled at 22 locations in Jena for several times. Some additional spider webs were sampled at other locations, mainly in Central Germany. For comparison with the spider web data, other non-classical samplings were performed. Three campaigns of moss bag biomonitoring were conducted in Jena and dust has been sampled from windows in Jena as well. Long-term dry and wet dust deposit was collected in open vessels at several locations in Central Germany. In addition, samples of selected materials that likely represent source terms of geogenic or anthropogenic dust have been taken. Tab. 3-1 gives an overview on the number of samples taken. In the following, sampling and sample processing will be described for the different sample materials.

Tab. 3-1: Overview on sample materials and the number of samples taken and processed in the course of this work.

Sample material	Number of samples taken	Number of sampling locations
Spider webs (repeated sampling)	265	22
Spider webs (additional samples)	31	26
Moss bags	50	20
Dust from windows	56	28
Long-term deposit	24	14
Source terms: agricultural soil	14	14
Source terms: loess	9	7
Source terms: anthropogenic sources	19	No sampling locations

3.1.1 Sampling of spider webs

Spider webs were first sampled in 2016 to test the applicability of this seldomly used biomonitoring method with regard to the analytical procedure (sample preparation, analysis, data quality). Afterwards, a high number of samples have been taken to generate the data set to be used for the identification of sources of PM. To cover both spatial and temporal variation, a repeated sampling has been performed at 22 locations in the city of Jena from 2016 to 2018 (see Fig. 3-4). The locations were named according to the most nearby type of traffic (CA: car traffic, PD: pedestrian area, RS: railroad station, TR: tram/train traffic, CA/TR: both car and tram/train traffic) and facilities/districts at the individual location. After the primal sampling in 2016, in 2017 and 2018 a periodic sampling has been performed from April to September, which proved to be a period with a sufficient amount of wheel webs for sampling. Samples were taken every six weeks with four locations being sampled every two weeks. Spring sampling campaigns were also part of Bachelor theses performed in the course of the project (BONRATH 2016; HERRSCHUH 2017; PERCHERMEIER 2016; SINZ 2017; SPERHAKE 2018). In total 265 spider webs samples were gained (see Tab. 3-1 and appendix Tab. A-1, Tab. A-2).

The webs were sampled by coiling them up on a plastic straw (polypropylene, PP, 25 cm length, 8 mm diameter), without touching the surface they are anchored to. One sample comprised all webs sampled at one location at a time. In most of the cases, webs were sam-

pled from handrails of bridges, as they are easy to access and webs are easily spotted on them. Selected impressions of webs and sampling locations are shown in Fig. 3-2.

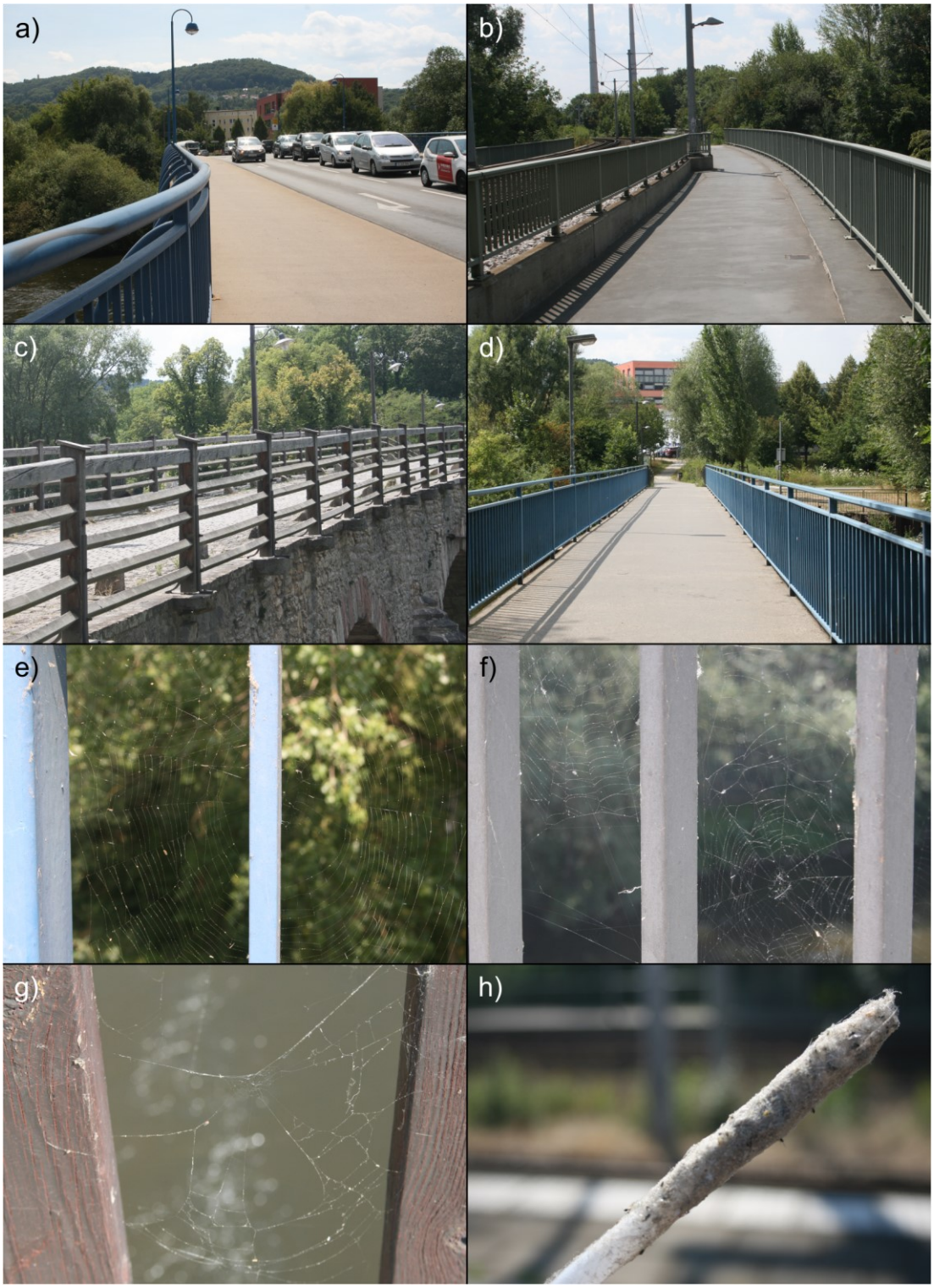

Fig. 3-2: Impressions of the sampling locations and sampling of spider webs in July 2018. a) CA-WIE, b) TR-ARE, c) PD-BUR, d) PD-LOB, e) optically rather clean web at CA-BUR_1, f) webs with visible coarse contaminants at CA/TR-CAM, g) web with demolished structure at PD-GRI, h) coiled up spider webs – dust load is visible by layer stack – gained at RS-PAR.

The height of the handrails varied between 0.89 m and 1.25 m but the lower approximately 50 cm above ground were not included in the sampling to avoid influences from spray water

bouncing back from the ground during rainfall events. Samples were stored in individual bags (polyethylene, PE) for transportation and storage until further processing. In the lab, the tangled webs were removed from the plastic straw and coarse objects like hairs or (parts of) insects were removed manually with tweezers (polyoxymethylene, POM). Afterwards, the samples were dried at 40 °C (heat cabinet UFE 500, Memmert GmbH & Co. KG) for at least 24 h and stored in 50 ml centrifuge tubes (PP, Greiner Bio-One GmbH) until further processing. Different attempts have been made to homogenize the samples, using a mortar and pestle, cryomilling with liquid nitrogen or bead milling (Bead Ruptor 24, biolabproducts GmbH). As none of these proved to work well for initial spider web samples, a homogenization was not performed. Nevertheless this can be considered irrelevant, as in most cases the whole sample was subjected to digestion in the following. The only exception are samples used for quality assurance (chapters 3.5 and 3.7), as they had to be split.

In addition to the repeated sampling in Jena, 31 spider web samples were taken at other locations, mainly in Central Germany (see Tab. 3-1 and appendix Tab. A-3). They were not only collected from handrails, but also from bushes and exteriors of buildings. In the latter case, the samples often contain funnel webs that cover a longer time span of exposure to ambient air compared to wheel webs. These samples have been taken to get an impression of samples from other locations/cities, or as they are expected to be influenced by only one source of PM. They will not be included in the data set of the repeated sampling but will be evaluated separately.

3.1.2 Moss bag biomonitoring

Three moss bag biomonitoring campaigns were performed in the city of Jena, with the aim of comparing analytical data gained from this method with analytical data gained from spider web biomonitoring. Moss bag biomonitoring is a more frequently applied biomonitoring method and has also already been reviewed (e.g. ARES et al. 2012). Thus, more data for comparison is available for this method than for spider web biomonitoring. The bags were exposed to ambient air at or some meters away from 20 locations of the spider web sampling (see Fig. 3-4). Two campaigns of an exposure time of ten weeks were performed in summer 2017 and winter 2018. An additional campaign with an exposure time of four weeks was performed in spring 2017 as part of the theses of HERRSCHUH (2017) and SINZ (2017). During each of the ten weeks campaigns, five moss bags were lost due to vandalism. More details on sampling dates as well as existing samples can be found in the appendix (Tab. A-4).

To prepare the bags, living individuals of the moss *Hypnum cupressiforme* were collected in a pine forest 15 km south of Jena (E 11.65419 N 50.80139 ETRS 1989). The sampling location is a rural area with forests and agricultural fields (distance to next road: 60 m, distance to next agricultural field: 63 m), thus only a background contamination of the moss can be expected. *Hypnum cupressiforme* was chosen due to both its high abundance in continental Europe and its high surface to volume and surface to mass ratios (ADAMO et al. 2008; BARANDOVSKI et al. 2015). Foreign objects like pine needles, soil fragments and fine gravel as

well as dead moss material were removed with tweezers (POM). Afterwards, the moss was rinsed three times with deionized water, using a 500 ml wide neck bottle of polyethylene terephthalate glycol (PETG, Kautex Textron GmbH & Co. KG) in which a portion of moss and a portion of water were shaken carefully for one minute, replacing the water two times. The bags (16 x 16 cm) were made of polyester mesh with a mesh size of 2 mm (Emil Lux GmbH & Co. KG) sewed with nylon thread (0.5 mm, Rayher Hobbykunst). Prior to filling, the bags were rinsed with diluted HNO_3 (Merck, subboiled) and ultrapure water (genPure UV-TOC, Thermo Fisher Scientific) successively. 3 g of the dry moss material were filled into each bag and the bags were sealed and stored in a PE pouch at room temperature until use.

For exposure, the bags were installed at street lamps (of the Kommunalservice Jena) in a height of approximately 2.5 m above ground to avoid vandalism. Plastic mountings, that prevent the bags from touching the metal lamp poles, were built for this purpose. The bags were tied to the mountings which were then tied to the lamp poles with cable ties of polyamide (PA, 380 x 7.6 mm). Impressions of the preparation and exposure are shown in Fig. 3-3. Moss was spaced out evenly in the bags at the beginning of the exposure period, but in most of the cases it assembled in the lower part of the bag throughout time (as shown in Fig. 3-3d).

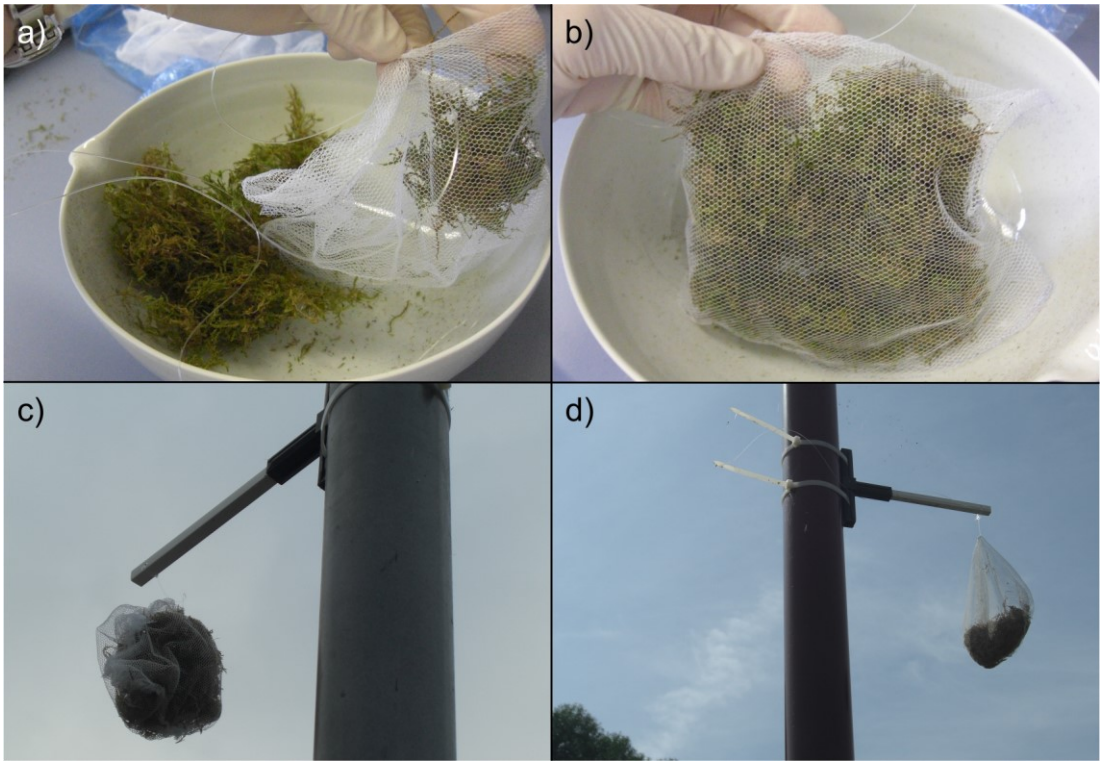

Fig. 3-3: Impressions of the preparation and exposure to ambient air of moss bags. a) Preparation of a bag in the laboratory, b) ready-made moss bag, c) bag installed at CA/TR-CAM at the beginning of the exposure period, d) bag at the end of an exposure period of ten weeks at PD-KUN.

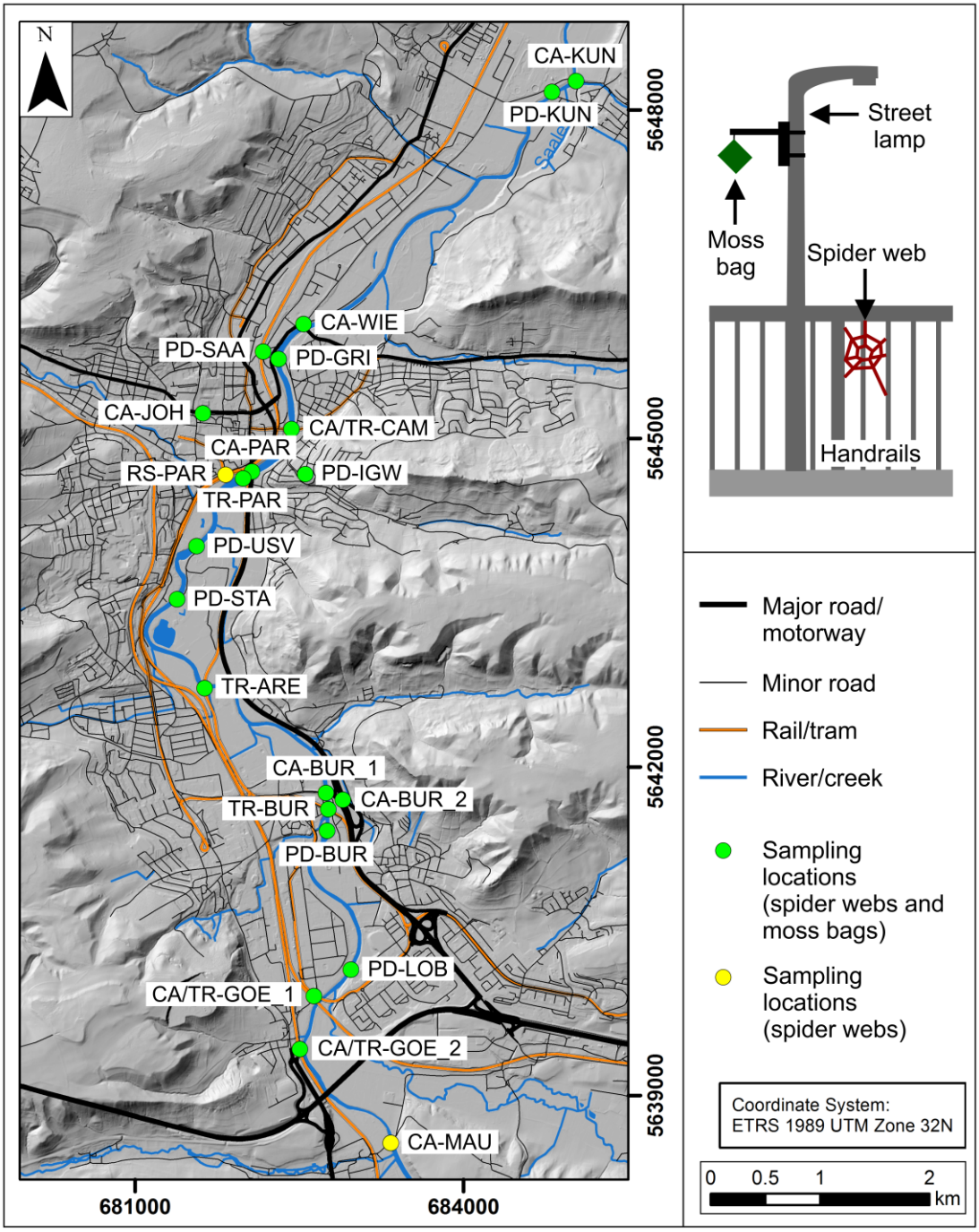

Fig. 3-4: Locations in the city of Jena where spider webs have been sampled repeatedly and moss bags were exposed to ambient air. Information on traffic routes and elevation above sea level has been derived from the Thuringian open geodata program (THÜRINGER LANDESAMT FÜR BODENMANAGEMENT UND GEOINFORMATION 2019).

After the set exposure time the bags were removed and stored in individual PE bags during transportation to the laboratory. There, the moss was removed from the bags and dried at 40 °C for several days. A part of each dry sample was cryomilled with liquid nitrogen (≥ 99.8%, Linde AG), using a porcelain mortar and pestle (W. Haldenwanger GmbH & Co. KG), and the milled samples were stored in 50 ml centrifuge tubes (PP, Greiner Bio-One GmbH) until chemical analysis. The non-milled samples were stored in PE bags for microscopic imaging. For detailed evaluation, only the samples with an exposure time to ambient

air of ten weeks were included, as exposure times of less than a month are often regarded as too short for the accumulation of a sufficient amount of particles (e.g. ARES et al. 2012). The campaign of four weeks has mainly been used to test preparation of the moss bags, sampling and sample processing. More details on this campaign can be found in the corresponding Bachelor theses of HERRSCHUH (2017) and SINZ (2017).

3.1.3 Dust from windows

To test another non-classical monitoring method for PM, that is not a biomonitoring method, and compare the results with those of the biomonitoring, dust deposit has been sampled from windows. At 28 locations in the city of Jena, dust has been sampled in two sampling campaigns: winter 2017/18 (04/12/17-24/01/18) and spring 2018 (23/03/18-16/04/18), yielding a total of 56 samples. Most of the locations are buildings of the Friedrich Schiller University Jena, while the others are buildings of the Studierendenwerk Thüringen, the Max Planck Institute for Biogeochemistry and a public bus stop of the Jenaer Nahverkehr GmbH. A map including the sampling locations is provided in Fig. 3-5. The locations were named according to street names or the according buildings, since not all locations could be assigned to a certain type of nearby traffic as performed for the spider web and moss bag biomonitoring. Location UHG_in for example is close to a major road (36 m) but located in a courtyard, preventing a major influence of road traffic. Also location BOT is close to a major road (18 m), but is expected to be shielded from its influence by surrounding trees. On the other hand, locations like FRU and NOL are located very close to tram lines and a major road (FRU: 11 m and 3 m, NOL: 41 m and 5 m) and expected to be strongly influenced by them.

For sampling a commercial window cleaning device (window vacuum cleaner WV 2 PREMIUM, Alfred Kärcher GmbH & Co. KG) was used. Deionized water was sprayed on the window glass from a short distance (30–50 cm) to suspend dust particles. The suspension was soaked up with the vacuum cleaner and collected in a small plastic container. A spacing of at least 3 cm was kept between the surface from which the sample was taken and both the window frames as well as big contaminations like bird droppings. A contamination of the dust sample with non-airborne substances should be avoided by this. Except from the location OTS (second floor), all samplings were done at ground floor windows in a height of 1.0–3.5 m above surface level. Several windows close to each other were vacuumed to form one sample. Total window areas were estimated and differ between the sampling locations (1.84–14.69 m^2). Further details for each sampling location can be found in the appendix (Tab. A-5, Tab. A-6) and in the thesis of ROMBACH (2018), who performed most of the sampling.

After sampling, the suspensions were transferred to individual 250 ml bottles (Nalgene, PP, Thermo Fisher Scientific) for transportation, storage and drying. Between the samplings at different locations, the window vacuum cleaner was rinsed with deionized water, excluding only the electric parts, to prevent cross-contamination of individual samples. In the laboratory, the samples were dried at 40 °C (two days up to two weeks, depending on the humidity of the sample), yielding 35–614 mg of dust particles for further analysis.

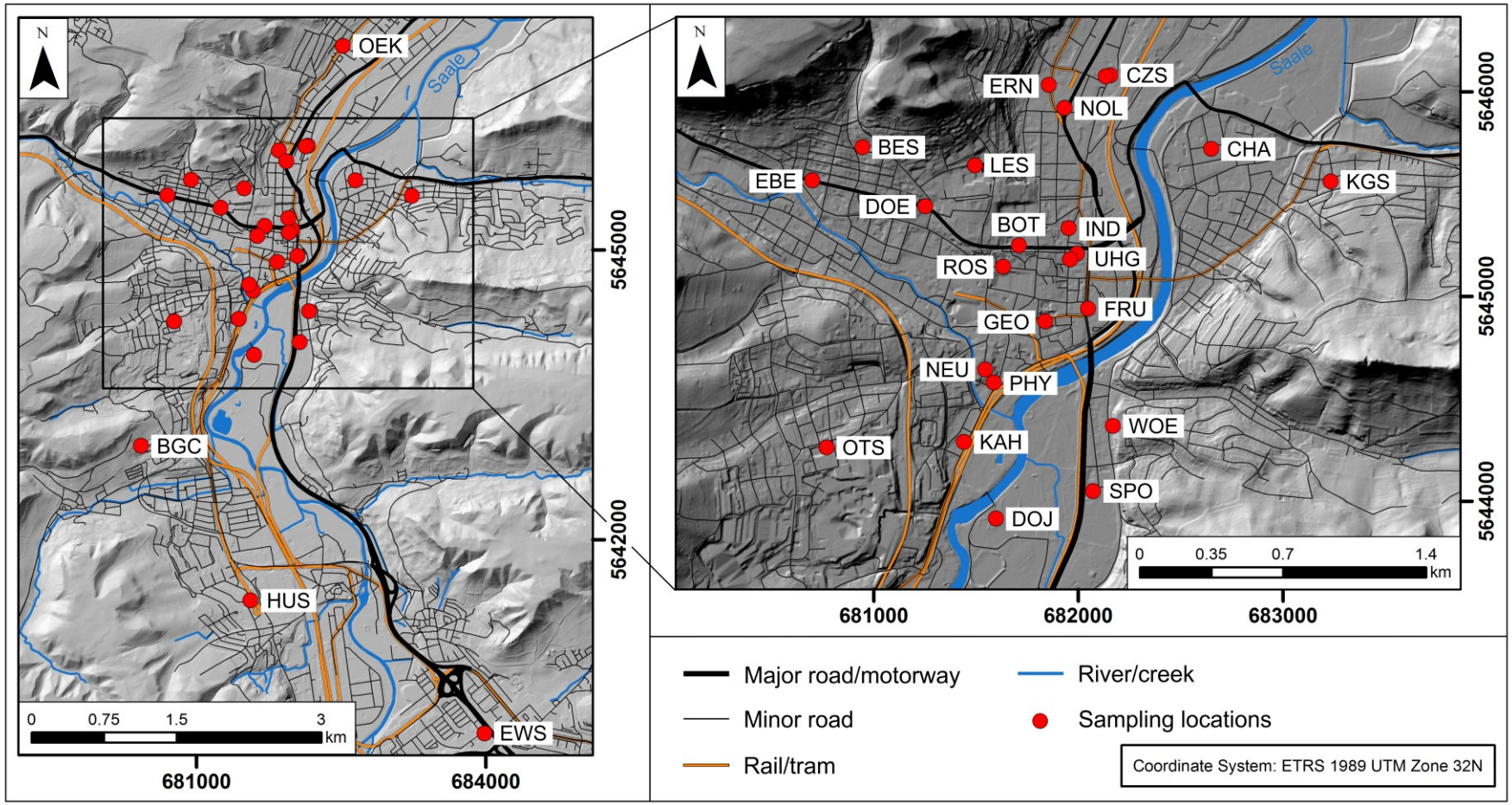

Fig. 3-5: Locations in the city of Jena where dust has been sampled from windows. Information on traffic routes and elevation above sea level is similar to Fig. 3-4.

3.1.4 Long-term dust deposit

At 14 locations in Central Germany dust deposit was collected on a long-term scale (several months up to one year) in a more classical attempt, as mentioned in 2.3. The locations were selected and named with regard to the different land use in their surroundings and the corresponding different nearby sources of dust particles: agriculture (AGR), airport (AIR), remote background (BGR), urban residential area (RES) and urban traffic (TRA). Most of the locations were provided by cooperation partners as well as third parties, e.g. the MOBICOS experimental container of the Helmholtz Centre for Environmental Research (AGR1), the Geodynamic Observatory Moxa of the Friedrich Schiller University Jena (BGR1), the Thüringer Landessternwarte Tautenburg (BGR2) and an airport in Central Germany (AIR1 and AIR2). The purpose of this has been both testing an easy to perform, classical sampling method and generating samples mainly influenced by a known source to get information on the source terms.

Measuring cups of PP (3 l, VITLAB GmbH) were used to collect dust deposit. At some locations, the cups were mounted directly on existing installations while at others they were installed on a wooden mounting that was built for this purpose and anchored into the ground. Fabric adhesive tape (Duck Tape®, silver) and cable ties (PA, 380 x 7.6 mm) were used to fix the cups. Where necessary, the water head was removed in between the samplings and merged with the corresponding sample to prevent an overflow. A plastic hose of polyvinyl chloride (PVC, 6 mm internal diameter, OBI GmbH & Co. KG) and PP bottles (0.5 and 1.0 l, Nalgene, Thermo Fisher Scientific) were used for this purpose. Besides from dry and wet dust deposit, other material like dead insects, algae and leaves could also be found in the vessels after the sampling period. Exemplary pictures are given in Fig. 3-6. Detailed information on the different appearances of the samples as well as the sampling locations and periods can be found in the appendix (Tab. A-7).

After the sampling period, the cups were deinstalled, covered with individual PE bags and transported upright to the laboratory to prevent spilling and/or loss of the samples. Insects, leaves and other foreign matter were sorted out of the samples with tweezers (POM) and rinsed with deionized water to obtain potential dust particles attached to them. Dry samples were rinsed off from the walls of the cups with deionized water and the rinsing suspensions were merged with the corresponding wet samples, where those existed. The suspensions were transferred stepwise into 50 ml centrifuge tubes (PP, Greiner Bio-One GmbH) and centrifuged for 15 min at 3000 rpm (Heraeus® Multifuge 3L), discarding the supernatants afterwards. The residues were dried at 40 °C, milled with a ceramic mortar and pestle and stored in the centrifuge tubes until further analysis.

Fig. 3-6: Examples of the different installations for the collection of long-term deposit (left) and the dry samples obtained at the respective locations in summer 2018. a) and b) AGR1, c) and d) AGR2, e) and f) RES3, g) and h) BGR1.

3.1.5 Samples representing source terms of urban dust

Samples of different potential sources of PM were taken to compare element patterns in them with patterns in the monitoring samples. Fig. 3-7 shows some impressions from the sampling; a table of all samples can be found in the appendix (Tab. A-8).

Agricultural soil has been sampled at 14 locations in Jena and its surroundings, as agriculture (in general) is expected to be a major source of PM in Europe (LELIEVELD et al. 2015). Soil particles are eroded preferentially from bare fields or suspended during activities like ploughing. The litter layer was removed, the uppermost 10 cm were sampled with a plastic shovel and samples were put in individual PE bags for transportation and storage. As the topsoil was sampled, those samples do not represent a purely geogenic/natural material, but are likely a mixed material containing also anthropogenic particles like coal fly ash transported over long distances. Higher contents of heavy metals in topsoils due to atmospheric deposition have been described for example by HOVMAND et al. (2008). All samples were dried at 40 °C for approximately seven days and afterwards wet sieved using a nylon sieve with a mesh size of 63 µm (Retsch GmbH) and tap water to avoid dissolution of easily soluble components. Drying was done prior to sieving to calculate amounts/proportions of selected grain size fractions in the sample in a corresponding project module of a M.Sc. student (SCHEUERER 2018). Only the fraction with a grain size smaller than 63 µm was used for further analysis as those particles are expected to be easily transported over longer distances, possibly reaching the city center of Jena. Samples with the prefix NL have been sampled at monitoring sites of the Thüringer Landesamt für Landwirtschaft und Ländlichen Raum, and all other samples were part of the named project module. Detailed descriptions of those samples and the sample preparation can be found in the corresponding report (SCHEUERER 2018).

In addition, loess has been sampled. This well sorted, aeolian sediment, deposited during the Quaternary glacial periods, occurs at several locations in Central Germany (PYE 1987). As it has already been transported in the air prior to deposition, it is regarded as a good material representing geogenic dust (PYE 1987). Nine samples have been taken from different outcrops. The surface layer was removed prior to sampling to avoid an influence of anthropogenic contaminants. Samples were taken with a plastic shovel from the C or Cv horizon (75 cm to 4 m below the litter layer) and put in individual PE bags for transportation and storage. The samples were dried for approximately five days (40 °C) and milled with an agate mortar and pestle to yield homogeneous samples. Both loess and soil samples were stored in PETG bottles (Kautex Textron GmbH & Co. KG) until further processing.

Seven samples were assigned to the source term tram/train. Three of them are residues/sediments that can be found inside tram tracks and were removed with a plastic shovel. Other samples consist of dust deposit collected from surfaces at tram/train stations using a clean plastic brush. All samples were stored in PETG bottles (Kautex Textron GmbH & Co. KG) and dried at 40 °C. Objects that could be identified as not being dust particles (e.g. hairs or small pebbles) were removed with tweezers (POM) prior to further processing.

To yield brake wear samples representing another source term, parts of a used brake pad and disc were rubbed against each other and the abraded fine material was collected. It was dried at 40 °C and stored in PETG bottles (Kautex Textron GmbH & Co. KG).

In the following, agricultural soil and loess samples are regarded as representing natural/geogenic dust while the tram/train samples as well as brake wear represent anthropogenic, traffic-related dust. Some other samples were taken as well to cover more sources of PM: charcoal, lignite and road salt. As for most of the latter samples element contents were below the limit of detection (LOD), they were not regarded further. Exhaust particles brushed off from the inside of exhaust pipes were regarded as another source term but did not yield enough material for chemical analysis.

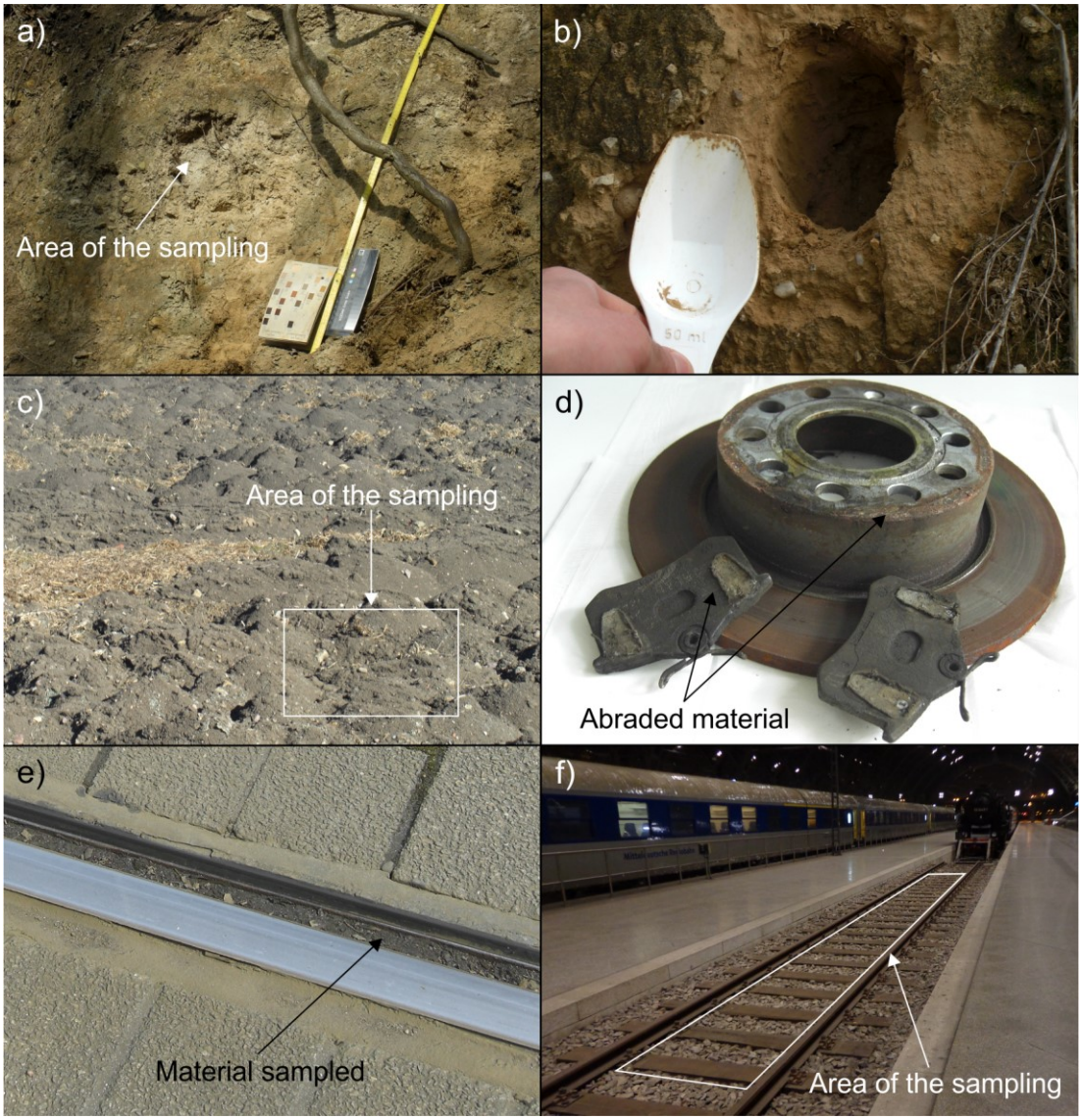

Fig. 3-7: Impressions of the sampling of materials representing different source terms of dust: loess (a) KP-1 and AB-1, b) NL-20.10.2016-4), agricultural soil (c), brake pad and disc (d), tram/train (e) residue from tram tracks AB-2, f) dust from wooden sleepers at an abandoned platform at the railroad station Leipzig NL-17.01.17-1).

3.2 Wet-chemical digestions

All samples were digested with aqua regia acording to DIN EN 16174 (2012) as a standardized procedure, using the microwave-assisted pressure digestion system MARS 5 Xpress and associated vessels of perfluoroalkoxy alkane (PFA, both: CEM GmbH). For this purpose, 6 ml HCl (35%, supra quality, Carl Roth) and 2 ml HNO_3 (65%, Merck, subboiled) were added to a maximum of 200 mg of the sample (precision scale BP210S, Sartorius AG). A prereaction of 20 min was allowed in the open vessel. Afterwards, the mixtures were heated to 175 °C within 15 min and kept at 175 °C for 10 min (closed vessel). The cooled mixtures were transferred to 25 ml volumetric flasks (polymethylpentene, PMP, Vitlab GmbH), filled up with ultrapure water (genPure UV-TOC, Thermo Fisher Scientific) and transferred to 50 ml centrifuge tubes (PP, Greiner Bio-One GmbH). After centrifugation at 3000 rpm for 15 min (Heraeus® Multifuge 3L), the clear supernatants were filled into 30 ml sample bottles (Nalgene high-density polyethylene, HDPE, Thermo Fisher Scientific) and stored until analysis.

Some samples of each sample material (spider webs, mosses, dust from windows, long-term deposit, loess, agricultural soil) were additionally subjected to a total digestion in a pressure digestion system (DAS, Pico Trace GmbH). 2.5 ml HNO_3 (65%, Merck, subboiled) were added to about 50 mg of each sample in the digestion vessels (polytetrafluoroethylene, PTFE, DAS, Pico Trace GmbH). In an initial step the mixtures were heated up to 45 °C within an hour and kept at that temperature for another hour. Afterwards, 2.5 ml 40% HF and 3 ml 70% $HClO_4$ (both: suprapur, Merck) were added to the cooled mixtures, which were then heated up to 180 °C within 8 h, kept at 180 °C for 12 h and cooled down. To evaporate the acids, the mixtures were heated up to 180 °C again within 4–5 h in the evaporation mode and kept at that temperature for 14 h. The remaining solids were dissolved in 2 ml HNO_3 (65%, Merck, subboiled), 0.6 ml HCl (35%, supra quality, Carl Roth) and 7 ml ultrapure water at 150 °C within 8 h. After cooling, the samples were filled up to 25 ml with ultrapure water in volumetric flasks (PMP, Vitlab GmbH) and transferred to 30 ml sample bottles (Nalgene HDPE, Thermo Fisher Scientific) for storage.

3.3 Chemical analyses

To obtain information on element contents, the digestion solutions were analyzed with inductively coupled plasma-optical emission spectroscopy (ICP-OES) and inductively coupled plasma-mass spectrometry (ICP-MS) at the Institute of Geosciences, Friedrich Schiller University Jena. The combination of the two methods enables the determination of element contents over a broad range, including also ultra trace components, but no information on the speciation of the elements is available. In addition, contents of carbon and nitrogen in the solid samples were determined in selected subsamples using an elemental analyzer at the Helmholtz Centre for Environmental Research, Magdeburg.

3.3.1 Inductively coupled plasma-optical emission spectroscopy

Contents of Al, Ca, Fe, K, Mg, Mn, Na, P, S, Si, Sr, Ti and Zr in the digestion solutions were determined with ICP-OES, using the spectroscope 725ES (Agilent Technologies) with a CCD-detector and the autosampler ASX 520 (Teledyne CETAC Technologies). This method is based on detecting and quantifying the characteristic radiation (characteristic wavelength) emitted by the excited analyte. The wavelengths are splitted and selected with a polychromator. Often, as it is also done in the 725ES, echelle optics are used for this purpose (SCHWEDT et al. 2016). The coupled plasma leads to atomisation, ionisation and excitation of the analyte, thus only element contents can be determined. ICP-OES is commonly used for multi-element analysis as excitation conditions can be adapted and the linear range of the calibration covers several orders of magnitude (OTTO 2014). Further details on the method can be found for example in OTTO (2014), SCHWEDT et al. (2016) or SKOOG et al. (2014).

The calibration was done using several standards: ICP multi-element standard solution IV (Certipur®, Merck) with Ag, Al, B, Ba, Ca, Cd, Co, Cr, Cu, Fe, K, Li, Mg, Mn, Na, Ni, Pb, Sr and Zn and two multi-element standards with five (Al, Ca, K, Mg, Na) and 17 (Al, B, Ca, Cd, Co, Cr, Cu, Fe, K, Mg, Mn, Mo, Na, Ni, Pb, V, Zn) elements (both: Bernd Kraft GmbH). In addition, single-element standards of the following elements were used: As, Fe, Mn, Mo, P, S, Si, Ti and V (Certipur®, Merck), Sb, Sn, U and Zr (AccuStandard) and W (Specpure®, Alfa Aesar).

3.3.2 Inductively coupled plasma-mass spectrometry

Contents of Ag, As, B, Ba, Cd, Ce, Co, Cr, Cu, Cs, Dy, Er, Eu, Gd, Hf (since 2017), Ho, La, Li, Lu, Mn, Mo, Nb (since 2017), Nd, Ni, Pb, Pr, Rb, Sb, Sc, Sm, Sn, Tb, Th, Ti, Tm, U, V, W (since 2017), Y, Yb, Zn and Zr in the digestion solutions were determined with ICP-MS, using the XSeries II quadrupole spectrometer with collision cell technology (Thermo Scientific) and the autosampler ASX 520 (Teledyne CETAC Technologies). Atomisation and ionisation in ICP-MS are similar to ICP-OES. Afterwards, analyte ions are separated in a mass filter according to their mass-to-charge ratio under vacuum conditions. In the present case a quadrupole mass filter was used, which can only be passed by one specific mass-to-charge ratio per time. Even though this indicates a scanning mode, ICP-MS is one of the most important multi-element methods for (trace) element analysis. This is based on its high selectivity, good accuracy and the LOD that is lower than the LOD for many optical (spectroscopical) methods (SKOOG et al. 2014). Further details on the method can be found for example in OTTO (2014), SCHWEDT et al. (2016) or SKOOG et al. (2014).

The following multi-element standards were used for calibration: 39-CMS-1, containing Ce, Dy, Er, Eu, Gd, Ho, La, Lu, Nd, Pr, Sc, Sm, Tb, Th, Tm, U, Y and Yb, 39-CMS-5, containing Ag, Al, Ca, Co, Cr, Cs, Cu, Fe, K, Li, Mg, Mn, Na, Ni, Rb, Sr and Zn and 39-IV-ICPMS-71B, containing Ge, Hf, Mo, Nb, Sb, Si, Sn, Ta, Te, Ti, W and Zr (all: Inorganic Ventures). In addition, single-element standards of As, B, Ba, Cd, Pb and V (all: Inorganic Ventures) were used. Re and Ru were used as internal standards (Certipur®, Merck).

3.3.3 Carbon contents

To get information on the bulk components of the different sample materials, contents of total carbon (C_{total}) and organic carbon (C_{org}) were detected in selected subsamples (mass between 0.1 and 0.3 mg). A CNS analyzer Vario EL cube (Elementar Analysensystem GmbH) was applied, using sulphanilic acid (for analysis, Merck) for the calibration. This elemental analysis is based on a high temperature combustion of the sample in the presence of oxygen followed by a reduction of nitrogen oxides to nitrogen (ELEMENTAR ANALYSENSYSTEME GMBH 2019). The resulting gases (CO_2, N_2, SO_2) are separated chromatographically and detected by a thermal conductivity detector. Further information can be found for example in OTTO (2014).

3.4 Microscopic imaging

Microscopic images of selected samples were taken with the digital microscope KEYENCE VHX-6000 (KEYENCE GmbH) with a magnification of 100X to 1,000X (Institute of Geosciences, Friedrich Schiller University Jena). Non-milled moss from moss bags was directly placed on the white or black object plate for this purpose. Spider webs were collected on glass slides at the monitoring site and covered with another glass slide to avoid damages during transportation. In the laboratory, webs were embedded in the thermoplastic mounting medium Cargille Meltmount*1.582 (Cargille-Sacher Laboratories Inc.) melted on a heating plate (PRÄZITHERM PZ 28-1, Harry Gestigkeit GmbH) and covered with a cover glass prior to imaging.

To get some reference images, additional materials (loess, exhaust particles, brake wear and two reference materials) were examined. Exhaust particles were brushed off from the inside of exhaust pipes of cars combusting diesel and gasoline fuel separately, using a commercial toothbrush (non-specified thermoplastic elastomer with bristles of nylon). A similar toothbrush was used to brush off brake wear particles from brake disks of parking cars. In addition, the reference materials SRM 1633a Trace Elements in Coal Fly Ash and SRM 1648a Urban Particulate Matter (both: National Institute of Standards and Technology) were used. For preparation, a small amount (less than 1 mm^3) of each dry sample and several drops of deionized water were spread on individual glass slides. After drying at 87 °C on the heating plate, the samples were embedded and covered similarly to the spider webs.

In addition, selected spider webs and mosses were examined with the scanning electron microscope (SEM) ULTRA PLUS (Carl Zeiss Microscopy GmbH, available at Institute of Geosciences, Friedrich Schiller University Jena) with a magnification of 900X to 25,000X. Images were captured with the SE2 detector and qualitative detection of Al, C, Ca, Cr, Cu, Fe, K, Mg, Na, O and Si was performed using the QUANTAX EDX system with a Xflash® 5010 detector (Bruker Corporation). Metal sample holders were equipped with carbon carrier material and for the spider webs a silicon carrier was added to parts of the sample holder. Moss shoots of some millimeters length were teared off the exposed moss and placed on the prepared sample

holders while spider webs were collected directly on the sample holders in the field. The samples were dried overnight (40 °C) and coated with 10 nm of carbon using the coating system Leica EM ACE600 (Leica Microsystems GmbH) and the associated carbon thread prior to imaging.

3.5 Quality assurance

The term quality assurance covers all actions that lead to information on quality and errors of the analytical findings (SCHWEDT et al. 2016). This is crucial to assess the reliability of the results and potentially adapt steps of the analytical process. A full quality assurance includes all steps of the analytical process from sampling to reporting of the results. It focuses mainly on influences of sample matrix, calibration and blank values as well as recovery, precision and accuracy. Only steps of the internal quality assurance were regarded in this work. Formally, internal quality assurance includes provision/revision of problem-oriented calibration, blank values, multiple determinations, recovery and analysis of reference materials (SCHWEDT et al. 2016). Calibrations for ICP-OES and ICP-MS are described in chapter 3.3. During each aqua regia digestion two blank samples were generated, filling the digestion vessels only with the acids and processing these in the same way as the other (twelve) samples. Each digestion solution was measured threefold during ICP-OES and ICP-MS. Measurement results are therefore mean values of these three measurements. Due to low sample weights, especially for spider webs and long-term deposits, multiple determinations (including also the digestion step) were not possible for the majority of the samples.

To calculate recovery rates representative for as many sample materials as possible, different reference materials were digested with aqua regia and analyzed according to the procedure described above. Standard reference material (SRM) 1648a Urban Particulate Matter (National Institute of Standards and Technology) has been chosen, as urban dust particles are of major interest in this work. In addition, SRM 1633a Trace Elements in Coal Fly Ash (National Institute of Standards and Technology) has been analyzed to include a fossil fuel combustion product. As representative for geogenic, soil-like material SOIL-7 Trace Elements in Soil (International Atomic Energy Agency) and BCR-146 sewage sludge from industrial origin (Community Bureau of Reference, European Commission) were chosen. In addition, two plant materials were analyzed that are expected to show similar recoveries as moss material: SRM 1575 Pine Needles (National Institute of Standards and Technology) and IPE 952 Grass mixture (Wageningen Evaluating Programs for Analytical Laboratories). For all materials recovery rates were calculated, relating the contents determined to the certified contents.

A reference material for spider webs was not available and the long-term deposits collected were expected to consist of different biological, geological and anthropogenic materials. Therefore, recovery rates were also calculated relating the contents after aqua regia digestion to those after total digestion for all sample materials. As especially for biological materials the results for some elements varied, outliers according to DIXON (1951, P = 99%) were removed prior to the calculation of mean recovery rates.

3.6 Data analysis

Data analysis has been performed using different software tools. Basic calculations like data pre-treatment, descriptive statistics and the calculation of correlation coefficients and enrichment factors (EFs) were performed with MS Excel (version 2010, Microsoft Corporation). Multivariate statistical methods were applied to cope with the large number of both element contents and samples regarded in this work and to take the multivariate structure of the data sets into account. For example, the data set of 28 selected element contents in 265 spider web samples from Jena (chapter 6) is the biggest one with 7,420 individual pieces of information. The software R (version 3.6.0) in combination with RStudio® (version 1.1.453) was used for multivariate statistics and most of the plots. Besides from basic packages, the packages ellipse, ggplot2, MASS, psych, scales and sfsmisc were used. A quick overview on the data prior to multivariate evaluation as well as some classification models have been done with PLS_Toolbox (version 8.7, Eigenvector Research).

3.6.1 Data pre-treatment and descriptive statistics

Prior to data analysis, values below the LOD were replaced by a random value between zero and the LOD. Elements with more than 5% of values below LOD were excluded from further examination. In case of the comparison of spider webs and moss bags (chapter 5) this has been set to 10% due to the low number of samples (n) for each sample material. Those two steps were performed for each subset of data for evaluation separately, leading to slightly different sets of variables. As lanthanides are known to behave similar to each other and are highly correlated in the data sets analyzed, only La as a representative has been included in detailed data analysis (e.g. SUZUKI et al. 2011). Otherwise, their high number and strong correlations might dominate the multivariate statistical analysis without adding further information. In addition, Sc was left out due to analytical problems that arose for materials with a high content of organic carbon and nitrogen and were ascribed to isobaric interferences of $^{45}Sc^{+}$ with $^{12}C^{16}O_2{}^{1}H^{+}$ and $^{14}N_2{}^{16}O^{1}H^{+}$ (MAY and WIEDMEYER 1998).

Data sets were tested for outliers either according to GRUBBS ($n > 30$, $P = 99\%$, 1969) or to DIXON ($n \leq 30$, $P = 99\%$, 1951). Outliers were removed for descriptive statistics and calculations of enrichment factors, but not for multivariate analysis. Statistical parameters were calculated for each element and the data was tested for normal distribution according to DAVID et al. ($P = 99\%$, 1954). As not all elements are normally distributed, robust statistical methods (methods that are less affected by non-normal distributions and outliers, e.g. using the median instead of the mean) were used for further data analysis whenever possible.

Prior to multivariate data analysis (cluster analysis, factor analysis and classification methods), data sets were autoscaled to give equal importance to all elements, independent from the order of magnitude of their contents. The autoscaled value z_{ij} of variable i in sample/object $_j$ is calculated according to the following formula

$$z_{ij} = \frac{x_{ij} - \bar{x_j}}{s_j} \tag{3-1}$$

with x_{ij}: content of variable i in sample j, $\bar{x_j}$: mean of all samples j at variable i and s_j: standard deviation of all samples j at variable i (EINAX et al. 1997).

3.6.2 Patterns of elements, enrichment factors and element correlations

Enrichment factors were calculated to assess a potential anthropogenic impact on PM. They compare contents in a sample with estimated average contents in the upper continental crust (UCC), the latter of which is regarded as a reference for geogenic/natural dust. In addition, a normalizing element is applied, that is expected to be derived only or mainly from natural sources. In this work, Al was used as normalizing element. It is a typical component of many rock-forming minerals and highest contents of Al in all sample materials regarded in this work were found in loess and soil samples (SALMINEN et al. 2005). EF_{Al} of an individual element I in a sample was calculated using element contents (c) in the sample and contents in the upper continental crust (WEDEPOHL 1995) as given in the following formula.

$$EF_{i,Al} = \frac{\left({}^{c_i}/_{c_{Al}}\right)_{sample}}{\left({}^{c_i}/_{c_{Al}}\right)_{UCC}} \tag{3-2}$$

Contents in UCC were determined with a variety of analytical methods, but mainly X-ray fluorescence has been used (WEDEPOHL 1995). Therefore, values for UCC are regarded as total contents. This has to be kept in mind when examining EFs, as in this work contents in the samples were determined after aqua regia digestion, not leading to total contents for some elements (chapter 3.7). EFs have been applied frequently in studies working on PM, street dust or biomonitoring methods (e.g. DE PAULA et al. 2015; MEGIDO et al. 2017; ZHENG et al. 2004). The level of the enrichment factor allows for an easy assessment if a sample is influenced by anthropogenic PM. Every author has set slightly different limits for EF to evaluate whether the dust regarded is of rather natural or anthropogenic origin. In this work, limits set by ENAMORADO-BÁEZ et al. (2015), RAGOSTA et al. (2008) and ZHU et al. (2015) are combined: EFs below five indicate a mainly natural origin and EFs above ten a mainly anthropogenic one. In between, a mixed origin is assumed (see e.g. Fig. 6-1). Similar to this work, the named authors did perform wet chemical digestions without HF (using HNO_3 or HNO_3 and H_2O_2), followed by ICP-MS or atomic absorption spectroscopy.

For the simple visualisation and optical assessment of element patterns in chapter 4.3, element contents are only divided by the respective contents in the upper continental crust, yielding normalized contents without using an additional normalizing element like Al (see e.g. Fig. 4-5).

To evaluate not only individual elements but also relations between elements, Spearman rank correlation coefficients were calculated. It is expected that combined elements with a high correlation hint to a potential source of PM, as in general the (metal) composition of PM is

source specific (FURUSJÖ et al. 2007). Some correlations of elements are known from the literature, e.g. the correlation of Cu and Sb that is typical for brake wear and a correlation of Co, Ni and V that is linked to oil combustion (JOHANSSON et al. 2009; KULKARNI et al. 2006). Correlations of elements found in the present study were compared to those found in the literature to get a first impression on potential sources of PM (e.g. chapter 5.3.4).

3.6.3 Cluster analysis

For several data sets, cluster analyses were calculated in the object space, meaning that the resulting dendrograms show groupings of elements. Cluster analysis is a method of unsupervised pattern recognition that is often performed as the first step of multivariate analysis to detect and visualise structures in data sets (EINAX et al. 1998; WISE et al. 2006). In the present case, a hierarchical, agglomerative method was used: At the beginning, each sample is regarded as a single cluster. Distances between all clusters are calculated and samples/clusters with the shortest distance are linked together (DU TOIT et al. 1986). This is repeated until all samples are merged in one cluster. Results are often depicted in a dendrogram, which can easily be assessed optically (WISE et al. 2006). It visualises the clustering and shows relative distances at which the (sub-)clusters are merged.

Methods of cluster analysis are characterized by how the distance is calculated and how the clusters are merged together (DANZER et al. 2001). For merging, Ward's algorithm was used. It forms clusters with a minimal increase of the within-group error sum of squares and is typically used for environmental data (e.g. DAVID et al. 2011; KÖTSCHAU et al. 2014). The algorithm leads to clear structures and stable clusters (EINAX et al. 1998). A cluster is regarded as stable if over a long range of relative distance in the dendrogram no further objects/variables are added to it. In the present case, squared Euclidean distances, that are typicall combined with Ward's algorithm, were applied. Broad differences are stressed with this distance measure, being calculated according to the following formula

$$d_{jk} = (x_j - x_k)(x_j - x_k)^T \tag{3-3}$$

with d_{jk}: distance between samples/clusters j and k, x_j and x_k: vectors of variables/element contents for samples j and k (WISE et al. 2006). Further information on cluster analysis can be found for example in DANZER et al. (2001) and WISE et al. (2006).

3.6.4 Factor analysis and principal component analysis

Factor analysis (FA) and principal component analysis (PCA) are another type of unsupervised learning to detect and visualise (hidden) structures in a data set (DANZER et al. 2001). Both methods focus on relations between variables and objects and are mathematically very similar to each other (SKRBIĆ and DURISIĆ-MLADENOVIĆ 2010). In environmental sciences, FA and PCA are often applied to detect sources of contamination, which is also an aim of the present work (e.g. EINAX et al. 1998; PRAVEENA et al. 2012).

The basic idea is that variations and relationships in a data set with correlated variables can be explained by weighted underlying factors/principal components (PCs) and, in case of the factor analysis, a residual error (YEOMANS and GOLDER 1982). Fig. 3-8 shows a matrix representation of the basic principle of FA. Mathematically, factors are linear combinations of the original variables. The model ($\mathbf{TP}^T$) of all factors (R) aims at maximizing the proportion of the variance in the original data set ($\mathbf{X}$) explained by the model (BRO and SMILDE 2014). In PCA, all variation is expected to be derived from common features (PCs). The matrix representation is similar to the one of FA, leaving out the matrix of the residuals. In FA factors do only explain common (shared) variance of the variables and residuals are specific for each variable (MANLY 2000). As a result of FA/PCA, matrices of scores and loadings are reported (BRO and SMILDE 2014). The loadings describe what a factor/PC represents – in case of the current work they hopefully describe sources of PM – while the scores describe which objects have a similar response.

As it can also be seen from Fig. 3-8, FA and PCA can be used to reduce dimensions ($R < I$). For elements with similar properties according to the samples, most of the variance of the data set is usually explained by the first few factors/PCs (MANLY 2000). This small number of latent factors/PCs allows for an easier interpretation than the original data set (PRAVEENA et al. 2012). There are several criteria that can be used to select the number of factors/PCs to be extracted. Most of them are based on the fact that FA and PCA are calculated by solving an eigenvalue problem. Criteria that were applied in this work are the scree-plot, the Kaiser-Guttman criterion (only factors/PCs with an eigenvalue greater than unity are extracted) and a high fraction of variance explained by the model (BRO and SMILDE 2014, EINAX et al. 1997; YEOMANS and GOLDER 1982). For FA, the model can also be rotated to faciliate its interpretation (WOLD et al. 1987). A rotation frequently used is for example the varimax rotation that yields factors with high loadings of only a few variables while all other loadings are close to zero (e.g. BAGUR et al. 2009; PRAVEENA et al. 2012; WEIß 2009).

Factor analyses in this work were performed according to the following procedure: First, the data set was subjected to PCA (using R), extracting all PCs possible as a basis for the selection of factors to be extracted. The number of relevant factors was selected based on a mixture of the criteria named above. Afterwards, a FA model with the selected number of factors and a varimax rotation was calculated for interpretation (using R). For the detailed FA in chapter 6.3, outliers were detected and removed prior to the procedure: PCAs were calculated for all relevant numbers of PCs to search for outliers (using PLS_Toolbox). They were detected by searching for objects with high Hotelling's T^2 (high leverage) and a high sum of squared residuals (Q residuals). More details on those measures as well as on FA and PCA in general can be found for example in BRO and SMILDE (2014).

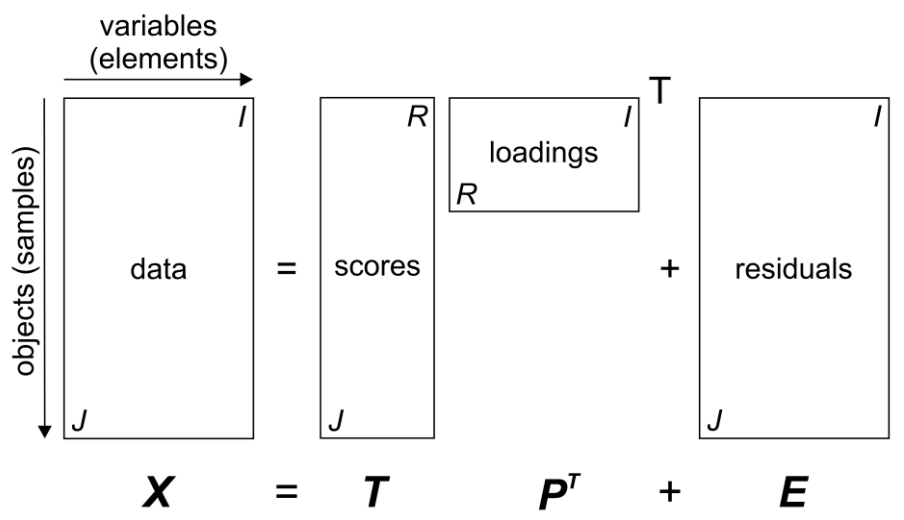

Fig. 3-8: Principle of factor analysis: The data set **X**, containing *J* objects and *I* variables, is described by factor scores **T** and factor loadings **P** of *R* factors, explaining the joint variance of the variables ($\mathbf{TP}^T$: factor analysis model), as well as residuals **E**.

3.6.5 Classification

Classification aims at sorting samples into given groups/classes. It leads to the qualitative response of class membership of a sample based on the set of variables measured for the sample (BALLABIO and TODESCHINI 2009). Classification models are built using a training set of data containing samples with known class membership and the corresponding variables measured. As class memberships of samples in the training set are given, classification belongs to the group of supervised pattern recognition techniques (WISE et al. 2006). The quality of a classification model is normally judged by rates of correct or false classification. Typical approaches to determine those rates are reclassification and cross-validation (DANZER et al. 2001). In reclassification, samples used to calculate the model are classified (reclassified) with the model. This does often lead to unreasonably low rates of false classification. A more realistic estimation of the quality of the model can be gained with cross-validation. The data set is divided into a training set for model calculation and a test set of samples to be classified. A typical split used also in the present work is 90% (training set) to 10% (test set). The split is repeated until every sample has been part of a test set once and rates of correct classification are determined for all test sets in total.

There are various approaches to calculate a classification model. In this work, linear discriminant analysis (LDA) was used most often. Similar to PCA it is calculated by solving an eigenvalue problem. The resulting model consists of discriminant functions with discriminant variables that are linear combinations of the original variables (MANLY 2000). The difference from PCA is the aim of the model which comes into effect in the input matrix of the eigenvalue problem. While PCA describes variation in the data set, LDA aims at a good separation of classes (DANZER et al. 2001). For this purpose, variance of the data set is split into variance between classes and variance within classes and the ratio between them (between-class-variance/within-class-variance) is maximized (EINAX et al. 1997; MANLY 2000). Anoth-

er method used to evaluate spider web samples is partial least squares-discriminant analysis (PLS-DA). As the name says, it calculates a PLS model that predicts the class number for each sample (WISE et al. 2006). In addition, usually a number of latent variables to retain in the model are chosen. Overall, PLS-DA is quite similar to LDA but includes advantages of PLS, mainly noise reduction and variable selection (WISE et al. 2006). Further information on PLS can be found for example in WOLD et al. (2001).

Other classification methods tested for the spider web data set in chapter 6.4 are k-nearest neighbours classification (kNN) and soft independent method of class analogy (SIMCA). In kNN, samples are grouped into the class of the nearest neighbour(s). Normally an odd number of neighbours is chosen (WISE et al. 2006). The method is non-parametric and can solve multiclass-problems, but kNN is very sensitive to the distance metric applied (BALLABIO and TODESCHINI 2009). In SIMCA every class is modeled individually by calculating a specific PCA model for every class. Thus, SIMCA describes the variation (which variables are responsible for the separation) and does a classification (WISE et al. 2006). Detailed information on all methods can be found for example in BALLABIO and TODESCHINI (2009).

For the evaluation of spider webs from 22 locations in Jena (chapter 6), all four models described were tested using PLS_Toolbox. Best rates of correct classification were found for LDA and PLS-DA, which were regarded in more detail. LDA models for evaluation were calculated with R and PLS-DA models were calculated in PLS_Toolbox, using the number of latent variables that has been chosen for FA of the same data set (chapter 6.3). For the comparison of different sample materials in chapter 7 LDA models were calculated with R.

3.7 Results of the quality assurance

Recovery rates were calculated for all elements certified in the respective reference materials (appendix Tab. A-9). As expected for plant materials, good rates (85% or higher) were found for almost all elements in the biological reference materials (SRM 1575, IPE 952) and the other rates are not substantially lower (≥ 70%). For IPE 952, rates substantially higher than 100% were found for Cd and Sb. As the material and the certificate are rather old (17 years), the certified values for the two elements might not be accurate and a contamination of the material by a former user cannot be ruled out completely. Only 60% of the recovery rates for soil-like reference materials SOIL-7 and BCR-146 are good. Remarkably low values were found for Al, Cu (only SOIL-7), Hf, K, Na, Si, Tb, Ti, U, Y, Yb and Zr. Most of the low recovery rates can be explained by the existence of silicate material that can usually not be dissolved completely by aqua regia in the reference materials (ENAMORADO-BÁEZ et al. 2013; STERNBECK et al. 2002). Al, K, Na and Si for example occur as parts of silicates like feldspar. Ti, which can be replaced by Hf and Zr, occurs in silicates like sphene and as an accessory element in pyroxene, amphibole, mica and garnet (SALMINEN et al. 2005).

For urban particulate matter (SRM 1648a), a lower number of good recovery rates (≥ 85%) was found. This corresponds to explanations given by LUMPP et al. (2012) who found that

matrices of real dust samples are often less critical than NIST 1648(a). As for soil-like materials, low rates were found for elements occuring in silicates (Al, Ce, K, Na, Rb and Ti). Also Cr, which cannot be dissolved if it occurs as chromite ($FeCr_2O_4$, SALMINEN et al. 2005), has a low rate. Reduced but not especially low values (≥ 70%) were found for elements that are expected to be derived to a large extent from anthropogenic sources (Co, Cu, Ni, Sr and V). A possible reason for that might be heat exposure, changing some particles to a non-soluble form prior to the deposition: Either the material was heated during production (e.g. Co, Ni as part of steel alloys), or the particles were heated during emission, like V from oil burning (AKINLUA et al. 2008; JOHANSSON et al. 2009). This complies with the results for SRM 1633a. For this coal fly ash (subjected to heat exposure during formation) only recovery rates that are substantially lower than 85% were found.

To take into account all sample materials regarded in this work, recovery rates were also calculated relating contents determined after aqua regia digestion to contents determined after total digestion of the same sample (appendix Tab. A-10). At first glance, it can be noticed that the standard deviations of these rates are higher than those for the rates calculated for reference materials. A slight increase is to be expected as the contents determined after total digestion were determined for each sample individually, while certified values for the reference materials (appendix Tab. A-11) are the same for each calculation. However, standard deviations above 15% or even 20% were found for some elements, mainly for spider webs. A reason might be heterogeneity of the spider web samples that could not be homogenized while reference materials are thoroughly homogenized powders. Samples that were subjected to both aqua regia and total digestion had to be split, even though they could not be homogenized totally. As most of the samples were digested as a whole, this is expected to be of minor influence for most of the samples.

Comparing contents after aqua regia digestion with contents after total digestion, good recovery rates (85% and higher) for all materials were found for Ca, Cu, Fe, Mn, Mo, P and Zn. Rates a little lower or a little more variable but still acceptable (≥ 70%) were found for Ce, Co, Eu, La, Mg, Ni, Pb, Sb, Sm, Th and V. A decrease of recovery rates from light to heavy rare earth elements (REE) shows that heavy REE are less soluble in aqua regia than light REE, which has also been described for natural conditions by DOŁĘGOWSKA et al. (2017). Al, Hf, Nb, Rb, Ti, U, Y, Yb and Zr show substantially low rates for all materials (except for Al, Rb and Y in moss bags). They are again plausible due to the presence of silicate material in the samples, either as key component (soil, loess, probably dust from windows) or as geogenic dust particles entrapped in biological material (spider webs, mosses). All elements have been named by SALMINEN et al. (2005) as elements that are part of silicate minerals or occur at trace level in rock-forming minerals.

For some elements, recovery rates are quite different (difference of more than 30%) for different sample materials. For Ba, Cd, K, Na, Nb, Nd, Pr, Sn, Sr, Ti and W the rates are lowest for soil and/or loess and higher for biological materials while for Cs and Li low rates were

found for biological materials. This indicates an occurrence of the elements in different binding states or phases, likely due to different sources. Ba for example can be derived from different anthropogenic sources (ENAMORADO-BÁEZ et al. 2015; SUVARAPU and BAEK 2017). Corresponding particles might be captured by spider webs and mosses, while the occurrence of Ba in soil and loess is driven by geogenic processes. Another example is K. In soil and loess it occurs mainly in insoluble silicates while it is a major plant nutrient and occurs in mosses in an easily soluble form (SCHEFFER and SCHACHTSCHABEL 2010; SCHUBERT 2006).

Overall, high recovery rates for biological reference materials demonstrate that the determination of element contents with ICP-OES and ICP-MS as performed in this project works well. Lower recovery rates for some elements in other reference materials show that aqua regia digestion does not lead to a total digestion of all components of the samples. Recovery rates calculated relating contents after aqua regia digestion to contents after total digestion reinforce these findings. While for 15 out of 41 elements the recovery rates for different sample materials are close to each other (difference of 20% or less: Ca, Co, Cu, Dy, Fe, Hf, Mg, Mn, Mo, P, U, V, Yb, Zn, Zr), 13 elements have substantially different rates for different materials (difference of more than 30%: Ba, Cd, Cs, K, Li, Na, Nb, Nd, Pr, Sn, Sr, Ti, W). Those variable rates hint to matrix-dependent binding forms in the different sample materials. Contents determined thus cannot be compared directly for different sample materials but rather element ratios, patterns or correlations should be compared. With regard to source identification, one has to keep in mind that with those measures a quantification of the amount of PM from the corresponding source(s) will not be possible.

4 Optical impressions and element patterns in different sample materials

In the course of this work, sample materials with different textures and chemical matrices were regarded. Especially for biological sample materials, differences in structure, surface and capture of particles can be seen on microscopic images (chapter 4.1). With regard to the bulk chemical matrix, some samples consist mainly of biological material while others likely consist of "pure" dust particles. To further take into account this chemical matrix, the carbon content in different sample materials is assessed (chapter 4.2).

As a potential first step towards the identification of sources of PM element patterns play an important role. Elements co-occuring in the same samples are likely derived from the same source. Therefore, element patterns of the different sample materials are regarded (chapter 4.3), comparing them also to patterns of samples that are expected to represent source terms.

4.1 Microscopic images of selected sample materials

Microscopic images of particles can supply a first indication on where individual particles are derived from (e.g. WEINBRUCH et al. 2014). Therefore, images of selected samples as well as materials representing source terms were captured with a digital microscope. To get an impression on potential appearances, materials representing different source terms have been examined first (see Fig. 4-1).

Loess (a) is regarded as an example for geogenic dust. It is characterized by translucent, angular minerogenic particles that are in the size range of coarse PM (coarse silt to fine sand particles, PYE 1987). Anthropogenic particles (b-f) on the other hand are often dark and cover a broad size range. Larger particles of tens to hundreds of micrometers might also be agglomerates formed when the particles were suspended in air, preferentially under wet conditions (STERNBECK et al. 2002). Brake wear material (b) is characterized by dark flakes without any preferential shape. The samples brushed off from exhaust pipes (representing exhaust emissions) are different for gasoline and diesel cars (c, d). For both of them, soot/exhaust particles are dark and likely agglomerate. In direct comparison, more particles and many small ones can be found in the exhaust pipes of diesel cars than in the ones of gasoline cars. Those particles might be (black) carbon either from fuel that did not burn down completely or from lubricants. This is in accordance with the report of the WHO, that names traffic as a major source of black carbon (WHO 2013). Big minerogenic particles that can be found in material from gasoline cars might have ended up in the exhaust pipes by resuspension of geogenic dust lying on the road, and direct deposit in the exhaust pipes depending on the routes of the individual cars (FURUSJÖ et al. 2007).

SRM 1648a Urban Particulate Matter (e) contains many dark, anthropogenic coarse and fine particles. Some of them are likely carbonaceous particles, as the corresponding certificate names a total carbon content of 12.7% and an organic carbon content of 10.5%. GÓRKA et al. (2018) did also identify a majority of the particles on SEM images of urban spider webs as

either organic and/or soot particles. The inorganic carbon content in SRM 1648a might be carbonate particles not visible on the image in (e), derived from the surroundings of St. Louis, Missouri, where the SRM 1648a material was sampled. According to the United States Geological Survey (USGS), sedimentary rocks containing carbonates like limestone occur in this area (USGS 1997). Dark, spherical particles are expected to be derived from burning processes, more specific from fossil fuel burning (GONZÁLEZ et al. 2016). The high abundance of dark, spherical particles in SRM 1633a Trace Elements in Coal Fly Ash (f) supports this assumption. Bigger particles are again expected to be agglomerates of either round or flaky anthropogenic particles (e.g. from tyre wear or exhaust emissions). In addition, some big, biogenic particles can be found in SRM 1648a. Due to their size, shape and composition they might be pollen or plant seeds.

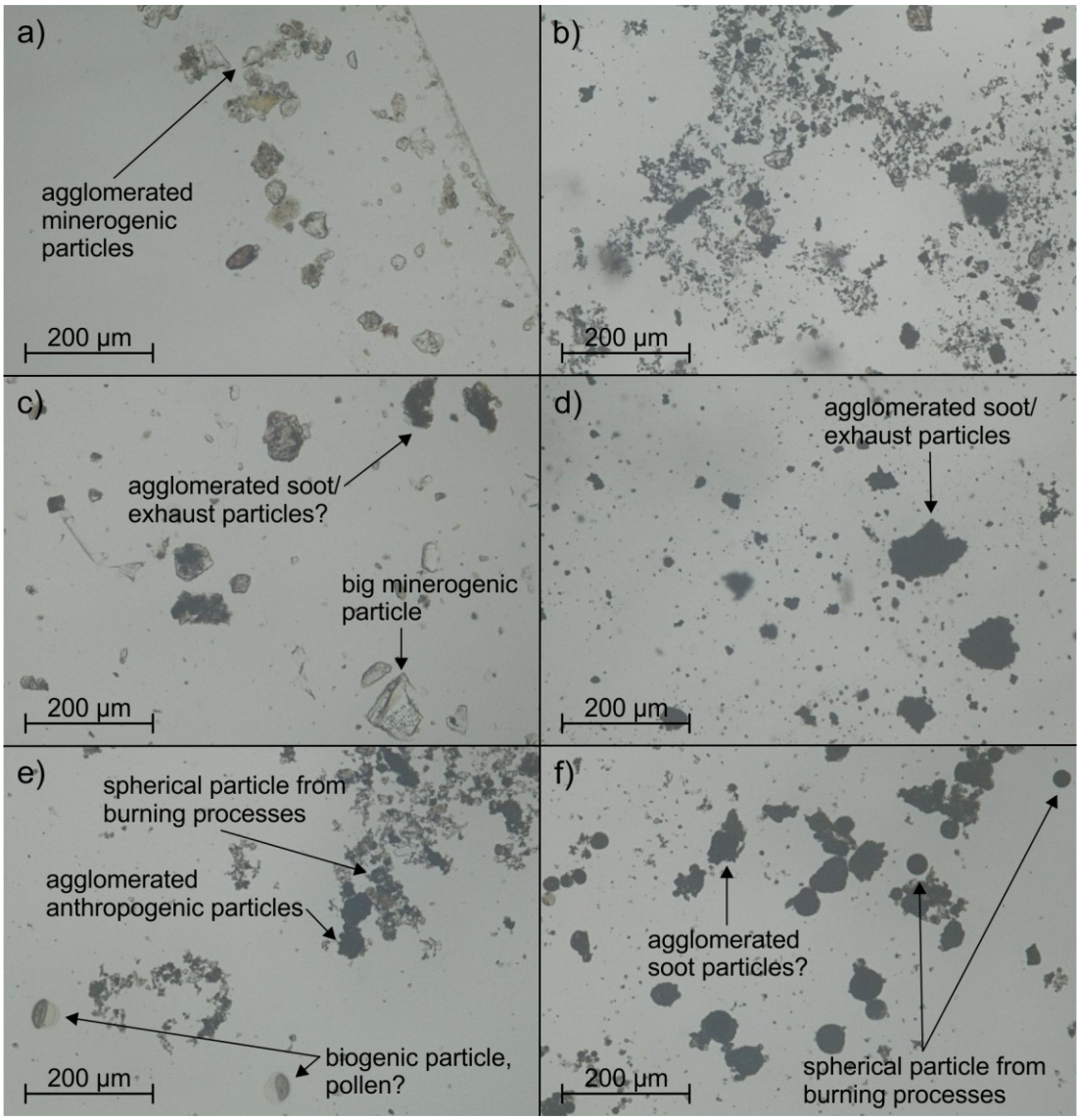

Fig. 4-1: Images of materials representing potential sources of PM taken with the digital microscope. a) loess, b) brake wear, c) exhaust particles (gasoline car), d) exhaust particles (diesel car), e) SRM 1648a Urban Particulate Matter, f) SRM 1633a Trace Elements in Coal Fly Ash.

Microscopic images of spider web and moss bag samples have been recorded to get an impression on how and which PM is captured by biomonitoring materials (appendix Fig. A-1). They are shown and discussed in detail also in chapter 5.3.1. Overall, spider webs can be zoomed in and focused better than mosses due to their planar structure and lower amount of biomass. Wheel webs exhibit a characteristic structure (Fig. A-1a) with a stable radial thread and a more flexible spiral thread with sticky droplets to capture prey (DAS et al. 2017). Particles attach preferentially to these droplets (c, e) while they do not seem to attach to a preferential place on the moss surface (d, f). Different types of particles captured by spider webs and moss bags can be seen and identified by comparing them to the images in Fig. 4-1: Coarse, translucent, angular particles are identified as minerogenic particles while small, dark particles are identified as being derived from anthropogenic sources. Translucent but rounded particles that can only be seen on the spider webs are thought to be biogenic particles. As the webs were sampled at the beginning of September, those might be plant seeds rather than pollen. Presumably biogenic particles are also captured by moss bags but cannot be distinguished from the moss material itself.

To realize a higher resolution and zoom as well as to analyze element contents in particles SEM images were captured. Single particles on spider webs and mosses from moss bags were examined (see Fig. 4-2). Measurements had to be taken more carefully than for example measurements of rock samples as mosses suffered from electrostatic charge and some spider webs ripped during EDX measurements. Due to the great number of particles, only selected individual particles were imaged with SEM. The results give an impression on the particles but might not cover all particle types (including also rare ones) that can be found.

Coarse particles (a-d) are often angular or even exhibit a prismatic, crystal-like shape (c). They contain elements that are typical for (alumo-)silicates (Al, O, Si and selected alkali and alkaline earth metals) or dolomite (Ca, Mg, O), both of which can be found in the surroundings of Jena (HOLLEMAN et al. 2007; SEIDEL 1993). The prismatic shape of Ca- and Si-based particles on SEM images has also been named by GONZÁLEZ et al. (2016). Those particles are identified as eroded geogenic particles. In accordance with this, GIERÉ and QUEROL (2010) described coarse particles as being mainly dust from mechanical processes, one of which is erosion of natural particles. The rhombohedral crystal shape in c) is typical for calcite and dolomite, containing Ca, Mg and O (OKRUSCH and MATTHES 2010). Agglomerates of fine particles (e, f) and single fine particles (g, h) do often contain Fe and O but no (other) elements typical for natural dust. Therefore, they are identified as anthropogenic particles. A preferential occurrence of anthropogenic particles in the fine fraction has also been named in other studies (e.g. DONGARRÀ et al. 2007; YADAV and RAJAMANI 2006). Further particles analyzed exhibit similar characteristics but in total more geogenic than anthropogenic particles were found.

Conclusion: Overall, three main groups of particles are present in the samples: Geogenic, translucent, angular/prismatic particles (identified by typical elements like Al, Ca, Mg, O, Si)

occur to a great extent in all biomonitoring samples and are in the size range of coarse PM. Other coarse particles, that could only be found on spider webs with the digital microscope, are biogenic particles like pollen or plant seeds. In contrast, fine particles (< 2.5 µm) are mainly anthropogenic, dark ones containing for example Fe and O. Potentially, they can also contain (black) carbon. Except for spherical particles from burning processes (URBAT et al. 2004), the group of anthropogenic particles could not be split up further with the microscopic methods presented.

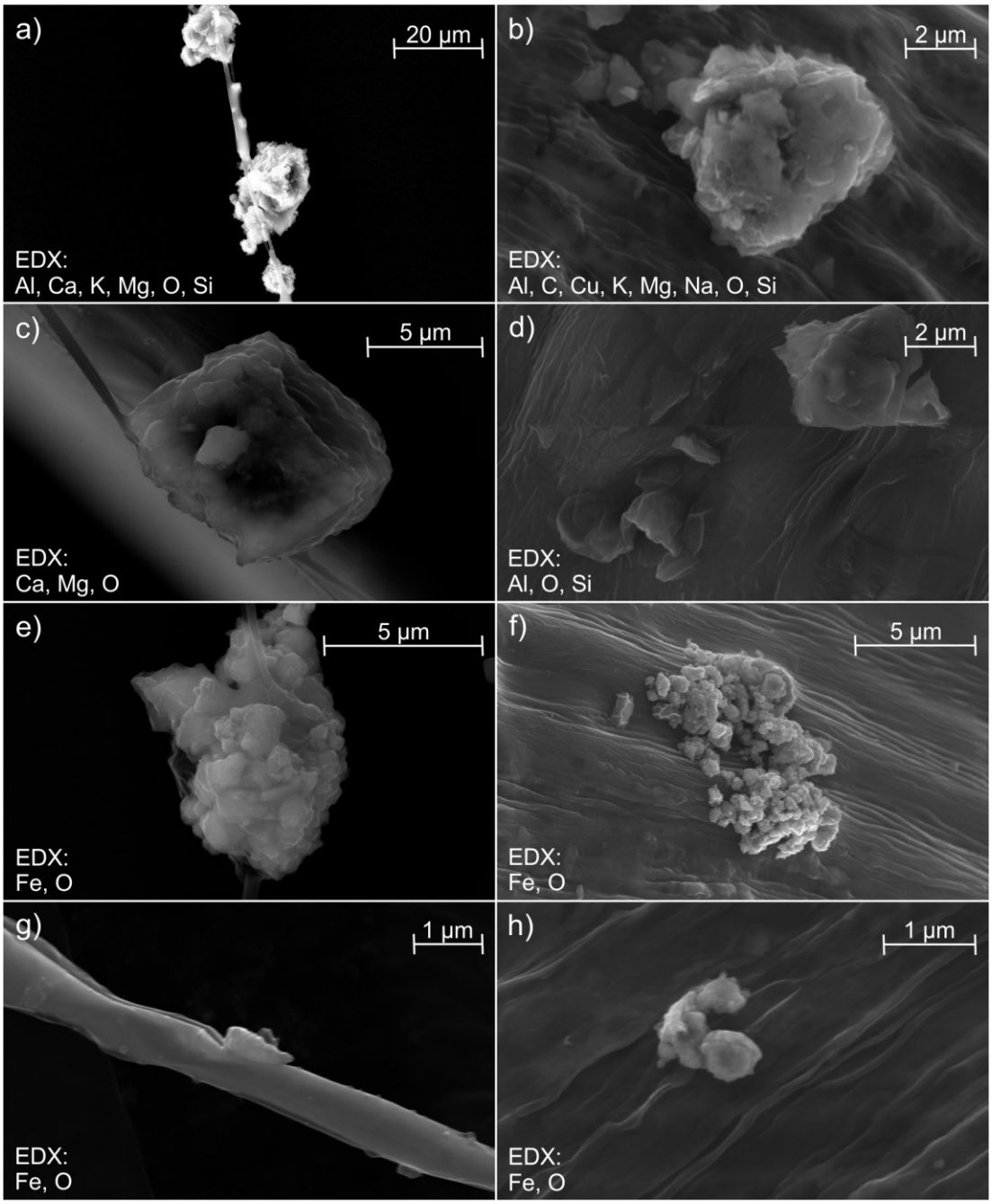

Fig. 4-2: SEM images (SE2 detector) of individual particles on spider webs (a, c, e, g) and mosses (b, d, f, h). Elements detected in the particles with the EDX system are named in the respective images. a)-d) coarse minerogenic particles/agglomerates of minerogenic particles like silicates, alumosilicates or dolomite, e)-h) fine individual or agglomerated particles of rather anthropogenic origin containing Fe and O.

4.2 Organic carbon as a potential variable to correct diluting effects of the biomass in selected sample materials

The sample materials regarded in this work exhibit different matrices/main constituents. This can be seen for example in Fig. 4-3, showing contents of C_{org} in the different sample materials as well as in SRM 1648a as an example for urban PM. Comparably low amounts of C_{org} can be found for loess, agricultural soil and dust from windows. This is in the expected range for loess and agricultural soil with values considerably lower than 50 mg/g (FLESSA et al. 2000; LOELL et al. 2011). For dust from windows low contents of C_{org} hint to a high amount of geogenic particles. Much higher amounts of C_{org} can be found for long-term deposit, moss bags and spider web samples, while SRM 1648a exhibits intermediate values.

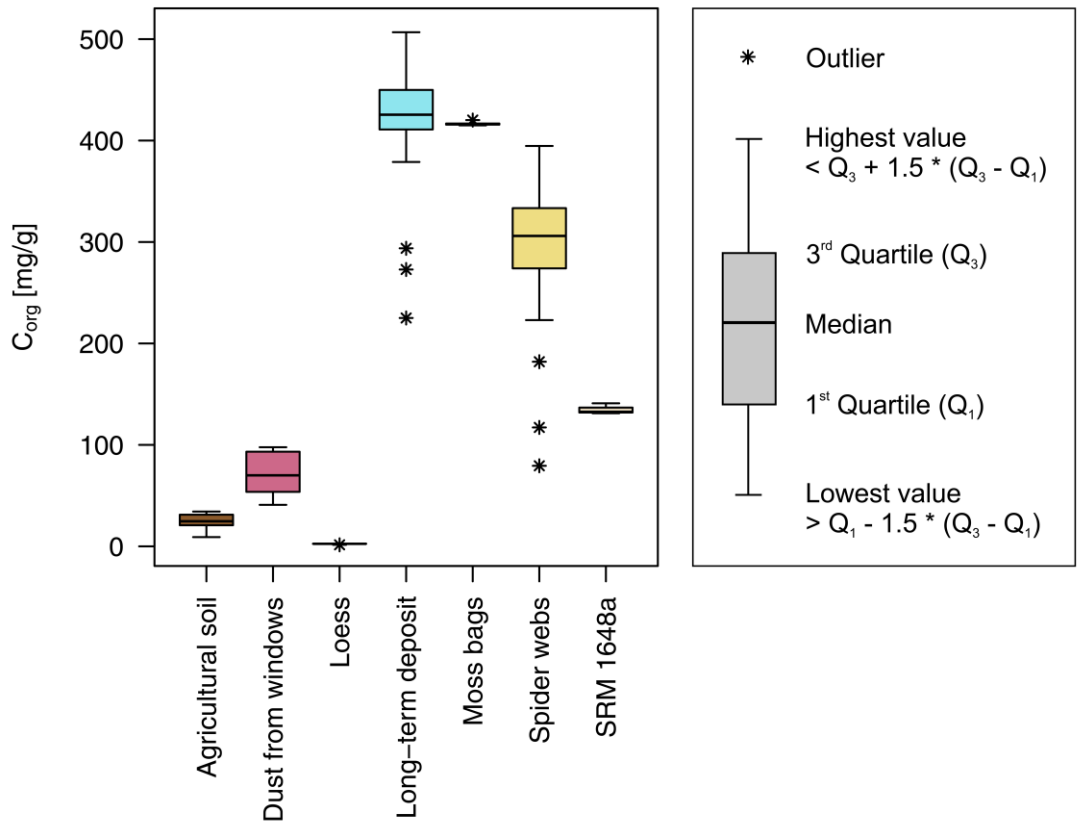

Fig. 4-3: Content of organic carbon in different sample materials: agricultural soil (number of samples (n) = 10), dust from windows (n = 10), loess (n = 5), long-term deposit (n = 23), moss bags (n = 6), spider webs (n = 25) and the reference material SRM 1648a Urban Particulate Matter (n = 3).

The values inherit a large variance for long-term deposit and spider web samples. For spider web samples this is expected to be due to the low weight of the webs themselves, leading to a high and flexible PM-to-total sample ratio. Different conditions of particle deposition might have influenced long-term deposit samples: Over the course of the year, a water head was often established inside the vessels. Algae growth and/or precipitation might have happened in the liquid phase, changing the composition of the subsequently dried sample material. Contents of C_{org} higher than the upper quartile for example were found in samples containing reddish or green flakes that might be precipitates and algae respectively.

The low variation for moss bags indicates that most of the C_{org} in moss bag samples is contained in the moss material and not in the particles collected on it during exposure to ambient air. Relatively consistent contents of C_{org} in the clean moss material can be expected as it consists of moss of only one species collected at a narrow spot.

C_{org} is expected to be directly connected to the amount of biomass in the samples, in particular for the two biomonitoring techniques applied. The biomass of spider webs and mosses acts as a carrier material for the dust particles, introducing a diluting effect. As an approach to correct for this effect and only compare (inorganic) dust particles, conversion factors (CFs) were calculated. They are multiplied with the measured content of an element to correct for either the content of C_{org} or the amount of biomass in the sample. If it is assumed that each sample does only consist of the sum of the elements determined and C_{org} or the biomass, the conversion factors can be calculated as indicated below.

$$CF_{C_{org}} = \frac{1}{1 - C_{org}\ [g/g]} \tag{4-1}$$

$$CF_{biomass} = \frac{1}{1 - biomass\ [g/g]} \tag{4-2}$$

The amount of biomass in the samples can be calculated from the amount of C_{org} using approximated sum formulas. This has been done for the two biomonitoring materials as well as for long-term deposit, whose high amount of C_{org} indicates a notable occurrence of biomass in the samples. For moss bag samples and long-term deposit the sum formula of cellulose $(C_6H_{10}O_5)_n$ has been applied while for spider webs $C_{3.38}H_{5.01}N_{1.06}O_{1.32}$ has been calculated from fractions of amino acid residues in spider silk named by WORK and YOUNG (1987). C_{org} is thus multiplied by 1.99 for spider webs and by 2.25 for moss bags and long-term deposit to yield the amount of biomass. In both formula 4-1 and 4-2 mean contents of C_{org} or the biomass were used for each sample material. Tab. 4-1 gives an overview of the conversion factors as well as the contents of C_{total} and C_{org} in the different materials. The higher measured content of C_{org} than of C_{total} in long-term deposit samples lies within the standard deviations of the two contents and is due to analytical uncertainties that were expected to amount to up to 10%.

To check for plausibility, the contents of trace elements were multiplied with the conversion factors and summed up. Fig. 4-4 shows this for the samples used to calculate the conversion factors. A noticeable change by applying CF_{Corg} can only be observed for long-term deposit, moss bags and spider webs, for which CF_{Corg} is substantially different from 1.0. The correction for biomass ($CF_{biomass}$) seems to be working well for moss bags and spider webs as, in contrast to the uncorrected ones, the summed corrected contents are in the same range. For long-term deposit the summed corrected contents show very high, implausible values that even exceed the limit of 1 g/g in some cases. Long-term deposit is possibly characterized by a

more complex composition of the biomass, including for example algea as described previously. This mixture cannot be described by the simple sum formula of cellulose.

Tab. 4-1: Content of C_{total} and C_{org} in different sample materials and conversion factors calculated from the latter to account for the dilution of dust particles by C_{org} or the biomass. Numbers with an asterisk were calculated leaving out an outlying value for C_{org}.

Sample material	Number of samples measured	C_{total} [mg/g] (measured)	C_{org} [mg/g] (measured)	Conversion factor C_{org}	Conversion factor biomass
Agricultural soil	10	45.2 ± 20.5	24.5 ± 7.9	1.0	-
Dust from windows	10	80.6 ± 22.0	71.2 ± 21.6	1.1	-
Loess	5	43.4 ± 31.3*	2.6 ± 0.1*	1.0*	-
Long-term deposit	23	404 ± 63.5	412 ± 66.0	1.7	13.9
Moss bags	6	429 ± 4.6	417 ± 1.8	1.7	16.1
Spider webs	25	301 ± 70.9	290 ± 75.4	1.4	2.4
SRM 1648a	3	139 ± 2.3	135 ± 5.3	1.2	-

Conclusion: Substantial amounts of biomass in the samples, diluting pure dust particles, lead to a high amount of C_{org} in spider webs, moss bags and long-term deposit samples. Factors to correct for this diluting effect were calculated from contents of C_{org} and theoretical sum formulas of the biomass. In general, those conversion factors seem to be working for the two biomonitoring methods. However, they do not work equally well for all materials and are not needed for geogenic materials like agricultural soil or loess. In addition, the uncertainty and variation of the determination of C_{org} is added to the uncertainty of the determination of trace element contents, leading to less reliable results. Therefore, only uncorrected contents are used in the following.

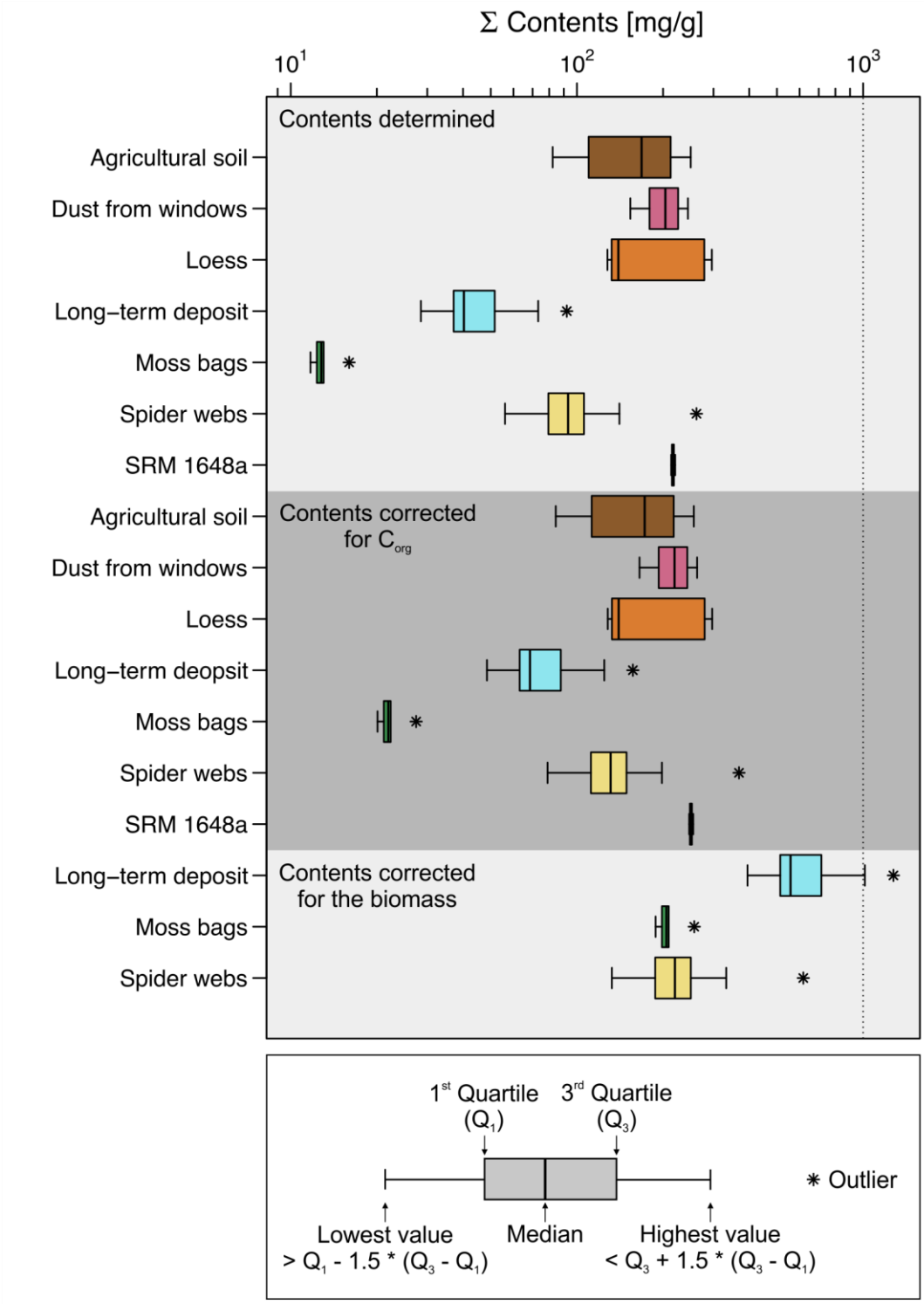

Fig. 4-4: Boxplot of the sum of 34 element contents measured in different sample materials, of contents corrected for C_{org} and of contents corrected for the biomass. The number of samples (n) varies according to the number of samples for which contents of C_{org} were determined: agricultural soil: n = 10, dust from windows: n = 10, loess: n = 5, long-term deposit: n = 23, moss bags: n = 6, spider webs: n = 25, SRM 1648a: n = 3.

4.3 Exemplary element patterns of samples and source terms

In this subsection, element contents in the different materials sampled to assess PM (spider webs, moss bags, dust from windows and long-term deposit) are evaluated with regard to

their levels, patterns and potential systematic differences between the sample materials. Overall, element contents are lowest in moss bags samples and highest in dust from windows. They range from 0.025 µg/g and 0.043 µg/g for Hf and Ag respectively in moss bags to 22,000 µg/g and 55,600 µg/g for Fe and Ca in dust from windows. This covers dimensions from ultra trace components (contents below 1 µg/g) to minor components (contents between 1 mg/g and 100 mg/g), but most of the contents are in the range of trace components (contents between 1 µg/g and 1,000 µg/g). Detailed numbers can be found in the appendix (Tab. A-12). Not all elements could be determined in all materials with less than 5% of the values below the LOD. Ag and As were excluded in the following as for at least two materials too many values are below the LOD. In addition, Hf, Nb and W were excluded since they were not determined in all samples.

Different levels of element contents can also be seen in the plot of median contents normalized to contents in UCC (WEDEPOHL 1995) in Fig. 4-5. They are expected to be due to the diluting effect of biological material in the samples: Values for moss bags (mainly biological material) are lowest, followed by spider web and long-term deposit samples (containing some biological material). Highest values can be found for dust from windows, that is expected to not be diluted by any biological material (except for potentially a few spores and pollen in the spring sampling campaign). As the overall element contents and patterns for spider web and long-term deposit samples are more similar to the pattern of dust from windows, which is regarded as a pure dust material, those materials might be more representative for dust samples than moss bags.

In general, element patterns look similar for all four materials. As different materials have been sampled at different locations, it might be assumed that the patterns reflect the background composition of PM in the sampling area. Median element contents therefore rather reflect homogeneously distributed PM from e.g. the geogenic background or diffusely distributed anthropogenic sources like domestic heating. Emissions from local sources are either rapidly dispersed in the air or only visible when regarding patterns of individual samples. Compared to UCC, all materials are depleted in alkali and alkaline earth metals as well as La, Th, Ti, U, Y and Zr due to the aqua regia digestion (chapter 3.7). To proof this, an optical comparison of element patterns and recovery rates can be found in the appendix (Fig. A-2). Readily soluble compounds containing alkali and alkaline earth metals have probably also been leached from dust particles on windows or mosses by rainfall. For other transition elements and p-block elements (except for Al, Si), recovery rates are around 100%. Patterns for those elements in Fig. 4-5 thus reflect dust samples without any effects from the digestion. Compared to other elements, e.g. an enrichment of Cu, Mo, Ni, Pb, S, Sb, Sn and Zn can be found.

The division by contents in UCC, yielding normalized contents, was done to allow for a more easy comparison of elements with contents of different orders of magnitude. Elements in this and all further similar plots are arranged according to the group they belong to in the period-

ic table and within this group ordered according to their molar weight, to reflect their chemical properties.

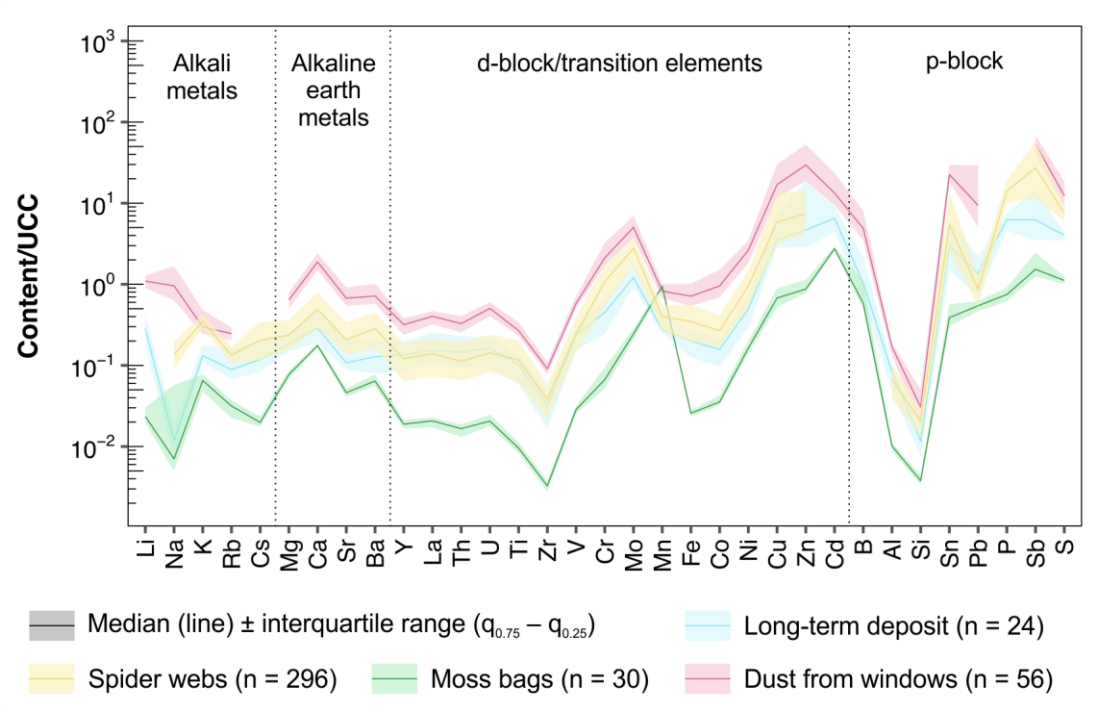

Fig. 4-5: Contents of elements determined in different sample materials divided by contents in the upper continental crust (UCC) given by WEDEPOHL (1995). All samples taken per sample material are aggregated except for moss bags, for which only the two campaigns of ten weeks of exposure time are aggregated. A dilution of dust particles by biological material is expected for all materials except for dust from windows (according to chapter 4.2).

Only for a few elements differences between the materials could be found. Moss bags for example show relatively high contents of Mn that are likely due to the occurrence of Mn in plants (STRASBURGER et al. 2014). Dust from windows has comparably high contents of Na, which are assumed to be derived from road salt applied in a cold period in the beginning of 2018, prior to the sampling in April 2018. Another possible reason for high Na contents in dust from windows could be selective leaching of Na containing compounds, that are often readily soluble in water, from particles still sticking to the window glass after sampling (HOLLEMAN et al. 2007). High values for P in spider webs and long-term deposit samples are assumed to be due to the individual biological material in the samples: Spider webs contain P for example in the aqueous coat forming sticky droplets to attach prey (VOLLRATH et al. 1990). High P contents in long-term deposit samples might be due to the growth of algae, containing significant amounts of P, in the temporarily existent water head in the vessels (MIDDELBURG 2019).

To detect sources of PM, single samples instead of median contents have to be regarded. An optical comparison of element patterns of single samples with patterns of source terms might give a first impression on major influences on the samples. For this purpose, samples of agricultural soil, loess, loose material collected from tram tracks and tram/train stations as well as particles brushed off from a used brake pad and lining have been analyzed. Fig. 4-6 shows

the corresponding contents normalized to UCC (see also appendix Fig. A-3). It shows that different element patterns can be expected for dust from natural/geogenic and anthropogenic sources. For agricultural soil and loess, the values are around one with lower values for elements for which lower recovery rates were found. Al, B, Ca, Cs, K, La, Mg, Rb, Th, U and Y have higher values for agricultural soil and loess, representing natural dust, than in traffic-related materials. Those are primarily geogenic elements occuring in rock forming minerals like feldspar and mica (Al, Cs, K, Rb) or in Triassic evaporites that occur in Jena and its surroundings (e.g. Ca, Mg). All other elements show higher contents in traffic-related samples than in geogenic ones. Particularly high normalized contents in traffic-related samples can be found for Ba (only brake wear), Cr, Cu, Fe (only brake wear), Mo, Sb, Sn and Zn with values greater than 10 up to greater than 1,000.

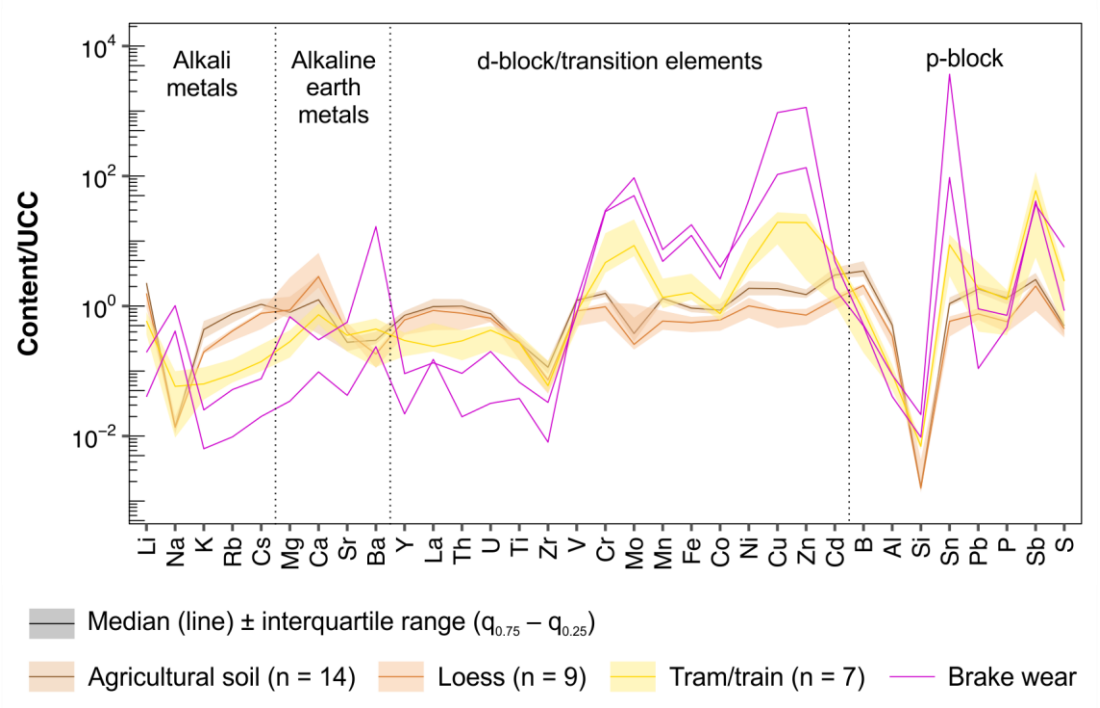

Fig. 4-6: Contents determined in samples representing different source terms divided by contents in the upper continental crust (UCC) given by WEDEPOHL (1995).

An optical comparison of element patterns of individual spider web samples with those of source terms has been done for selected samples. This is likely only possible for samples with only one (known) major source of PM, as otherwise element patterns will be mixed. For all comparisons, high contents of K, Na, P and S should not be regarded as these elements occur in the webs themselves (RACHOLD et al. 1992; WORK and YOUNG 1987).

Fig. 4-7 shows element patterns of spider web samples taken at the location CA-KUN (low amount of traffic, next to an agricultural field) in comparison with the overall pattern for agricultural soils that includes all different soil types close to the location (BUNDESANSTALT FÜR GEOWISSENSCHAFTEN UND ROHSTOFFE 2005). Levels and patterns for samples and the source term are similar for most of the elements: Normalized contents are mainly around one or lower and high values much greater than five, as found for the traffic related source

terms, cannot be found. This supports the thesis that a main source of PM in those samples is erosion and redeposition of agricultural soil. Different patterns for samples and source term were found for Ba, Cu, K, Na, P, S, Sb, Sn and Zn. High values for Ba, Cu, Sb, Sn and Zn might describe a (minor) influence of car traffic on the spider web samples. High normalized contents were found for them in brake material in Fig. 4-6 and they have also been named in the literature as being derived from brake wear (e.g. STERNBECK et al. 2002).

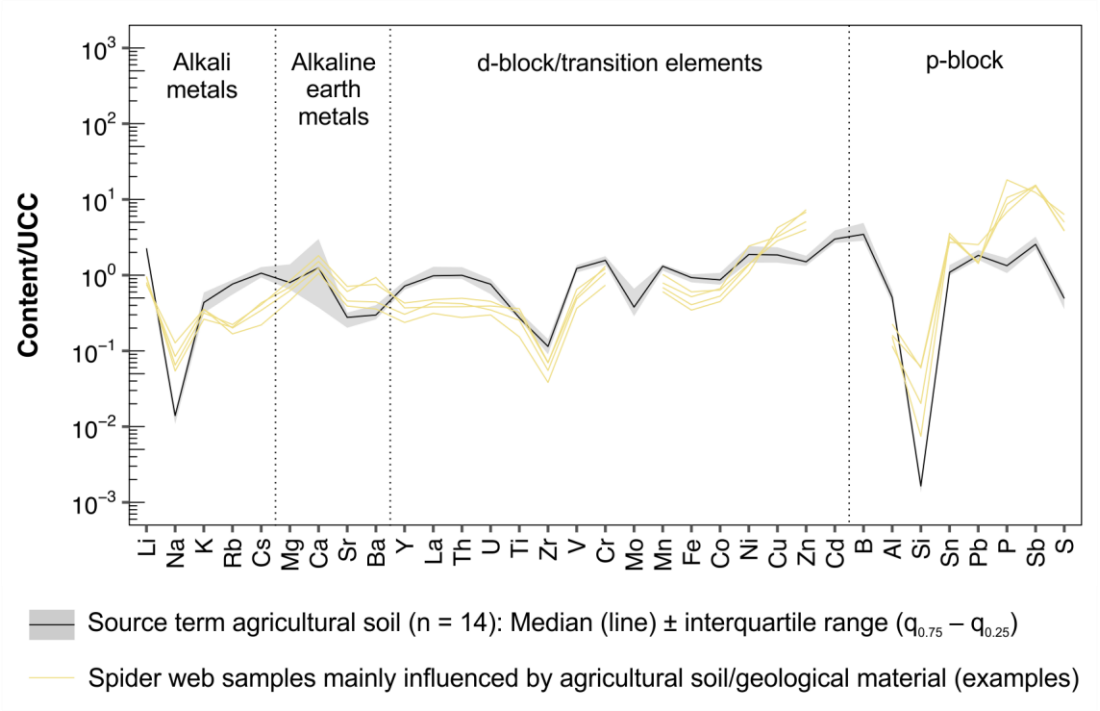

Fig. 4-7: Comparison of contents determined in selected spider web samples from location CA-KUN, surrounded by agricultural fields, and agricultural soils from the surroundings of Jena, standardized to contents in the upper continental crust (UCC) given by WEDEPOHL (1995).

Similar comparisons were done for the source terms tram/train and brake wear (appendix Fig. A-4, Fig. A-5). Matching patterns for samples and the source term can also be found for spider web samples from location TR-ARE (close to tram and train tracks surrounded by meadows) and the source term tram/train (Fig. A-4). They exhibit values below one for elements of geogenic origin (alkali and alkaline earth metals, Al, La, Si, Th, Ti, U, Y, Zr) and higher values for other transition and p-block elements. Despite the diluting effect of spider web biomass, higher normalized contents in spider web samples were found for Ba, Cr and Ni that occur in steel alloys (GUÉGUEN et al. 2012; LAHD GEAGEA et al. 2007). Thus, abrasion of tram/train tracks made of steel is likely a major source of PM captured in the spider webs regarded here. This is not consistent with the samples representing the source term since loose material collected from tram tracks did also contain sand particles that ensure proper adhesion of the tram wheels, but dilute abraded steel particles (ARIAS-CUEVAS and LI 2011). Either few sand particles were applied/still present at the spider web sampling location TR-ARE (where trams run quite fast) or sand particles were too coarse to be transported over several meters in air to handrails of spider web sampling. The latter might be deduced from

microscopic images in chapter 4.1, showing bigger sizes for silicate containing particles than for Fe containing particles which might be derived from steel abrasion.

Samples from location CA-BUR_1 (next to a busy road) were compared with the patterns of the source term brake wear (Fig. A-5). This source term has very high normalized contents (> 100) of Cu, Sn and Zn. Given the diluting effect of the web material itself, comparatively high normalized contents of Cu, Sn and Zn can also be found in the spider web samples regarded here. Therefore, car traffic is likely a major source of PM entrapped in those samples. In addition, normalized contents of alkaline earth metals as well as of La, Th, Ti, U, Y and Zr are nearly as high as the ones in samples influenced by geogenic/soil dust in Fig. 4-7, indicating that also a remarkable amount of geogenic particles has been entrapped by the spider webs. This is likely street dust (including natural particles), resuspended by driving vehicles. GÓRKA et al. (2018) for example mentioned resuspended soil material as a potential major source of PM in cities. Geogenic particles might also be derived from abrasion of road construction materials like grit or asphalt (FANG et al. 2005; STERNBECK et al. 2002).

Besides from influences of local sources of PM, an optical comparison of element patterns can also reveal temporal changes and/or individual, short-term events emitting dust particles. An example for this is given in Fig. 4-8. Spider web samples taken at four different days from handrails of a bridge crossing a motorway (Liebertwolkwitz, Saxony) are compared with samples representing the source term brake wear as well as with a soil sample taken at an acre close to the bridge. Element patterns of spider web samples drawn with a yellow line are quite similar to each other and to the element patterns of the source term brake wear with high normalized contents of Ba, Cu, Mo, Sb, Sn and Zn. In contrast, for the spider web sample drawn with a black line higher normalized contents of Ca, Cs, La, Mg, Rb, Th, Ti, Y and Zr can be found. The pattern for those elements is more similar to the pattern of the soil sample. The black sample has been taken at the exact day when crop was harvested at the nearby field from which the soil sample was taken. It can thus be inferred that PM at the sampling location of the spider webs is influenced by car traffic on the motorway most of the time, but other, temporarily occuring emissions like soil resuspension during agricultural activities can change this.

Conclusion: In summary, contents of the elements regarded in this work are mainly in the range of trace components with median element patterns being similar for all four sample materials (spider webs, moss bags, dust from windows, long-term deposit). Those patterns likely describe the background composition of PM in the sampling area. By comparing element patterns of individual samples with patterns of materials representing potential sources, an identification of sources of PM in the particular samples has been expected. This could be shown for selected samples and the source terms soil dust, tram/train and brake wear. Nevertheless this only works if there is a prominent major source and for more reliable results, a broader data basis for source terms would be needed (including also samples from other potential anthropogenic sources). Covering all potential sources with a reasonably high

number of samples however has been beyond the scope of this work. As sources have been regarded individually in other studies (e.g. CESARI et al. 2012; STERNBECK et al. 2002; WANG et al. 2003), literature data on element patterns/correlations will mainly be used in the following.

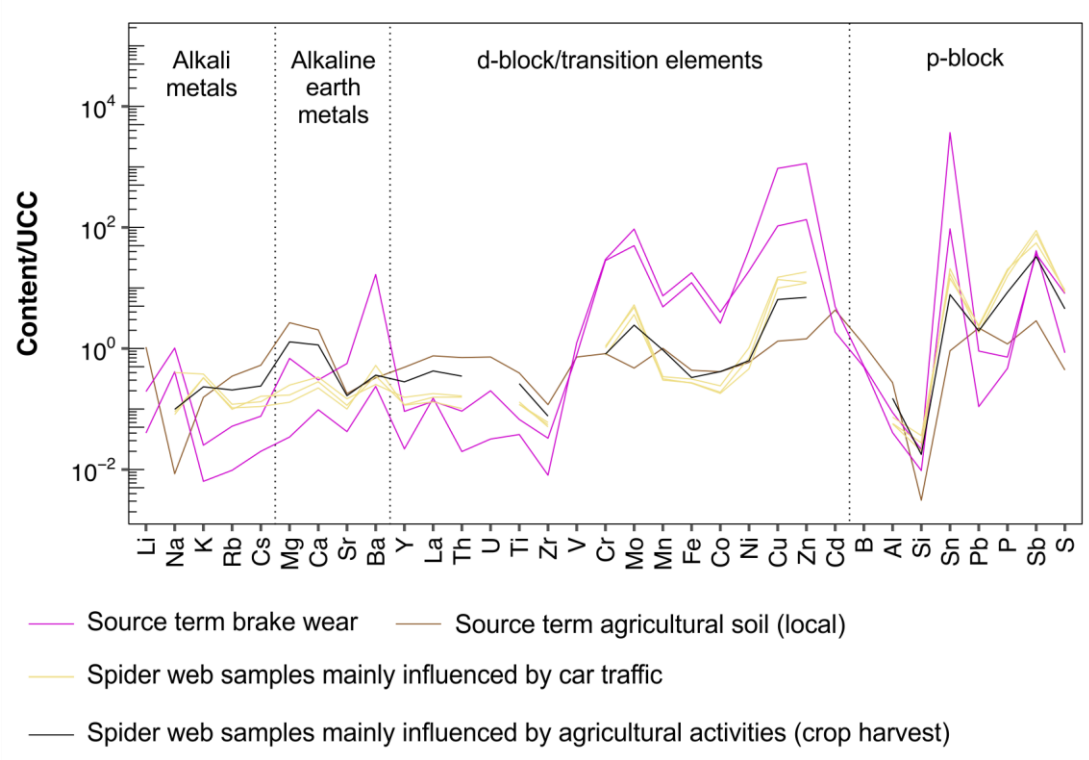

Fig. 4-8: Comparison of contents in spider web samples taken at a bridge crossing a motorway close to Liebertwolkwitz (Saxony), in a soil sample taken close to the bridge and in samples representing the source term brake wear, standardized to contents in the upper continental crust (UCC) given by WEDEPOHL (1995).

5 Comparison of spider web and moss bag biomonitoring to detect sources of urban particulate matter

Chapter 5 corresponds to a manuscript under review for the journal Environmental Monitoring and Assessment together with the co-authors listed.

Neele van Laaten[1,2], Dirk Merten[2], Wolf von Tümpling[3], Thorsten Schäfer[2] and Michael Pirrung[2]

[1] International Max Planck Research School for Global Biogeochemical Cycles, Max Planck Institute for Biogeochemistry, Hans-Knöll-Straße 10, 07745 Jena, Germany

[2] Institute of Geosciences, Applied Geology, Friedrich Schiller University Jena, Burgweg 11, 07749 Jena, Germany

[3] Helmholtz Centre for Environmental Research – UFZ, Brückstraße 3a, 39114 Magdeburg, Germany

Abstract

Atmospheric particulate matter has become a major issue in urban areas from both a health and an environmental perspective. In this context, biomonitoring methods are a potential complement to classical monitoring methods like impactor samplers, being spatially limited due to higher costs. Monitoring using spider webs is compared with the more common moss bag technique in this study, focusing on element contents, element ratios and the applicability for source identification.

Spider webs, exposed to ambient air for one day, and moss bags with *Hypnum cupressiforme*, exposed for ten weeks, were sampled at 15 locations with different types of traffic in the city of Jena, Germany. In the samples contents of 35 elements, mainly trace metals, were determined using inductively coupled plasma-optical emission spectroscopy (ICP-OES) and mass spectrometry (ICP-MS) after aqua regia digestion.

Significantly higher element contents in spider webs than in moss bags were found and could not be ascribed completely to a diluting effect by the biological material in the samples. Different mechanisms of particle retention by the two materials are therefore assumed.

Besides, more significant correlations between elements have been found for the spider web data set. Those patterns allow for an identification of different sources of particulate matter (e.g. geogenic dust, brake wear), while correlations between elements in the moss bags show a rather general anthropogenic influence. Therefore, it is recommended to use spider webs for the short-term detection of local sources while moss bag biomonitoring is a good tool to show a broader, long-term anthropogenic influence.

5.1 Introduction

Particulate matter (PM) in the atmosphere is regarded as one of the major environmental and health issues worldwide, especially in urban areas, where people are exposed to enhanced levels of PM (FURUSJÖ et al. 2007; LANDRIGAN et al. 2018). The exposure to PM leads to health issues as premature mortality, with up to 3.15 million estimated deaths per year worldwide, (lung) cancer, respiratory and cardiovascular diseases (LELIEVELD et al. 2015; WHO 2013). Besides, the atmospheric transport of particles influences element cycling in the environment, e.g. by the deposition of metals onto soils or into forest ecosystems (FANG et al. 2005). In the atmosphere PM scatters and absorbs radiation and particles can act as cloud condensation nuclei depending on their composition (GIERÉ and QUEROL 2010). Enhanced levels of PM thus influence both weather and, on a longer time scale, climate.

Threshold values for atmospheric PM and metals attached to it have thus been set (e.g. 2004/107/EC; 2008/50/EC) and monitoring stations have been installed in many urban areas. Due to high costs and need of space, most of the cities only hold one or a few stations (KARDEL et al. 2011). As levels and composition of PM can change rapidly within hundreds or even tens of meters, those stations have only a poor spatial coverage (SALMOND and MCKENDRY 2009). An often discussed, simple and cost-effective complement are biomonitoring techniques (SZCZEPANIAK and BIZIUK 2003): Airborne pollutants are adsorbed by a variety of biological materials that are sampled in the area of interest and analyzed. Typical matrices are mosses, lichen and plant leaves, but also tree bark and needles have been used so far (NOROUZI et al. 2015; TRETIACH et al. 2011; URBAT et al. 2004). The advantage of biomonitoring methods is its lack of need for both power supply and maintenance, leading to low sampling costs. Furthermore, plants are widely distributed, hence a large number of sampling sites is accessible (VUKOVIC et al. 2016).

An advanced technique is moss bag biomonitoring. Moss of a selected species from a remote place is put into bags of plastic mesh and exposed to ambient air at the locations of interest (ARES et al. 2012). Afterwards, the contents of selected elements in the individual samples are determined (ADAMO et al. 2011; ANICIC et al. 2009; DI PALMA et al. 2017). There has been a growing scientific interest in this technique within the last decades, as it is more controllable than classical moss monitoring and can be applied at every desired location (ARES et al. 2012).

Another biomonitoring technique is the collection of spider webs, to whose adhesive silk dust particles can attach. This method has only been studied a few times so far (e.g. RACHOLD et al. 1992; RYBAK 2015; XIAO-LI et al. 2006). If the webs are not collected too often, the method is rather non-invasive and spider webs can be found at many locations in urban areas. They can be collected easily, for example from fences, handrails and walls (RYBAK 2015; XIAO-LI et al. 2006). Spiders can survive adverse surroundings with high metal contents and can be found in many climate zones, thus the method might be applied in many countries (AYEDUN et al. 2013).

To the best of our knowledge, no systematic comparison between the sampling of spider webs and moss bag biomonitoring has been done so far. Both methods have been applied individually, showing their suitability to assess levels of atmospheric pollution. Contents of numerous trace elements (mainly heavy metals) in spider web and moss bag samples from the same locations shall be determined and compared in this work. The questions we address in this paper are: (a) Do the two biological materials show the same retention of dust particles? (b) Do the individual data sets contain patterns that can be used to identify sources of PM? And (c) Are the patterns and the resulting grouping of samples similar for both biomonitoring methods?

5.2 Material and methods

5.2.1 Monitoring sites

For sampling, 15 locations in the city of Jena were chosen (Fig. 5-1). Jena is a medium-sized city in Central Germany without big industries, therefore the local air quality is expected to be mainly influenced by traffic on two railroad lines, two federal highways and a motorway. As the city is located in a valley formed by the river Saale, the sampling locations cover its north-south orientation and include locations with car traffic (prefix CA), tram and train transport (TR) as well as areas reserved only for pedestrians (PD).

5.2.2 Moss bag and spider web biomonitoring

For the preparation of the moss bags *Hypnum cupressiforme* was collected in a pine forest about 15 km south of Jena (UTM 32 N E 687024 N 5631097). Foreign objects like pine needles and soil fragments as well as dead moss material were removed manually before the moss was rinsed three times with deionized water and dried at 40 °C. The bags were made of polyester mesh (16 x 16 cm, 2 mm mesh size) sewed with nylon thread, rinsed with diluted HNO_3 (Merck, subboiled) and ultrapure water (genPure UV-TOC, Thermo Scientific) before use. Approximately 3 g of the dry moss were filled into each bag and the bags were stored in a polyethylene (PE) pouch until exposure. The bags were hung up at lamp posts 2.5 m above ground level using plastic mountings that kept the moss away from the metal lamp poles. After ten weeks (from June to August 2017) the bags were removed. Spider webs were sampled from the upper half of handrails (0.5–1.2 m above ground level) by coiling the webs up on the upper half of a plastic straw (polypropylene, PP). The webs available at one site made up one sample containing tens up to two hundred of intertwined individual webs. All samples were stored in individual PE bags during transportation to the lab.

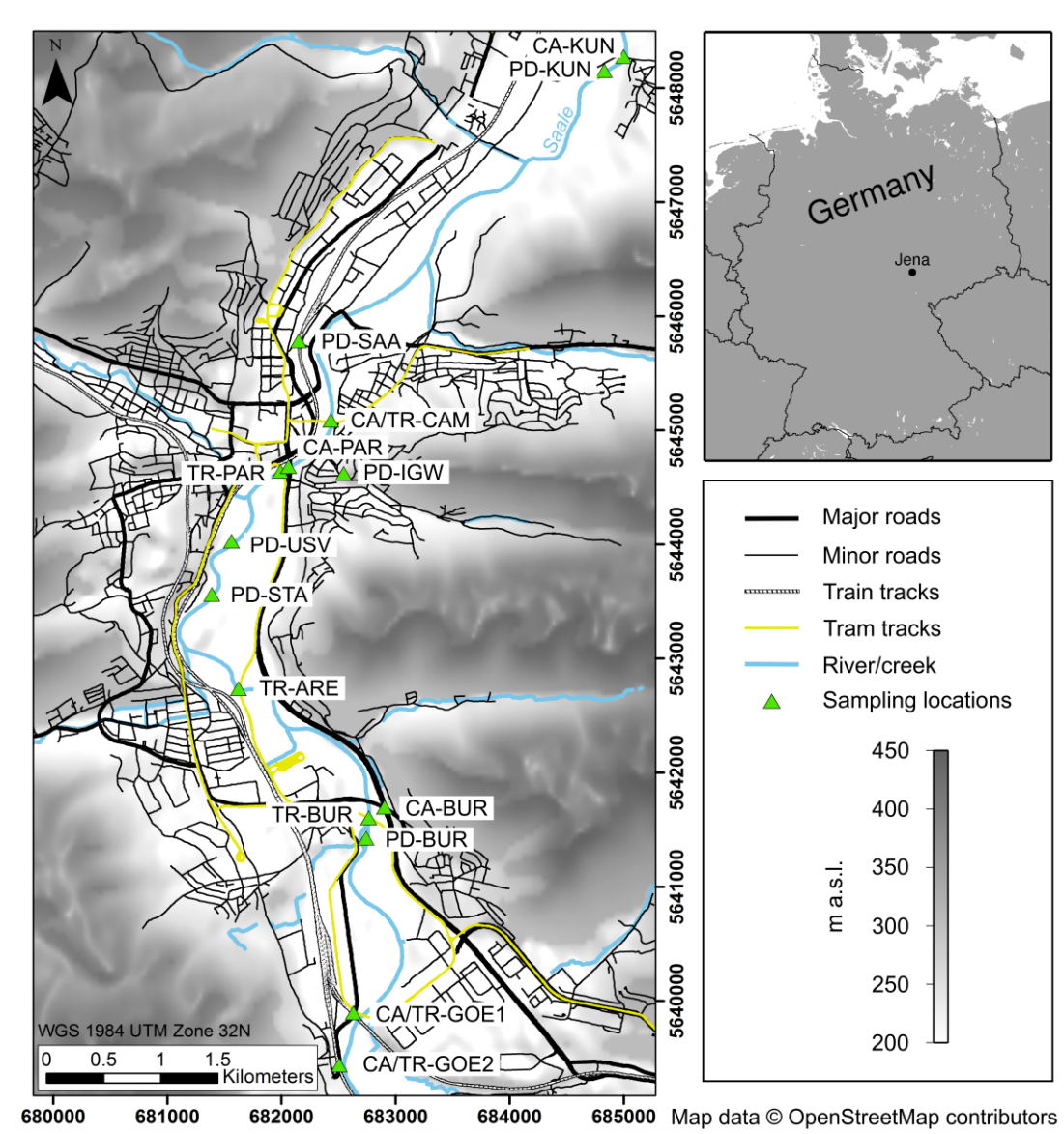

Fig. 5-1: Map of the city of Jena including traffic routes and the sampling locations coded according to the nearby type of traffic. CA: car traffic, CA/TR: car and tram/train traffic, PD: pedestrian areas, TR: tram/train traffic. The map has been created using SRTM3 topography data (USGS 2004) and GMT (WESSEL et al. 2013).

5.2.3 Sample preparation and analysis

Mosses were removed from the bags and dried at 40 °C. Each sample was cryomilled using liquid nitrogen and a ceramic mortar and pestle. The spider webs were first removed from the plastic straws. Coarse objects like insects or hairs were sorted out manually using plastic tweezers before drying at 40 °C. All samples were digested with aqua regia (related to DIN EN 16174:2012) using the microwave system MARS 5 Xpress and vessels of perfluoroalkoxy alkane (both: CEM GmbH). For this, 6 ml 35% HCl (supra quality, Carl Roth) and 2 ml 65% HNO_3 (Merck, subboiled) were added to up to 200 mg of the individual samples. A pre-reaction of 20 min took place in open vessels. Afterwards the vessels were closed, the mixtures were heated to 175 °C within 15 min and kept at 175 °C for 10 min. After cooling down, the digestion mixtures were filled up to 25 ml with ultrapure water in volumetric flasks

(polymethylpentene, PMP, Vitlab) and transferred to 50 ml centrifuge tubes (PP, Greiner Bio-One). After centrifugation (3000 rpm, 15 min), the clear supernatants were transferred to 30 ml sample bottles (high-density PE, Thermo Scientific) and stored until further processing.

In addition, total digestions of selected samples were performed using a pressure digestion system (DAS, Pico Trace) with vessels of polytetrafluoroethylene. For this, 2.5 ml 65% HNO_3 (Merck, subboiled) were added to 50 mg of the sample, heated up to 45 °C within 1 h and kept at 45 °C for 1 h. After cooling down, 2.5 ml 40% HF and 3 ml 70% $HClO_4$ (both: suprapur, Merck) were added, the mixture was heated up to 180 °C within 8 h and kept at that temperature for 12 h. The cooled mixture was heated up to 180 °C again within 4–5 h in the evaporation mode and kept there for 14 h to evaporate the acids. The remaining solids were dissolved in 2 ml HNO_3 (Merck, subboiled), 0.6 ml HCl (suprapur, Carl Roth) and 7 ml ultrapure water within 8 h at 150 °C and filled up to 25 ml with ultrapure water in volumetric flasks (PMP, Vitlab).

Contents of Al, Ca, Fe, K, Mg, Mn, Na, P, S, Si, Sr and Ti were analyzed by ICP-OES (inductively coupled plasma-optical emission spectroscopy, 725ES, Agilent Technologies) and contents of Ag, As, B, Ba, Cd, Co, Cr, Cs, Cu, La, Li, Mo, Nb, Ni, Pb, Rb, Sb, Sn, V, W, Y, Zn and Zr were analyzed by ICP-MS (inductively coupled plasma-mass spectrometry, XSeries II, Thermo Scientific). For quality assurance standard reference materials SRM 1648a Urban Particulate Matter, SRM 1575 Trace Elements in Pine Needles (both: National Institute of Standards and Technology), and IPE 952 Grass mixture (Wageningen Evaluating Programs for Analytical Laboratories) were digested with aqua regia and analyzed according to the description above.

Contents of organic and total carbon as well as nitrogen were determined in selected samples using a Vario EL cube element analyser (Elementar Analysensystem GmbH).

5.2.4 Microscopy

Microscopic pictures of the sample materials were taken with the digital microscope KEYENCE VHX-6000 (KEYENCE GmbH) with a magnification of 100X – 1,000X. Non-milled moss from moss bags was placed directly on the object plate while spider webs were collected on glass slides at the monitoring sites, embedded in a thermoplastic mounting medium (Cargille Meltmount*1.582, Cargille-Sacher Laboratories Inc.) and covered with a cover glass.

5.2.5 Data handling and statistical evaluation

Data pre-treatment, calculations and univariate statistics were done using MS Excel 2010 (Microsoft Corporation). Contents below the limit of detection (LOD) were replaced by a random value between zero and the LOD and element measurement series with more than 10% of values below the LOD were excluded from further examination (namely Ag and As). The data was checked for outliers according to DIXON (1951, P = 99%) and statistical param-

eters as well as the test for normal distribution according to DAVID et al. (1954, P = 99%) were calculated for the data without outliers. Significant differences between spider webs and moss bags were tested for each element using the Wilcoxon signed-rank test (BORTZ et al. 2008, P = 99%). Additionally, the Spearman rank correlation between elements in spider webs and moss bags was calculated for each element. Cluster analyses of the autoscaled data including outliers were done with the software R using Ward's algorithm with squared Euclidean distances. Graphical visualisations were edited with CorelDRAW Graphics Suite 2017 (Corel Corporation).

5.3 Results and discussion

5.3.1 Microscopy

The microscopic images of the two different sample materials (Fig. 5-2) show that the ratio of deposited PM to biological material is much larger for spider webs than for moss bag samples. Besides, particles can be seen and zoomed in better on spider webs as the structure is less complex and can be fixed on a glass slide. Particles can be seen on the surface of moss material after exposure to ambient air (c, e, g), but not before (a). Black particles are attached to the surface of moss exposed at a car traffic location (c) and to a smaller extent to moss exposed at a pedestrian area (g). In contrast, on moss exposed at a tram and train transport location (e) many big, white, sub-rounded particles can be found. Those are likely quartz and/or feldspar sand and silt particles added on the tracks to increase the adhesion of the wheels (ARIAS-CUEVAS and LI 2011).

Fresh spider webs (b) have characteristic sticky droplets at which particles adhere after exposure (d, f, h; for comparison see VOLLRATH and TILLINGHAST 1991). The highest amount of PM can be found on webs from a car traffic location (d). This is mainly black, flocculent material similar to brake wear (see Fig. 4-1), while some oval, translucent particles were identified as windblown plant material. At the tram and train transport location (f) fewer and smaller particles can be found. Compared to the moss sample there are less translucent mineral particles but some bigger, brownish particles that are considered as plant material. Only very few particles adhere to the spider web taken at a pedestrian area (h).

Possibly the big and heavy minerogenic particles found on mosses are too heavy to attach to spider webs while particles of biologic origin might not be distinguished optically from the moss material. Those differences are expected to influence the element patterns discussed in the following. Besides, the easy optical inspection of spider web samples strengthens the superior suitability of spider webs to sample PM as stated by RYBAK and OLEJNICZAK (2014).

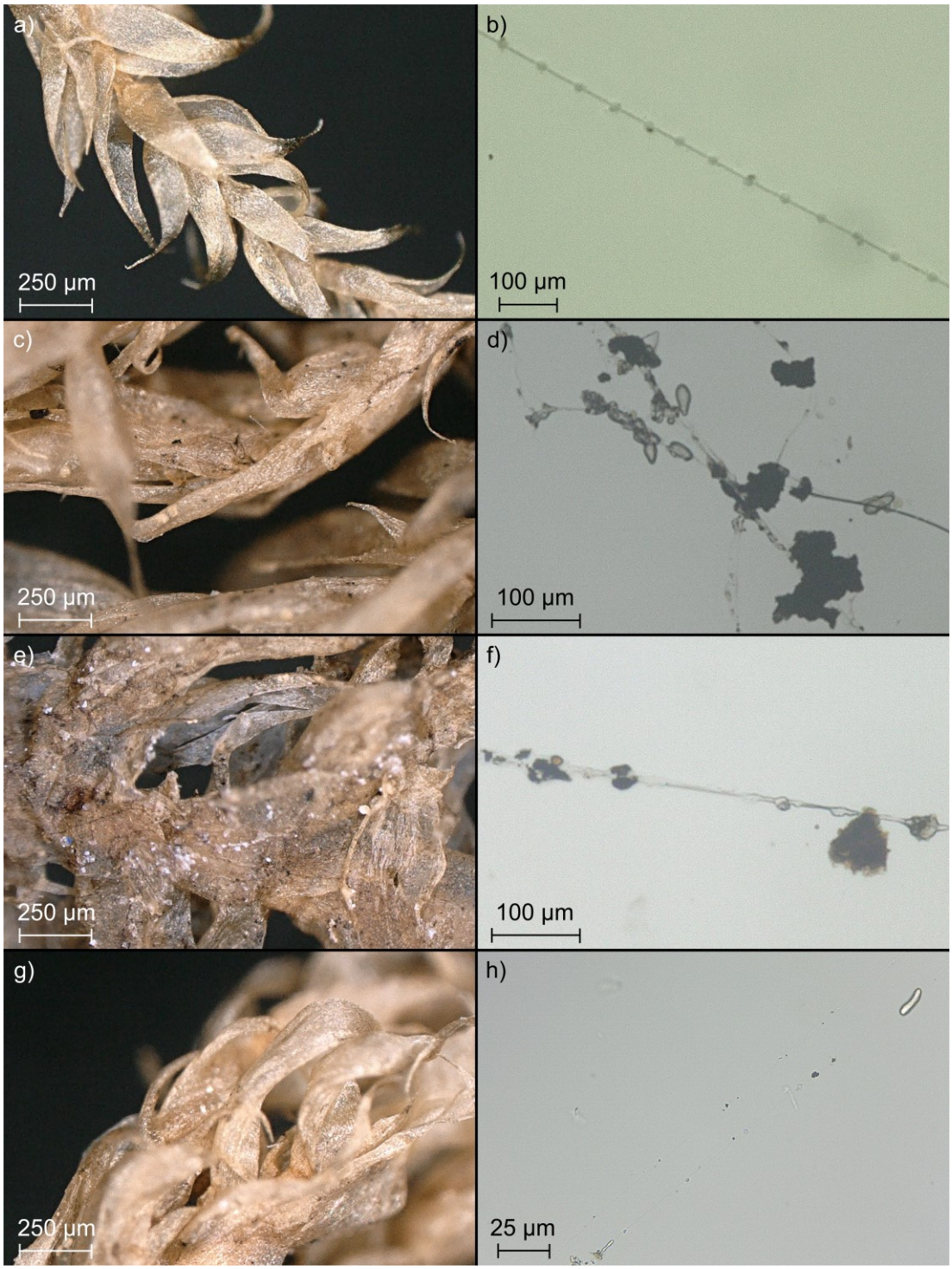

Fig. 5-2: Microscopic images of sample material (left: moss, right: spider webs) from locations with different types of traffic. a) moss prior to exposure, b) fresh spider web early in the morning, c) and d) CA-PAR (car traffic), e) and f) TR-ARE (tram and train transport), g) and h) PD-IGW (pedestrian area).

5.3.2 Quality assurance

The recovery rates for elements in biological reference materials (SRM 1575, IPE 952) are for most of the elements greater than 90% (lowest rate: 76 ± 9%). For SRM 1648a (Urban Particulate Matter) recovery rates are greater than 90% only for some elements and substantially lower (below 70%) for Al, Cr, K, Na, Rb and Ti. The latter might be due to the fact that urban

particulate matter often contains some geogenic particles of which silicates like feldspar (containing Al, K, Na and Rb) as well as chromite ($FeCr_2O_4$) are not dissolved in aqua regia (SALMINEN et al. 2005). Detailed numbers can be found in chapter 3.7.

Recovery rates were also calculated relating the contents after aqua regia digestion to those after total digestion for both sample materials (chapter 3.7). They are greater than 90% for Ca, Co, Cu, Fe, Mg, Mn, Mo, P, Sb, Sr and Zn and substantially lower (below 70%) for Nb, Ti and Zr. As the tendencies are similar for both sample materials and for SRM 1648a, element contents cannot be regarded as total contents, however, element patterns can be compared to each other. Taking the standard deviations into account, considerably different recovery rates calculated for biological materials can only be found for Al, Cs, K, Na and Rb. Relations of contents for those elements thus have to be regarded carefully.

5.3.3 Differences between the sample materials

In accordance with the optical observations, the median of the measured contents of elements in spider webs is generally higher than in moss bag samples with factors ranging from 2 to 15 for most of the elements (e.g. B: 21.3 µg/g in spider webs and 9.00 µg/g in moss bags or Sn: 13.1 µg/g in spider webs and 0.895 µg/g in moss bags). For Na and P, the factors are 29 and 36, respectively. Detailed numbers can be found in Tab. 5-1. While a majority of contents is in the range of trace components (1,000 µg/g ≥ median ≥ 1 µg/g), a higher number of minor components (10% ≥ median ≥ 1,000 µg/g) can be found for spider webs and the number of ultra trace components (median ≤ 1 µg/g) is higher for moss bag samples. Only for Cd and Mn the contents are higher in moss bag samples. This difference between the sample materials is significant (Wilcoxon signed-rank test, P = 99%) for all elements except Cd and Pb.

Contents for moss bag samples are in the range or at least in the same order of magnitude than contents for moss bag samples using *Hypnum cupressiforme* in urban areas in the literature. ADAMO et al. (2011) for example found 0.26 µg/g of Cd, 5.4 µg/g of Cr and 1,140 µg/g of Mg in a study in Naples, Italy, while TRETIACH et al. (2011) found 0.42 µg/g, 5.05 µg/g and 1,020 µg/g respectively in a study from Trieste, Italy. Median contents in moss bags in this study were 0.291 µg/g Cd, 2.28 µg/g Cr and 1,160 µg/g Mg. Besides, the contents are higher than those in naturally occuring *Hypnum cupressiforme* from Ljubljana municipality (BERISHA et al. 2017). For spider webs, more differences between contents in the literature and contents determined in this study have been found. XIAO-LI et al. (2006) for example found contents one to two orders of magnitude higher for Cd (0.85–3.37 µg/g) and Pb (35.4–290 µg/g) in webs from Wuhan (China) than we found in this work with 9.31 µg/g Pb. In the cited study, older webs (age up to 60 days) were used which might be a reason for higher contents compared to those in one day old webs in the present study. Besides, levels of PM and its metal contents might be higher in Wuhan than in Jena. Some differences might also be due to the various digestion methods used as they can show different recovery rates. Silicate particles for example can only be digested totally by HF that was used by ADAMO et al.

(2011) while most of the other studies cited used a digestion with HNO_3 and H_2O_2 (BERISHA et al. 2017; RYBAK 2015; XIAO-LI et al. 2006).

Tab. 5-1: Median (µg/g) and interquartile range (IQR) of the measured contents in moss bags and spider webs (n = 15). Minor components: 10% ≥ median ≥ 1000 µg/g, trace components: 1000 µg/g ≥ median ≥ 1 µg/g, ultra trace components: median ≤ 1 µg/g, underlined: content in moss bags higher than in spider webs, bold: data without the (upwards) outlier (n = 14), italics: no normal distribution, m: number of elements per column.

Element	Minor components				Trace components				Ultra trace components			
	Moss bags		Spider webs		Moss bags		Spider webs		Moss bags		Spider webs	
	Median	IQR	Median	IQR	Median	IQR	Median	IQR	Median	IQR	Median	IQR
Al			3,650	2,570	714	17						
B					9.00	5.30	21.3	6.1				
Ba					45.2	14.1	161	285				
Ca	**5,160**	**249**	12,900	10,800								
Cd									0.291	0.032	0.260	0.100
Co							2.44	0.92	0.379	0.121		
Cr					2.28	0.92	**29.9**	**25.0**				
Cs									0.104	0.016	0.500	0.384
Cu					***7.85***	***2.97***	79.8	74.2				
Fe			9,630	9,380	**766**	**143**						
K	***1,320***	***2232***	12,300	2,100								
La							3.32	2.59	0.600	0.202		
Li							5.60	4.54	0.560	0.232		
Mg	1,160	74	2,990	1,510								
Mn					522	90.5	168	144				
Mo							3.60	4.37	**0.329**	**0.086**		
Na			3,700	1,630	127	48.0						
Nb									**0.133**	**0.045**	0.940	0.610
Ni					2.60	0.65	18.6	10.7				
P			13,900	5,460	**387**	**78.6**						
Pb					9.31	2.60	11.1	4.68				
Rb					**2.44**	**0.48**	10.9	4.49				
S	1,000	117	9,150	2,350								
Sb							6.30	9.62	**0.459**	**0.176**		
Si	1,140	319	5,490	3,000								
Sn							13.1	12.5	**0.895**	**0.431**		
Sr					15.3	2.94	56.4	37.0				
Ti					28.2	8.05	252	185				
V					1.52	0.28	10.1	5.3				
W									**0.092**	**0.023**	**0.415**	**0.239**
Y							1.66	1.17	0.347	0.093		
Zn					42.3	14.0	375	293				
Zr							7.33	2.73	**0.661**	**0.232**		
m	5		9		16		20		12		4	

The spider web data shows higher variation (higher interquartile ranges compared to the median) than the moss bag data. This might be ascribed to the fact that spider webs could not be (cryo)milled and thus are more heterogeneous than moss samples. Besides, the sampling process is more heterogeneous for the spider webs than for the moss bags: Webs are

woven by individual spiders and thus the material can vary. The influence of the (levelling) amount of biological material is also smaller for spider webs than for moss bag samples. To correct for this, the contents measured in the samples were divided by one minus the fraction of the biomass in the samples. In geochemistry, the content of organic carbon in the samples is often used to calculate the fraction of biomass in a sample (e.g. PRIBYL 2010; VILLARES et al. 2003). As mosses and spider webs are dissimilar biological materials, we used an adapted approach with different sum formulas in combination with the mean content of organic carbon in the two materials. For moss bags $C_{12}H_{20}O_{10}$ (cellulose) has been used and for spider webs we applied $C_{3.38}H_{5.01}N_{1.06}O_{1.32}$, a sum formula approximated from the fractions of amino acid residues named by WORK and YOUNG (1987). Fig. 5-3 shows boxplots for the sum of all element contents and for cumulated contents corrected for the biomass as described. For the latter the difference between the sample types decreases noticeably for the median from a factor of 6.2 to 1.2. Still, the difference is significant with no significant difference for Al, Ba, Co, Cs, La, Li, Mo, Nb, Ni, Rb, Si, Ti, V, W and Y. This leads to two different conclusions: Either the diluting influence of the biomass cannot be corrected for completely by this approach or the influence can be corrected for completely and the remaining differences are due to systematic contrasts of the retention of PM by the two biological materials.

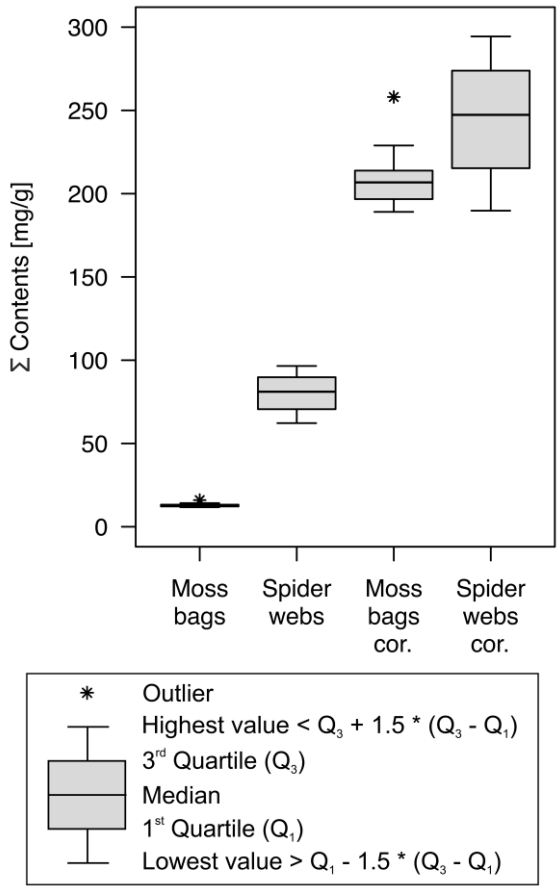

Fig. 5-3: Boxplot of the sum of all element contents measured in moss bag and spider web samples and of contents corrected for the amount of biomass (cor.).

Independent from the significant difference, the corrected contents are in the same range. For some comparison that might be helpful, e.g. to qualitatively differentiate between polluted and unpolluted areas.

5.3.4 Element patterns

To discover element patterns, that are expected to describe different sources of PM, Spearman rank correlation coefficients (calculated using the contents measured) can be used. The comparison of correlation coefficients within the individual sample materials (Tab. 5-2) shows that only some significant correlations are found for both materials and a higher number is found for the spider web than for the moss bag data set. Thus, a stronger relation between the elements in spider webs is deduced. The (joint) coefficients can be regarded as forming sub-matrices with predominantly significant coefficients that are ascribed to the different sources of PM or influences of the sample material. The joint sub-matrix of K, P and S likely describes the dilution of PM by the biological material: Correlations of K, P and S with other elements are negative and the elements are included in both spider webs and mosses (RACHOLD et al. 1992; STRASBURGER et al. 2014; WORK and YOUNG 1987). Al, Co, La, Nb, Ti, V, Y, Zr form another joint sub-matrix that is ascribed to PM of geogenic origin like natural and anthropogenically influenced soil erosion. For La, Nb, Y and Zr high values in soils in Central Germany with areas of Quarternary loess deposits, which are typical for the surroundings of Jena (SEIDEL 1993), have been mentioned by SALMINEN et al. (2005). Cu, Sb, Sn and Zn correlating with each other have been ascribed to brake wear in the literature (BERISHA et al. 2017; FURUSJÖ et al. 2007; JOHANSSON et al. 2009). Therefore, this sub-matrix likely describes brake wear as a part of the influence of automobile traffic to PM.

For spider webs, the sub-matrix describing (resuspended) geogenic PM is bigger than the joint matrix, containing elements which are typical for either calcareous rocks (Ca, Mg, Sr) or marine evaporates (B, Cs, Li) that can also be found in the surroundings of Jena (SALMINEN et al. 2005; SEIDEL 2003). In addition, a matrix of Cr, Fe, Mo and Ni can be found for the spider web data but not for the moss bags. Those elements are ascribed to the abrasion of rail and/or tram tracks consisting of steel alloys containing all four elements (JOHANSSON et al. 2009; LAHD GEAGEA et al. 2007). Solely for the moss bag samples, significant correlation coefficients with many other elements can be found for Co, Cr, Fe, Ni, Si, W and Zn. Especially Co, Cr, Fe, Ni and Zn have been described as being mainly of anthropogenic origin and derived from different sources (DONGARRÀ et al. 2007; RYBAK 2015; SUVARAPU and BAEK 2017). The comparison of correlation coefficients shows that the influence of types of traffic is more pronounced in the spider web data set while a more diffuse anthropogenic influence can be seen in the moss bag data set.

Tab. 5-2: Joint correlation matrices (Spearman rank correlation) for moss bags and spider webs. Only significant correlations (P = 99%) are regarded. The color code shows if the correlation is significant for the moss bag data set (turquoise, n = 61), the spider webs data set (yellow, n = 114) or both (purple, n = 85); - indicates a negative correlation. Different sub-matrices are formed for moss bag and spider web samples.

	Rb	K	S	P	Si	W	Al	Ca	Li	Sr	B	Y	Cs	Mg	Ti	Nb	La	Zr	Pb	V	Co	Cd	Ba	Mn	Fe	Cr	Ni	Mo	Cu	Sb	Sn	Zn	Na
Rb																																	
K															-	-										-							
S					-		-	-	-	-		-	-	-	-		-	-	-	-													
P							-	-	-	-		-	-	-	-	-	-	-	-	-	-												
Si																																	
W																																	
Al																																	
Ca																																	
Li																																	
Sr																																	
B																																	
Y																																	
Cs																																	
Mg																																	
Ti																																	
Nb																																	
La																																	
Zr																																	
Pb																																	
V																																	
Co																																	
Cd																																	
Ba																																	
Mn																																	
Fe																																	
Cr																																	
Ni																																	
Mo																																	
Cu																																	
Sb																																	
Sn																																	
Zn																																	
Na																																	

Significant r_s for both sample matrices

Significant r_s for moss bags

Significant r_s for spider webs

\- Negative correlation

The fact that there are only very few significant correlation coefficients between the sample materials (Tab. 5-3) further strengthens the differences between the two monitoring methods. If the sample materials would accumulate PM in identical ways, significant correlation coefficients for the same element in moss bag and spider web samples should be expected. A correlation like that can only be calculated for Cu, Sb, Sn and Zn that have been already ascribed to brake wear or car traffic in a broader sense. Most striking is also the correlation of Ba in moss bags with Al, Ca, Cd, Cs, La, Li, Mg, Pb, Sr, Y and Zr in spider webs. Most of them have already been discussed as being of geogenic/natural origin. Cd and Pb are almost completely of anthropogenic origin, but with a variety of sources and often cannot be ascribed to a single source but more to diffuse pollution (ENAMORADO-BÁEZ et al. 2015; SUVARAPU and BAEK 2017). Ba on the other hand can be derived from both natural and anthropogenic sources as it can be found in sedimentary rocks like sulfates that occur in the surroundings of Jena (SEIDEL 2003) and it can be found in unleaded fuel, lubricant oils and brake fillings as well (STERNBECK et al. 2002). This correlation between the sample materials might therefore be due to diffusely distributed PM from different sources, likely resuspended by driving vehicles.

Tab. 5-3: Spearman rank correlation coefficients between moss bag and spider web data. Only significant correlations (P = 99%) are shown. A distinct correlation between the same elements in the two matrices can only be calculated for Cu, Sb, Sn and Zn (grey background).

Spider webs / Moss bags	Al	Ca	Li	Sr	Y	Cs	Mg	Nb	La	Zr	Pb	Cd	Cr	Ni	Mo	Cu	Sb	Sn	Zn
Nb													0.65		0.75				
Zr																	0.67		
Ba	0.68	0.77	0.75	0.79	0.69	0.78	0.66		0.68	0.69	0.65	0.71							
Ni														0.67					
Mo															0.67	0.80	0.77	0.82	0.75
Cu																0.86	0.84	0.85	0.85
Sb																0.65	0.73	0.66	0.76
Sn																0.83	0.89	0.84	0.85
Zn																0.75	0.71	0.78	0.71
Na								0.65											

5.3.5 Cluster analyses

To identify sources of PM and effectively distinguish or group sampling locations, multivariate methods can be applied. In some studies this has already been done, but only for single data sets (e.g. BARANDOVSKI et al. 2015; RAGOSTA et al. 2008). Here, cluster analyses have been performed with the contents measured in moss bags and spider webs and the resulting dendrograms are contrasted with each other (Fig. 5-4). At a relative distance of 15% four stable clusters can be found for the moss bag samples. While the location with the highest traffic volume (CA-PAR) is clearly cut off, the other clusters cannot be ascribed to a specific source or circumstance. They contain locations with different type of nearby traffic, different

elevation and different location in the town. In contrast, at 15% relative distance the spider web samples are clearly distinguished according to the nearby type of traffic, coinciding with the results of RYBAK and OLEJNICZAK (2014), who suggested spider webs as a useful indicator of traffic emissions, but with respect to polycyclic aromatic hydrocarbons.

Overall, the differences between moss bag and spider web biomonitoring might not only be due to differences in texture and relation of sample material to PM as described above, but also to different sampling approaches. While wheel webs, that were sampled in this study, are renewed nearly every day, mosses need several weeks to accumulate a significant amount of PM (ARES et al. 2012; NENTWIG 1980). Thus, the latter give integrated values over a longer period. In addition, the sampling height is different for the two methods: Mosses were sampled 2.5 m above ground level and the spider webs at 0.5–1.2 m. As the bottom meters of the atmosphere show rapid changes, different compositions of PM might reach the two sampling levels. Near ground level emissions like those from traffic are likely more pronounced next to the surface while the influence of mixing, leading to less local variation, increases with height. Even though CAPOZZI et al. (2016a) described a main influence by traffic for moss bags in a height of 4 m, it is assumed that in this study the influence of mixing already becomes relevant at an exposure height of 2.5 m. The air circulation will also only transport smaller particles into a height of 2.5 m in relation to a height between 0.5 and 1.2 m as it could be seen also on the microscopic images. Bigger particles have a stronger influence on the element pattern which likely leads to better discrimination of the sampling locations. From a health perspective, a lower height might be of greater interest, as this is the height of inhalation for children, which suffer disproportionally much from PM exposure (FANG et al. 2005; LANDRIGAN et al. 2018). Still it might not be possible to expose moss bags next to ground level as they will likely be damaged or touched by people, which is unlikely for the spider webs.

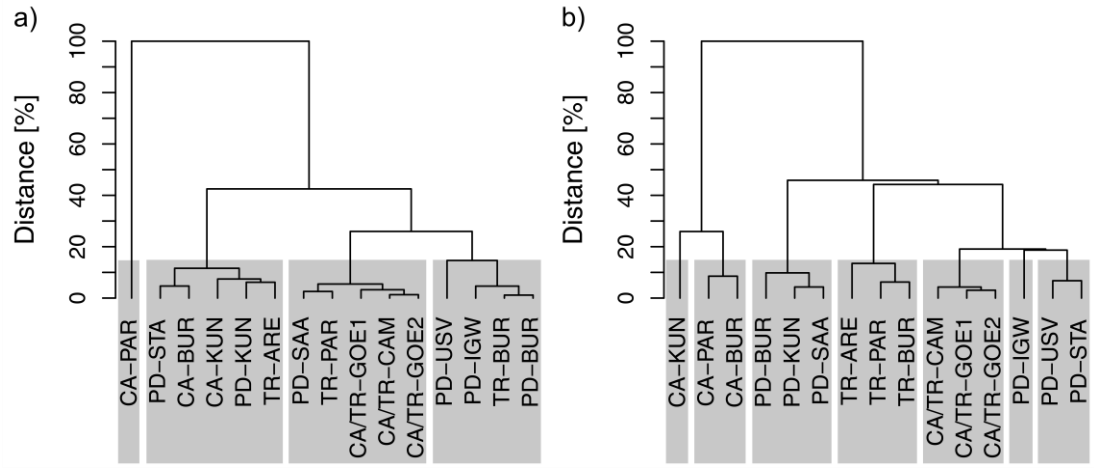

Fig. 5-4: Dendrograms (Ward's algorithm, squared Euclidean distances) depicting the cluster analyses of moss bags (a) and spider webs (b). At 15% relative distance the sampling locations are separated according to the nearby sort of traffic (CA: car, PD: pedestrian, TR: tram/train, CA/TR: car and tram/train) within the spider web data set. A similar pattern cannot be seen within the moss bag data set.

5.4 Conclusion

In this work two different biomonitoring methods for particulate matter (PM) have been compared, analyzing amounts and patterns of (trace) elements in the samples as well as their potential use for monitoring and source identification. Element contents are significantly higher in spider webs than in moss bag samples. A calculation to account for the diluting effect of the biological material leads to fewer but still existing significant differences, hinting to different adsorptions of dust particles. This can also be seen partially in microscopic images of the samples. Element patterns, detected by correlation coefficients and cluster analyses, can be found for the two sample materials. For spider webs, they can clearly be ascribed to different sources of PM, leading to a clustering of the sampling locations in accordance to the type of nearby traffic. This source identification is less pronounced for the moss bag data set with an undefined clustering of the sampling locations. As a result, it is recommended to use moss bags for long-term screening on a rather regional scale. For a local, short-term source identification spider web data should be used to exploit the higher variance in the data, the smaller influence of the biological material and the stronger relations between the elements. Further studies might focus on possibly different capture mechanisms for PM of the biological materials, which has not been a major part of this study.

6 Repeated spider web biomonitoring in the city of Jena, Germany and its utilization to detect sources of particulate matter

Spider web biomonitoring and in particular its potential use for the identification of sources of PM has been a key point of this work. Spider web data will be discussed in detail in this chapter, mainly focusing on the repeated sampling at 22 locations in the city of Jena (in spring 2016 and every six weeks from April to September in 2017 and 2018). To get a first impression, element contents in the samples as well as enrichment factors of single elements are regarded (chapter 6.1).

To identify sources of PM, connections between elements are regarded in a multivariate approach. This is based on the assumption that the chemical composition allows for understanding the origin of PM (e.g. ORDÓÑEZ et al. 2003; RAGOSTA et al. 2008). NORRA et al. (2004) for example did state that different types of land use in urban areas can be distinguished by their specific element patterns. Spearman rank correlations as well as a cluster analysis were calculated for this purpose (chapter 6.2). To take into account also the different sampling locations as well as to confirm or deny the primal source identification, a factor analysis was calculated and evaluated thoroughly (chapter 6.3). Results of the latter do also tell how much of the variance of the data set is explained by one source.

When working with environmental samples, an important aspect is to assess how representative the regarded samples are. To answer this question, classification models are used both by applying cross-validation and by classifying samples from locations that were not part of the repeated sampling (chapter 6.4). In addition, the inter-annual variability is assessed, again by using classification models (chapter 6.5).

6.1 Contents of (trace) elements measured in spider webs

A total number of 52 elements in the samples has been determined in this work. Descriptive statistical numbers for 28 elements are regarded in this chapter. A detailed table of these numbers can be found in the appendix (Tab. A-13). The decrease of the number of elements by nearly a half is due to analytical problems dealing with Sc, using only La as a representative for lanthanide elements and elimination of elements due to too many values below the LOD.

Highest contents were found for elements that occur either in biological (K, Na, P and S) or in geogenic material (Al, Ca, Fe, Mg and Si). They range between 14,600 µg/g (Ca) and 3,150 µg/g (Mg) and are in the range of minor components. All other elements are in the range of trace components with values from 379 µg/g (Zn) down to 1.14 µg/g (Th). Most of the contents found in this work have the same order of magnitude as contents in the literature and only some show a difference of maximum one order of magnitude (e.g. HOSE et al. 2002; RYBAK et al. 2012; RYBAK et al. 2015; XIAO-LI et al. 2006). As this difference can often be noted for selected sampling locations in the present work, it might be due to different local sources of PM. Remarkably higher contents of Ca in this study for example are expected

to be derived from geogenic dust, as a lot of carbonate rocks occur in Jena and its surroundings (SEIDEL 1993). For Cr, Fe and Ni higher values were found in this study at locations with tram/train traffic. This type of traffic has not been regarded in the literature and thus higher contents might be due to local emissions from tram/train traffic. Nevertheless, it has to be noted that contents of several elements are only given by RYBAK (2015) with 16 elements, while all other studies on spider webs focus on very few elements.

The order of the elements (Ca > Fe > K > … > Al > … > Mg > Zn > Ti > Mn > … > Cu > … > Cr > Ni > … > Pb > … > Co) is similar to the one RYBAK (2015) names, who found Ca > Fe > K > Al > Zn > Mg > Ti > Mn > Cu > Pb > Ni > Cr > Co in spider webs from Wrocław, Poland. Similar orders were found for PM_{10} with slight differences that might be due to either local sources of dust or differences between the analytical methods. For PM_{10} samples from Augsburg, Germany, Fe > Ca > K > Mg > Cu > Zn > Mn > Cr > Pb > Ni > Ti has been found (GU et al. 2011) and for samples from Madrid SALVADOR et al. (2004) found Fe > Ca > K > Mg > Pb > Cu > Zn > Ti > Mn > Cr > Ni.

In addition to contents of elements, variation of the data series should be regarded. It can provide first information on which elements can be used to identify sources of PM and is expressed as the interquartile range (IQR) as percentage of the median in this work. For half of the elements this number is around 100%. Substantially bigger numbers were found for Cu, Sb, Sn, Ti and Zn, indicating a pronounced inhomogeneous distribution. Those elements are expected to be suited to identify heterogeneously distributed, anthropogenic sources of PM in the following. On the other hand, substantially lower numbers were found for K, Mn, Na, P, Rb, S and Si which are either part of the spider webs themselves (K, Na and S) or derived from a natural (background) source, e.g. Si from geogenic material (RACHOLD et al. 1992; WORK and YOUNG 1987). They do likely describe a homogeneous characteristic of PM and the web material itself. This finding corresponds well with the explanation given by ORDÓÑEZ et al. (2003), indicating that a homogeneous distribution of heavy metals is typical for natural sources while a heterogeneous distribution hints to anthropogenic ones.

If an element is derived from a natural or anthropogenic source can also be assessed using enrichment factors. In this work EFs using Al as normalizing element, abbreviated as EF_{Al}, are regarded. For the spider web samples, grouped according to the type of traffic at the sampling locations, they are shown in Fig. 6-1. Mainly EFs greater than one can be found, indicating either a relative enrichment of all of the elements or comparably low contents of Al in the samples (ENAMORADO-BÁEZ et al. 2015). The latter likely explains some of the enrichment, as Al is not totally dissolved during aqua regia digestion (chapter 3.7). An either mixed or pronounced anthropogenic enrichment can be found for transition elements (starting from the sixth group in the periodic table) and p-block elements. These elements do typically occur in man-made products. Cr, Fe, Mn and Ni for example can be found in steel alloys while galvanized materials contain Zn (HUBER et al. 2016; JOHANSSON et al. 2009). For some of these elements, comparably high EFs can be found for a selected type of nearby traffic,

indicating that these elements are typical for PM at these locations. Those are mainly Ba, Cr, Fe, Mn and Ni for tram/train traffic. In contrast, alkali and alkaline earth metals are mainly of natural origin. They occur in rocks and soils, therefore geogenic sources do often predominate (SALMINEN et al. 2005). This is likely also true for Ba and Ca, whose higher EFs are due to their greater occurrence in Triassic evaporites like the ones occuring in the area of Jena compared to UCC (LIPPMANN et al. 2005; OKRUSCH and MATTHES 2010). Higher EFs found for K do also not implicitly indicate an anthropogenic influence, as spider webs are enriched in K by nature (RACHOLD et al. 1992).

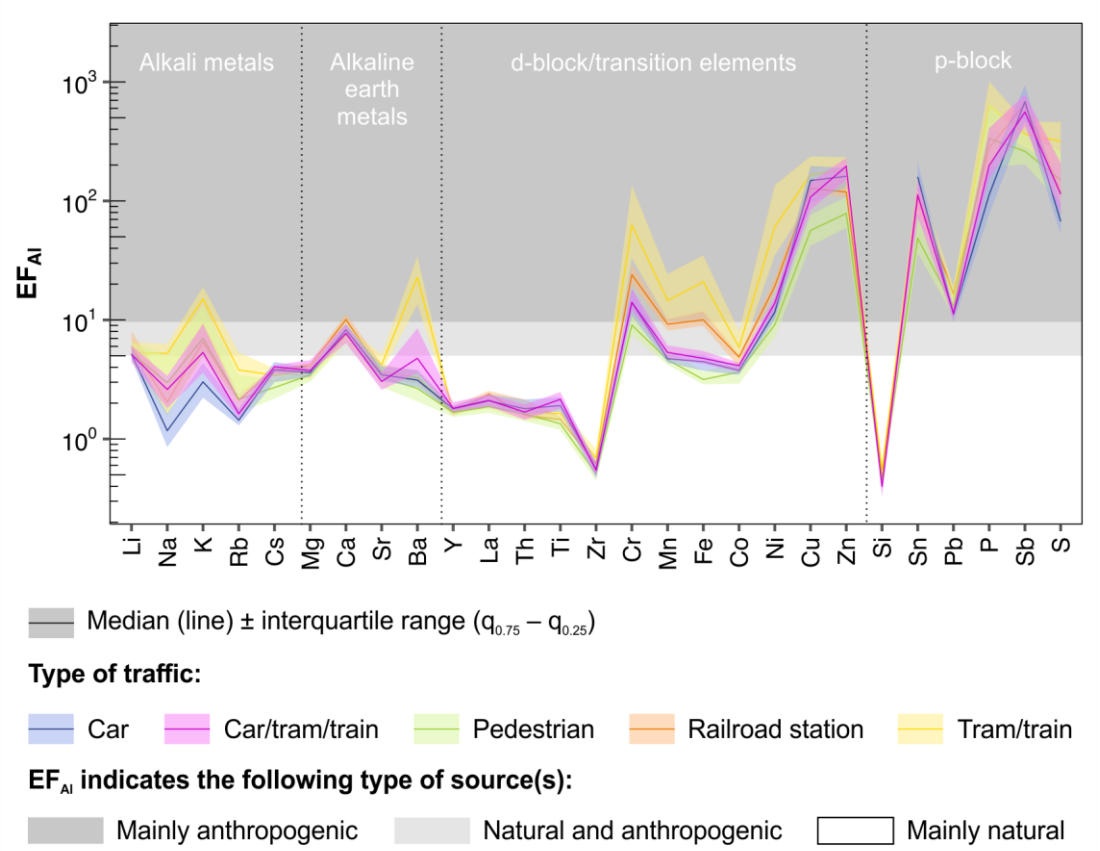

Fig. 6-1: Enrichment factors of elements in spider webs from locations with different types of traffic: car (n = 107), car/tram/train (n = 27), pedestrian (n = 80), railroad station (n = 9) and tram/train (n = 42). Al has been used as internal normalizing element and contents in the upper continental crust given by WEDEPOHL (1995) were used as geogenic reference.

As influences on locations within a group might still vary, median EFs for each location can be regarded in addition (appendix Tab. A-14). With this approach, differences between types of location and within a type of location become (more) visible: Substantially higher EFs of Ba, Cr, Fe, Mn and Ni at locations with tram/train traffic are especially true for location TR-ARE, which is distant from any car traffic and has both tram and train traffic. It can also be seen that Sn and Zn have especially high EFs at some of the locations with car traffic and Sb spans a broad range of numbers from below 100 to above 1,000.

For comparison, EF_{Al} has been calculated with the same formula for contents in spider webs from Wrocław, Poland, as given by RYBAK (2015). The numbers are in the same range for

Co, Cr, Fe, K and Mg, while a higher enrichment can be calculated for Ca, Cu, Mn, Ni, Pb, Ti and Zn in spider web samples from Wrocław compared to the samples from Jena. Slight differences that can be found are expected to be due to different local sources of PM rather than differences in e.g. the analytical methods, as they occur only for some elements. Other EFs from the literature can be used for comparison as well but were calculated using other references for contents in the upper continental crust. RACHOLD et al. (1992) for example found similar values for EF_{Al} for Ca, Co, Cr, Fe, K, Ni and Ti in a spider web sample from Hamburg, Germany. Substantially higher EFs for Pb, Sb and Zn in the cited study might be due to the fact that the sampling was performed prior to the complete phase-out of leaded gasoline in Europe and more severe emission regulations defined in e.g. 2008/50/EC (98/70/EC; HUBER et al. 2016). For PM_{10} samples from Gijón, Spain, MEGIDO et al. (2017) found similar tendencies for EF_{Al}: EFs greater than 100 were found for Cr, Cu, Ni, Pb, Sb, Sn and Zn. Generally higher EFs for PM_{10} samples with substantially lower ones for P and S are due to the (diluting) effect of biomass in the spider web samples containing P and S. EFs for elements occuring in spider silk (like K, Na and S) thus have to be regarded with care.

Conclusion: Evaluating data series for single elements already shows which elements are rather derived from geogenic or from anthropogenic sources. The latter are mainly heavy metals or p-block elements for which large EFs and a high variation of the data series can be found. Anthropogenic PM therefore is characterized by a heterogeneous distribution. For selected elements, EFs do also inherit substantial differences between the different types of nearby traffic, possibly allowing for a separation of those sampling locations in the following. Those are Ba, Cr, Fe, Mn and Ni (high EFs for tram/train traffic) and Sn and Zn (high EFs for car traffic).

6.2 Groups of elements with similar behaviour and element patterns

To assess the similarity of elements, a cluster analysis was performed. The smaller the distance between two elements in the resulting dendrogram, the more similar they behave (DU TOIT et al. 1986). Additionally, the longer the distance for which a cluster persists (no further elements are added), the more stable the cluster is (DANZER et al. 2001). In this study, similarity is expected to be due to emission of the elements from the same source.

The dendrogram for the cluster analysis of 28 elements in the space of the 265 samples (collected 2016-2018) is shown in Fig. 6-2. At a relative distance of 25% four clusters can be found that can be ascribed to different sources and properties of the samples. The first one (cluster I) consists of Cs, Cu, Sb, Sn, Zn and Zr forming a rather stable cluster. Four of the elements, Cu, Sb, Sn and Zn, have been shown previously to be anthropogenically enriched in the samples. All four of them occur in brake wear (HEINRICHS and BRUMSACK 1997; STERNBECK et al. 2002). JOHANSSON et al. (2009) also pointed out that the correlation of Cu and Sb is a clear indication for brake wear. Thus, cluster I is ascribed to brake wear from automobile traffic. Cluster II contains 13 elements of which only Pb has been shown to be anthropogenically enriched. All other elements (Al, Ca, Co, La, Li, Mg, Rb, Si, Sr, Th, Ti and

Y) are not (highly) enriched in the samples and most of them have been named as elements describing the geogenic background (FURUSJÖ et al. 2007; ORDÓÑEZ et al. 2003). Therefore, these elements are ascribed to geogenic dust blown into the valley from the hillsides and surroundings of the city. An exception is Rb, which is quite distant from the geogenic elements and rather connected to biomass than to geogenic particles (MEGIDO et al. 2017).

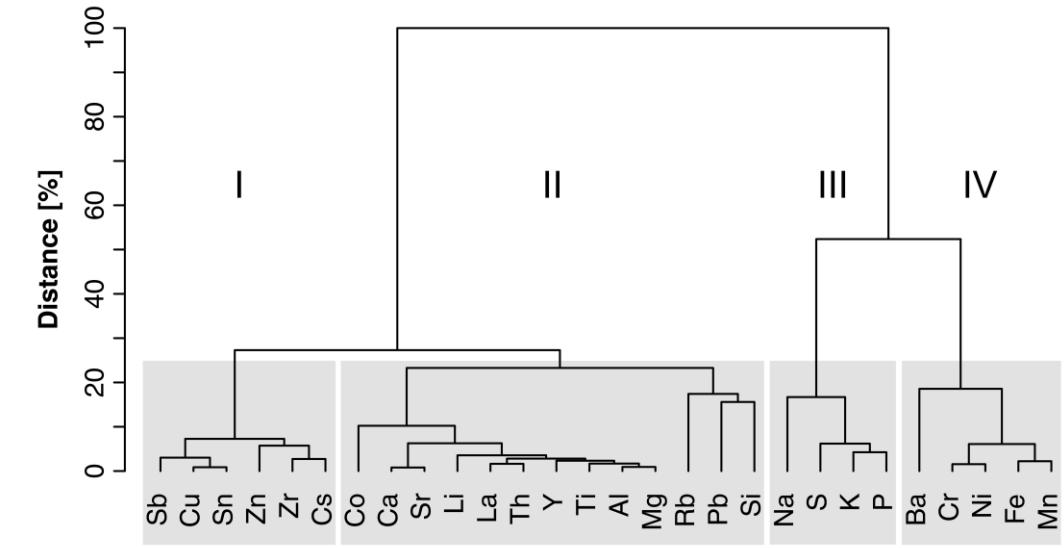

Fig. 6-2: Dendrogram (Ward's algorithm, squared Euclidean distances) depicting the cluster analysis of 28 elements in spider web samples from Jena in the object space (265 samples, collected 2016–2018). At a relative distance of 25% four clusters are formed.

Cluster III contains K, Na, P and S that have been described previously as part of biological material. S for example is part of the amino acid residues forming the spider silk (WORK and YOUNG 1987). The two alkali metals K and Na have been mentioned by RACHOLD et al. (1992) to be enriched in spider web material. Thus, their occurrence in the samples is not only due to natural dust, as deduced in chapter 6.1, but also to the biological material itself. Cluster IV consists of Ba, Cr, Fe, Mn and Ni. Those are mainly typical anthropogenic elements occuring in various products and processes. A group of products that can contain all of the elements are steel alloys (JOHANSSON et al. 2009; MEGIDO et al. 2017). Also Ba, which is often regarded as being rather derived from geogenic sources (e.g. ORDÓÑEZ et al. 2003), has been connected to steel products (LAHD GEAGEA et al. 2007). As there are no big steel producing or processing industries in Jena and its direct surroundings, cluster IV is ascribed to abrasion of steel emitted from traffic. In the following it has to be checked if this is emitted mainly by car traffic, mainly by tram/train traffic or by both of them.

As clusters I, II and IV are ascribed to different sources of PM, two of them being related to traffic, contents of the corresponding elements should vary for different types of nearby traffic. An exemplary element for each cluster is shown in Fig. 6-3. The representatives for clusters I (Zn) and II (Mg) show much higher contents in samples from locations with car traffic. In addition to brake wear particles (cluster I), car traffic thus also seems to increase the amount of geogenic PM. This is likely due to enhanced resuspension of homogeneously dis-

tributed natural dust by driving vehicles. In contrast, Ni as a representative for cluster IV shows high contents in samples from locations with tram/train traffic. The cluster has previously been ascribed to steel abrasion and can now be ascribed concretely to abrasion of tram/train tracks. As expected for the biological material, no substantial differences can be found for contents of K (representative of cluster III) in samples from different locations.

To reveal not only the most prominent but all connections between elements, Spearman rank correlation coefficients (r_s) were calculated (appendix Tab. A-15). Sub-matrices of elements strongly correlated with each other can be found that are, as expected, similar to the results of the cluster analysis: A sub-matrix of Cr, Fe, Mn and Ni (r_s = 0.85–0.95), one of Cu, Sb, Sn and Zn (r_s = 0.89–0.96) and a sub-matrix containing Al, Ca, Co, Cs, La, Li, Mg, Sr, Th, Ti, Y and Zr (r_s = 0.81–0.99) can be found. In the latter, the connection of Cs and Zr with other mainly geogenic elements becomes more visible than in the dendrogram. High correlation coefficients between Cu, Sb, Sn and Zn on one hand and elements in the sub-matrix of geogenic elements on the other (r_s = 0.69–0.86) confirm the assumption drawn before that geogenic PM is preferentially resuspended at locations with car traffic. For Na, Rb and Si no high correlation with any element can be found. This shows that their occurrence in a cluster does not indicate a same origin of the elements but they are merged to the most fitting cluster as they have to be part of a cluster. Another new finding is the fact that the elements of cluster III are not as closely connected to each other as the elements in other clusters (r_s = 0.28–0.78). In addition, the only negative correlations in the correalation matrix are found for K and P with other elements. On one hand this confirms the assumption that they are connected to the biological material diluting elements occuring mainly in dust particles. On the other hand, S seems to behave differently from K and P, even though they form one cluster in the dendrogram, as no significant negative correlations can be found for it.

RYBAK (2015) did also calculate Spearman rank correlation coefficients for her spider web samples from Wrocław, Poland. Some results are in line with current findings, but there are also differences, likely due to differences in local sources, host rock geology and the sampling method. She found for example high correlations between Cr, Cu, Ni and Zn and ascribed them to traffic as one source while in the present study the source traffic can be split up further with Cr and Ni belonging to tram/train track abrasion and Cu and Zn belonging to car traffic. A possible reason might be the lower number of six sampling sites in Wrocław, that did not include any tram/train traffic location. Few correlations with Ca in the Wrocław samples are likely due to differences in the local host rock geology and soil types. In addition, no negative correlation of K with other elements was found. A reason might be the sampling of funnel webs instead of wheel webs in the study of RYBAK (2015), as the chemical composition of spider silk can be highly variable (RACHWAŁ et al. 2018; WORK and YOUNG 1987).

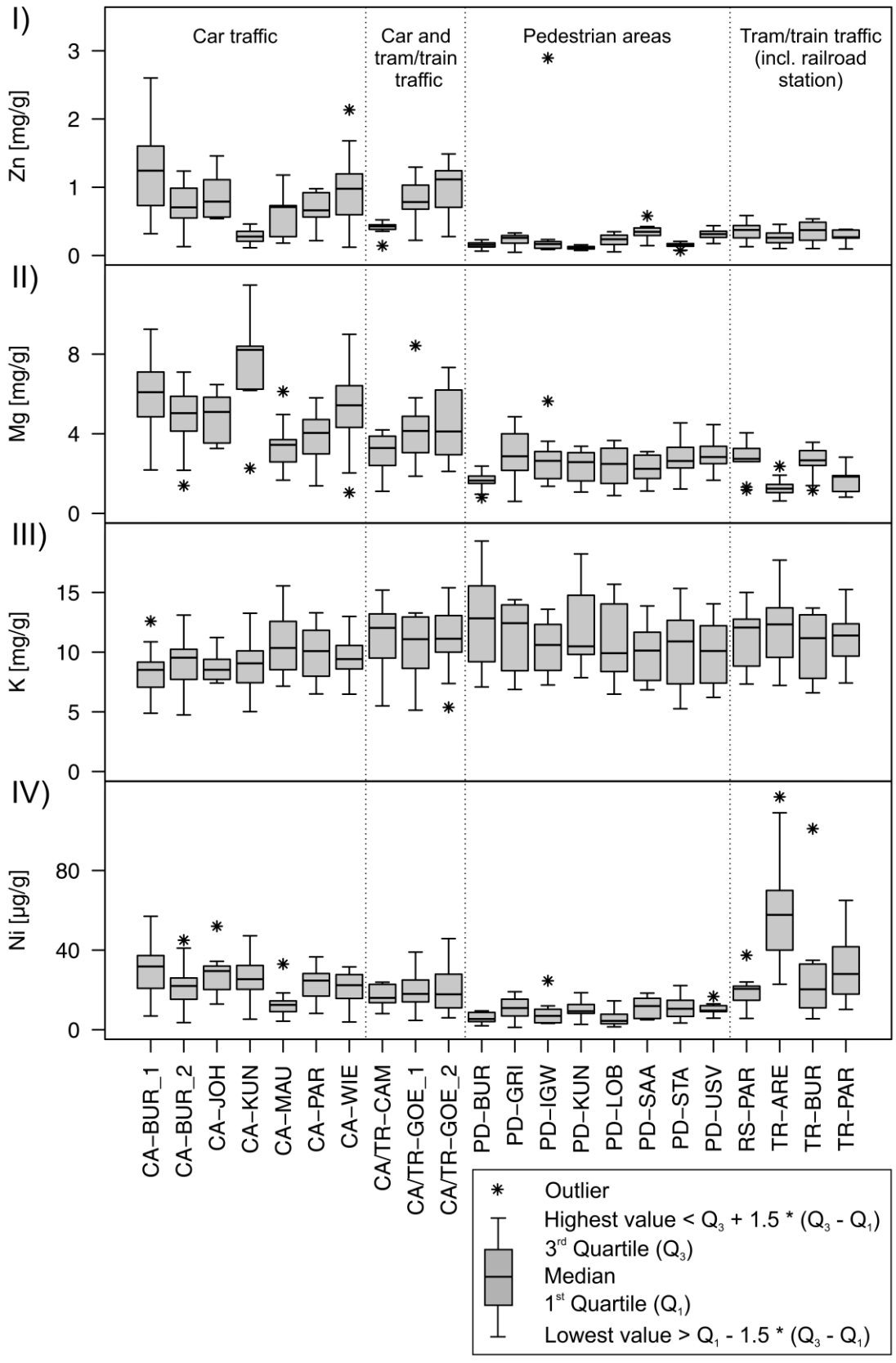

Fig. 6-3: Exemplary element contents in spider webs from the different sampling locations as representatives for the clusters in the dendrogram. I) Cs, Cu, Sb, Sn, Zn, Zr, II) Al, Ca, Co, La, Li, Mg, Pb, Rb, Si, Sr, Th, Ti, Y, III) K, Na, P, S, IV) Ba, Cr, Fe, Mn, Ni.

Conclusion: This approach shows that not only the dendrogram itself but also other features should be used to assess all connections between the elements and yield reliable results. Overall, three to four potential sources of PM could be identified by the cluster analysis and by regarding contents per sample location for exemplary elements: brake wear, geogenic dust, possibly exhaust emissions (Pb) and steel abrasion from tram/train tracks. Further information could be gained by examining correlation coefficients that do also exhibit that Na, Rb and Si are quite dissimilar to all other elements.

6.3 Identification of sources of urban particulate matter

By not only regarding element patterns but also their connections with the objects, primal source identifications can be confirmed or denied and additional sources might be found. For this purpose, principal component analysis and factor analysis were used. In contrast to cluster analysis, elements can be assigned to more than one factor, allowing for the identification of different influences on the particular element. In addition, variance explained by the groups of elements can be assessed with these tools.

First, a principal component analysis with all 265 samples was performed. For models with four to six principal components (most suiting according to criteria named in chapter 3.6.4) five samples showed a high leverage (high Hotelling's T^2) and a high sum of squared residuals (Q residuals). Those five samples where thus removed from the data set and a factor analysis with varimax rotation was calculated and evaluated for source identification for the 260 samples left. Even though the Guttman-Kaiser criterion and the screeplot (appendix Fig. A-6) would indicate a model with five factors (explaining already more than 80% of the variance), six factors were extracted. This has been done to separate the influence of Na and Rb from the one of Si. The correlation matrix has already shown that they are not (highly) correlated and with only five factors they would be merged in the fifth factor. Tab. 6-1 gives an overview on the factor loadings and communalities. All elements show high loadings for one or maximum two factors and except for Ba, Co, Na and Pb high communalities can be reached. For all factors, high (positive) scores are connected to high contents of the elements with which they are highly loaded.

In the course of the evaluation, the factors are ascribed to the following sources of PM or underlying properties of the samples: geogenic/natural dust (factor 1), brake wear (factor 2), abrasion of tram/train tracks (factor 3), an influence of changing pollen drift in spring (factor 5), an influence of the sample weight (factor 6) and the spider web material itself (factor 4). This assignment will be explained in detail in the following paragraphs.

Factor 1 explains nearly half of the variance explained by the model and is highly loaded with Al, Ca, Co, Cs, La, Li, Mg, Mn, Pb, Sr, Th, Ti, Y, Zn and Zr. These are mainly elements that are part of cluster II in the cluster analysis, except for Cs, Zn and Zr (cluster I) as well as Mn (cluster IV). The latter are good examples for elements being allocated to more than one group of elements (more than one source of PM) in contrast to the dendrogram. Many of the

elements in factor 1, like Al, Ca, Li, Mg, Sr and Ti, have already been discussed as being mostly of geogenic origin. Therefore, factor 1 is ascribed to resuspension of geogenic/soil particles. As described in chapter 2.4, Jena is located in a valley surrounded by many agricultural fields. Agricultural activities like ploughing or leaving fields fallow can enhance the erosion of geogenic/soil material which is then transported into the city and resuspended by driving vehicles (GUÉGUEN et al. 2012).

Tab. 6-1: Factors loadings and communalities (h_i^2) resulting from the factor analysis (varimax rotation) of 260 spider web samples from 22 locations in Jena as well as variance explained by the factors. Only factor loadings with an absolute value higher than 0.50 are shown.

Element	Factor 1	Factor 2	Factor 3	Factor 4	Factor 5	Factor 6	h_i^2
Al	0.92						0.96
Ba			0.63				0.35
Ca	0.89						0.89
Co	0.71						0.59
Cr			0.91				0.85
Cs	0.69	0.61					0.89
Cu		0.85					0.92
Fe			0.90				0.85
K				0.86			0.92
La	0.89						0.87
Li	0.87						0.84
Mg	0.91						0.93
Mn	0.58		0.74				0.79
Na				0.57	-0.52		0.66
Ni			0.95				0.87
P				0.85			0.87
Pb	0.72						0.63
Rb					0.74		0.80
S				0.88			0.82
Sb		0.85					0.95
Si						0.92	0.96
Sn		0.84					0.93
Sr	0.85						0.79
Th	0.91						0.89
Ti	0.83						0.88
Y	0.93						0.95
Zn	0.55	0.69					0.78
Zr	0.67	0.58					0.84
Variance explained [%]	39	15	14	10	4	4	-

The same is true for factor 6 that is highly loaded only with Si and describes 4% of the variance. A plot of the factor scores of those two factors shows that they jointly describe an influence of the sample weight (see Fig. 6-4) on the data set. Most of this effect is nevertheless inherited in factor 6. The effect is likely due to the use of aqua regia digestion: A higher ex-

cess of acids for low sample weights may lead to a higher percentage of silicates in the sample being digested, as only the use of HF ensures a quantitative digestion of alumosilicate materials (SASTRE et al. 2002, see also chapter 3.7). Since most of the spider web samples were very light, it was not possible to prevent this by always using the same sample weight per amount of acids. In addition, most of the samples with a high weight have been taken at locations with car traffic (see Fig. 6-5). Road dust has been described by many authors as containing noticeably high amounts of mineral dust resuspended by driving vehicles which might not be properly dissoluted by aqua regia (e.g. ADAMO et al. 2011; SANTACATALINA et al. 2010). Therefore, a part of factor 1 together with factor 6 is ascribed to effects of the digestion.

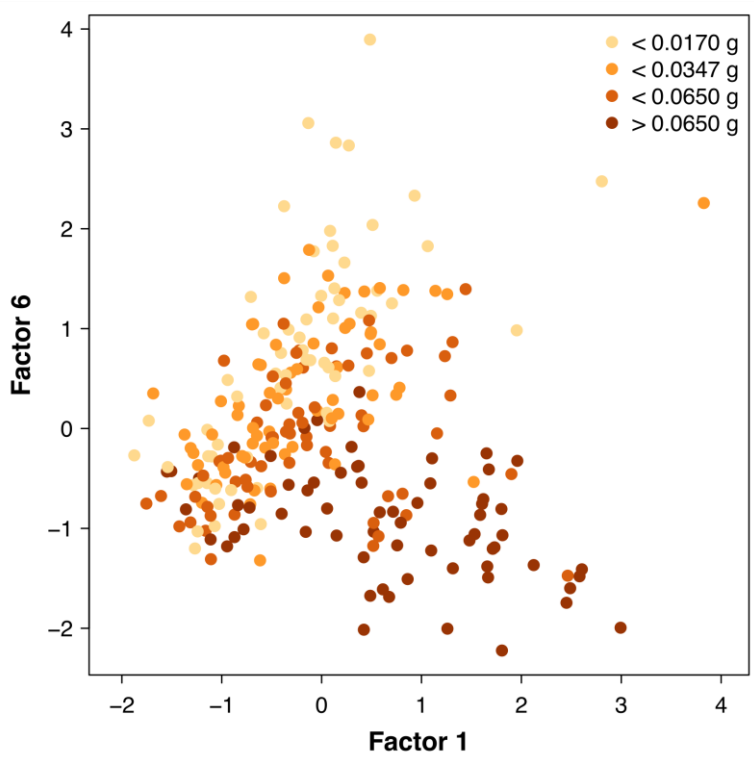

Fig. 6-4: Plot of the factor scores for factors 1 and 6 (factor analysis with varimax rotation) of 260 spider web samples from Jena, color coded according to the sample weight (4 quartiles).

Factor 2, explaining 15% of the variance, is highly loaded with Cs, Cu, Sb, Sn, Zn and Zr (similar to cluster I). The correlation between Cu, Sb, Sn and Zn has already been ascribed to brake wear. This is still assumed as the factor has high scores (> 2.0) for samples from two locations with a high amount of car traffic (CA-BUR_1 and CA-JOH, see Fig. 6-6). At both locations cars have to brake at a frequented junction, thus an amplified occurrence of brake wear particles is probable. The third factor, explaining 14% of the variance, is highly loaded with Ba, Cr, Fe, Mn and Ni (similar to cluster IV) and has been ascribed to steel abrasion of tram/train tracks. Very high scores can be found for samples from location TR-ARE with both tram and train traffic and without any car traffic in the surroundings (see Fig. 6-6). Compared to previous studies, this is a further piece of information as abraded steel particles were connected to steel parts of driving cars or brake wear in those studies (e.g. FURUSJÖ et al. 2007; HUBER et al. 2016; KUMMER et al. 2009).

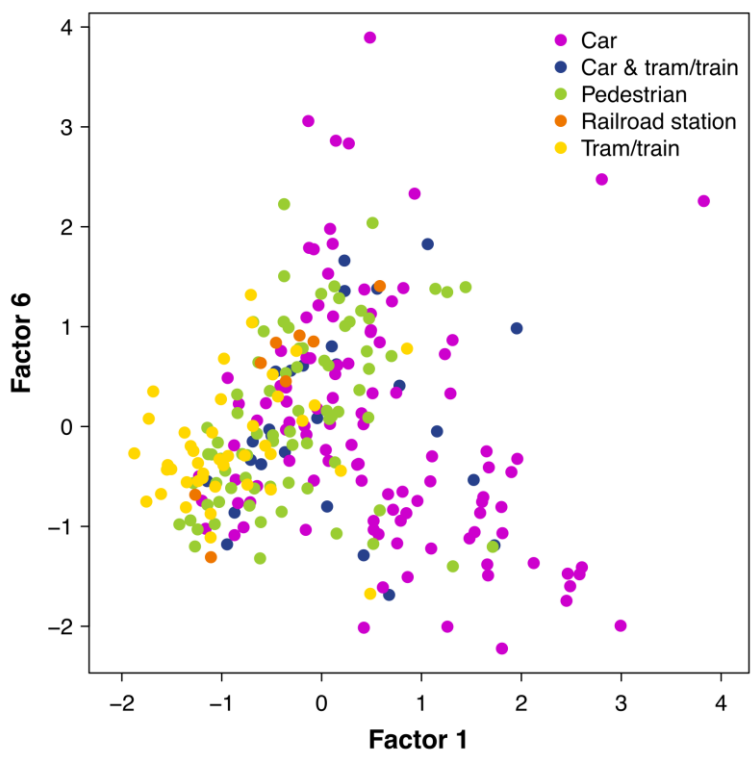

Fig. 6-5: Plot of the factor scores for factors 1 and 6 (factor analysis with varimax rotation) of 260 spider web samples from Jena, color coded according to the type of nearby traffic.

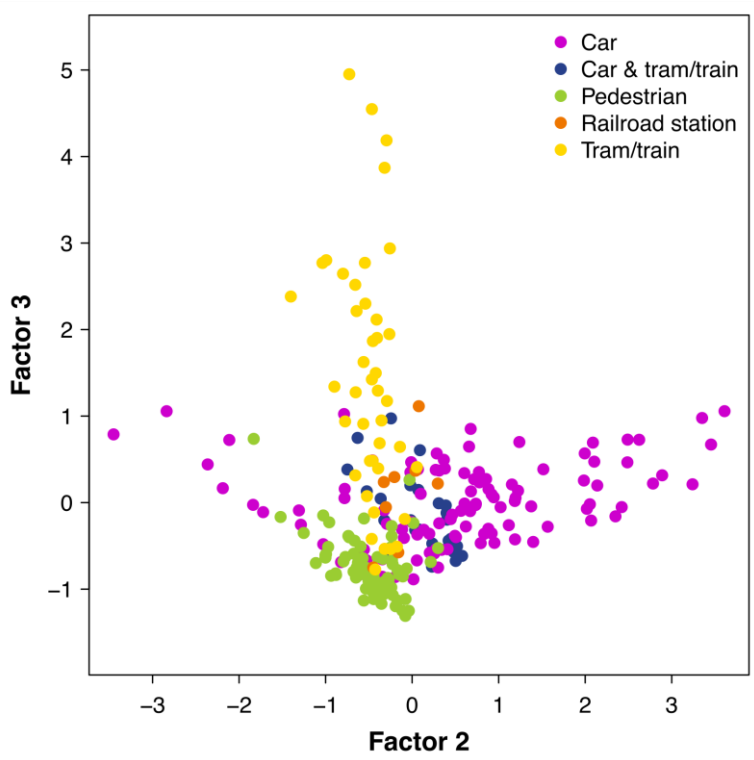

Fig. 6-6: Plot of the factor scores for factors 2 and 3 (factor analysis with varimax rotation) of 260 spider web samples from Jena, color coded according to the type of nearby traffic.

The remaining two factors 4 and 5 explain 10% and 4% of the variance respectively. A slight seasonal influence on the data can be seen in Fig. 6-7, where samples have been color coded according to the expected dominant type of pollen: trees (April to 15th May), grasses (16th

May to end of July) and mugwort (August and September). High and low scores of factor 5 are mainly found for samples taken in early to mid spring (tree pollen). The factor has a high positive loading of Rb and a high negative loading of Na. Rb is a tracer for plant biomass (pollen) that dilutes the spider web biomass (containing Na according to RACHOLD et al. 1992), but adds no other metals to the sample. An example for this is a group of ten samples taken at the end of April 2018 that is separated from all other samples in Fig. 6-7 by high scores for factor 5. In April 2018, warm temperatures (mean: 14 °C) several degrees higher than the longtime average were detected in Jena while only two weeks before temperatures were below 0 °C (ERNST-ABBE-HOCHSCHULE JENA 2019). This rapid increase might have induced a very quick development of pollen of different tree species at a time, being present in the corresponding samples. An influence of different pollen drift might thus be described by factor 5.

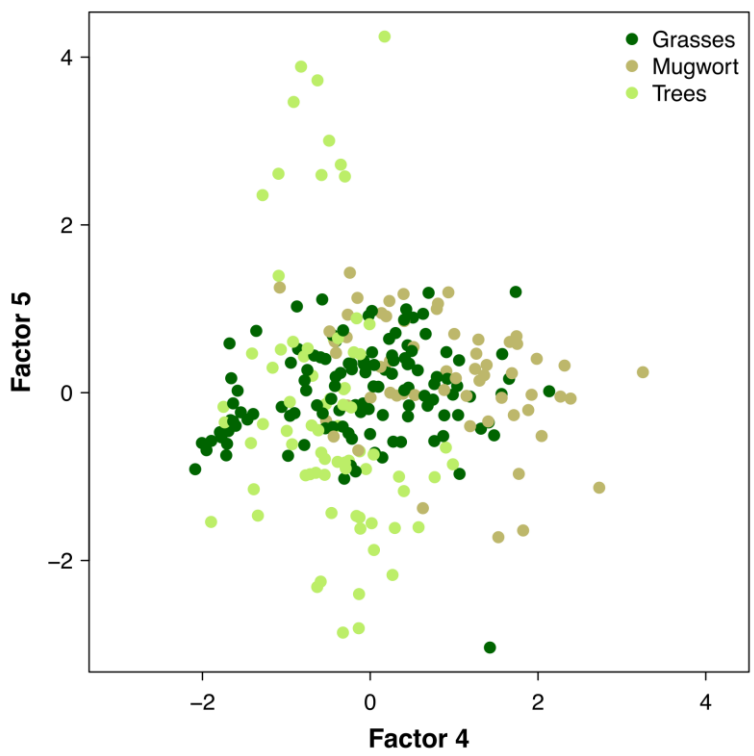

Fig. 6-7: Plot of the factor scores for factors 4 and 5 (factor analysis with varimax rotation) of 260 spider web samples from Jena, color coded according to the expected predominant type of pollen (April – 15th May: trees, 16th May – July: grasses, August and September: mugwort).

The scores plot for factors 4 and 5 was color coded according to other different criteria to check for further potential sources of PM: days without rain before the sampling, district of the sampling location (intra-urban versus suburban), sample weight, type of nearby traffic, wind direction at the day of the sampling, wind force (Beaufort scale) and year of the sampling. None of these led to a clear distinction of groups or identification of an influence on the data set. This meets the expectations for factor 4, that is highly loaded with K, Na, P and S. Those elements have been ascribed to the influence of biological material which should be rather uniform compared to e.g. anthropogenic local sources of PM.

So far, factor analysis to detect sources of PM has only been done once for spider web samples. RYBAK (2015) calculated a factor analysis for spider web samples from three locations in Wrocław, Poland, that were expected to be polluted by either motor traffic or a nearby slag heap of a former chromite ore smelter. These expected pollutions have been found in two factors, describing 87% of the variance. The factors extracted in the present factor analysis explain nearly the same amount of variance in the data set. Thus, an explained variance of 80–90% seems to be suitable for spider web data. As the data set presented here contains more locations that were also sampled at different times, variation in this data set likely covers more sources and temporal changes as discussed for example for factor 5. Traffic as a source of PM could be identified in both studies, but in the present work this can be split into two different sources. Since several mainly geogenic elements are included in the present study, it also covers the influence of mineral/soil dust which has not been regarded by RYBAK (2015). This source should not be disregarded, as soil has been named a major contributor of PM on a global scale (MEGIDO et al. 2017). BIAN et al. (2003) for example stated that natural and anthropogenic mineral dust account for up to half of the total annual aerosol emissions.

Conclusion: The tool of factor analysis of element contents was suitable to identify sources of PM entrapped in spider webs in the city of Jena. Six factors were extracted of which the first three ones, explaining nearly 70% of the variance, can clearly be related to the sources geogenic dust, brake wear (car traffic) and abrasion of tram/train tracks (rail traffic). Traffic therefore seems to be the major anthropogenic issue of PM in Jena. It could also be shown that elements can be essentially emitted/influenced by more than one source (Cs, Zn and Zr in geogenic dust and brake wear and Mn in geogenic dust and abrasion of tram/train tracks). Apart from the clear sources, influences of pollen drift in spring and of the spider web material itself as well as a minor influence of the sample weight could be found.

6.4 Reclassification of pre-defined types of nearby traffic and classification of further spider web samples

The factor analysis has shown that the trace element composition of spider web samples from Jena is influenced to a great extent by particles emitted by different types of traffic. Therefore, a grouping of samples should also work the other way around, identifying types of nearby traffic of a sampling location by examining element contents of the corresponding samples. Different classification models were tested for this purpose (appendix Tab. A-16). They can also be used to review results of a PCA/FA (e.g. SKRBIĆ and DURISIĆ-MLADENOVIĆ 2010). In the following only linear discriminant analysis and partial least squares-discriminant analysis with six latent variables (number of latent variables extracted for the factor analysis) are regarded, since they exhibit the best rates of reclassification and cross-validation.

A major advantage of classification models is the classification of new/unknown samples based on their measured features (in this case element contents). In contrast to the multivariate analyses performed so far (cluster analysis, PCA, FA), classification models allow for the

assignment of further samples to groups/classes even after the model was calculated. Nevertheless, a method of unsupervised learning like cluster analysis, PCA of FA should be calculated prior to a classification model since for those methods classes/class memberships do not need to be known as they have to for a classification.

Five types of nearby traffic were applied as classes ("car", "car & tram/train", "pedestrian", "railroad station" and "tram/train"). In addition, models were calculated with only three classes (incorporating "car & tram/train" into the class "car" and "railroad station" into the class "tram/train") to yield classes with more members and avoid problems during cross-validation. Tab. 6-2 lists the rates of correct classification for the two methods and the two sets of classes. Rates of correct classifications are fairly good, ranging between 82% (PLS-DA, 5 classes) and 92% (3 classes) for reclassification and 78% (PLS-DA, 5 classes) and 90% (LDA, 3 classes) for cross-validation, which gives more reliable results (DANZER et al. 2001).

Tab. 6-2: Rates of correct classification of a linear discriminant analysis (LDA) and a partial least squares-discriminant analysis (PLS-DA) calculated with 260 spider web samples from Jena classified to either five or three different types of nearby traffic.

Classes	**Classification**	**LDA**	**PLS-DA (6 latent variables)**
Car (n = 106) Car & tram/train (n = 27) Pedestrian (n = 76) Railroad station (n = 9) Tram/train (n = 42)	Reclassification	88%	82%
	Cross-validation	83%	78%
Car (n = 133) Pedestrian (n = 76) Tram/train (n = 51)	Reclassification	92%	92%
	Cross-validation	90%	88%

These results emphasize the influence of traffic on element contents from another perspective: While classification models focus on the best distinction between groups/classes, factor analysis focuses on explaining most of the variance in the data set. Fig. 6-8 gives an optical impression on the discrimination of the samples. It shows the 260 samples used to build the LDA model in the space of the linear discriminant functions (LDFs) 1 and 2. They explain most of the between-group variance, namely 57% and 31%. The first LDF separates the class "car" from the class "tram/train". Differences between those two classes are therefore the biggest ones between the five classes. LDF 2 separates the class "pedestrian" from the others. It has to be noted that there is an intersection area where the classes overlap, meaning that they are not completely separated (at least not by LDF 1 and 2). As expected before, the classes "car & tram/train" and "railroad station" can be incorporated in the classes "car" and "tram/train" respectively. They might be cut off by LDF 3 and LDF 4, but their separating power is low.

In addition, class means of the individual elements (means of autoscaled element contents for each class) can be regarded (appendix Tab. A-17). Like factor loadings, they can be as-

sessed to find underlying relations. For Al, Ca, Cs, Mg, Sr, Th, Ti and Y, that have been ascribed to the source of geogenic/soil dust, means are comparably high for the class "car" and low for "tram/train". This finding does indicate that the biggest differences between PM at locations with car traffic and tram/train traffic are not the various direct emissions from traffic, but more likely the different rates of resuspension of geogenic/soil dust. The class "pedestrian" as the third big one is mainly characterized by low class means of elements that have been identified as emitted by brake wear (Cu, Sb, Sn, Zn) or tram/train track abrasion (Cr, Fe, Mn, Ni) and exhibit high class means for the related classes. As extreme means can only be found for the three big classes while the classes "car & tram/train" and "railroad station" are inbetween them, the two small classes might be incorporated in the three bigger ones as it has been done in the approach with three classes.

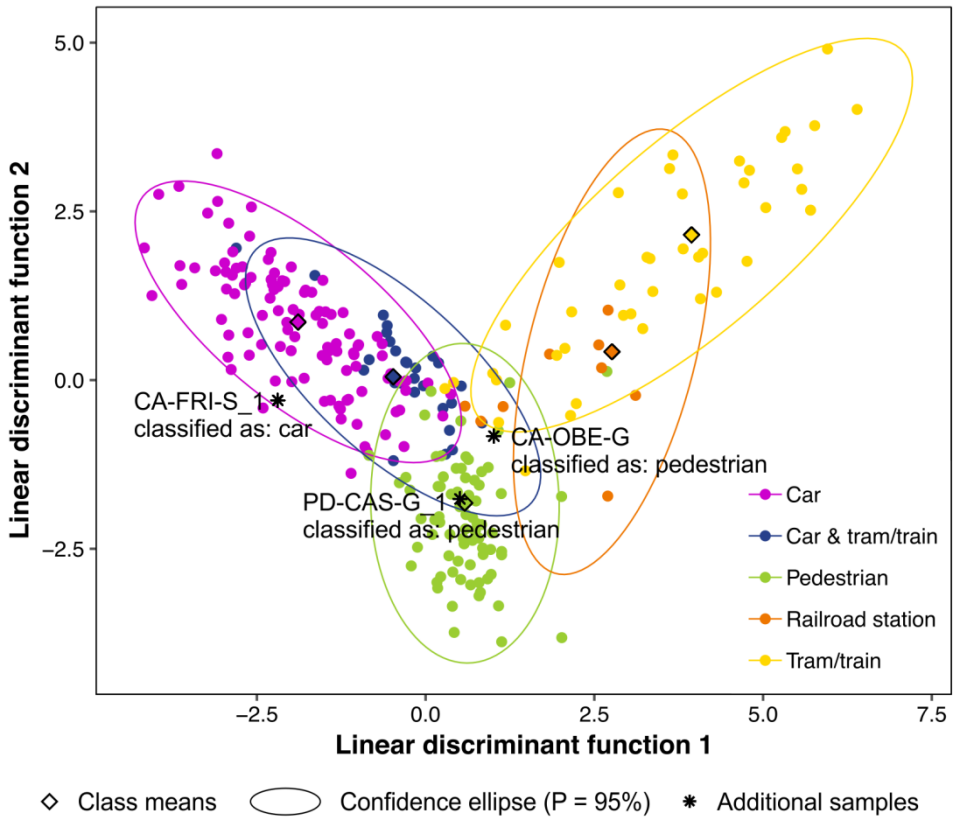

Fig. 6-8: Plot of 260 spider web samples (used to calculate the model) in the space of the first two linear discriminant functions. Asterisks show three exemplary additional samples and how they are classified by the model.

A classification of new samples based on their measured features (in this case element contents) has been done with 28 spider web samples from additional locations, using the classification model. Only samples that can be grouped into one of the classes incorporated in the model were used. This classification shall also show how representative the model is for samples from other locations in Central Germany since not all additional samples were taken in Jena. Examples for the classification of new samples are shown in Fig. 6-8. Samples that are rather close to a class mean (e.g. PD-CAS-G_1) are correctly classified while samples that lie at the edge of a class or even outside the confidence ellipse might not be classified correctly.

CA-OBE-G for example has been taken at a road with a low amount of car traffic but is classified as a "pedestrian" sample by the classification model.

Pre-defined and assigned classes according to the LDA model can be found in Tab. 6-3. Additional samples taken in Jena are correctly classified, showing that samples from other locations but within the sampling grid of the samples used to build the model can be nicely classified. Regarding the samples taken in the city of Suhl, those from locations with a high amount of car traffic (CA-SCH-S, CA-FRI-S_1, CA-FRI-S_2) are correctly classified, while samples from locations with existent but less car traffic are not. Similar results can be found for the city of Greiz, where samples from locations with tram/train traffic or pedestrian areas are correctly classified, but samples from locations with car traffic are classified as "pedestrian". Like Jena, both cities are located in Thuringia and in a valley, but they exhibit a smaller size (Greiz: 20,000 inhabitants, Suhl: 35,000 inhabitants), likely connected to a lower amount and influence of car traffic (THÜRINGER LANDESAMT FÜR STATISTIK 2019). An indication for this are also the annual means for PM_{10} measured at federal monitoring stations. The value for Jena (category "urban background") amounts to 18 µg/m³, while for the station in Suhl, close to a main road (category "urban traffic"), only 16 µg/m³ were determined (UMWELTBUNDESAMT 2019). Furthermore, the local climate might vary between the cities, influencing particle distribution and resuspension. Similar results can be found for other additional spider web samples (e.g. CA-LIE_1, CA-LIE_2, CA-AIR), leading to an overall rate of correct classification of 61%.

As far as the author knows, no classification has been done with spider web samples to assess PM so far. The findings discussed however show that this can be a useful tool for the assessment of air quality. Classification models might allow for a simplified assessment and comparison of dust samples, as only a set number of classes is regarded, which can still incorporate various pieces of information like element contents. This could be a useful tool for non-experts that do not want to focus on a broad number of detailed information. Nevertheless, classification models should be interpreted carefully (e.g. taking into account intersections of classes as described here). Substantial effort would also be needed to build the model, as the data set used for this has to cover all types of land-use/major sources influencing PM in the area of interest. An application of such a model would for example allow for the identification of changing influences at a set monitoring location, if the new samples are grouped into another class.

Conclusion: The classification model approach does work in general. For samples from the same city it allows for an assessment of major influences on new/unknown samples. Individual models have to be built for each city/area of interest, covering their individual features resulting from e.g. traffic density, amount of rail versus car traffic and urban ventilation capacity. For the city of Jena, three main classes could be found, being linked to the types of nearby traffic to the sampling locations: "car", "tram/train" and "pedestrian". The biggest difference between these classes is the one between locations with car traffic and with

tram/train traffic. It has been shown to be driven to a big extent by the different rates of re-suspension of geogenic/soil dust. The third class of samples from pedestrian areas is characterized mainly by low contents/class means.

Tab. 6-3: Pre-defined classes and classification according to the linear discriminant analysis (calculated with 260 spider web samples from Jena) for additional spider web samples.

Location/ sampling campaign	Sample ID	Pre-defined class	Class according to the LDA	Correctly classified?
Meckenbach, Rhineland-Palatinate	PD-MEC	Pedestrian	Pedestrian	Yes
Sampling campaign in Suhl, southern Thuringia 20th July 2016	CA-SCH-S	Car	Car	Yes
	CA/TR-RAI-S	Car & tram/train	Pedestrian	No
	CA-FRI-S_1	Car	Car	Yes
	CA-BUS-S_3	Car	Pedestrian	No
	CA-BUS-S_2	Car	Car & tram/train	No
	CA-BUS-S_1	Car	Car & tram/train	No
	CA-FRI-S_2	Car	Car	Yes
Sampling campaign in Greiz, eastern Thuringia 7th June 2016	TR-RAI-G_1	Tram/train	Tram/train	Yes
	TR-RAI-G_2	Tram/train	Tram/train	Yes
	PD-ELS-G	Pedestrian	Pedestrian	Yes
	PD-WEI-G	Pedestrian	Pedestrian	Yes
	CA-FRI-G_1	Car	Pedestrian	No
	CA-MOL-G	Car	Pedestrian	No
	CA-OBE-G	Car	Pedestrian	No
	PD-CAS-G_2	Pedestrian	Pedestrian	Yes
	PD-CAS-G_1	Pedestrian	Pedestrian	Yes
Greiz, 4th July 2018	CA-FRI-G_2	Car	Pedestrian	No
Additional samples taken in Jena	CA/TR-GOE-J	Car & tram/train	Car & tram/train	Yes
	CA/TR-BUR-J	Car & tram/train	Car & tram/train	Yes
	RS-GOE-J	Railroad station	Railroad station	Yes
	CA/TR-CAM-J	Car & tram/train	Car & tram/train	Yes
Großheringen	RS-GRO	Railroad station	Railroad station	Yes
Bridge crossing a motorway close to Liebertwolkwitz, Saxony	CA-LIE_1	Car	Pedestrian	Yes
	CA-LIE_2	Car	Pedestrian	Yes
	CA-LIE_3	Car	Car	No
	CA-LIE_4	Car	Car	No
Motorway bridge at an airport in Central Germany	CA-AIR	Car	Pedestrian	No
Correct classification				61%

6.5 How representative are samples from only one year?

When assembling data to assess PM or to build a classification model, a question arising might be: How many samples are needed and how representative is a selected (sub)set of the data? One potential variation that needs to be covered by the data set is the inter-annual variation of weather conditions. The question to be answered is if data acquired in only one year is representative for other years. In the course of this study, a similar, repeated sampling of

spider webs in Jena has been performed both in 2017 and in 2018 (April to September in each case). Local weather conditions in the two years have been quite different (see Tab. 6-4): In 2018, the amount of rainfall has been substantially lower and air temperatures have been much higher than in 2017. This might have influenced both particle amount and composition of PM. To give an impression on potential differences between the two years in the data set, selected element contents in samples from locations TR-ARE and CA-BUR_2 are shown in the appendix (Fig. A-7 and Fig. A-8). Classification models (LDA and PLS-DA) with the same 28 elements as in Tab. A-17 were built individually for each year, using all the samples (from 22 locations in Jena) acquired in this year. Afterwards, each model was used to classify samples from the other year. Rates of correct classification for the different models can be found in Tab. 6-5.

Tab. 6-4: Mean air temperature and rainfall during the sampling periods of spider webs in 2017 and 2018 (MAX PLANCK INSTITUTE FOR BIOGEOCHEMISTRY 2019).

Parameter	Year	April	May	June	July	August	September	Overall
Temperature [°]	2017	7.7	14.8	18.2	19.0	18.7	13.0	15.3
	2018	13.2	16.3	18.5	21.1	20.5	15.3	17.5
Rainfall [mm]	2017	37	53	65	92	81	18	346
	2018	16	37	11	48	19	58	189

Rates of correct classification of samples from the other year are comparable for both years and only a little lower than the rates for the cross-validation of the model built with 260 samples from three years (see Tab. 6-2). They range between 76% and 79% for five classes and 81% and 89% for three classes. Therefore, current data sets for single years seem to cover mainly the same conditions: If data from one year covered a broad range of meteorological and environmental conditions and data from the other one covered only a part of it, classifications would be expected to be much better for the second one. For both sets of classes (either five or three ones), classification of samples from the other year with the LDA model is better for one year while PLS-DA works better for the other one. Thus, none of the methods is inferior. Given the comparably big differences between weather conditions of the years 2017 and 2018, these findings give a good impression. To further test this, comparable data sets from more years would be needed. Within the course of a PhD project this has not been possible.

Conclusion: On the present data base, changing weather conditions between the years do not seem to influence the composition of PM in the city of Jena. Still, they might influence the total amount of PM but this does not influence the classification as data sets were autoscaled prior to multivariate analysis. This does indicate that one year of sampling yields enough samples to build a classification model. Rates of correct classification would not be very close to 100% but due to the overlap of classes as found in chapter 6.4, classification models in this case will presumably never reach a rate of 100%.

Tab. 6-5: Rates of correct classification of a linear discriminant analysis (LDA) and a partial least squares-discriminant analysis (PLS-DA) calculated from spider web data for one year and applied to spider web data of the other year.

Classes	Data set to build the model	Classification	LDA	PLS-DA (6 latent variables)
Car Car & tram/train Pedestrian Railroad station Tram/train	2017	Reclassification (2017 data)	93%	86%
		Classification of 2018 data	76%	79%
	2018	Reclassification (2018 data)	93%	82%
		Classification of 2017 data	78%	76%
Car Pedestrian Tram/train	2017	Reclassification (2017 data)	96%	90%
		Classification of 2018 data	86%	81%
	2018	Reclassification (2018 data)	95%	92%
		Classification of 2017 data	83%	89%

6.6 Summary

The detailed evaluation in this chapter shows that spider webs are a useful tool to assess air quality with regard to (trace) element distributions and to identify sources of PM in the city of Jena. Resuspended geogenic/soil dust is the source describing the largest part of the variation, identified by Al, Ca, Co, Cs, La, Li, Mg, Pb, Sr, Th, Ti, Y, Zn and Zr. Two directly traffic-related sources could be identified: brake wear, identified by Cu, Sb, Sn and Zn, and abrasion of steel tram/train tracks, identified by Ba, Cr, Fe, Mn and Ni. In addition, an influence on the element patterns of the biological material of the webs themselves could be found (K, Na, P, Rb and S). A cluster analysis could be utilized to preliminary identify those sources of PM. To confirm and quantify sources/connections between elements, a factor analysis was performed. In addition, a pronounced anthropogenic enrichment of Cr, Cu, Ni, Pb, Sb, Sn and Zn could be found in spider web samples from the city of Jena.

The differences between types of nearby traffic (land-use) at the sampling locations are rather distinct and allow for a classification of the samples. An evaluation of the classification model showed, that the difference between PM at car traffic locations and PM at tram/train traffic locations is mainly based on rates of resuspension: At car traffic locations, high levels of elements ascribed to geogenic/soil dust can be found while those levels are comparably low at tram/train traffic locations. Samples from pedestrian areas, the third main class, are characterized by low element contents in general.

This is one of the few studies so far using spider web biomonitoring in combination with factor analysis to identify sources of PM. For the first time, as far as the author knows, also a classification was applied. It proved to be a useful tool for the assessment of PM, incorporat-

ing much detailed information but providing simple results (class memberships). Applying classification models did also show that new studies and models will have to be performed and calculated individually for other cities/areas of interest. Within the current study area, no remarkable influence of an inter-annual variability of element contents in spider web samples could be found. One year of sampling has thus been shown to be representative if no big changes (e.g. building and opening of new motorways or factories) occur.

7 Comparison of biomonitoring and other tested non-classical methods to sample urban particulate matter

Different non-classical methods to sample urban PM have been tested in this PhD project. A comparison of the two biomonitoring techniques has already been described in chapters 5. Nevertheless, other methods applied show different characteristics and might lead to other results with regard to element contents and source identification. In addition, the feasibility of both sampling and sample preparation directly influence the size of the data set for evaluation, which might be of interest for further studies. Therefore, all four materials sampled to assess PM – spider webs, moss bags, dust from windows and long-term deposit – are compared in this chapter, focusing on feasibility (chapter 7.1), the number of elements that might be used for evaluation (chapter 7.2), (anthropogenic) influences on the data set (chapter 7.3) and potential source identifications (chapter 7.4). In addition, selected samples of different materials collected close to each other are compared (chapter 7.5).

7.1 Feasibility of the sampling and the sample preparation

All samplings and sample preparations are easier than common methods with for example cascade impactors that require expensive equipment and power supply (e.g. RYBAK 2015; URBAT et al. 2004). However, as described in chapter 3.1, sampling and sample preparation did vary for the different sample materials. For higher numbers of samples small differences between the individual samplings and sample preparations might become more important (see Fig. 3-1 for reference). The feasibility of these steps influences the overall amount of samples that can be taken.

Spider webs were sampled directly without further preparation. The sampling was easy as no bulky equipment was needed and all handrails were readily accessible. The most time consuming step has been the hand sorting to remove foreign objects like insects or hairs. Less effort in sample preparation was only needed for the dust samples from windows. For the latter material, the sampling took a little longer and equipment had to be carried around. The number of windows that could be probed in a row was also limited by battery life of the window vacuum cleaner: In the winter sampling campaign, sometimes only two or three locations could be probed per day.

For long-term deposit, equipment had to be built prior to the installation and further equipment like a driller and a hammer as well as the installations for the vessel itself were needed for the assembly of the sampling constructions. Besides, over the course of the year the height of the water head had to be checked regularly and water had to be removed when the vessels were almost filled. This has been of major relevance in autumn and winter, mainly for the 2017 sampling campaign. In the laboratory, removing excess water took up to two hours and only a limited number of samples could be processed in parallel.

The most complex preparation before exposure was needed for the moss bags. Moss had to be collected at a rural location in high amount, cleaned and dried. In addition, the bags had

to be prepared and afterwards were filled with dry moss material. In this project, also customized plastic mountings were produced manually. This took about 15 min per mounting which are not included in Fig. 3-1, as the mountings can be and have been reused for multiple sampling campaigns after careful cleaning. Therefore, even though moss bags have been exposed to ambient air at the same locations where spider webs have been sampled, sampling has been less flexible for moss bags than for spider webs.

Apart from the processing of the samples, an important aspect is the exposure time of the samples which is directly connected to the (practicable) frequency of the sampling. It has been shown by frequent sampling at four locations (CA-BUR_1, CA-BUR_2, CA-WIE and TR-ARE) that spider webs can even be sampled every two weeks from spring to autumn without noticeably reducing the number of spiders at the locations. For wheel webs as they have been regarded in this work, PM in the samples does only reflect the last day(s) before the sampling, allowing for a comparably high temporal resolution. For other methods, the period of exposure to ambient air has been longer. It has already been mentioned that moss bags have to be exposed for at least a month (ARES et al. 2012). In this project, ten weeks of exposure time were selected. A period of even three months has been kept between the sampling of dust from windows in order to allow for adhesion of a sufficient amount of material. Moss bags and dust from windows thus can point out seasonal variation. Long-term deposit samples did even represent PM from an entire year. Shorter exposure periods might not be possible as even with this period small amounts of samples were gained. Therefore, long-term deposit is rather suitable to show either average pollution levels (over time) or possibly reflect source terms if installed at an adequate location.

Conclusion: Spider webs are most flexible with regard to sampling and frequency of the sampling. In contrast, other materials cover PM from a longer frequency (months to a year) without the need for repeated sampling.

7.2 Elements quantified in the different sample materials

The extent of the data analysis and the conclusions drawn depend on which elements are included in the evaluation. Especially for multivariate tools, data sets combining different elements might lead to different results. In the first instance, this depends on which elements in the data set do not show too many values below the LOD and thus do not have to be excluded. As described in chapter 3.3, contents of up to 52 elements were determined in the samples. Elements were excluded from the data set if contents were below the LOD for more than 5% of the samples. Tab. 7-1 lists those elements for the different sample materials (excluding Hf, Nb, Sc, and W as described previously). The table does also include REE besides La that were not regarded in detail in this work but might be useful for other projects.

Spider webs show the greatest number of elements that could not be quantified while long-term deposit samples show the lowest number. Elements to be excluded vary for the different sample materials, but often several REE could not be quantified. An unexpected fact is the

exclusion of P from the dust from windows data set, as remaining P contents above the LOD in dust samples from windows are high (median: 1,331 µg/g) compared to other elements. This is due to the analytical method. P was determined with ICP-OES that is not as sensitive as ICP-MS, which has been used to determine contents of trace elements. In addition, Cd and V could not be quantified in all the spider web samples. These elements would have been of interest since Cd in PM is considered as purely anthropogenic and V is regarded as a tracer for oil combustion since it is enriched in fossil fuels (MEGIDO et al. 2017; NORRA and STÜBEN 2004; SUVARAPU and BAEK 2017).

Tab. 7-1: Elements for which too many analytical results (more than 5%) were below the limit of detection (LOD), listed for the different sample materials. Those elements were excluded from further data analysis.

Sample material	Elements with more than 5% of the values < LOD
Spider webs (n = 265)	Ag, As, B, Cd, Er, Eu, Ho, Lu, Mo, Tb, Tm, V, Yb
Moss bags (n = 30)	As, Lu, Tm
Dust from windows (n = 56)	Ag, As, Cs, Eu, Ho, Lu, P, Tb, Tm
Long-term deposit (n = 24)	As

If an element cannot be quantified does also depend on the sample weight used for digestion. The lower the sample weight, the higher is the LOD, leading to more contents that cannot be quantified. In the present case, different sample weights had to be used due to the local variation of dust accumulation. Only for moss bag samples, a fixed amount of around 200 mg of the sample has been available all the times. Tab. 7-2 gives an overview on the sample weights used for aqua regia digestion. They are lowest for spider webs and dust from windows, which both also exhibit a high variation of the sample weight.

Tab. 7-2: Weights of samples weighted in for the aqua regia digestion and corresponding interquartile rages (IQRs) for the different sample materials.

Statistical measure	Spider webs (n = 265)	Moss bags (n = 30)	Dust from windows (n = 56)	Long-term deposit (n = 24)
Median [g]	0.0345	0.2008	0.0448	0.1301
Minimum [g]	0.0033	0.1885	0.0010	0.0371
Maximum [g]	0.2005	0.2109	0.1975	0.2012
IQR [g]	0.0481	0.0059	0.0598	0.1065
IQR*100%/Median [%]	139	3	134	82

In the following, the same 26 elements will be regarded in the different materials to allow for a direct comparison. This includes Al, Ba, Ca, Co, Cr, Cu, Fe, K, La, Li, Mg, Mn, Na, Ni, Pb, Rb, S, Sb, Si, Sn, Sr, Th, Ti, Y, Zn and Zr. For long-term deposit, samples with only dry deposition (AIR2, RES5_1 and RES5_2) are excluded from further analysis: As they exhibit higher contents of most of the elements, clustering and variance explained will otherwise mainly focus on the difference between only dry and combined dry and wet deposition.

Conclusion: Overall, moss bags and long-term deposit samples are superior if a high number of elements, especially REE, are of interest for the evaluation. Nevertheless, a large number of

elements could be quantified in each sample material, allowing for a statistical evaluation (chapter 7.4). The obliged exclusion of the mainly anthropogenic elements Cd and V from the data set may be a disadvantage of the spider webs that should be regarded if those elements are of special interest.

7.3 Detectable anthropogenic influences on the samples

In this chapter, enrichment factors are assessed to figure out for which elements in which sample material anthropogenic influences can be assumed. Median EFs per sample material are shown in Fig. 7-1. In general, an anthropogenic enrichment (EF > 10) can be found for Cu, Ni, Pb, S, Sb, Sn and Zn in all sample materials while EFs for Co, Cr, K and Mn hint to a mixed origin from both natural and anthropogenic sources (5 ≤ EF ≤ 10). Higher EFs for Ca and Ba do not hint to an anthropogenic enrichment but are due to their occurrence in local host rocks (SEIDEL 1993), especially in Muschelkalk, with contents higher than those in UCC. Enrichments of Na in dust from windows and Mn in mosses have already been ascribed to the application of road salt in winter and occurrence in plant material respectively in chapter 4.3.

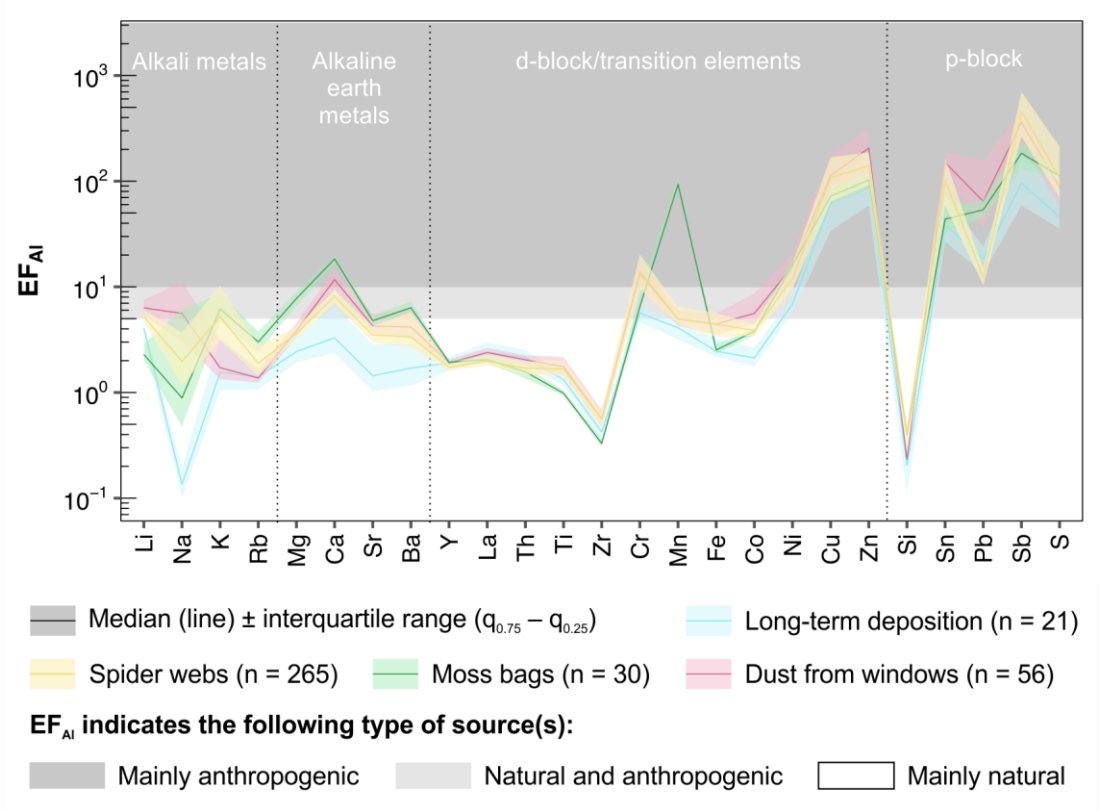

Fig. 7-1: Overall enrichment factors of elements in different sample materials: spider webs, moss bags, dust from windows and long-term deposit. Al has been used as internal normalizing element and contents in the upper continental crust given by WEDEPOHL (1995) were used as geogenic reference.

Big differences in EFs can be found for Pb and Sb. For Pb, highest EFs were calculated for dust from windows and moss bags while lowest EFs were found for spider webs. Pb is emitted by many anthropogenic sources, mainly ones connected to burning processes like exhaust emissions and coal combustion (KUMMER et al. 2009; QIANG et al. 2015; ZHU et al.

2015). They emit mainly ultra-fine particles (UFP), which stay suspended in the atmosphere for longer timescales compared to bigger particles like geogenic or abraded ones (HERTEL and GOODSITE 2009; LAHL and STEVEN 2005). An enrichment of Pb in UFP does therefore become more important with increasing height of the sampling (spider webs: maximum 1.1 m, moss bags: 2.5 m, dust from windows: maximum 2 m, long-term deposit: usually 1 m). EFs for Sb are lowest in long-term deposit samples. They are the only material that has also been sampled in rural areas. As a low importance of Sb from natural sources was pointed out by SALMINEN et al. (2005), Sb might act as a tracer for only anthropogenic PM. This corresponds to highly enriched contents of Sb that have been found in both urban and industrial areas in previous works (e.g. DONGARRÀ et al. 2007; GUÉGUEN et al. 2012).

As Al is used as an internal referencing element, the patterns overlap more than the ones for contents normalized to UCC in Fig. 4-5. It has to be kept in mind that Al is not totally dissoluted during aqua regia digestion (chapter 3.7). Some of the EFs thus might be a little too high. Low recovery rates do also lead to low values for some other elements like Si or Zr.

Different types of nearby land-use were noted down for the long-tern deposit samples. Patterns of EFs grouped according to those land-uses (as for types of nearby traffic in Fig. 6-1) exhibit different shapes, indicating land-use specific emissions (see Fig. 7-2). Apparent findings are higher EFs of Ca, K, Mg, Na, Rb and S in the sample from an airport and higher EFs of Ba, Cr, Cu, Fe, Mn, Sb and Sn (steel abrasion and brake wear) in samples from traffic-related locations (both road and rail transport). High EFs of S in the airport sample have been expected, as S is an element typical for aviation-related PM and has been recommended as tracer for aircraft emissions (SHIRMOHAMMADI et al. 2018; VANDER WAL et al. 2016). In addition, soil material containing Ca, K, Mg, Na and Rb might be resuspended with rates above average by turbine movements and resulting local winds. As the patterns overlap, an optical evaluation is not straightforward. Differences in EFs between various types of nearby traffic as found for spider web samples in Fig. 6-1 could not be found for moss bags, even though they were exposed to ambient air at the same locations as the spider webs (appendix Fig. A-9): The patterns for different types of traffic for moss bag samples are close to each other.

For moss bags, dust from windows and long-term deposit two sampling campaigns were performed (see Fig. 7-3). Different EFs for selected elements in the two campaigns hint to temporal changes of sources of PM. In moss bags, differences between summer and winter can be found for K, Na and Rb. Higher EFs of Na in winter have been ascribed to the application of road salt before. K and Rb are expected to be derived from biomass burning, leading to higher contents in moss bag samples in winter times (BARI and KINDZIERSKI 2016; MEGIDO et al. 2017). For dust from windows, only the difference in Na can be found: Higher EFs for Na were calculated for the spring sampling campaign, reflecting dust accumulated from December 2017 to March/April 2018. This includes the main part of the winter season when road salt was applied. A slight difference not between seasons but between years can be

found for long-term deposit. For 2018, a higher enrichment of some geogenic elements (Ba, Ca, Co, K, Mg, Rb and Sr) could be found in long-term deposit. As discussed in chapter 6.5, less rainfall happened in 2018, which has likely led to more erosion from dry soils. Therefore, geogenic dust is expected to have accumulated in the sampling vessels.

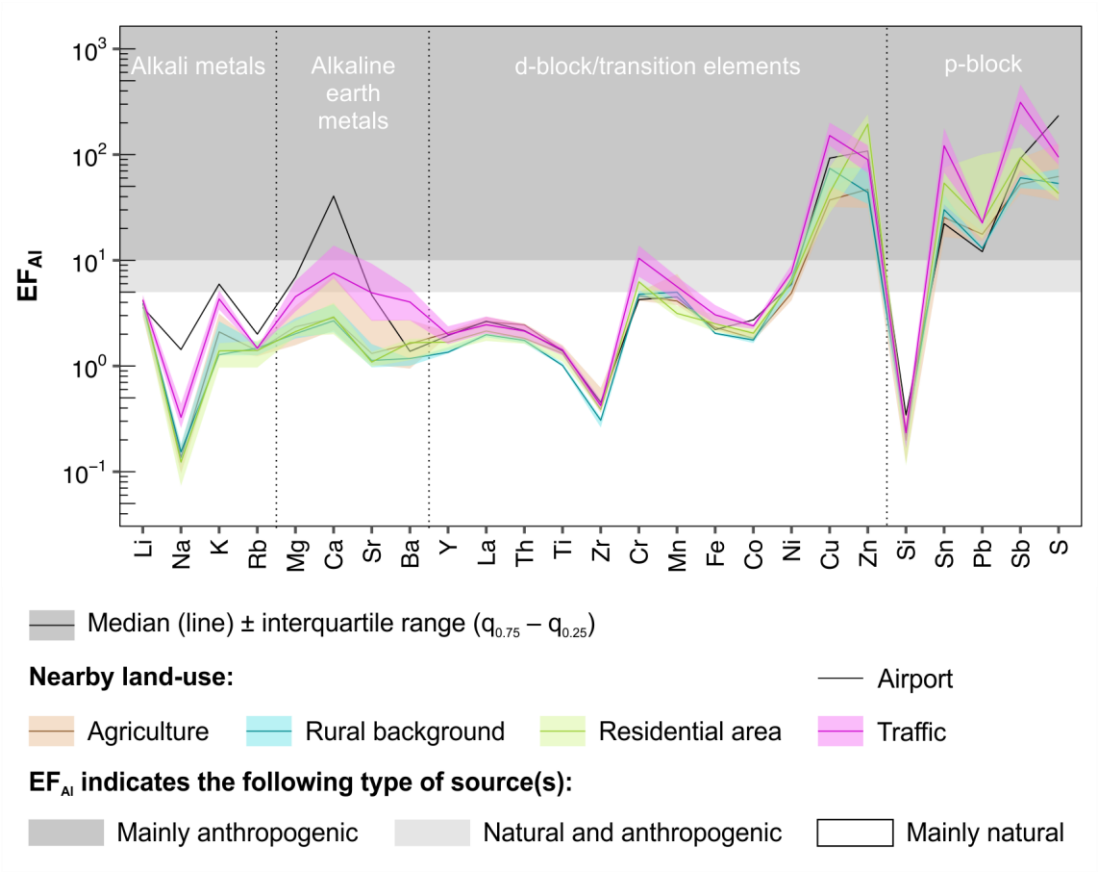

Fig. 7-2: Enrichment factors of elements in long-term deposit samples from locations with different nearby land-use: agriculture (n = 6), airport (n = 1), residential area (n = 7), rural background (n = 3) and traffic (n = 4). Al has been used as internal normalizing element and contents in the upper continental crust given by WEDEPOHL (1995) were used as geogenic reference.

Not two but various sampling campaigns were performed for spider webs. For comparison with Fig. 7-3, EFs of samples from two selected campaigns in April (spring) and August (late summer) 2017 are shown in Fig. 7-4. The patterns look similar and do not show any clear differences. The only striking features are broad distributions of contents of K and Na with higher contents of Na in spring samples and higher contents of K in late summer samples. Both elements occur naturally in spider webs (RACHOLD et al. 1992). Since the chemical composition of spider silk varies for different silk types, these variations might reflect the proportion of different silk types (e.g. spiral and radial thread) in the samples or an evolution of silk types over a spider's lifespan (VOLLRATH 1999; WORK and YOUNG 1987). Another possible reason might be changing contents of plant residues and parts of insects, containing K and Na as essential elements, that were too small to be removed (HOLLEMAN et al. 2007).

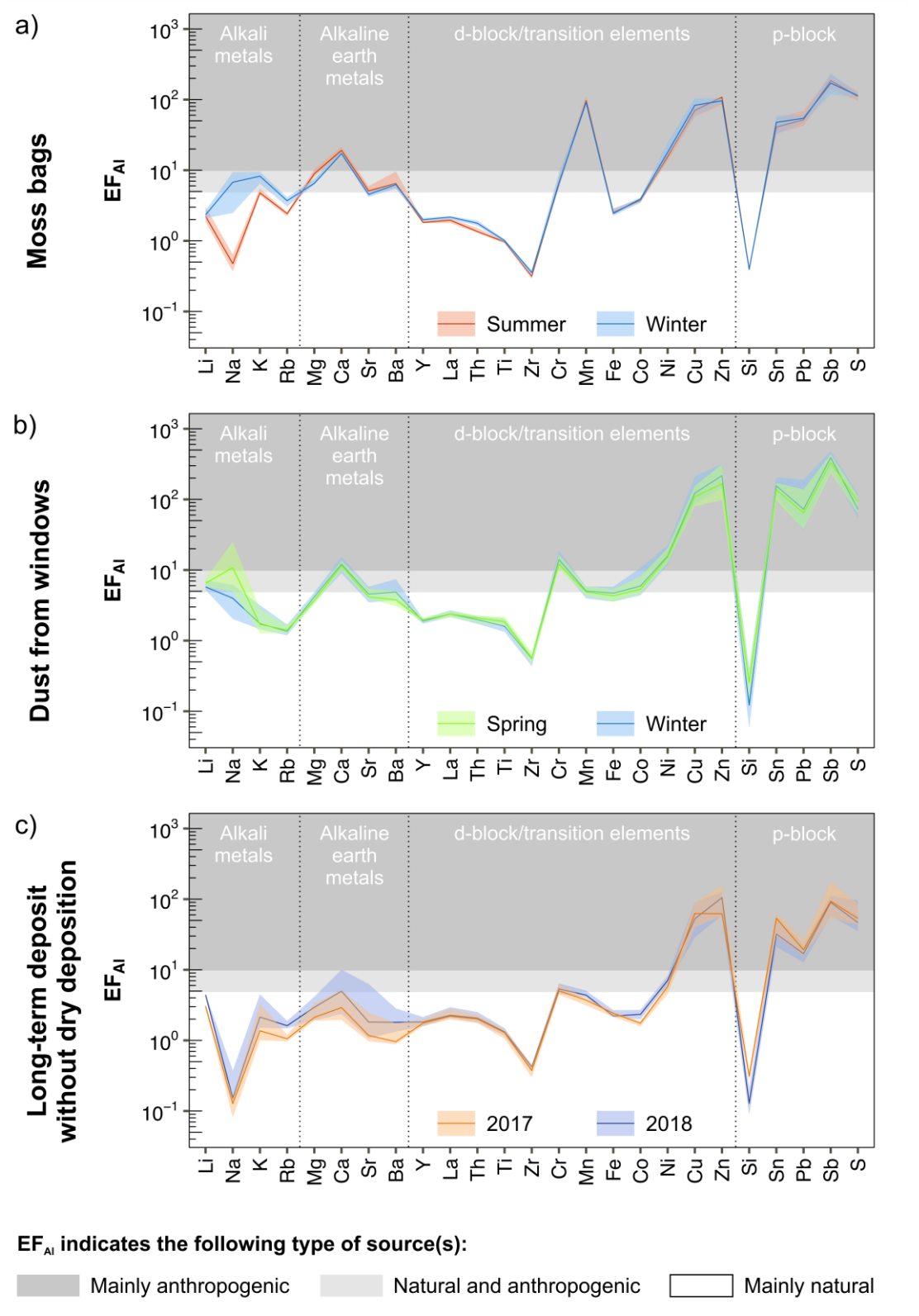

Fig. 7-3: Enrichment factors of elements in different sample materials per sampling campaign: a) moss bags (n = 15 per campaign), b) dust from windows (n = 28 per campaign), c) long-term deposit (2017: n = 9, 2018: n = 12). Al has been used as internal normalizing element and contents in the upper continental crust given by WEDEPOHL (1995) were used as geogenic reference.

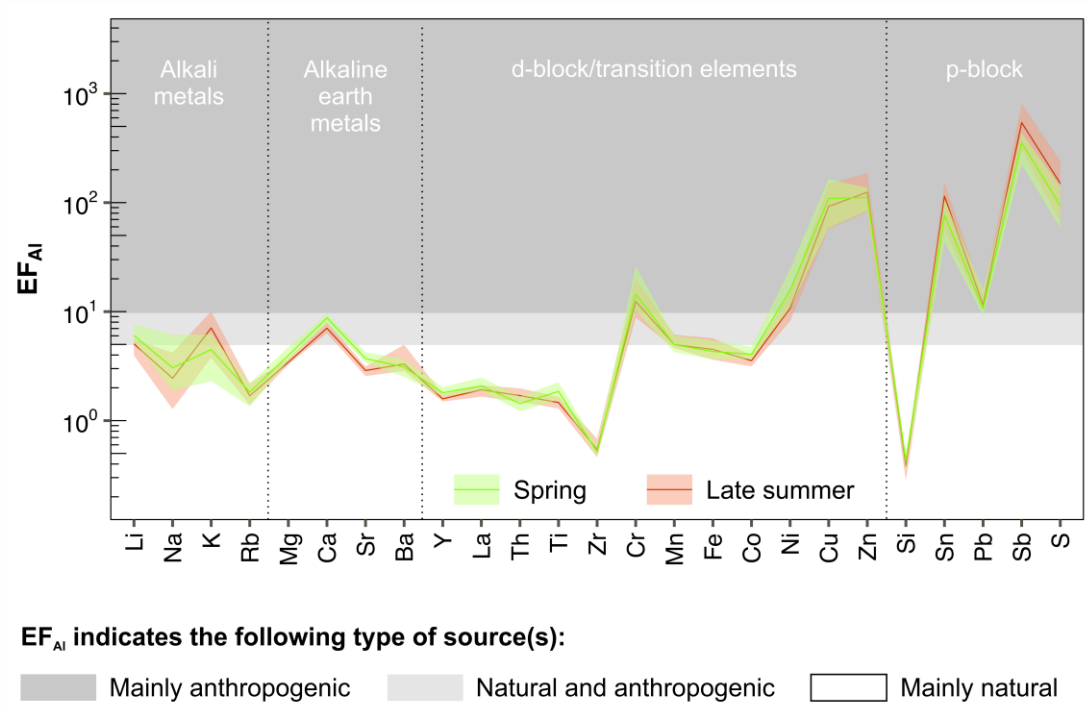

Fig. 7-4: Enrichment factors of elements in spider webs of two different sampling campaigns in 2017 (n = 22 per campaign). Al has been used as internal normalizing element and contents in the upper continental crust given by WEDEPOHL (1995) were used as geogenic reference.

Conclusion: The anthropogenic enrichment of the same elements (Cu, Ni, Pb, S, Sb, Sn and Zn) for all four sample materials shows that there are no systematic differences with regard to identifying a general anthropogenic influence. The biological dilution effect is reduced to some extent by the calculation of EFs as the patterns are close to each other. Apart from spider webs (chapter 6.1), an identification of sources of PM by examining EFs is also possible with the long-term deposit samples. In this case traffic (comparably high EFs for Ba, Cr, Cu, Fe, Mn, Sb and Sn) and aviation (Ca, K, Mg, Na, Rb, S) could be identified as sources. EFs do also allow for the identification of seasonal/annual change of sources for selected elements in moss bags (K, Na, Rb), dust from windows (Na) and long-term deposit (Ba, Ca, Co, K, Mg, Rb, Sr), while seasonal changes of spider web samples seem to reflect changes of the webs themselves or of varying dilution by organic material from pollen or insects.

7.4 Links between elements and source identification

Links between elements were assessed using correlation coefficients and cluster analyses as done in chapter 6.2 for spider webs. To give an overall impression on the strength of element connections, median and upper quartile ($q_{0.75}$) of all the absolute Spearman rank correlation coefficients (r_s) between the 26 elements are shown in Tab. 7-3. They indicate how closely elements are connected. Strongest links between elements can be found for spider web samples and lowest for dust samples from windows. However, for all four materials, $q_{0.75}$ is within the range of significant correlation coefficients, indicating that there are sufficiently high correlations between elements allowing for a multivariate evaluation of all four data sets.

Tab. 7-3: Median and upper quartile ($q_{0.75}$) of absolute Spearman rank correlation coefficients (r_s) for the different sample materials. Limits for significant r_s were taken from/calculated according to HEDDERICH and SACHS (2016).

Statistical measure	Spider webs	Moss bags	Dust from windows	Long-term deposit
n	265	30	56	21
Significant $\|r_s\|$	≥ 0.16	≥ 0.464	≥ 0.35	≥ 0.551
Median ($\|r_s\|$)	0.64	0.44	0.29	0.44
$q_{0.75}$ ($\|r_s\|$)	0.87	0.63	0.47	0.79

Elements linked to each other are also to some extent different for the sample materials. This can be seen in the dendrograms of the cluster analyses (see Fig. 7-5). For reasons of comparison, the relative distance at which four clusters are formed for the spider webs (30%) has been chosen for evaluation for all dendrograms. For spider webs, those four clusters have been identified as describing brake wear (cluster I), resuspension of natural/geogenic dust (cluster II), the influence of the spider web material (cluster III) and steel abrasion (cluster IV) in chapter 6.2. For the moss bags data set, six clusters are found. An identification of reasons for the clustering and/or connected sources of PM cannot be done only with the dendrogram. Cu, Sb, Sn and Zn for example, that have been identified previously to be derived from brake wear, form a cluster together with Ca, Fe and Sr that are of rather natural origin (HEINRICHS and BRUMSACK 1997; SALMINEN et al. 2005; STERNBECK et al. 2002). At the same time, other elements that have been in the cluster describing geogenic dust in spider webs (e.g. Al, Co, Ti) are part of another cluster (VI) for the moss bags.

Similar results can be found for long-term deposit with only three rather stable clusters. Similar to the dendrogram for moss bags, elements that have previously been ascribed to geogenic and to anthropogenic PM are combined in the clusters, especially in the big cluster III, that hampers an easy source identification. As a result of the low correlations between elements in dust from windows (sub-)clusters are merged at a comparably high relative distance for this material. At the relative distance of 30% nine clusters, some of them containing only one or two elements, can be found. An identification of sources of PM with only two elements that are even not closely linked to each other seems not to be suitable. Wrong conclusions might be drawn, especially for elements like Fe or Zn that can be emitted from different sources (ENAMORADO-BÁEZ et al. 2015; SUVARAPU and BAEK 2017).

Factor analyses were calculated for all four data sets to potentially identify sources of PM. To hopefully get factors with a similar amount of elements with high loadings, the same number of factors was extracted for all materials. A number of five factors was chosen as it does meet the Guttman-Kaiser criterion for spider webs and moss bags, and biomonitoring methods are of major interest in this work. Results for the different materials will be discussed shortly but not as detailed as for the spider webs in chapter 6.3. Tables of the factor loadings can be found in the appendix (Tab. A-18, Tab. A-19, Tab. A-20, Tab. A-21). For all materials, high scores correspond to high contents of the elements with which the factor is highly loaded.

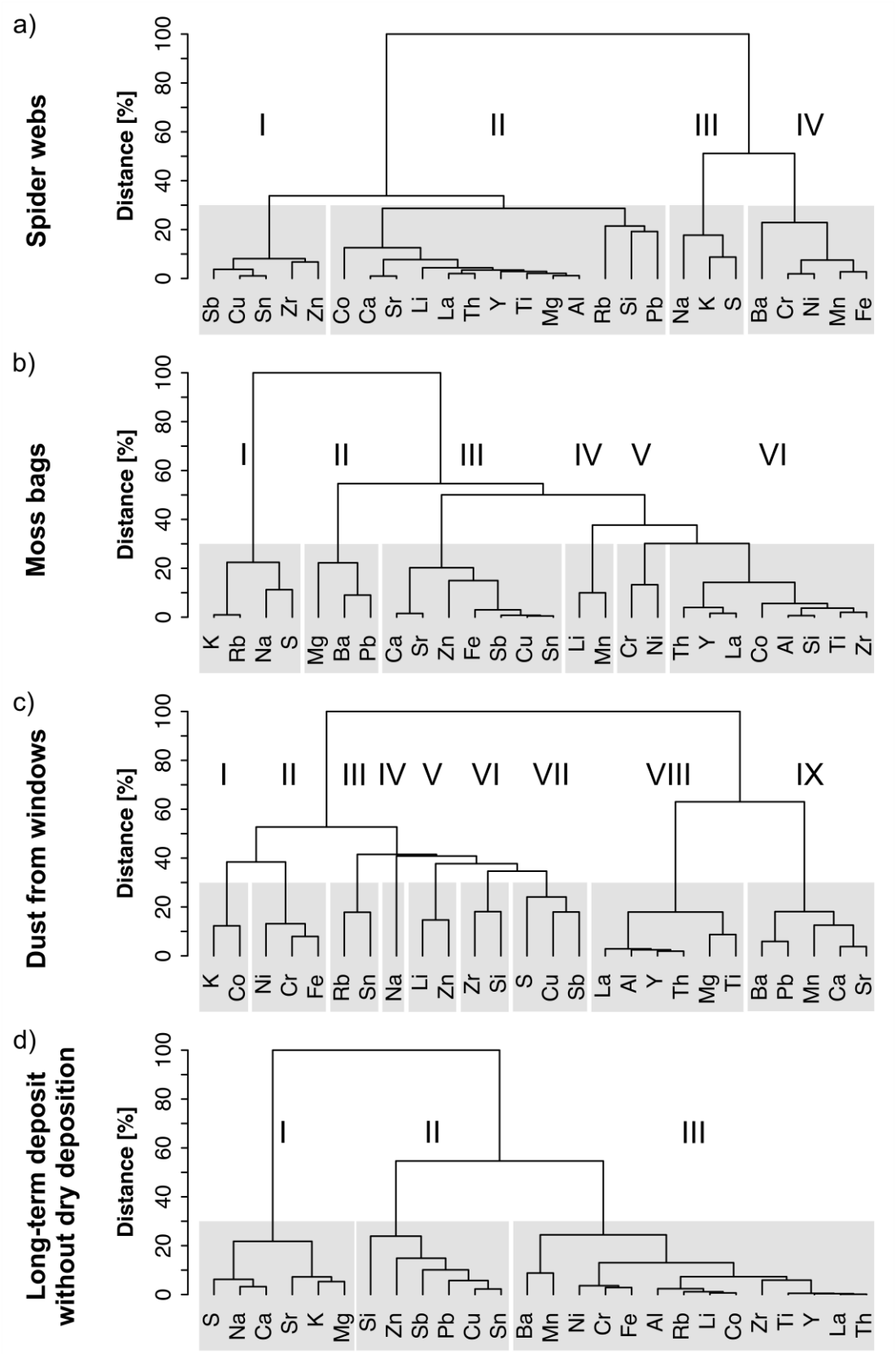

Fig. 7-5: Dendrograms (Ward's algorithm, squared Euclidean distances) depicting the cluster analyses for samples of four different materials in the object space: a) spider webs, b) moss bags, c) dust from windows, d) long-term deposit. Different numbers of clusters are formed at the same relative distance (in case of the grey boxes 30%).

Factor scores for spider webs are again quite similar to the results in chapter 6.3 (appendix Fig. A-10): Two factors describe traffic-related sources of PM, namely brake wear (factor 2: high loadings of Cu, Sb, Sn, Zn) and abrasion of tram/train tracks (factor 3: Ba, Cr, Fe, Mn, Ni). Factors 1 and 4 have been ascribed to resuspension of geogenic/natural dust (factor 1: Al, Ca, Co, La, Li, Mg, Pb, Si, Sr, Th, Ti, Y, Zr) and the influence of the spider web material (factor 4: K, Na, S).

Plots of selected factor scores for moss bags are shown in Fig. 7-6. Factor 1 has high loadings for both elements that have been described to be typical for resuspended geogenic/natural dust (Al, Ca, Co, Si, Sr, Ti, Y, Zr) as well as elements typical for brake wear (Cu, Sb, Sn, Zn) and Fe. This factor separates samples from the location CA-PAR, characterized by a high amount of car traffic, from all other samples. The high number of driving vehicles might lead to both enhanced emissions from traffic and to enhanced resuspension, whirling up many particles up to the height of the moss bags (2.5 m). Especially brake wear is expected to be high at this location, since it is located in between two intersection where cars often have to either accelerate or brake. Factors 2 and 3 describe the difference between the sampling campaigns/seasons. Factor 2 is assumed to describe the influence of heating in private households in winter times using various fuels: It has higher scores for samples from the winter campaign and high loadings of K, Mg, Na, Rb, S and Th. K and Rb are parts of wooden biomass and might be emitted from biomass burning (MEGIDO et al. 2017; STRASBURGER et al. 2014; VIANA et al. 2008) while S and Th can be emitted from coal and oil combustion (SALMINEN et al. 2005; WHO 2013).

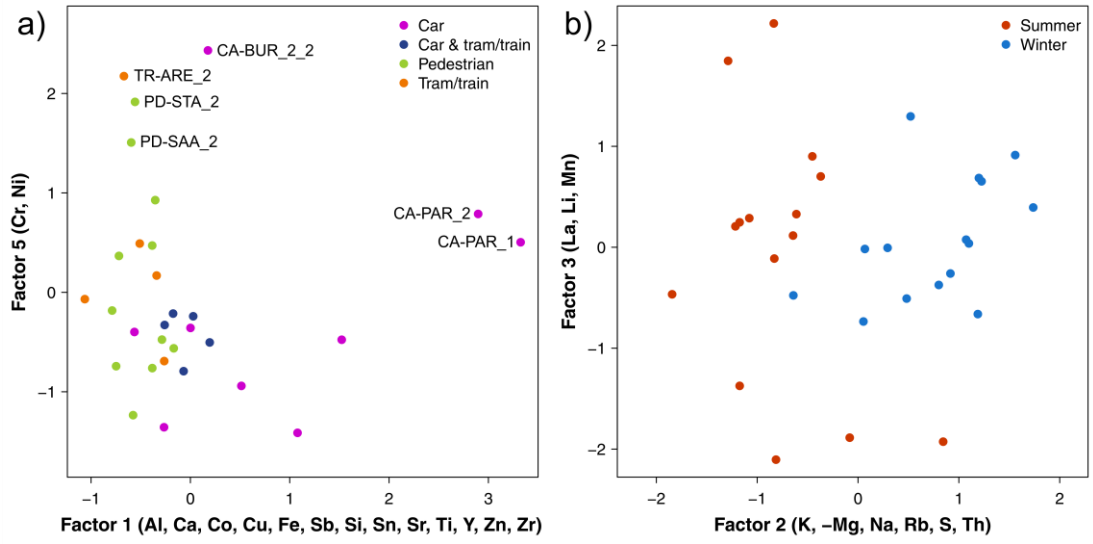

Fig. 7-6: Plot of selected factor scores (a) factors 1 and 5, b) factors 2 and 3, factor analysis with varimax rotation) of 30 moss bag samples from Jena and contents of 26 elements.

A slight seasonal influence also comes into effect for factor 5. It is highly loaded with Cr and Ni that can also be emitted from oil combustion (MEGIDO et al. 2017; SUVARAPU and BAEK 2017). Samples with high scores have been exposed to ambient air next to train routes with diesel locomotives in winter time (except for CA-BUR_2_2). More stable atmospheric layers

in winter might have inhibited a vertical mixing and led to a horizontal distribution of emissions from diesel locomotives that does not occur in summer (HERTEL and GOODSITE 2009; UMWELTBUNDESAMT 2009). Nevertheless, this assumption has to be accepted under reserve as it is only based on two elements that can occur in other emissions, like those of gasoline-powered vehicles, as well. Factor 4, that is not shown, does not lead to any separation. As it is highly loaded with Ba and Pb that do both occur in oil, gasoline and lubricants, this factor is expected to reflect a general urban (background) pollution level induced by fuel and lubricant burning in traffic (KUMMER et al. 2009; YADAV and RAJAMANI 2006).

Fig. 7-7 shows plots of selected factor scores for dust from windows. All of the factors separate single sampling locations from the others. This hints to strong differences between the sampling locations, either because there is a strong difference between PM at the locations or because there is an influence of the respective building, e.g. eaves, facade materials or paints on walls/window frames. Factor 1 is highly loaded with elements that have been ascribed to resuspension of geogenic/natural dust (Al, La, Li, Mg, Mn, Na, Th, Ti and Y). It exhibits high scores for samples from the location DOJ which is located in a park and close to sports grounds with lots of bare sand. Soil and/or sand might have been resuspended and ended up at the windows at location DOJ. Factor 2 has high loadings both for Pb, S and Zn that are typical for fuel combustion as well as Ba, Ca and Sr that are expected to be derived from geogenic dust (ORDÓÑEZ et al. 2003; SUVARAPU and BAEK 2017; WHO 2013). It separates samples from the location KGS with high scores from all others. KGS is located in a residential area with many private households burning fossil fuels for heating purpose in winter. Besides, the location is close to both a sports ground and an allotment garden, from which resuspended soil material might be derived.

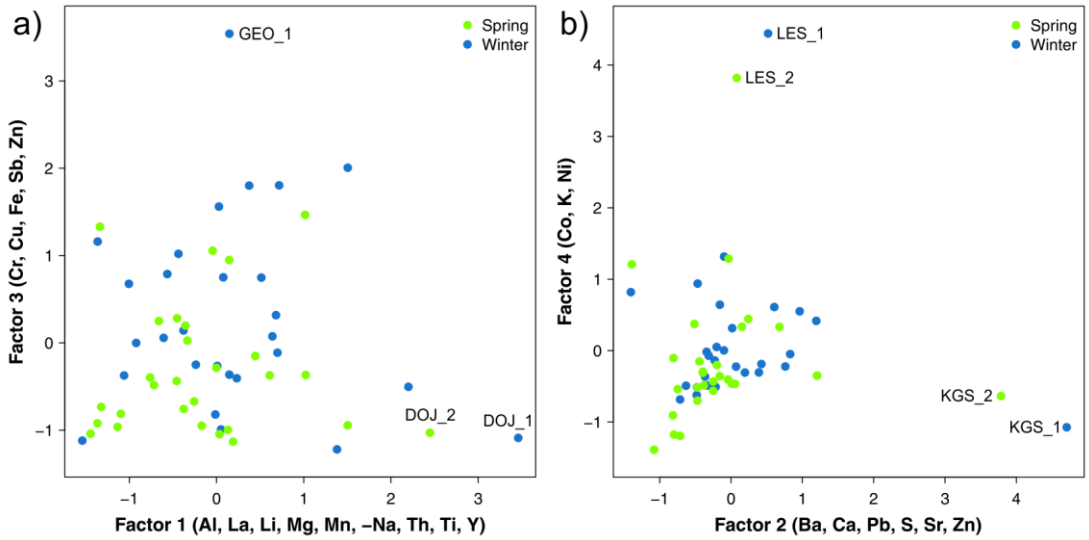

Fig. 7-7: Plot of selected factor scores (a) factors 1 and 3, b) factors 2 and 4, factor analysis with varimax rotation) of 56 dust samples collected from windows in Jena and contents of 26 elements.

Elements typical for steel abrasion (Cr, Fe) as well as brake wear (Cu, Sb, Zn) show high loadings for factor 3. Scores of this factor are remarkably high for the sample GEO_1, which

has been taken next to the main tram and bus stop in the city center in winter. Due to stable atmospheric layers or atmospheric inversion in winter, emissions from both tram and bus traffic might have accumulated in this sample (UMWELTBUNDESAMT 2009). Factor 4 separates samples taken next to a small mechanical/metalworking facility (location LES) from all others. High loadings of Co, K and Ni of this factor might be derived from either special steel alloys processed there or combustion of lubricants used in machines applied (JOHANSSON et al. 2009; KULKARNI et al. 2006).

Plots of selected factor scores for long-term deposit are shown in Fig. 7-8. A clear source identification can be done for factor 4. It separates the sample taken at an airport (AIR1) from all others and has high loadings of Ca, Na and S. High contents of Na and S were also found in PM collected next to the Los Angeles International Airport (SHIRMOHAMMADI et al. 2018). They occur in aircraft fuels while Ca occurs in lubricants applied in aircraft engines (VANDER WAL et al. 2016). In winter times, Na might also be derived from road salt applied on the runway. Factor 1 is highly loaded both with elements typical for geogenic dust (Al, Co, La, Li, Rb, Th, Ti, Y, Zr) and with elements typical for traffic-related steel abrasion emissions (Cr, Fe, Ni). It is expected that this factor describes the proportion of dry to wet deposition material in the samples, as if samples with only dry deposition are included those exhibit even much higher scores. The values of the scores are remarkably high, showing that there are big differences between the samples.

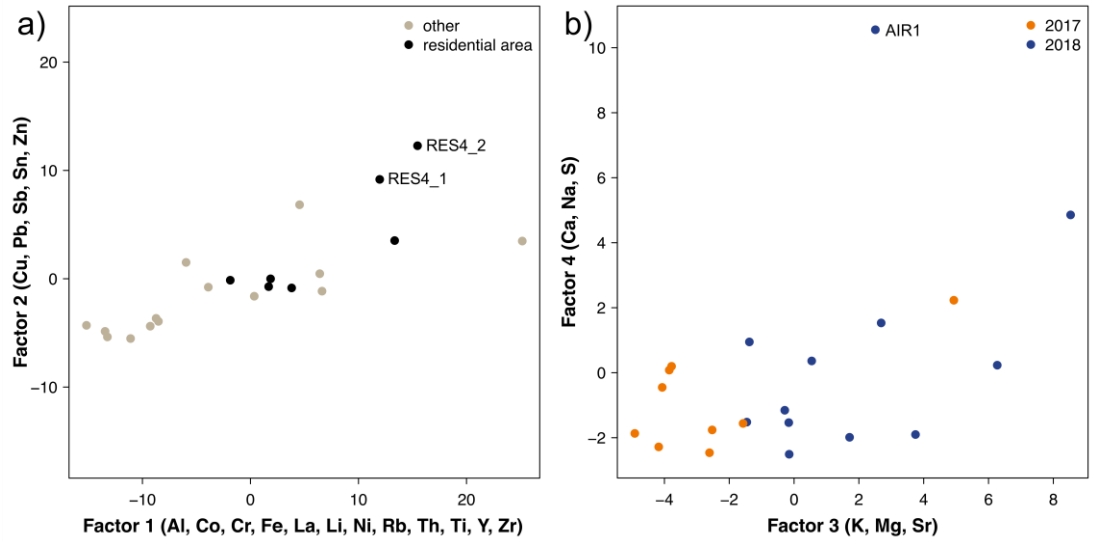

Fig. 7-8: Plot of selected factor scores (a) factors 1 and 2, b) factors 3 and 4, factor analysis with varimax rotation) of 21 long-term deposit samples from Central Germany and contents of 26 elements.

Factor 2 has high loadings of Cu, Sb, Sn and Zn (brake wear) and Pb (exhaust emissions, KUMMER et al. 2009). Highest scores are found for samples collected in the city of Leipzig (RES4). Possibly this factor reflects the urban (background) contamination from traffic in Leipzig that with its 589,000 inhabitants is much bigger than Jena, where all other samples from residential areas were collected (STATISTISCHES LANDESAMT SACHSEN 2019). This corresponds to PM_{10} contents in the air in 2018: While for both cities the urban background

concentration was 18 µg/m³, contents measured at locations of urban traffic in Leipzig are comparably high, with one of them ("Leipzig, Lützner Str. 36", 28 µg/m³) exhibiting the highest content of all monitoring stations in Central Germany (UMWELTBUNDESAMT 2019). Factor 3 describes the difference between the years of the sampling and is highly loaded with K, Mg and Sr. In 2017 there has been more rainfall (MAX PLANCK INSTITUTE FOR BIOGEOCHEMISTRY 2019), leading to higher soil moisture with less eolian erosion, from which K, Mg and Sr might be derived (SALMINEN et al. 2005).

Conclusion: This gives a first impression on which information and source identification might be possible with the different materials. Links between element contents are sufficiently high for all four materials to be subjected to a multivariate analysis but different results were obtained. Spider webs are most suited to identify sources of PM (a natural and two traffic-related ones in this case) using statistical methods, while further materials might be used to answer other questions. Rather general pollution levels as well as locations with notably different PM and seasonal/annual changes of PM could for example be identified with data from moss bags and long-term deposit. Dust from windows might in general not be as suitable to assess trends of PM as the three other materials: Comparably low links between elements were found and very local features, that might not (only) be due to PM, govern the data set.

7.5 Samples from locations in close proximity to each other

Different materials could not be sampled at the same locations, except for spider webs and moss bags (chapter 5). Nevertheless, selected samples have been taken at locations less than 300 m away from each other. Exemplary ones are regarded in the following to assess if the different materials sampled in one area show similar enrichments of elements relative to all samples of that material. For that purpose, the median element content (for all samples of the sample material) was subtracted from the element content in the sample of interest and the result was divided by the interquartile range. This shall reduce the influence of systematic differences between sample materials, as only relative enrichment/depletion are regarded. For spider webs, the median of all element contents determined at the location of interest was used instead of an individual content. Elements are ascribed to sources as described in chapter 6, except for the explanation where new citations are given.

Fig. 7-9 compares samples from location EBE (dust from windows, in this case at a bus stop) and TRA1 (long-term deposit) as examples of a location next to car traffic. They were taken close to the same part of a main road (distance around 300 m) with a horizontal distance from the runway of 2 m for dust from windows and 28 m for long-term deposit. Most of the elements show inverse behaviours: A majority of the values is above zero for dust from windows but below zero for long-term deposit. In dust from windows, high values can be found for Sb and Sn derived from brake wear. This pattern can also be found for long-term deposit, but only with small positive values. An enrichment in dust from windows can also be observed for Ti, that is likely derived from abrasion of white road marking paint containing

TiO_2 (HUBER et al. 2016). Values below zero can be found for alkali metals in dust from windows while alkaline earth metals exhibit positive values. An enrichment of all of them would be expected if they were derived from resuspension of geogenic dust. A reason for this selective enrichment might be abrasion of road material containing only selected geogenic elements (JOHANSSON et al. 2009). In the long-term deposit sample, Ba, Ca, Na and Sr are characterized by high positive values. They can be found in local host rocks of Muschelkalk and Buntsandstein, e.g. as carbonates or sulfates (HOLLEMAN et al. 2007; SEIDEL 2003), and are expected to be derived from soil developed on those host rocks next to the sampling vessel (e.g. during heavy rainfall).

There seem to be two main effects leading to differences between the samples from locations EBE (dust from windows) and TRA1 (long-term deposit). The first one is the difference in distance to the main road. Similar results were found for example for topsoil samples collected next to roads: Magnetic susceptibility of the samples, which is expected to be correlated to anthropogenic contaminants, decreased within only a few meters distance from the road in selected studies (VENUTI et al. 2016; WAWER et al. 2015). The second one is the difference between the exposure periods: Dust from windows does reflect approximately summer and autumn PM, while long-term deposit was sampled over the course of a whole year.

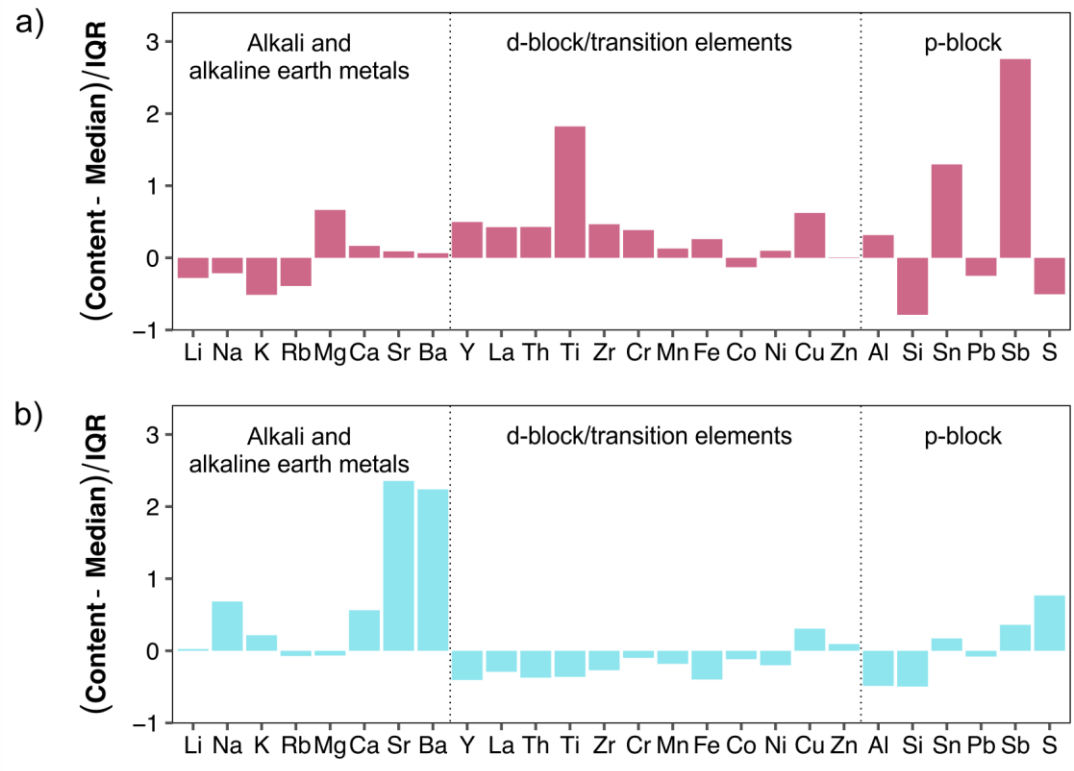

Fig. 7-9: Local element enrichment/depletion in comparison to the overall data sets of different sample materials, expressed as difference from the median content divided by the interquartile range (IQR). Samples collected close to the same main road are regarded: a) dust from windows, location EBE, winter sampling campaign, b) long-term deposit, location TRA1, 2018 sampling campaign.

Locations PHY (dust from windows) and RS-PAR (spider webs) close to the same railway station are compared in Fig. 7-10. Positive values can be found for almost all elements in dust

from windows, including both geogenic and traffic-related ones. The latter are elements typical for steel abrasion (Cr, Fe, Mn) as well as brake wear (Cu, Sb, Sn). Windows at location PHY are not only next to the railway station but also to tram tracks and the moderately frequented road passing the railway station. In addition to elements typical for abrasion of train tracks (Ba, Cr, Fe, Mn and Ni), coarse particles from traffic-related abrasion processes and horizontally resuspended road dust can therefore reach the windows at PHY.

In contrast, for spider webs at RS-PAR, negative values can be found for many geogenic elements. This major difference is expected to be due to a height difference: Handrails at the railroad station used for spider web sampling are located some meters above ground. It is expected that comparably big geogenic particles at the ground (e.g. as part of road dust) do readily fall to the ground after resuspension (ALLEN et al. 2001; GIERÉ and QUEROL 2010). Only a small portion of geogenic particles, for example particles resuspended from tram tracks and platforms, might thus be entrapped by the spider webs at the railroad station. As expected for a train traffic location, a pattern of steel abrasion with positive values for Cr, Fe, Mn and Ni can be found in spider webs at location RS-PAR. Positive values are also found for Cu and Sb, that hint to brake wear, possibly derived from braking (freight) trains.

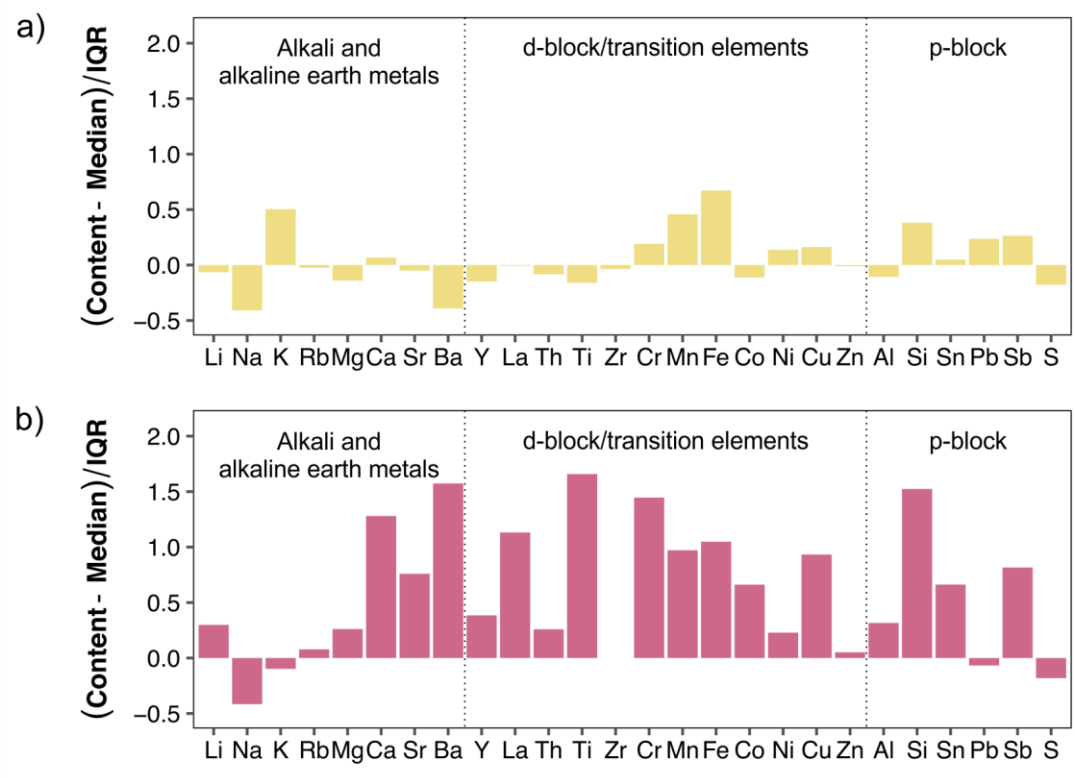

Fig. 7-10: Local element enrichment/depletion in comparison to the overall data sets of different sample materials, expressed as difference from the median content divided by the interquartile range (IQR). Samples collected close to the same railway station and main road are regarded: a) dust from windows, location PHY, winter sampling campaign (the value for Zr has been removed as an outlier), b) spider webs, location RS-PAR.

Fig. 7-11 compares samples from location PD-IGW (spider webs and moss bags) and RES2 (long-term deposit) collected in the same residential area (east and west of a building). For all

materials comparably low contents of anthropogenic, traffic-related elements can be found. Results for the moss bag and spider webs are similar with negative values for most of the elements. This meets the expectations for a residential area. The sampling locations exhibit a higher elevation above sea level than the city center and all other sampling locations in Jena. Horizontally suspended, anthropogenic particles in the city center thus cannot reach PD-IGW and RES2. For the moss bag, positive values can be found for Ba, K, Mg, Pb and Rb. The bag was hung close to treetops, wherefore K, Mg and Rb might have been derived from surrounding plant biomass (MEGIDO et al. 2017; STRASBURGER et al. 2014).

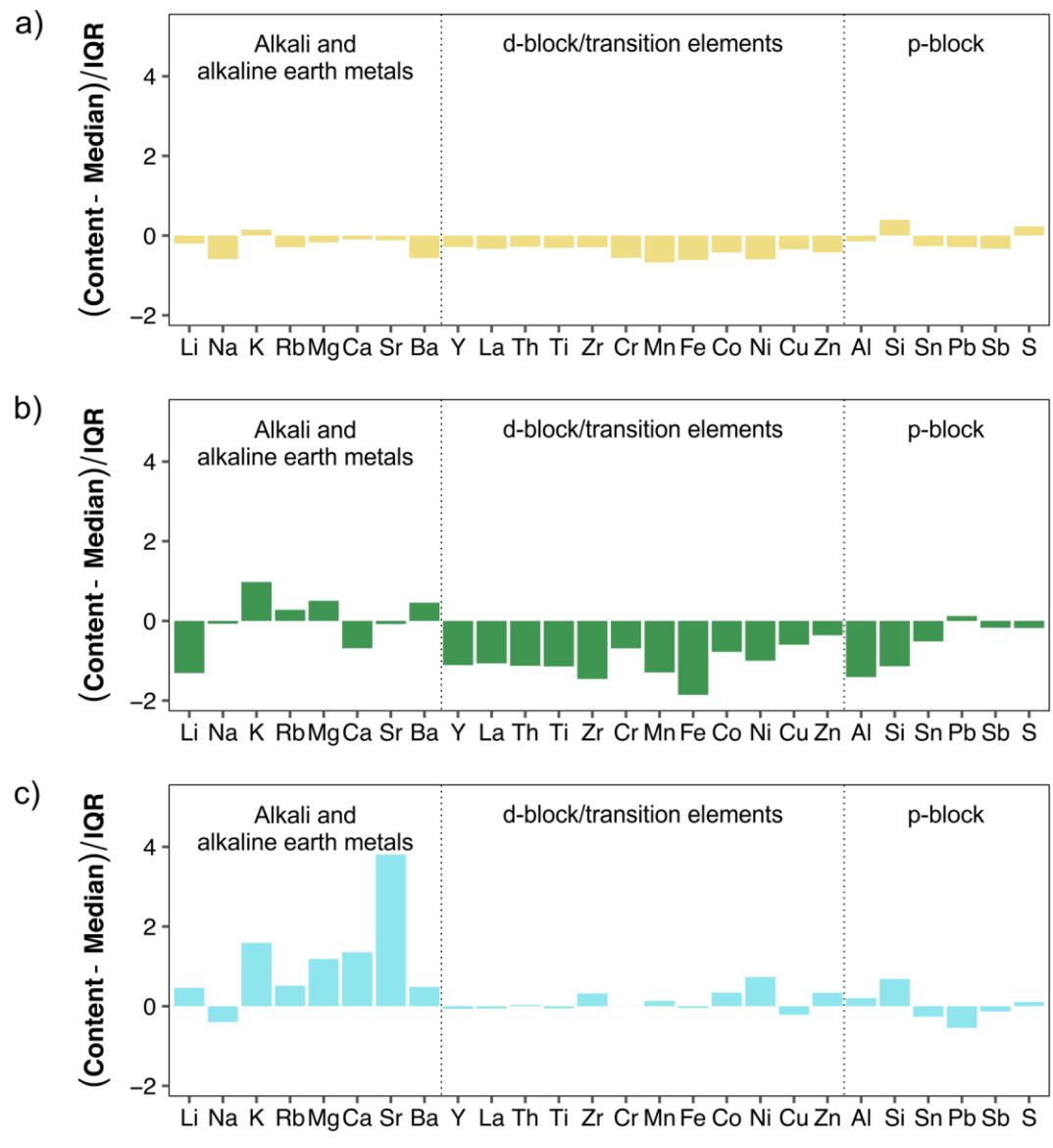

Fig. 7-11: Local element enrichment/depletion in comparison to the overall data sets of different sample materials, expressed as difference from the median content divided by the interquartile range (IQR). Samples from the same property are regarded: a) spider webs, location PD-IGW b) moss bags, location PD-IGW, summer sampling campaign, c) long-term deposit, location RES2, 2018 sampling campaign.

For long-term deposit (Fig. 7-11c) negative values can only be found for few elements. RES2 is sheltered from the side of the property facing the city center and the nearby road by a

building. Highly positive values for alkali and alkaline earth metals as well as Co, Si and Zr are thus expected to reflect PM transported from the eastern side, that is not sheltered. At this side, construction works were done during the exposure/sampling period. In the course of excavation, soil developed on the local host rocks as well as eroded host rock particles might have been suspended and ended up in the sampling vessel. Those would be mainly gypsum from the Upper Buntsandstein and carbonates from the Lower Muschelkalk (chapter 2.4). Spider webs and the moss bag have been sheltered from this eastern side source by the building, thus geogenic particles might not have reached them to a great extent. This effect of buildings being obstacles for particles has also been described by HERTEL and GOODSITE (2009). Positive values for Ni and Zn in the long-term deposit sample are not ascribed to natural PM but are rather derived from (galvanized) metal parts like rain gutters at the building close to the sampling vessel (only 2 m distance). For further campaigns thus a bigger distance to buildings should be kept, like it has been done for example at the location BGR1 (Geodynamic Observatory Moxa).

Conclusion: In general, already identified patterns of expected local sources/nearby types of traffic could be found in all samples (e.g. Ba, Cr, Fe, Mn and Ni from abrasion of train tracks). Nevertheless, element contents in the samples are often governed by small differences between the sampling locations like a change of only a few meters in horizontal or vertical distance to a road or obstacles like buildings. As a conclusion, sampling locations should be chosen carefully to make them more comparable. This could include using only locations with sealed surfaces, a set sampling height and distance (range) to roads and a reasonable distance to buildings/obstacles.

7.6 Summary

The comparison of different non-classical methods to sample PM stresses both similarities and differences of them with regard to feasibility, (anthropogenic) enrichment of elements in the materials, links between elements and their potential use to identify sources of PM. Sampling and sample preparation were not complex for all four methods. Sampling proved to be even easier for the biomonitoring methods (spider webs and moss bags) compared to dust from windows and long-term deposit. However, also other features influence the suitability of a method: The sample weight for example has been limited for all materials, except for moss bags, preventing repeated determinations and leading to higher LODs.

Even though anthropogenic enrichments of elements detected by calculations of EFs are almost similar for all materials (clear anthropogenic enrichment of Cu, Ni, Pb, S, Sb, Sn, Zn), dendrograms show different groupings of elements. Furthermore, the strength of the connection/correlation between elements is different for the four materials. The spider web samples show strongest correlations while the dust samples from windows inherit weakest ones. A clear identification of sources of PM using a factor analysis has been possible mainly with the spider web data set. An airport-related source has in addition been identified with long-term deposit. All other analyses did often lead to a separation of single locations or a

separation of the two sampling campaigns performed. Those separations could not be ascribed to sources of PM in general but other features like seasonal changes in sources or local hotspots. Other factors did not lead to a separation of samples, wherefore a more homogeneous distribution is assumed (e.g. Ba, Pb in moss bags). As a conclusion, overall levels of contamination or seasonal changes might be assessed better with moss bags or long-term deposit samples than with spider web samples that reflect mainly local sources.

In addition, exemplary comparisons reveal that relative enrichment/depletion of elements can be different even on small scales (tens of meters). A horizontal or vertical difference of a few meters or bigger obstacles can change the relative element patterns, underlining the strong spatial variation of urban PM and demanding for a careful selection of sampling locations.

8 General conclusions and recommendations

The need for low-cost, non-classical methods to sample and assess PM has been pointed out previously (e.g. chapter 1). Four different methods (spider web biomonitoring, moss bag biomonitoring, collection of dust from windows and collection of long-term deposit) have been compared in this work, regarding feasibility as well as their potential to detect anthropogenic influences and sources of PM. The main focus has been on spider web biomonitoring, for which broader sampling campaigns and a more detailed evaluation were performed.

In this study, especially spider webs have been shown to be a useful biomonitor to identify local sources of PM. By multivariate analyses of trace element contents in the webs, three sources could be detected in the exemplary environment of the city of Jena: geogenic/natural dust resuspended by driving vehicles (Al, Ca, Co, Cs, La, Li, Mg, Mn, Pb, Sr, Th, Ti, Y, Zn, Zr), brake wear (representing car traffic with Cu, Sb, Sn, Zn) and abrasion of tram and train tracks (representing rail transport with Ba, Cr, Fe, Mn, Ni). As there are no big industries in Jena, a major anthropogenic influence in the form of traffic meets the expectations for a medium-sized city located in a valley. In addition, a classification model could be built, allowing for the integration of new samples from the city of Jena into the classes “car”, “tram/train” and “pedestrian”. A model like this might allow for a more easy assessment of sources of PM and/or air quality in general. It has been shown that single models have to be built for every city/area of interest individually. Studies like this could be an important first step towards the improvement of air quality.

Of the three other methods, one source, airport emissions, could be identified with long-term deposits. Apart from that, moss bag and long-term deposit data sets only give hints to sources with geogenic and anthropogenic elements being combined in some clusters and factors. Both data sets are rather characterized by differences between the two respective sampling campaigns, revealing seasonal (moss bags) and annual (long-term deposit) changes. In addition, they reveal locations with notably different PM (potential hotspots). The data set for dust from windows is characterized by very local features of which it cannot be told if they are derived from PM or from other features like window frames, facade paint of the building or rain gutters. In the form presented here, this approach therefore seems to be least suitable to monitor PM and identify sources.

As an overall conclusion, both scientific and rather practical aspects are discussed in this chapter. The more practical approach highlights potentials and drawbacks of the different methods and gives recommendations for potential applications (chapter 8.1). Further scientific questions that should or might be tackled to yield additional information are outlined in the outlook (chapter 8.2).

8.1 Potential, drawbacks and recommendations for the application of non-classical methods to sample particulate matter

All four non-classical methods to sample PM presented in this work are easy to perform and cheap. The low price of the sampling can be regarded as a major benefit, since 92% of all pollution-related mortality, demanding for air quality improvement, occurs in low- and middle-income countries (LANDRIGAN et al. 2018). Compared to classical air quality monitoring stations in containers, no or only little space is needed for non-classical methods. As a result, application of the methods presented is more flexible and a dense sampling network can be realized. This has been shown by the establishment of 22 locations for spider web sampling, 20 locations for moss bag biomonitoring and 26 locations at which dust from windows has been collected, compared to only one state-owned monitoring station in Jena.

In contrast to high-volume samplers, the methods presented here cannot be used to determine volume concentration in µg/m³, as no air masses from which particles are derived are measured. Therefore, compliance with threshold values given in µg/m³ cannot be checked. Instead, the focus of the methods presented here is on composition of PM. Contents of far more elements than demanded by legislation (with only As, Cd, Hg, Ni and Pb; 2004/107/EC; 2008/50/EC) were determined in the different sample materials. As a result, these methods cannot replace classical air quality monitoring but might be used as an amendment to yield more information, especially on spatial heterogeneity of metal contents and sources of PM.

To choose the best of the approaches presented in this work for a certain monitoring purpose, several aspects have to be considered. As background information for this, advantages and disadvantages of the four methods as well as the respective exposure periods and sampling heights are listed in Tab. 8-1. Some recommendations are given in the following. They will focus on spider web and moss bag biomonitoring as well as the collection of long-term deposit, since it has been shown that dust from windows reflects very local influences. If the latter method is of interest, it is recommended to use structures more simple and comparable to each other than windows of buildings. An option, at least with regard to traffic-related PM, might be glass shelters at bus stops, constructed using the same standards.

The most important aspect for the choice of an appropriate method is the aim of the particular monitoring approach. If source identification is of major interest, spider web biomonitoring is the most suitable of the methods tested. In contrast to that, if the surveyance of a rather general pollution level is the aim, moss bags biomonitoring or sampling of long-term deposit are better suited. In addition, exposure period and frequency of the sampling have to be considered. Short-term effects for example can only be detected with spider web biomonitoring, while moss bag biomonitoring or the collection of long-term deposit are recommended if PM from a longer exposure period or in winter time is of interest.

Tab. 8-1: Advantages and disadvantages of the four different non-classical methods to sample particulate matter regarded in this work. In bold: aspects considered the most important ones.

Sample material	Advantages	Disadvantages
Spider webs	➢ **High temporal resolution of a few days** (even biweekly sampling did not lead to a decrease in abundance of webs) ➢ **No risk of vandalism** ➢ **Source-specific element patterns can be detected** ➢ Easy: no laboratory conditions needed until aqua regia digestion ➢ Good accumulation of particles (high PM-to-total sample ratio)	➢ **Lack of wheel webs in winter time** ➢ **Several elements below the LOD** ➢ **Possible leaching of alkali and alkaline earth metals by rainfall** ➢ Depends on occurrence of webs ➢ Few webs (low sample weight) at some locations (merging of samples would be needed for higher sample weights) ➢ Carbon content in PM (without the webs) cannot be determined
	Exposure period: One day up to a few days Sampling height: 0.50–1.25 m	
Moss bags	➢ **Constant and high sample weight** ➢ **Reflects general pollution levels** ➢ **Most frequently used method** ➢ Independent from natural occurence, sampling locations can be chosen almost freely (if e.g. a special sampling pattern is needed) ➢ Flexible adjustment of the exposure period	➢ **Possible loss due to vandalism** ➢ **Poor accumulation of particles** (low PM-to-total sample ratio) ➢ Carbon content in PM (without the moss) cannot be determined ➢ Permissions are needed for the installation
	Exposure period: 10 weeks, in general at least one month Sampling height: Flexible, in this case 2.5 m	
Dust from windows	➢ **Only dust particles without any substantial amount of diluting (bio)mass** ➢ No sample preparation needed except for drying ➢ Areas with windows cover most of the area of interest in cities	➢ **Battery of the window vacuum needs to be charged every few hours** ➢ **Reflects very local effects** ➢ Permissions are needed for the sampling ➢ Drying of the samples takes up to two weeks
	Exposure period: Several months Sampling height: Flexible, in this case 1.0–3.5 m	
Long-term deposit	➢ **Reflects PM from a long period** ➢ Most similar to classical monitoring with passive samplers	➢ **Preferably only at controlled, private or hidden locations** ➢ **Potential water head has to be checked for and removed every few weeks/months** ➢ Potential growth of solid material (e.g. algae, precipitates) in case of an existing water head ➢ Strong differences between only dry and dry and wet deposition ➢ Low amount of samples ➢ Permissions are needed for the installation
	Exposure period: 1 year Sampling height: Approximately 1 m (if installed at ground level)	

The exposure/sampling height also influences the meaning of the results. If one is interested in personal exposure, especially to vulnerable people like children or people in wheelchairs, spider web biomonitoring at low sampling heights like from handrails is recommended. In contrast, moss bags were exposed to ambient air at a height of 2.5 m and can even be exposed at greater height (e.g. ADAMO et al. 2011; DI PALMA et al. 2017). Thus, they can be used to assess air quality in different heights, as it has been done for example by CAPOZZI et al. (2016a).

Applying the methods presented here is potentially of greatest interest in cities. The two biomonitoring methods are recommended for urban monitoring as moss bags and spider webs can be installed and/or sampled from existing structures. At public locations an installation of vessels to collect long-term deposit is not recommended since sampling requires some free space and the samples might be contaminated accidentally or due to vandalism.

A practical aspect to be considered is the demand for blank values. If those are needed, one might either adapt moss bag biomonitoring or use long-term deposit samples, which are expected to be blank-free (if only dust deposition reaches the vessels). Even though moss bag biomonitoring has been named as a method with known blank values (e.g. ARES et al. 2012; TRETIACH et al. 2011), lower contents of most of the elements were found after exposure compared to contents prior to exposure in this work. This is possibly due to leaching by rainfall. However, if moss bags are exposed to ambient air with a roofing, blank values can be gained from moss prior to exposure (e.g. ZECHMEISTER et al. 2006).

8.2 Outlook

Results shown and discussed in chapters 4 to 7 give a good first impression on potentials and possible applications of some non-classical methods to monitor PM. In the future, these methods might be applied as a complement to classical air quality monitoring approaches. As discussed, local differences of PM on small scales can be covered with these methods and contents of far more elements are detectable than those usually considered by classical monitoring. Due to the cheap and easy nature of both sampling and transport of the samples, especially spider web biomonitoring and the collection of long-term deposit might be performed in the framework of citizen science in the future. This approach to include citizens in monitoring campaigns to yield more data has already been applied in some studies, for example to monitor PM, reefs or plant distribution, and growing interest is expected (CÉSAR DE SÁ et al. 2019; COMMODORE et al. 2017; LAU et al. 2019). Nevertheless, the highest potential for a soon, broad application is likely given for moss bag biomonitoring, as it has already been studied intensively (e.g. ARES et al. 2012; CAPOZZI et al. 2016b).

Comparisons in chapters 5.3.4, 5.3.5 and 7.4 have already shown that different methods might lead to different results. It should therefore be worked out in the future if measurements by e.g. federal monitoring stations and the non-classical monitoring approach of choice reflect the same PM or, more generally, which method reflects urban PM (with regard

to a certain question) best. While only few studies have been published on this topic so far it would be helpful if any of the methods presented in this work is to be applied in combination with classical monitoring (stations). Some aspects of this have been touched for the two biomonitoring methods but detailed studies on them have been beyond the scope of this work. Results in chapter 5.3.3 for example suggest that there might be differences in particle retention by moss and spider web surfaces. Further work thus should be done on examining single particles entrapped in the biomonitoring materials, e.g. by detailed SEM measurements.

With regard to source identification, other measurements might be applied in future studies, for example measurements of isotopic ratios. Isotopic fingerprinting has been used in several studies on PM to trace sources, as many of them have distinct isotopic signatures (e.g. GUÉGUEN et al. 2012; LAHD GEAGEA et al. 2007). YU et al. (2016) for example have mentioned that isotopic methods might lead to additional results in comparison with multivariate statistical evaluations of element contents, as they have been done here.

Apart from the identification of sources of PM, a potential quantification of the influences of the individual sources to total amounts of PM has been named as an aim in chapter 1. This could not be done with the multivariate methods applied (cluster analysis and factor analysis), as they exploit variation in the data set but no total contents. Other statistical methods like positive matrix factorization or chemical mass balance are typically used for this purpose (e.g. HADLEY 2017; LOWENTHAL et al. 2014; TAO et al. 2017). Programs are available for these methods, but they are not adapted to samples gained with non-classical monitoring (e.g. UNITED STATES ENVIRONMENTAL PROTECTION AGENCY 2019). Due to this and to time limitations, these approaches were no longer pursued in this thesis but might be tackled in the future.

To the author's knowledge, this has been the first study sampling spider webs repeatedly from a large number of sampling locations and using them for source identification. The general applicability of spider web biomonitoring to detect local sources of PM has been shown by this. Since it could be demonstrated that results will likely differ for every city (chapter 6.4), individual sampling campaigns based on the recommendations presented in this work could be repeated in the future to assess air quality in other cities. An application of spider web biomonitoring at locations close to industrial facilities to test their use with regard to the detection of industrial sources could for example be performed.

References

Adamo, P., R. Bargagli, S. Giordano, P. Modenesi, F. Monaci, E. Pittao, V. Spagnuolo and M. Tretiach (2008). Natural and pre-treatments induced variability in the chemical composition and morphology of lichens and mosses selected for active monitoring of airborne elements. Environ. Pollut. 152, pp. 11–19.

Adamo, P., S. Giordano, A. Sforza and R. Bargagli (2011). Implementation of airborne trace element monitoring with devitalised transplants of Hypnum cupressiforme Hedw.: assessment of temporal trends and element contribution by vehicular traffic in Naples city. Environ. Pollut. 159, pp. 1620–1628.

Akinlua, A., N. Torto and T. R. Ajayi (2008). Determination of rare earth elements in Niger Delta crude oils by inductively coupled plasma-mass spectrometry. Fuel 87, pp. 1469–1477.

Al-Khashman, O. A. (2004). Heavy metal distribution in dust, street dust and soils from the work place in Karak Industrial Estate, Jordan. Atmos. Environ. 38, pp. 6803–6812.

Allen, A. G., E. Nemitz, J. P. Shi, R. M. Harrison and J. C. Greenwood (2001). Size distributions of trace metals in atmospheric aerosols in the United Kingdom. Atmos. Environ. 35, pp. 4581–4591.

Anicic, M., M. Tomasevic, M. Tasic, S. Rajsic, A. Popovic, M. V. Frontasyeva, S. Lierhagen and E. Steinnes (2009). Monitoring of trace element atmospheric deposition using dry and wet moss bags: accumulation capacity versus exposure time. J. Hazard. Mater. 171, pp. 182–188.

Ansmann, A., J. Bösenberg, A. Chaikovsky, A. Comerón, S. Eckhardt, R. Eixmann, V. Freudenthaler, P. Ginoux, L. Komguem, H. Linné, M. Á. L. Márquez, V. Matthias, I. Mattis, V. Mitev, D. Müller, S. Music, S. Nickovic, J. Pelon, L. Sauvage, P. Sobolewsky, M. K. Srivastava, A. Stohl, O. Torres, G. Vaughan, U. Wandinger and Wiegner (2003). Long-range transport of Saharan dust to northern Europe: The 11-16 October 2001 outbreak observed with EARLINET. J. Geophys. Res. 108, pp. D24, 4783.

Apte, J. S., K. P. Messier, S. Gani, M. Brauer, T. W. Kirchstetter, M. M. Lunden, J. D. Marshall, C. J. Portier, R. C. H. Vermeulen and S. P. Hamburg (2017). High-Resolution Air Pollution Mapping with Google Street View Cars: Exploiting Big Data. Environ. Sci. Technol. 51, pp. 6999–7008.

Ares, A., J. R. Aboal, A. Carballeira, S. Giordano, P. Adamo and J. A. Fernandez (2012). Moss bag biomonitoring: a methodological review. Sci. Total Environ. 432, pp. 143–158.

Arias-Cuevas, O. and Z. Li (2011). Field investigations into the adhesion recovery in leaf-contaminated wheel–rail contacts with locomotive sanders. P. I. Mech. Eng. F-J. Rai. 225, pp. 443–456.

Ayedun, H., A. Adewole, B. G. Osinfade, R. O. Ogunlusi, B. F. Umar and S. A. Rabiu (2013). The use of spider webs for environmental determination of suspended trace metals in industrial and residential areas. J. Environ. Chem. Ecotoxicol. 5, pp. 21–25.

Bagur, M. G., S. Morales and M. López-Chicano (2009). Evaluation of the environmental contamination at an abandoned mining site using multivariate statistical techniques--the Rodalquilar (Southern Spain) mining district. Talanta 80, pp. 377–384.

Ballabio, D. and R. Todeschini (2009). Multivariate classification for qualitative analysis. Ed. by Sun, D.-W. Infrared spectroscopy for food quality analysis. Academic Press, Amsterdam, pp. 83–104.

Barandovski, L., M. V. Frontasyeva, T. Stafilov, R. Sajn and T. M. Ostrovnaya (2015). Multi-element atmospheric deposition in Macedonia studied by the moss biomonitoring technique. Environ. Sci. Pollut. R. 22, pp. 16077–16097.

Bari, M. A. and W. B. Kindzierski (2016). Eight-year (2007-2014) trends in ambient fine particulate matter (PM2.5) and its chemical components in the Capital Region of Alberta, Canada. Environ. Int. 91, pp. 122–132.

Berisha, S., M. Skudnik, U. Vilhar, M. Sabovljevic, S. Zavadlav and Z. Jeran (2017). Trace elements and nitrogen content in naturally growing moss Hypnum cupressiforme in urban and peri-urban forests of the Municipality of Ljubljana (Slovenia). Environ. Sci. Pollut. R. 24, pp. 4517–4527.

Bian, H. and C. S. Zender (2003). Mineral dust and global tropospheric chemistry: Relative roles of photolysis and heterogeneous uptake. J. Geophys. Res. 108, pp. 4672.

Blissett, R. S., N. Smalley and N. A. Rowson (2014). An investigation into six coal fly ashes from the United Kingdom and Poland to evaluate rare earth element content. Fuel 119, pp. 236–239.

Blundell, A., J. A. Hannam, J. A. Dearing and J. F. Boyle (2009). Detecting atmospheric pollution in surface soils using magnetic measurements: A reappraisal using an England and Wales database. Environ. Pollut. 157, pp. 2878–2890.

Bock, Rudolf (2005). Handbuch der analytisch-chemischen Aufschlussmethoden. Wiley-VCH, Weinheim, 327 pages (in German).

Bonrath, A. (2016). Metallgehalte in natürlichen und anthropogen beeinflussten Stäuben im Stadtgebiet Jenas. B.Sc. thesis, Friedrich Schiller University Jena, Germany, 97 pages (in German).

Bortz, J., G. A. Lienert and K. Boehnke (2008). Verteilungsfreie Methoden in der Biostatistik. Springer, Berlin, Heidelberg, 929 pages (in German).

Bro, R. and A. K. Smilde (2014). Principal component analysis. Anal. Methods 6, pp. 2812–2831.

Bundesanstalt für Geowissenschaften und Rohstoffe (2005). Bodenkundliche Kartieranleitung, Hannover, 438 pages (in German).

Bundesregierung der Bundesrepublik Deutschland (1999). Bundes-Bodenschutz- und Altlastenverordnung (BBodSchV). Bundesgesetzblatt Teil I Nr. 36, pp. 1554–1582 (in German).

Bundesregierung der Bundesrepublik Deutschland (2010). Neununddreißigste Verordnung zur Durchführung des Bundes-Immissionsschutzgesetzes (Verordnung über Luftqualitätsstandards und Emissionshöchstmengen - 39. BImSchV). Bundesgesetzblatt Teil I Nr. 40, pp. 1065–1104 (in German).

Capozzi, F., S. Giordano, J. R. Aboal, P. Adamo, R. Bargagli, T. Boquete, A. Di Palma, C. Real, R. Reski, V. Spagnuolo, K. Steinbauer, M. Tretiach, Z. Varela, H. Zechmeister and J. A. Fernandez (2016a). Best options for the exposure of traditional and innovative moss bags: A systematic evaluation in three European countries. Environ. Pollut. 214, pp. 362–373.

Capozzi, F., S. Giordano, A. Di Palma, V. Spagnuolo, F. de Nicola and P. Adamo (2016b). Biomonitoring of atmospheric pollution by moss bags: Discriminating urban-rural structure in a fragmented landscape. Chemosphere 149, pp. 211–218.

Cattani, E., M. J. Costa, F. Torricella, V. Levizzani and A. M. Silva (2006). Influence of aerosol particles from biomass burning on cloud microphysical properties and radiative forcing. Atmos. Res. 82, pp. 310–327.

César de Sá, N., H. Marchante, E. Marchante, J. A. Cabral, J. P. Honrado and J. R. Vicente (2019). Can citizen science data guide the surveillance of invasive plants? A model-based test with Acacia trees in Portugal. Biol. Invasions (Biological Invasions) 21, pp. 2127–2141.

Cesari, D., D. Contini, A. Genga, M. Siciliano, C. Elefante, F. Baglivi and L. Daniele (2012). Analysis of raw soils and their re-suspended PM10 fractions: Characterisation of source profiles and enrichment factors. Appl. Geochem. 27, pp. 1238–1246.

Chand, V. and S. Prasad (2013). ICP-OES assessment of heavy metal contamination in tropical marine sediments: A comparative study of two digestion techniques. Microchem. J. 111, pp. 53–61.

Cohen, A. J., M. Brauer, R. Burnett, H. R. Anderson, J. Frostad, K. Estep, K. Balakrishnan, B. Brunekreef, L. Dandona, R. Dandona, V. Feigin, G. Freedman, B. Hubbell, A. Jobling, H. Kan, L. Knibbs, Y. Liu, R. Martin, L. Morawska, C. A. Pope, H. Shin, K. Straif, G. Shaddick, M. Thomas, R. van Dingenen, A. van Donkelaar, T. Vos, C. J. L. Murray and M. H. Forouzanfar (2017). Estimates and 25-year trends of the global burden of disease attributable to ambient air pollution: an analysis of data from the Global Burden of Diseases Study 2015. Lancet 389, pp. 1907–1918.

Commodore, A., S. Wilson, O. Muhammad and Svendsen, E.Pearce, J. (2017). Community-based participatory research for the study of air pollution: a review of motivations, approaches, and outcomes. Environ. Monit. Assess. 189, pp. 378–407.

Dai, Q., L. Li, J. Yang, B. Liu, X. Bi, J. Wu, Y. F. Zhang, L. Yao and Y. Feng (2016). The fractionation and geochemical characteristics of rare earth elements measured in ambient size-resolved PM in an integrated iron and steelmaking industry zone. Environ. Sci. Pollut. R. 23, pp. 17191–17199.

Danzer, K., H. Hobert, C. Fischbacher and K.-U. Jagemann (2001). Chemometrik: Grundlagen und Anwendungen. Springer, Berlin, Heidelberg, 408 pages (in German).

Das, R., A. Kumar, A. Patel, S. Vijay, S. Saurabh and N. Kumar (2017). Biomechanical characterization of spider webs. J. Mech. Behav. Biomed. 67, pp. 101–109.

David, H. A., H. O. Hartley and E. S. Pearson (1954). The Distribution of the Ratio, in a Single Normal Sample, of Range to Standard Deviation. Biometrika 41, pp. 482–493.

David, T., P. Krebs, D. Borchardt and W. von Tümpling (2011). Element patterns for particulate matter in stormwater effluent. Water Sci. Technol. 63, pp. 3013–3019.

de Paula, P. H. M., V. L. Mateus, D. R. Araripe, C. B. Duyck, T. D. Saint'Pierre and A. Gioda (2015). Biomonitoring of metals for air pollution assessment using a hemiepiphyte herb (Struthanthus flexicaulis). Chemosphere 138, pp. 429–437.

DIN EN 16174 (2012). Sludge, treated biowaste and soil - Digestion of aqua regia soluble fractions of elements. Deutsches Institut für Normung e. V.

Di Palma, A, F. Capozzi, V. Spagnuolo, S. Giordano and P. Adamo (2017). Atmospheric particulate matter intercepted by moss-bags: Relations to moss trace element uptake and land use. Chemosphere 176, pp. 361–368.

Dixon, W. J. (1951). Ratios Involving Extreme Values. Ann. Math. Stat. 22, pp. 68–78.

Dmuchowski, W. and A. Bytnerowicz (2009). Long-term (1992-2004) record of lead, cadmium, and zinc air contamination in Warsaw, Poland: determination by chemical analysis of moss bags and leaves of Crimean linden. Environ. Pollut. 157, pp. 3413–3421.

Dołęgowska, S., A. Gałuszka and Z. M. Migaszewski (2017). An impact of moss sample cleaning on uncertainty of analytical measurement and pattern profiles of rare earth elements. Chemosphere 188, pp. 190–198.

Dongarrà, G., E. Manno, D. Varrica and M. Vultaggio (2007). Mass levels, crustal component and trace elements in PM10 in Palermo, Italy. Atmos. Environ. 41, pp. 7977–7986.

Du Toit, S. H. C., A. G. W. Steyn and R. H. Stumpf (1986). Graphical Exploratory Data Analysis. Springer, New York, 314 pages.

Ealo, M., A. Alastuey, A. Ripoll, N. Pérez, M. C. Minguillón, X. Querol and M. Pandolfi (2016). Detection of Saharan dust and biomass burning events using near-real-time intensive aerosol optical properties in the north-western Mediterranean. Atmos. Chem. Phys. 16, pp. 12567–12586.

Einax, J. W., D. Truckenbrodt and O. Kampe (1998). River Pollution Data Interpreted by Means of Chemometric Methods. Microchem. J. 58, pp. 315–324.

Einax, J. W., H. W. Zwanziger and S. Geiss (1997). Chemometrics in environmental analysis. VCH, Weinheim, Cambridge, 384 pages.

Elementar Analysensysteme GmbH (Oct. 2019). vario EL cube (in German). URL: https://www.elementar.de/de/produkte/organische-elementaranalyse/vario-el-cube.html.

Ellenberg, J. (2012). Geologie erleben: Saale-Holzland und Jena. Jenzig, Golmsdorf, 132 pages (in German).

Enamorado-Báez, S. M., J. M. Abril and J. M. Gómez-Guzmán (2013). Determination of 25 Trace Element Concentrations in Biological Reference Materials by ICP-MS following Different Microwave-Assisted Acid Digestion Methods Based on Scaling Masses of Digested Samples. ISRN Anal. Chem. 2013, pp. 1–14.

Enamorado-Báez, S. M., J. M. Gómez-Guzmán, E. Chamizo and J. M. Abril (2015). Levels of 25 trace elements in high-volume air filter samples from Seville (2001–2002): Sources, enrichment factors and temporal variations. Atmos. Res. 155, pp. 118–129.

Environmental Protection Agency (2013). 78 FR 3085: National Ambient Air Quality Standards for Particulate Matter. Federal Register 78, pp. 3085–3287.

Ernst-Abbe-Hochschule Jena (Jul. 2019). Klimatologische Messstation: Ausgewählte graphische Darstellungen (in German). URL: http://wetter.mb.fh-jena.de/station/index.html.

European Environment Agency (May 2019). European Pollutant Release and Transfer Register. URL: https://prtr.eea.europa.eu/#/areaoverview.

European Union (1998). Directive 98/70/EC of the European Parliament and of the Council of 13 October 1998 relating to the quality of petrol and diesel fuels and amending Council Directive 93/12/EEC. Official Journal of the European Union L 350, pp. 58–67.

European Union (2004). Directive 2004/107/EC of the European Parliament and of the Council of 15 December 2004 relating to arsenic, cadmium, mercury, nickel and polycyclic aromatic hydrocarbons in ambient air. Official Journal of the European Union L 23, pp. 3–16.

European Union (2008). Directive 2008/50/EC of the European Parliament and the Council of 21 May 2008 on ambient air quality and cleaner air for Europe. Official Journal of the European Union L 152, pp. 1–43.

Fang, G.-C., Y.-S. Wu, S.-H. Huang and J.-Y. Rau (2005). Review of atmospheric metallic elements in Asia during 2000–2004. Atmos. Environ. 39, pp. 3003–3013.

Flentje, H., B. Briel, C. Beck, M. Collaud Coen, M. Fricke, J. Cyrys, J. Gu, M. Pitz and W. Thomas (2015). Identification and monitoring of Saharan dust: An inventory representative for south Germany since 1997. Atmos. Environ. 109, pp. 87–96.

Flessa, H., B. Ludwig, B. Heil and W. Merbach (2000). The Origin of Soil Organic C, Dissolved Organic C and Respiration in a Long-Term Maize Experiment in Halle, Germany, Determined by13C Natural Abundance. J. Plant Nutr. Soil Sc. 163, pp. 157–163.

Furusjö, E., J. Sternbeck and A. P. Cousins (2007). PM10 source characterization at urban and highway roadside locations. Sci. Total Environ. 387, pp. 206–219.

Gieré, R. and X. Querol (2010). Solid Particulate Matter in the Atmosphere. Elements 6, pp. 215–222.

González, A. G. and O. S. Pokrovsky (2014). Metal adsorption on mosses: Toward a universal adsorption model. J. Colloid Interf. Sci. 415, pp. 169–178.

González, L. T., F. E. L. Rodríguez, M. Sánchez-Domínguez, C. Leyva-Porras, L. G. Silva-Vidaurri, K. Acuna-Askar, B. I. Kharisov, J. F. Villarreal Chiu and J. M. Alfaro Barbosa (2016). Chemical and morphological characterization of TSP and PM2.5 by SEM-EDS, XPS and XRD collected in the metropolitan area of Monterrey, Mexico. Atmos. Environ. 143, pp. 249–260.

Goodman, G. T. and T. M. Roberts (1971). Plants and Soils as Indicators of Metals in the Air. Nature 231, pp. 287–292.

Górka, M., W. Bartz and J. Rybak (2018). The mineralogical interpretation of particulate matter deposited on Agelenidae and Pholcidae spider webs in the city of Wrocław (SW Poland): A preliminary case study. J. Aerosol Sci. 123, pp. 63–75.

Grantz, D. A., J. H. B. Garner and D. W. Johnson (2003). Ecological effects of particulate matter. Environ. Int. 29, pp. 213–239.

Grubbs, F. E. (1969). Procedures for Detecting Outlying Observations in Samples. Technometrics 11, pp. 1–21.

Gu, J., M. Pitz, J. Schnelle-Kreis, J. Diemer, A. Reller, R. Zimmermann, J. Soentgen, M. Stoelzel, H.-E. Wichmann, A. Peters and J. Cyrys (2011). Source apportionment of ambient particles: Comparison of positive matrix factorization analysis applied to particle size distribution and chemical composition data. Atmos. Environ. 45, pp. 1849–1857.

Guéguen, F., P. Stille, V. Dietze and R. Gieré (2012). Chemical and isotopic properties and origin of coarse airborne particles collected by passive samplers in industrial, urban, and rural environments. Atmos. Environ. 62, pp. 631–645.

Hadley, O. L. (2017). Background PM2.5 source apportionment in the remote Northwestern United States. Atmos. Environ. 167, pp. 298–308.

Hedderich, J. and L. Sachs (2016). Angewandte Statistik. Springer Spektrum, Berlin, 969 pages (in German).

Heinrichs, H. and H.-J. Brumsack (1997). Anreicherung von umweltrelevanten Metallen in atmosphärisch transportierten Schwebstäuben aus Ballungszentren. Ed. by Matschullat, J. Geochemie und Umwelt. Springer, Berlin, pp. 25–36 (in German).

Herrschuh, L. (2017). Vergleich von Methoden zur Feinstaubuntersuchung im Stadtgebiet Jena und Umgebung. B.Sc. thesis, Friedrich Schiller University Jena, Germany, 99 pages (in German).

Hertel, O. and M. E. Goodsite (2009). Urban Air Pollution Climates throughout the World. Ed. by Harrison, R. M. and R. E. Hester. Air Quality in Urban Environments. Royal Society of Chemistry, Cambridge, pp. 1–22.

Holleman, A. F., E. Wiberg and N. Wiberg (2007). Lehrbuch der anorganischen Chemie. de Gruyter, Berlin, 2149 pages (in German).

Hose, G. C., J. M. James and M. R. Gray (2002). Spider webs as environmental indicators. Environ. Pollut. 120, pp. 725–733.

Hovmand, M. F., K. Kemp, J. Kystol, I. Johnsen, T. Riis-Nielsen and J. M. Pacyna (2008). Atmospheric heavy metal deposition accumulated in rural forest soils of southern Scandinavia. Environ. Pollut. 155, pp. 537–541.

Huber, M., A. Welker and B. Helmreich (2016). Critical review of heavy metal pollution of traffic area runoff: Occurrence, influencing factors, and partitioning. Sci. Total Environ. 541, pp. 895–919.

IPCC (2013). Climate Change 2013: The Physical Science Basis. Contribution of Working Group I to the Fifth Assessment Report of the Intergovernmental Panel on Climate Change. Ed. by Stocker, T. F., Qin, D., Plattner, G.-K., Tignor, M., Allen, S. K., Boschung, J., Nauels, A., Xia, Y., Bex, V. and P. M. Midgley. Cambridge University Press, Cambridge, New York, 1535.

Johansson, C., M. Norman and L. Burman (2009). Road traffic emission factors for heavy metals. Atmos. Environ. 43, pp. 4681–4688.

Kardel, F., K. Wuyts, B. A. Maher, R. Hansard and R. Samson (2011). Leaf saturation isothermal remanent magnetization (SIRM) as a proxy for particulate matter monitoring: Inter-species differences and in-season variation. Atmos. Environ. 45, pp. 5164–5171.

Koch, H. G. (1953). Wetterheimatkunde von Thüringen. VEB Gustav Fischer Verlag, Jena, 190 pages (in German).

Kötschau, A., G. Büchel, J. W. Einax, R. Meißner, W. von Tümpling and D. Merten (2014). Element pattern recognition and classification in sunflowers (Helianthus annuus) grown on contaminated and non-contaminated soil. Microchem. J. 114, pp. 164–174.

Kulkarni, P., S. Chellam and M. P. Fraser (2006). Lanthanum and lanthanides in atmospheric fine particles and their apportionment to refinery and petrochemical operations in Houston, TX. Atmos. Environ. 40, pp. 508–520.

Kummer, U., J. Pacyna, E. Pacyna and R. Friedrich (2009). Assessment of heavy metal releases from the use phase of road transport in Europe. Atmos. Environ. 43, pp. 640–647.

Lahd Geagea, M., P. Stille, M. Millet and T. Perrone (2007). REE characteristics and Pb, Sr and Nd isotopic compositions of steel plant emissions. Sci. Total Environ. 373, pp. 404–419.

Lahl, U. and W. Steven (2005). Feinstaub - eine gesundheitspolitische Herausforderung. Pneumologie 59, pp. 704–714 (in German).

Landrigan, P. J., R. Fuller, N. J. R. Acosta, O. Adeyi, R. Arnold, N. Basu, A. B. Baldé, R. Bertollini, S. Bose-O'Reilly, J. I. Boufford, P. N. Breysse, T. Chiles, C. Mahidol, A. M. Coll-Seck, M. L. Cropper, J. Fobil, V. Fuster, M. Greenstone, A. Haines, D. Hanrahan, D. Hunter, M. Khare, A. Krupnick, B. Lanphear, B. Lohani, K. Martin, K. V. Mathiasen, M. A. McTeer, C. J. L. Murray, J. D. Ndahimananjara, F. Perera, J. Potočnik, A. S. Preker, J. Ramesh, J. Rockström, C. Salinas, L. D. Samson, K. Sandilya, P. D. Sly, K. R. Smith, A. Steiner, R. B. Stewart, W. A. Suk, van Schayck, O. C. P., G. N. Yadama, K. Yumkella and M. Zhong (2018). The Lancet Commission on pollution and health. Lancet 391, pp. 462–512.

Lau, C. M., A.l A. Kee-Alfian, Y. A. Affendi, J. Hyde, A. Chelliah, Y. S. Leong, Y. L. Low, P. A. Megat Yusup, V. T. Leong, A. Mohd Halimi, Y. Mohd Shahir, R. Mohd Ramdhan, A. G. Lim and N. I. Zainal (2019). Tracing Coral Reefs: A Citizen Science Approach in Mapping Coral Reefs to Enhance Marine Park Management Strategies. Front. Mar. Sci. 6, pp. 265–273.

Lelieveld, J., J. S. Evans, M. Fnais, D. Giannadaki and A. Pozzer (2015). The contribution of outdoor air pollution sources to premature mortality on a global scale. Nature 525, pp. 367–371.

Lelieveld, J., K. Klingmüller, A. Pozzer, U. Pöschl, M. Fnais, A. Daiber and T. Münzel (2019). Cardiovascular disease burden from ambient air pollution in Europe reassessed using novel hazard ratio functions. Eur. Heart J., pp. 1–7.

Li, N., X. Long, X. Tie, J. Cao, R. Huang, R. Zhang, T. Feng, S. Liu and G. Li (2016). Urban dust in the Guanzhong basin of China, part II: A case study of urban dust pollution using the WRF-Dust model. Sci. Total Environ. 541, pp. 1614–1624.

Lippmann, R., T. Voigt, C. Baunack, K. Föhlisch and H. Lützner (2005). Geochemische Zyklen im Unteren Muschelkalk (Typus-Profil der Jena-Formation, Steudnitz). Z. geol. Wiss. 33, pp. 27–50 (in German).

Loell, M., W. Reiher and P. Felix-Henningsen (2011). Contents and bioavailability of rare earth elements in agricultural soils in Hesse (Germany). J. Plant Nutr. Soil Sc. 174, pp. 644–654.

Lowenthal, D. H., A. W. Gertler and M. W. Labib (2014). Particulate matter source apportionment in Cairo: Recent measurements and comparison with previous studies. Int. J. Environ. Sci. Te. 11, pp. 657–670.

Lumpp, R., M. Klein, E. Bieber, F. Bunzel, U. Eckermann, C. Frels, W. Günther, C. Hagemann, C. Koch, A. Olschewski and C. Temme (2012). Vergleich verschiedener Aufschlussverfahren zur Elementbestimmung in Schwebstaub und Staubniederschlag. Gefahrst. Reinhalt. L. 72, pp. 64–71 (in German).

Mägdefrau, K. (1929). Geologischer Führer durch die Trias um Jena. Verlag von Gustav Fischer, Jena, 52 pages (in German).

Mahowald, N. M., S. Engelstaedter, C. Luo, A. Sealy, P. Artaxo, C. Benitez-Nelson, S. Bonnet, Y. Chen, P. Y. Chuang, D. D. Cohen, F. Dulac, B. Herut, A. M. Johansen, N. Kubilay, R. Losno, W. Maenhaut, A. Paytan, J. M. Prospero, L. M. Shank and R. L. Siefert (2009). Atmospheric Iron Deposition: Global Distribution, Variability, and Human Perturbations. Annu. Rev. Mar. Sci. 1, pp. 245–278.

Makishima, A., K. Kobayashi and E. Nakamura (2002). Determination of Chromium, Nickel, Copper and Zinc in Milligram Samples of Geological Materials Using Isotope Dilution High Resolution Inductively Coupled Plasma-Mass Spectrometry. Geostand. Geoanal. Res. 26, pp. 41–51.

Manly, B. F. J. (2000). Multivariate statistical methods: A primer. Chapman & Hall/CRC, Boca Raton Fla., 215 pages.

Max Planck Institute for Biogeochemistry (May 2019). Data from Weather Station Beutenberg. URL: https://www.bgc-jena.mpg.de/wetter/.

May, T. W. and R. H. Wiedmeyer (1998). A Table of Polyatomic Interferences in ICP-MS. Atom. Spectrosc. 19, pp. 150–155.

Megido, L., L. Negral, L. Castrillon, B. Suarez-Pena, Y. Fernandez-Nava and E. Maranon (2017). Enrichment factors to assess the anthropogenic influence on PM10 in Gijon (Spain). Environ. Sci. Pollut. R. 24, pp. 711–724.

Middelburg, J. J. (2019). Marine Carbon Biogeochemistry. Springer International Publishing, Cham, 118 pages.

Ministry of Ecology and Environment, The People's Republic of China (2012). Ambient air quality standard GB 3095-2012. China Environmental Science Press (in Chinese).

Moreno, T., X. Querol, A. Alastuey, J. Pey, M. C. Minguillón, N. Pérez, R. M. Bernabé, S. Blanco, B. Cárdenas and W. Gibbons (2008). Lanthanoid Geochemistry of Urban Atmospheric Particulate Mattaer. Environ. Sci. Technol. 42, pp. 6502–6507.

Myhre, G., D. Shindell, F.-M. Bréon, W. Collins, J. Fuglestvedt, J. Huang, D. Koch, J.-F. Lamarque, D. Lee, B. Mendoza, T. Nakajima, A. Robock, G. Stephens, T. Takemura and H. Zhang (2013). Anthropogenic and Natural Radiative Forcing. Ed. by IPCC. Climate Change 2013: The Physical Science Basis. Contribution of Working Group I to the Fifth Assessment Report of the Intergovernmental Panel on Climate Change. Cambridge University Press, Cambridge, New York, pp. 659–740.

Nentwig, W. (1980). Wie funktionieren Spinnennetze? Biologie in unserer Zeit 10, pp. 117–119 (in German).

Norouzi, S., H. Khademi, A. Faz Cano and J. A. Acosta (2015). Using plane tree leaves for biomonitoring of dust borne heavy metals: A case study from Isfahan, Central Iran. Ecol. Indic. 57, pp. 64–73.

Norra, S. and D. Stüben (2004). Trace Element Patterns and Seasonal Variability of Dust Precipitation in a Low Polluted City – The Example of Karlsruhe/Germany. Environ. Monit. Assess. 93, pp. 203–228.

Okrusch, M. and S. Matthes (2010). Mineralogie: Eine Einführung in die spezielle Mineralogie, Petrologie und Lagerstättenkunde. Springer, Berlin, Heidelberg, 661 pages (in German).

Oldfield, F., A. Hunt, M. D. H. Jones, R. Chester, J. A. Dearing, L. Olsson and J. M. Prospero (1985). Magnetic differentiation of atmospheric dusts. Nature 317, pp. 516–518.

Ordóñez, A., J. Loredo, E. de Miguel and S. Charlesworth (2003). Distribution of heavy metals in the street dusts and soils of an industrial city in northern Spain. Arch. Environ. Con. Tox. 44, pp. 160–170.

Otto, M. (2014). Analytische Chemie. Wiley-VCH, Weinheim, 674 pages (in German).

Perchermeier, K. (2016). Charakterisierung von anthropogen und natürlich beeinflussten Stäuben in Jena. B.Sc. thesis, Friedrich Schiller University Jena, Germany, 133 pages (in German).

Praveena, S. M., O. W. Kwan and A. Z. Aris (2012). Effect of data pre-treatment procedures on principal component analysis: a case study for mangrove surface sediment datasets. Environ. Monit. Assess. 184, pp. 6855–6868.

Pribyl, D. W. (2010). A critical review of the conventional SOC to SOM conversion factor. Geoderma 156, pp. 75–83.

Pye, K. (1987). Aeolian dust and dust deposits. Academic Press, London, United Kingdom, 334 pages.

Qiang, L., W. Yang, L. Jingshuang, W. Quanying and Z. Mingying (2015). Grain-size distribution and heavy metal contamination of road dusts in urban parks and squares in Changchun, China. Environ. Geochem. Hlth. 37, pp. 71–82.

Rachold, V., H. Heinrichs and H.-J. Brumsack (1992). Spinnenweben: Natürliche Fänger atmosphärisch transportierter Feinstäube. Naturwissenschaften 79, pp. 175–178 (in German).

Rachwał, M., J. Rybak and W. Rogula-Kozłowska (2018). Magnetic susceptibility of spider webs as a proxy of airborne metal pollution. Environ. Pollut. 234, pp. 543–551.

Ragosta, M., R. Caggiano, M. Macchiato, S. Sabia and S. Trippetta (2008). Trace elements in daily collected aerosol: Level characterization and source identification in a four-year study. Atmos. Res. 89, pp. 206–217.

Rampazzo, G., M. Masiol, F. Visin, E. Rampado and B. Pavoni (2008). Geochemical characterization of PM10 emitted by glass factories in Murano, Venice (Italy). Chemosphere 71, pp. 2068–2075.

Rombach, J. (2018). Untersuchung von Feinstaub im Stadtgebiet Jena mithilfe der Analyse von Fensterstaub und moss bags. M.Sc. thesis, Friedrich Schiller University Jena, Germany, 185 pages (in German).

Russell, A. G. and B. Brunekreef (2009). A Focus on Particulate Matter and Health. Environ. Sci. Technol. 43, pp. 4620–4625.

Rybak, J. (2015). Accumulation of Major and Trace Elements in Spider Webs. Water Air Soil Poll. 226, pp. 105–116.

Rybak, J. and T. Olejniczak (2014). Accumulation of polycyclic aromatic hydrocarbons (PAHs) on the spider webs in the vicinity of road traffic emissions. Environ. Sci. Pollut. R. 21, pp. 2313–2324.

Rybak, J., I. Sówka and A. Zwoździak (2012). Preliminary Assessment of Use of Spider Webs for the Indication of Air Contaminants. Environ. Prot. Eng. 38, pp. 175–181.

Rybak, J., I. Spówka, A. Zwoździak, M. Fortuna and K. Trzepla-Nabagło (2015). Evaluation Of The Usefulness Of Spider Webs As An Air Quality Monitoring Tool For Heavy Metals. Ecol. Chem. Eng. S 22, pp. 389–400.

Salminen, R., M. J. Batista, M. Bidovec, A. Demetriades, B. de Vivo, W. de Vos, M. Duris, A. Gilucis, V. Gregorauskiene, J. Halamić, P. Heitzmann, A. Lima, G. Jordan, G. Klaver, P. Klein, J. Lis, J. Locutura, K. Marsina, A. Mazreku, P. J. O'Connor, S. Å. Olsson, R.-T. Ottesen, V. Petersell, J. A. Plant, S. Reeder, I. Salpeteur, H. Sandström, U. Siewers, A. Steenfelt and T. Tarvainen (2005). Geochemical atlas of Europe. Part 1 - Background Mnformation, Methodology and Maps. Geological Survey of Finland, Espoo, 526 pages.

Salmond, J. A. and I. G. McKendry (2009). Influences of Meteorology on Air Pollution Concentrations and Processes in Urban Areas. Ed. by Harrison, R. M. and R. E. Hester. Air Quality in Urban Environments. Royal Society of Chemistry, Cambridge, pp. 23–41.

Salvador, P., B. Artíñano, D. G. Alonso, X. Querol and A. Alastuey (2004). Identification and characterisation of sources of PM10 in Madrid (Spain) by statistical methods. Atmos. Environ. 38, pp. 435–447.

Santacatalina, M., C. Reche, M. C. Minguillón, A. Escrig, V. Sanfelix, A. Carratalá, J. F. Nicolás, E. Yubero, J. Crespo and A. Alastuey (2010). Impact of fugitive emissions in ambient PM levels and composition: A case study in Southeast Spain. Sci. Total Environ. 408, pp. 4999–5009.

Sastre, J., A. Sahuquillo, M. Vidal and G. Rauret (2002). Determination of Cd, Cu, Pb and Zn in environmental samples: Microwave-assisted total digestion versus aqua regia and nitric acid extraction. Anal. Chim. Acta 462, pp. 59–72.

Scheffer, F. and P. Schachtschabel (2010). Lehrbuch der Bodenkunde. Spektrum Akademischer Verlag, Heidelberg, 569 pages (in German).

Scheuerer, F. (2018). Ermittlung geogener Hintergrundwerte für die Feinstaubkonzentration im Stadtgebiet von Jena. report, Friedrich Schiller University Jena, Germany, 56 pages (in German).

Schubert, Sven (2006). Pflanzenernährung. Ulmer, Stuttgart, 224 pages (in German).

Schwedt, G., T. C. Schmidt and O. J. Schmitz (2016). Analytische Chemie: Grundlagen, Methoden und Praxis. Wiley-VCH, Weinheim, 544 pages (in German).

Seidel, G. (1993). Geologie von Jena, 68 pages (in German).

Seidel, G. (2003). Geologie von Thüringen. Schweizerbart, Stuttgart, 601 pages (in German).

Shirmohammadi, F., C. Lovett, M. H. Sowlat, A. Mousavi, V. Verma, M. M. Shafer, J. J. Schauer and C. Sioutas (2018). Chemical composition and redox activity of PM0.25 near Los Angeles International Airport and comparisons to an urban traffic site. Sci. Total Environ. 610-611, pp. 1336–1346.

Sinz, R. (2017). Analyse der Staubinhaltsstoffe von im Stadtgebiet Jena beprobten Spinnweben und Moss Bags mit dem Ziel, Quellen des Feinstaubs zu identifizieren. B.Sc. thesis, Friedrich Schiller University Jena, Germany, 73 pages (in German).

Skoog, D. A., F. J. Holler and S. R. Crouch (2014). Instrumentelle Analytik: Grundlagen - Geräte - Anwendungen. Springer, Berlin, 1200 pages (in German).

Skrbić, B. and N. Durisić-Mladenović (2010). Chemometric interpretation of heavy metal patterns in soils worldwide. Chemosphere 80, pp. 1360–1369.

Sperhake, F. (2018). Geochemische Signaturen von Spinnweben im Stadtgebiet Jenas im Frühjahr 2018. B.Sc. thesis, Friedrich Schiller University Jena, Germany, 83 pages (in German).

Statistisches Landesamt Sachsen (Sep. 2019). Bevölkerung des Freistaates Sachsen jeweils am Monatsende ausgewählter Berichtsmonate nach Gemeinden (in German). URL: https://www.statistik.sachsen.de/download/010_GB-Bev/Bev_Z_Gemeinde_akt.pdf.

Sternbeck, J., Å. Sjödin and K. Andréasson (2002). Metal emissions from road traffic and the influence of resuspension—results from two tunnel studies. Atmos. Environ. 36, pp. 4735–4744.

Strasburger, E., F. C. Noll, A. F. W. Schimper, J. W. Kadereit, C. Körner, B. Kost and U. Sonnewald (2014). Lehrbuch der Pflanzenwissenschaften. Springer Spektrum, Berlin, 919 pages (in German).

Suvarapu, L. N. and S.-O. Baek (2017). Determination of heavy metals in the ambient atmosphere. Toxicol. Ind. Health 33, pp. 79–96.

Suzuki, Y., S. Hikida and N. Furuta (2011). Cycling of rare earth elements in the atmosphere in central Tokyo. J. Environ. Monitor. 13, pp. 3420–3428.

Świetlik, R., M. Strzelecka and M. Trojanowska (2013). Evaluation of traffic-related heavy metals emissions using noise barrier road dust analysis. Pol. J. Environ. Stud. 22, pp. 561–567.

Szczepaniak, K. and M. Biziuk (2003). Aspects of the biomonitoring studies using mosses and lichens as indicators of metal pollution. Environ. Res. 93, pp. 221–230.

Tao, J., L. Zhang, J. Cao, L. Zhong, D. Chen, Y. Yang, L. Chen, Z. Zhang, Y. Wu, Y. Xia, S. Ye and R. Zhang (2017). Source apportionment of PM2.5 at urban and suburban areas of the Pearl River Delta region, south China - With emphasis on ship emissions. Sci. Total Environ. 574, pp. 1559–1570.

Thüringer Landesamt für Bodenmanagement und Geoinformation (Apr. 2019). Landesprogramm "Offene Geodaten" (in German). URL: https://www.geoportal-th.de/de-de/Downloadbereiche/Download-Offene-Geodaten-Th%C3%BCringen.

Thüringer Landesamt für Statistik (Apr. 2019). Bevölkerung der Gemeinden, erfüllenden Gemeinden und Verwaltungsgemeinschaften nach Geschlecht in Thüringen (in German). URL: https://statistik.thueringen.de/datenbank/TabAnzeige.asp?tabelle=gg000102%7C%7C.

Tretiach, M., E. Pittao, P. Crisafulli and P. Adamo (2011). Influence of exposure sites on trace element enrichment in moss-bags and characterization of particles deposited on the biomonitor surface. Sci. Total Environ. 409, pp. 822–830.

Umweltbundesamt (2007). Die Nebenwirkungen der Behaglichkeit: Feinstaub aus Kamin und Holzofen, 8 pages (in German).

Umweltbundesamt (2009). Feinstaubbelastung in Deutschland, 22 pages (in German).

Umweltbundesamt (2012). Luftqualität 2011: Feinstaubepisoden prägen das Bild, 19 pages (in German).

Umweltbundesamt (Apr. 2019). Jährliche Auswertung Feinstaub (PM10) - 2018 (in German). URL: https://www.umweltbundesamt.de/dokument/jaehrliche-auswertung-feinstaub-pm10-2018-excel.

United States Environmental Protection Agency (Oct. 2019). Positive Matrix Factorization Model for environmental data analyses. URL: https://www.epa.gov/air-research/positive-matrix-factorization-model-environmental-data-analyses.

Urbat, M., E. Lehndorff and L. Schwark (2004). Biomonitoring of air quality in the Cologne conurbation using pine needles as a passive sampler—Part I: Magnetic properties. Atmos. Environ. 38, pp. 3781–3792.

USGS (1997). Bedrock geologic map of the St. Louis 30' x 60' Quadrangle, Missouri and Illinois.

USGS (2004). Shuttle Radar Topography Mission, 3 Arc Second Scene, Unfilled Unfinished 2.0. Global Land Cover Facility, University of Maryland, College Park, Maryland, February 2000, Maryland.

Vander Wal, R. L., V. M. Bryg and C.-H. Huang (2016). Chemistry characterization of jet aircraft engine particulate matter by XPS: Results from APEX III. Atmos. Environ. 140, pp. 623–629.

Venuti, A., L. Alfonsi and A. Cavallo (2016). Anthropogenic pollutants on top soils along a section of the Salaria state road, central Italy. Ann. Geophys. Italy 59, pp. G0544.

Verein Deutscher Ingenieure - VDI (2013). VDI 2119 Part 4: 2013-06: Ambient air measurements - Sampling of atmospheric particles > 2,5 µm on an acceptor surface using the Sigma-2 passive sampler - Characterisation by optical microscopy and calculation of number settling rate and mass concentration. VDI/DIN-Handbuch Reinhaltung der Luft, Band 4: Analysen- und Messverfahren I (in German).

Viana, M., T.A.J. Kuhlbusch, X. Querol, A. Alastuey, R. M. Harrison, P. K. Hopke, W. Winiwarter, M. Vallius, S. Szidat, A.S.H. Prévôt, C. Hueglin, H. Bloemen, P. Wåhlin, R. Vecchi, A. I. Miranda, A. Kasper-Giebl, W. Maenhaut and R. Hitzenberger (2008). Source apportionment of particulate matter in Europe: A review of methods and results. J. Aerosol Sci. 39, pp. 827–849.

Villares, R., X. Puente and A. Carballeira (2003). Heavy metals in sandy sediments of the Rías Baixas (NW Spain). Environ. Monit. Assess. 83, pp. 129–144.

Voigt, T., L. Katzschmann, A. Nestler and G. Hecht (2000). Exkursionsführer - Trias in Thüringen, 54 pages (in German).

Vollrath, F. (1999). Biology of spider silk. Int. J. Biol. Macromol. 24, pp. 81–88.

Vollrath, F., W. J. Fairbrother, R. J. P. Williams, E. K. Tillinghast, D. T. Bernstein, K. S. Gallagher and M. A. Townley (1990). Compounds in the droplets of the orb spider's viscid spiral. Nature 345, pp. 526–528.

Vollrath, F. and E. K. Tillinghast (1991). Glycoprotein glue beneath a spider web's aqueous coat. Naturwissenschaften 78, pp. 557–559.

Vukovic, G., M. Anicic Urosevic, S. Skrivanj, T. Milicevic, D. Dimitrijevic, M. Tomasevic and A. Popovic (2016). Moss bag biomonitoring of airborne toxic element decrease on a small scale: A street study in Belgrade, Serbia. Sci. Total Environ. 542, pp. 394–403.

Wang, Y.-F., K.-L. Huang, C.-T. Li, H.-H. Mi, J.-H. Luo and P.-J. Tsai (2003). Emissions of fuel metals content from a diesel vehicle engine. Atmos. Environ. 37, pp. 4637–4643.

Wawer, M., T. Magiera, G. Ojha, E. Appel, G. Kusza, S. Hu and N. Basavaiah (2015). Traffic-Related Pollutants in Roadside Soils of Different Countries in Europe and Asia. Water Air Soil Poll. 226, pp. 216–229.

Wedepohl, K. H. (1995). The composition of the continetal crust. Geochim. Cosmochim. Ac. 59, pp. 1217–1232.

Weinbruch, S., A. Worringen, M. Ebert, D. Scheuvens, K. Kandler, U. Pfeffer and P. Bruckmann (2014). A quantitative estimation of the exhaust, abrasion and resuspension components of particulate traffic emissions using electron microscopy. Atmos. Environ. 99, pp. 175–182.

Weiß, C. H. (2009). Datenanalyse und Modellierung mit STATISTICA. Oldenbourg, München, 449 pages (in German).

Wessel, P., W. H. F. Smith, R. Scharroo, J. Luis and F. Wobbe (2013). Generic Mapping Tools: Improved Version Released. Eos Trans. AGU (Eos, Transactions, American Geophysical Union) 94, pp. 409–410.

WHO (2006). WHO Air quality guidelines for particulate matter, ozone, nitrogen dioxide and sulfur dioxide: Global update 2005, 22 pages.

WHO (2013). Review of evidence on health aspects of air pollution - REVIHAAP Project, 309 pages.

Wise, B. M., N. B. Gallagher, R. Bro, J. M. Shaver, W. Windig and R. S. Koch (2006). Chemometrics Tutorial for PLS_Toolbox and Solo.

Wold, S., K. Esbensen and P. Geladi (1987). Principal component analysis. Chemometr. Intell. Lab. 2, pp. 37–52.

Wold, S., M. Sjöström and L. Eriksson (2001). PLS-regression: a basic tool of chemometrics. Chemometr. Intell. Lab. 58, pp. 109–130.

Work, R. W. and C. T. Young (1987). The Amino Acid Compositions of Major and Minor Ampullate Silks of Certain Orb-Web-Building Spiders (Araneae, Araneidae). J. Arachnol. 15, pp. 65–80.

Xiao-li, S., P. Yu, G. C. Hose, C. Jian and L. Feng-xiang (2006). Spider Webs as Indicators of Heavy Metal Pollution in Air. B. Environ. Contam. Tox. 76, pp. 271–277.

Yadav, S. and V. Rajamani (2006). Air quality and trace metal chemistry of different size fractions of aerosols in N–NW India—implications for source diversity. Atmos. Environ. 40, pp. 698–712.

Yang, H., Y. Peng, J. Tian, J. Wang, J. Hu and Z. Wang (2016). Spiders as excellent experimental models for investigation of heavy metal impacts on the environment: A review. Environ. Earth. Sci. 75, pp. 1059.

Yeomans, K. A. and P. A. Golder (1982). The Guttman-Kaiser Criterion as a Predictor of the Number of Common Factors. Statistician 31, pp. 221.

Yu, Y., Y. Li, B. Li, Z. Shen and M. K. Stenstrom (2016). Metal enrichment and lead isotope analysis for source apportionment in the urban dust and rural surface soil. Environ. Pollut. 216, pp. 764–772.

Zechmeister, H. G., S. Dullinger, D. Hohenwallner, A. Riss, A. Hanus-Illnar and S. Scharf (2006). Pilot study on road traffic emissions (PAHs, heavy metals) measured by using mosses in a tunnel experiment in Vienna, Austria. Environ. Sci. Pollut. R. 13, pp. 398–405.

Zheng, J., M. Tan, Y. Shibata, A. Tanaka, Y. Li, G. Zhang, Y. Zhang and Z. Shan (2004). Characteristics of lead isotope ratios and elemental concentrations in PM10 fraction of airborne particulate matter in Shanghai after the phase-out of leaded gasoline. Atmos. Environ. 38, pp. 1191–1200.

Zhu, X., Y Kuang, J. Li, R. Schroll and D. Wen (2015). Metals and possible sources of lead in aerosols at the Dinghushan nature reserve, southern China. Rapid Commun. Mass Sp. 29, pp. 1403–1410.

Appendix

Tab. A-1: Locations in the city of Jena where spider webs were sampled repeatedly. Numbers in brackets indicate the year (2016, 2017, 2018), the length is the summed length of all railings - part 1.

Location	Coordinates [°] (ETRS 1989)		Number of samples	Description
	Longitude	Latitude		
CA-BUR_1	11.59880	50.89874	24 (3, 10, 11)	Metal railings (blue paint), concrete ground height: 1.02 m, length: 87 m bridge hightly frequented by cars distance railings to road: 2.2 m
CA-BUR_2	11.60108	50.89794	21 (0, 10, 11)	Metal railings (light grey paint), concrete ground height: 1.01 m, length: 150 m bridge highly frequented by cars distance railings to road: 1.5 m
CA-JOH	11.58458	50.93007	10 (1, 5, 4)	Metal railings (powder-coated), ground: slabs height: 1.21 m, length: 53 m walkway close to a road highly frequented by cars distance railings to road: 2.5–10.0 m
CA-KUN	11.63418	50.95638	9 (1, 4, 4)	Metal railings (light grey paint), concrete ground height: 1.01 m, length: 75 m close to agricultural land and cement plant distance railings to road: 0.5–1.6 m
CA-MAU	11.60571	50.86984	9 (1, 4, 4)	Metal railings (blue paint), concrete ground height: 1.01 m, length: 140 m bridge sparsely frequented by cars Close to agricultural land distance railings to road: 1.6 m
CA-PAR	11.59061	50.92503	12 (4, 4, 4)	Metal railings (light grey paint), ground: slabs height: 1.21 m, length: 146 m bridge highly frequented by cars distance railings to road: 5.5 m
CA-WIE	11.59824	50.93688	22 (1, 10, 11)	Metal railings (blue paint), concrete ground height: 1.25 m, length: 91 m bridge highly frequented by cars distance railings to road: 3.0 m
CA/TR-CAM	11.59608	50.92854	9 (2, 3, 4)	Metal railings (light grey paint), concrete ground height: 1.00 m, length: 160 m bridge highly frequented by cars, trams, buses distance railings to road: 4.25 m
CA/TR-GOE_1	11.59629	50.88184	9 (1, 4, 4)	Metal railings (blue/white paint), concrete ground height: 1.22 m, length: 234 m bridge moderately frequented by cars crosses tram and train tracks distance railings to road: 3.0 m
CA/TR-GOE_2	11.59429	50.87777	9 (1, 4, 4)	Metal railings (blue/white paint), concrete ground height: 1.22 m, length: 192 m bridge moderately frequented by cars crosses train tracks distance railings to road: 3.0 m
PD-BUR	11.59864	50.89555	10 (2, 4, 4)	Wooden railings, limestone ground height: 1.20 m, length: 286 m bridge for pedestrians and cyclists

Tab. A-2: Locations in the city of Jena where spider webs were sampled repeatedly. Numbers in brackets indicate the year (2016, 2017, 2018), the length is the summed length of all railings - part 2.

Location	Coordinates [°] (ETRS 1989)		Number of samples	Description
	Longitude	Latitude		
PD-GRI	11.59457	50.93427	12 (3, 5, 4)	Wooden railings, asphalted ground height: 1.12 m, length: 156 m bridge for pedestrians and cyclists
PD-IGW	11.59743	50.92432	10 (1, 5, 4)	Metal railings (light grey paint) ground: roofing felt height: 0.89 m, length: 38 m handrails of a patio ca. 3 m above the ground trees and bushes in the surroundings
PD-KUN	11.63170	50.95531	9 (1, 4, 4)	Wooden railings, roof and ground height: 1.23 m, length: 110 m bridge for pedestrians and cyclists close to agricultural land and cement plant
PD-LOB	11.60114	50.88403	10 (2, 4, 4)	Metal railings (blue paint), asphalted ground height: 1.23 m, length: 90 m bridge for pedestrians and cyclists trees and bushes in the surroundings
PD-SAA	11.59242	50.93490	9 (1, 4, 4)	Metal railings (grey paint/ galvanized) ground: slabs height: 1.20 m, length: ca. 100 m pedestrian underpass beneath tram rails
PD-STA	11.58048	50.91517	10 (2, 4, 4)	Metal railings (black paint), asphalted ground height: 1.21 m, length: 76 m bridge for pedestrians and cyclists next to parking with unpaved ground
PD-USV	11.58318	50.91930	10 (2, 4, 4)	Metal railings (blue paint/galvanized) concrete ground height: 1.14 m, length: 134 m bridge for pedestrians and cyclists paint peels off
RS-PAR	11.58763	50.92500	9 (1, 4, 4)	Metal railings (grey paint/galvanized) ground: slabs height: 1.10 m, length: 744 m train platforms, ca. 4 m above the ground distance railings to tracks: 4.6 m
TR-ARE	11.58341	50.90767	22 (1, 10, 11)	Metal railings (light grey paint) asphalted ground height: 1.20 m, length: 100 m bridge used by trams, pedestrians, cyclists distance railings to track: 3.0 m
TR-BUR	11.59905	50.89714	10 (2, 4, 4)	Metal railings (light grey paint), concrete ground height: 1.20 m, length: 91 m bridge used by trams, pedestrians, cyclists, very few cars distance railings to tracks: 6.0 m
TR-PAR	11.58957	50.92469	10 (2, 4, 4)	Metal railings (light grey paint), concrete ground height: 1.02 m, length: 204 m bridge used by trams, pedestrians, cyclists distance railings to tracks: 2.5–4.7 m

Tab. A-3: Sampling locations where additional spider web samples (other than the 22 locations of the repeated sampling in the city of Jena) have been taken.

Sample ID	Coordinates (ETRS 1989)		Expected nearby source (pre-defined class)	Comments
	Latitude	Longitude		
PD-MEC	7.09692	49.61567	Pedestrian	Meckenbach, Rhineland-Palatinate
CA-SCH-S	10.68961	50.60467	Car	Sampling campaign in Suhl, southern Thuringia 20th July 2016
CA/TR-RAI-S	10.68402	50.60630	Car & tram/train	
CA-FRI-S_1	10.68624	50.60941	Car	
CA-BUS-S_3	10.69092	50.61023	Car	
CA-BUS-S_2	10.69134	50.61037	Car	
CA-BUS-S_1	10.69174	50.61066	Car	
CA-FRI-S_2	10.69328	50.61170	Car	
TR-RAI-G_1	12.19739	50.65273	Tram/train	Sampling campaign in Greiz, eastern Thuringia 7th June 2016
TR-RAI-G_2	12.19739	50.65273	Tram/train	
PD-ELS-G	12.20041	50.65490	Pedestrian	
PD-WEI-G	12.19939	50.65505	Pedestrian	
CA-FRI-G_1	12.19838	50.65567	Car	
CA-MOL-G	12.20516	50.65585	Car	
CA-OBE-G	12.20478	50.65654	Car	
PD-CAS-G_2	12.19719	50.65810	Pedestrian	
PD-CAS-G_1	12.19692	50.65870	Pedestrian	
CA-FRI-G_2	12.19838	50.65567	Car	Greiz, 4th July 2018
NA-MAU	11.60707	50.86828	Natural background	Additional samples taken in Jena
CA/TR-GOE-J	11.59489	50.88377	Car & tram/train	
CA/TR-BUR-J	11.59325	50.89843	Car & tram/train	
RS-GOE-J	11.59325	50.89843	Railroad station	
CA/TR-CAM-J	11.59183	50.92593	Car & tram/train	
RS-GRO	12.02232	51.26718	Railroad station	Großkorbetha, Saxony-Anhalt
CA-LIE_1	12.48923	51.27262	Car	Bridge crossing a motorway close to Liebertwolkwitz, Saxony
CA-LIE_2	12.48923	51.27262	Car	
CA-LIE_3	12.48923	51.27262	Car	
CA-LIE_4	12.48923	51.27262	Car	
AG-TAU	12.51666	51.37705	Agriculture	Taucha-Plösitz, Saxony
CA-AIR	12.22414	51.42458	Car	Motorway bridge at an airport in Central Germany
AG-NIE	11.15874	51.94169	Agriculture	Nienhagen (Halberstadt), Saxony-Anhalt

Tab. A-4: Locations of the moss bag biomonitoring and overview on where samples were gained (existing sample). Locations written in italics are some meters away from the spider web sampling while at all other locations moss bags were exposed directly where spider webs were sampled.

Location	Coordinates [°] (ETRS 1989)		Existing sample		
	Longitude	Latitude	Sampling 1 15/05 – 09/06/17 25 days	Sampling 2 09/06 – 17/08/17 69 days	Sampling 3 23/01 – 04/04/18 71 days
CA-BUR_1	11.59880	50.89874	yes	no	yes
CA-BUR_2	11.60108	50.89794	yes	yes	yes
CA-JOH	*11.58418*	*50.93025*	*yes*	*no*	*yes*
CA-KUN	11.63418	50.95638	yes	yes	yes
CA-PAR	11.59061	50.92503	yes	yes	yes
CA-WIE	11.59824	50.93688	yes	no	yes
CA/TR-CAM	*11.59654*	*50.92856*	*yes*	*yes*	*no*
CA/TR-GOE_1	11.59629	50.88184	yes	yes	yes
CA/TR-GOE_2	11.59429	50.87777	yes	yes	yes
PD-BUR	11.59864	50.89555	yes	yes	no
PD-GRI	11.59457	50.93427	yes	no	yes
PD-IGW	*11.59756*	*50.92470*	*yes*	*yes*	*yes*
PD-KUN	*11.63131*	*50.95555*	*yes*	*yes*	*no*
PD-LOB	11.60114	50.88403	yes	no	no
PD-SAA	11.59242	50.93490	yes	yes	yes
PD-STA	*11.58084*	*50.91484*	*yes*	*yes*	*yes*
PD-USV	*11.58291*	*50.91950*	*yes*	*yes*	*yes*
TR-ARE	*11.58349*	*50.90694*	*yes*	*yes*	*yes*
TR-BUR	11.59905	50.89714	yes	yes	yes
TR-PAR	11.58957	50.92469	yes	yes	no

Tab. A-5: Details for the sampling locations where dust has been sampled from windows in the city of Jena - part 1.

Location	Coordinates [°] (ETRS 1989)		Window area (estimated) [m²]	Height above ground [m]	Nearest potential PM source	Sampling dates	Particle mass obtained in spring [g]	Remarks
	Longitude	Latitude						
BES	11.57495	50.93486	2.10	1.20–2.80	Minor road (directly)	10/01/18 11/04/18	0.0538	Some grilled windows
BGC	11.56655	50.91020	9.60	1.40	Urban background	18/01/18 11/04/18	0.1195	Protected from wind
BOT	11.58558	50.93038	9.50	1.20	Main road (18 m)	18/12/17 29/03/18	0.1865	-
CHA	11.59954	50.93187	13.37	1.28	Urban background	17/01/18 23/03/18	0.1000	-
CZS_in	11.59238	50.93750	2.56	1.10–1.30	Urban background	11/12/17 26/03/18	0.0767	Courtyard
CZS_out	11.59257	50.93754	1.93	1.33	Construction works (16 m)	11/12/17 26/03/18	0.6139	-
DOE	11.57930	50.93216	4.22	1.80	Main road (5 m)	10/01/18 28/03/18	0.0798	-
DOJ	11.58349	50.91844	4.37	1.00–1.60	Urban background	24/01/18 06/04/18	0.1335	-
EBE	11.57163	50.93332	3.36	1.40	Main road (3 m)	18/12/17 28/03/18	0.1242	Bus stop
ERN	11.58867	50.93719	3.28	1.90	Road (3 m) Tram (7 m)	10/01/18 26/03/18	0.0817	-
EWS	11.61574	50.88223	3.05	2.10	Main road (25 m)	13/12/17 28/03/18	0.1409	-
FRU	11.59060	50.92747	2.88	1.20	Main road (3 m)	17/01/18 06/04/18	0.3998	-
GEO	11.58756	50.92684	5.68	2.50	Road (6 m) Tram(6 m)	18/01/18 29/03/18	0.0795	-
HUS	11.58179	50.89554	4.31	1.05–1.60	Tram (25 m)	13/12/17 28/03/18	0.1817	-

Tab. A-6: Details for the sampling locations where dust has been sampled from windows in the city of Jena - part 2.

Location	Coordinates (ETRS 1989)		Window area (estimated) [m²]	Height above ground [m]	Nearest potential PM source	Sampling dates	Particle mass obtained in spring [g]	Remarks
	Longitude	Latitude						
IND	11.58964	50.93120	7.29	1.00–1.60	Minor road (directly)	15/12/17 23/03/18	0.0492	-
KAH	11.58163	50.92175	5.90	2.00	Road (4 m)	19/12/17 03/04/18	0.3607	-
KGS	11.60773	50.93253	3.73	1.20	Road (3 m)	19/12/17 16/04/18	0.1421	Grilled windows
LES	11.58326	50.93360	5.05	1.40	Urban background	17/01/18 23/03/18	0.1017	Windows with shutters
NEU	11.58322	50.92483	6.80	2.40	Urban background	16/01/18 10/04/18	0.1065	-
NOL	11.58943	50.93612	2.64	3.50	Main road (5 m)	10/01/18 26/03/18	0.0353	-
OEK	11.59861	50.94681	4.80	1.80	Road (10 m)	11/01/18 06/04/18	0.1889	-
OTS	11.57213	50.92151	6.00	2nd floor	Urban background	24/01/18 05/04/18	0.0836	Substantially higher
PHY	11.58386	50.92430	3.99	1.25	Road (3 m)	16/01/18 10/04/18	0.0677	-
ROS	11.58489	50.92932	1.84	1.85	Urban background	11/01/18 28/03/18	0.0350	-
SPO	11.59059	50.91923	10.86	1.25	Main road (64 m) Tram (81 m)	18/01/18 10/04/18	0.1061	-
UHG_in	11.58940	50.92961	10.16	1.41	Urban background	04/12/17 10/04/18	0.0835	Courtyard
UHG_out	11.58976	50.92978	14.69	1.60–1.82	Main road (24 m)	04/12/17 10/04/18	0.3168	Smoking area
WOE	11.59203	50.92218	2.66	1.10	Road (23 m)	24/01/18 06/04/18	0.0348	-

Tab. A-7: Details of the sampling of long-term deposit: coordinates, duration of the accumulation and appearance of the samples. Locations were named according to the nearby land use: AGR – agriculture, AIR – airport, BGR – background location, RES – residential area, TRA – traffic.

Location	Coordinates [°] (ETRS 1989)		Duration [days]	Appearance	Remarks
	Longitude	Latitude			
AGR1	11.15869	51.94153	139	Brown liquid, containing plant leaves, seed capsules and small larvae	Larvae could not be removed quantitatively
			369	Reddish brown, dry residue, containing snail shells, small plant leaves and some plastic particles	The upper part of the cup broke during the sampling
AGR2	12.48923	51.27739	177	Brown liquid, red, flaky sediment	-
			369	Dark green, dry residue, containing at least one big beetle	-
AGR3	12.51666	51.37705	158	Green liquid, containing many green flakes and some plant leaves	-
			324	Greenish brown liquid, containing dark green flakes and plant leaves	-
AIR1	12.27023	51.41387	365	Dark green, dry residue, containing insects, grass and small gravel	-
AIR2	12.20749	51.42082	365	Only few yellow to greyish particles	Only dry deposition
BGR1	11.61452	50.64494	372	Greenish liquid, containing a green sediment with some plant parts	-
BGR2	11.71070	50.97942	139	Reddish brown liquid, containing many small larvae	Larvae could not be removed quantitatively
			353	Reddish brown, flaky, dry residue, containing some bird droppings	-
RES1	11.56655	50.91020	unknown	Slightly red liquid, containing red flakes and a few wasps	-
			370	Brownish, crumbly residue, containing some dead wasps	-
RES2	11.59755	50.92461	363	Few dark brown liquid, containing many tree leaves	-
RES3	11.61163	50.96027	210	Brownish liquid, containing reddish green flakes and some insects	Small insects could not be removed
			366	Red, flaky, dry residue, containing many small black insects	Small insects could not be removed
RES4	12.42059	51.31425	359	Brown liquid, red and green flakes	-
			364	Brownish, dry residue, containing plant parts and a grasshopper	-
RES5	12.42059	51.31425	359	Greyish, powdery deposit, containing some plant seeds	Roofed, only dry deposition
			366	Yellow to greyish, powdery deposit, containing few parts of plants	
TRA1	11.57578	50.93239	188	Brown liquid, containing reddish flakes, larvae and plant needles	Larvae could not be removed quantitatively
			354	Greenish brown, dry residue, containing many tree needles	-
TRA2	12.42722	51.35190	152	Brownish liquid, containing plant leaves, seed capsules and larvae	Larvae could not be removed quantitatively
			353	Few brown liquid, containing a sediment mainly of plant leaves	-

Tab. A-8: Overview on the samples representing different source terms of PM. Soil types were taken from the German Bodenübersichtskarte 1:200,000 and named according to the German Bodenkundliche Kartieranleitung (BUNDESANSTALT FÜR GEOWISSENSCHAFTEN UND ROHSTOFFE 2005).

Sample type	**Sample ID**	**Coordinates [°] (ETRS 1989)**		**Comments**
		Longitude	**Latitude**	
Agricultural soil	NL-28.02.17-1	11.39434	50.92336	Soil type: Rendzina
	NL-28.02.17-2	11.34917	51.06641	Soil type: Tonmergel-Rendzina
	NL-28.02.17-3	11.32968	51.06641	Soil type: Schwarzerde
	NL-28.02.17-4	11.32316	51.05523	Soil type: Braunschwarzerde
	19.1-2	11.56256	50.97301	Soil type: Rendzina
	19.1-3	11.49543	50.93442	Soil type: Rendzina
	23.1-2	11.63461	50.96423	Soil type: Vega
	23.1-3	11.56055	50.94360	Soil type: (Para-)Rendzina
	24.1-4	11.56094	50.87878	Soil type: Rendzina
	30.1-1	11.61140	50.85693	Soil type: Vega
	30.1-2	11.64923	50.87893	Soil type: Braunerde
	1.2-1	11.64092	50.92908	Soil type: Pelosol
	1.2-2	11.64425	50.91981	Soil type: Pelosol
	7.2-2	11.62258	50.92395	Soil type: (Para-)Rendzina
Loess	KP-1	11.59595	50.90796	Jena, outcrop below the fault "Studentenrutsche"
	AB-1	11.59595	50.90796	Jena, outcrop below the fault "Studentenrutsche"
	KP-10	11.60628	50.95592	Jena, new outcrop "Rautal"
	KP-11	11.60647	50.95614	Jena, old outcrop "Rautal"
	AB-10	11.60647	50.95614	Jena, old outcrop "Rautal"
	NL-20.10.2016-1	11.70484	51.12974	Bad Kösen, next to a limestone quarry
	NL-20.10.2016-2	11.70484	51.12974	Bad Kösen, next to a limestone quarry
	NL-20.10.2016-3	11.70475	51.12426	Bad Kösen, limestone quarry
	NL-20.10.2016-4	11.80558	51.23037	Freyburg (Unstrut), northwestern part of an abandoned gravel pit
Tram/train	AB-2	11.59001	50.92388	Jena, residue from tram tracks close to the location TR-PAR
	MP-20.04.17-2	12.41669	51.31145	Leipzig, residue from tram tracks at the tram stop "Völkerschlachtdenkmal"
	P1	11.58349	50.90720	Jena, residue from tram tracks close to the location TR-ARE
	NL-17.01.17-1	12.38215	51.34587	Leipzig, railroad station, dust from wooden sleepers at an abandoned platform
	NL-24.01.17-1	12.38215	51.34587	Leipzig, railroad station, dust from a granite base at a platform
	NL-31.01.17-1	12.38215	51.34587	Leipzig, railroad station, dust from a concrete base at a platform
	NL-06.07.18-6	12.37442	51.34107	Leipzig, dust deposit on wall panels at the tram stop "Markt"
Brake wear	NL-03.05.18-2	-	-	Used brake disc
	NL-03.05.18-3	-	-	Used brake linings
Agricultural soil Liebertwolkwitz	MP-12.07.2016-2	12.48590	51.27411	Additional sample taken close to the location where additional spider webs were sampled (location CA-LIE)

Tab. A-9: Recovery rates [%] of elements certified in different standard reference materials. The materials were digested and measured according to the standard procedure including aqua regia digestion as described above (n: number of samples, -: no certified content). Green: good rates (≥ 85%), yellow: 70% ≤ recovery rate < 85%, red: poor rates (< 70%), blue: irrationally high rates (> 110%).

Element	SRM 1648a (n = 5)	SRM 1633a (n = 3)	SRM 1575 (n = 3)	IPE 952 (n = 3)	SOIL-7 (n =3)	BCR-146 (n = 3)
Al	56±2	24±2	96±2	-	-	43±0
As	89±4	88±2	-	-	98±9	-
B	-	-	-	76±9	-	-
Ba	-	-	-	99±2	-	-
Ca	99±2	61±1	96±1	96±1	-	95±0
Cd	105±5	75±5	-	115±3	106±5	106±4
Ce	67±2	-	-	-	86±1	-
Co	70±5	-	-	83±3	91±4	92±2
Cr	26±1	35±3	96±17	105±9	77±1	90±4
Cs	-	-	-	-	98±2	-
Cu	79±5	48±0	90±3	96±7	68±3	92±2
Dy	-	-	-	-	70±2	-
Eu	-	-	-	-	92±2	-
Fe	93±2	75±0	98±4	108±5	-	96±1
Hf	-	-	-	-	10±1	-
K	53±2	23±1	96±1	101±1	-	56±0
La	-	-	-	-	90±0	-
Li	-	-	-	104±5	-	-
Mg	88±4	35±1	-	93±0	-	82±1
Mn	101±2	53±2	101±1	100±2	108±1	104±1
Mo	-	-	-	100±1	-	-
Na	49±2	29±1	-	95±1	-	35±0
Nd	-	-	-	-	82±2	-
Ni	78±5	53±1	-	97±3	-	92±3
P	-	-	93±1	97±0	-	115±1
Pb	105±7	49±1	100±3	105±4	97±1	98±2
Rb	48±5	21±1	89±0	-	70±0	-
S	92±1	-	-	98±0	-	-
Sb	101±4	67±5	-	129±1	96±6	-
Sc	-	-	-	-	90±0	-
Si	-	1±0	-	-	-	2±0
Sm	-	-	-	-	94±2	-
Sr	84±2	48±1	97±2	102±1	84±1	-
Tb	-	-	-	-	68±2	-
Th	-	37±2	93±2	-	85±3	-
Ti	50±3	-	-	-	-	4±0
U	-	53±2	82±3	-	52±3	-
V	83±3	47±1	-	90±3	96±2	-
Y	-	-	-	-	64±2	-
Yb	-	-	-	-	40±2	-
Zn	85±8	53±1	-	99±1	89±1	97±1
Zr	-	-	-	-	8±0	-

Tab. A-10: Contents after aqua regia digestion divided by contents after total digestion for elements in different sample materials and in SRM 1648a (n: number of samples, *: outlier removed, underlined: SD ≥ 15%, -: contents below the LOD). Green: good rates (≥ 85%), yellow: 70% ≤ rate < 85%, red: poor rates (< 70%), blue: high rates (> 110%), grey: remarkably different rates (difference ≥ 30%).[1)]

Element	Spider webs (n = 12)	Moss bags (n = 6)	Dust from windows (n = 7)	Long-term deposit (n = 7)	Agricultural soil (n = 6)	Loess (n = 5)	SRM 1648a (n = 5)
Al	63±15	84±3	57±6	58±7	64±12	59±6	60±4
Ba	79±25	89±2	82±13	54±18	53±10	40±4	79±6
Ca	102±7*	104±1*	105±9	104±12	95±9	102±3	100±3
Cd	-	91±4	95±16	92±11	70±18	41±5	97±10
Ce	90±27	90±7	94±10	79±12	99±4	93±8	74±5
Co	95±5*	97±6	97±2*	77±7	92±3	92±5	84±2
Cs	64±15	74±4	85±12	61±13	94±11	95±4	56±13
Cu	92±21	96±7	104±15	85±6	100±3	85±1	94±9
Dy	72±8*	77±4	77±7	63±11	72±9	67±3	64±6
Er	63±14	74±8	66±7	53±8	57±11	54±5	59±4
Eu	76±17	-	92±9	73±12	95±4	89±7	71±7
Fe	98±11	109±3	95±11	100±4*	91±3	92±2	97±3
Gd	83±11*	87±11	90±11	71±10	89±4	82±6	68±6
Hf	23±9	20±5	16±4	15±4	11±8	-	24±1
K	90±8*	99±4	56±13	68±19	46±11	38±8	59±3
La	88±22	88±7	96±11	78±11	97±6	89±7	70±5
Li	88±24	111±55	84±9	69±14	88±6	91±5	62±6
Mg	93±15	104±1*	88±3*	95±6	93±5	84±2	93±4
Mn	110±13	111±2	102±4	110±9	97±3	110±4	104±2
Mo	96±17	96±4*	106±15	99±12	89±13	89±14	96±4
Na	79±19	83±11	68±23	19±6	12±10	9±5	50±3
Nb	53±12	58±8	38±2*	45±6	20±5	-	55±3
Nd	88±22	90±6	100±10	82±14	104±4	99±9	72±6
Ni	84±31	83±21	100±9	71±19	103±4	90±2	81±20
P	102±8	110±6	96±12	113±17	93±3	95±2	103±2
Pb	89±12	95±2	99±15	89±10	89±4	74±2	99±9
Pr	88±24	90±7	100±10	83±14	104±5	102±10	73±7
Rb	59±12	75±2	59±7	48±9	68±15	62±9	54±7
Sb	94±9*	97±12	98±13*	82±21	82±6	73±5	92±10
Sm	86±23	93±10	99±12	82±14	102±4	99±7	74±6
Sn	92±24	119±18	192±15	89±9	77±12	67±6	74±8
Sr	92±15	100±5	88±9	83±16	66±15	84±15	84±4
Th	84±26	81±9	87±11	71±12	87±6	86±3	64±7
Ti	42±11	47±7	33±14	37±5	24±2	24±2	56±4
U	63±15	67±11	72±5	57±14	55±8	54±12	70±6
V	89±10*	93±16	87±12	82±8	84±10	73±8	92±3
W	94±59*	82±15	71±15	73±8*	26±6	-	89±6
Y	68±12	85±4	68±6	58±8	67±10	59±4	65±2
Yb	55±11	67±6	58±6	45±7	48±12	45±3	55±3
Zn	94±59	91±6	98±11	85±5	98±3	86±2	91±10
Zr	23±9	22±5	18±3	14±4	12±8	7±1	22±1

[1)] Ag, As, Ho, Lu, Tb, Tm: below the LOD; B, Cr, S, Si: formation of volatiles (e.g. CrO_2Cl_2) during total digestion (BOCK 2005; MAKISHIMA et al. 2002). Sc: problems for materials with high C_{org}, ascribed to isobaric interferences of $^{45}Sc^+$ with $^{12}C^{16}O_2{}^1H^+$ and $^{14}N_2{}^{16}O^1H^+$ (MAY and WIEDMEYER 1998).

Tab. A-11: Certified element contents [µg/g] and relative standard deviations (rel. SD) [%] in different standard reference materials given by the associated certificates (-: no certified content available). For SOIL-7 and some contents in BCR-146 no rel. SD was available.

Element	SRM 1648a		SRM 1633a		SRM 1575		IPE 952		SOIL-7	BCR-146	
	Mean	rel. SD	Mean	rel. SD	Mean	rel. SD	Mean	rel. SD	Mean	Mean	rel. SD
Al	34,300	4	143,000	7	545	6	-	-	-	47,600	-
As	115.5	3	145	10	-	-	-	-	13.4	-	-
B	-	-	-	-	-	-	7.01	23	-	-	-
Ba	-	-	-	-	-	-	19.1	13	-	-	-
Ca	58,400	3	1.11	1	4,100	5	5,400	7	-	101,400	-
Cd	73.7	3	1.00	15	-	-	2.91	11	1.3	77.7	3
Ce	54.6	4	-	-	-	-	-	-	61	-	-
Co	17.93	4	-	-	-	-	0.273	17	8.9	11.8	6
Cr	402	3	196	3	2.6	8	3.69	13	60	784	-
Cs	-	-	-	-	-	-	-	-	5.4	-	-
Cu	610	11	118	3	3.0	10	14.5	9	11	934	3
Dy	-	-	-	-	-	-	-	-	3.9	-	-
Eu	-	-	-	-	-	-	-	-	1.0	-	-
Fe	39,200	5	94,000	1	200	5	493	9	-	18,500	-
Hf	-	-	-	-	-	-	-	-	5.1	-	-
K	10,560	5	18,800	3	3,700	5	37,600	6	-	4,800	-
La	-	-	-	-	-	-	-	-	28	-	-
Li	-	-	-	-	-	-	0.448	25	-	-	-
Mg	8,130	1	4,550	2	-	-	1,680	7	-	19,900	-
Mn	790	6	179	4	675	2	81.5	8	631	588	4
Mo	-	-	-	-	-	-	5.68	8	-	-	-
Na	4240	1	1,700	6	-	-	1,300	12	-	2,200	-
Nd	-	-	-	-	-	-	-	-	30	-	-
Ni	81.1	8	127	3	-	-	6.74	8	-	280	6
P	-	-	-	-	1,200	17	4,260	5	-	25,800	-
Pb	6,550	5	72.4	1	10.8	5	6.55	11	60	1,270	2
Rb	51.0	3	131	2	11.7	1	-	-	51	-	-
S	55,100	7	-	-	-	-	3,640	7	-	-	-
Sb	45.4	3	6,8	6	-	-	0.125	14	1.7	-	-
Sc	-	-	-	-	-	-	-	-	8.3	-	-
Si	-	-	228,000	4	-	-	-	-	-	106,700	-
Sm	-	-	-	-	-	-	-	-	5.1	-	-
Sr	215	8	830	4	4.8	4	7.99	9	108	-	-
Tb	-	-	-	-	-	-	-	-	0.6	-	-
Th	-	-	24.7	1	0.037	8	-	-	8.2	-	-
Ti	4021	2	-	-	-	-	-	-	-	17,400	-
U	-	-	10.2	1	0.020	20	-	-	2.6	-	-
V	127	9	297	2	-	-	3.07	10	66	-	-
Y	-	-	-	-	-	-	-	-	21	-	-
Yb	-	-	-	-	-	-	-	-	2.4	-	-
Zn	4800	6	220	5	-	-	82.0	7	104	4,059	2
Zr	-	-	-	-	-	-	-	-	185	-	-

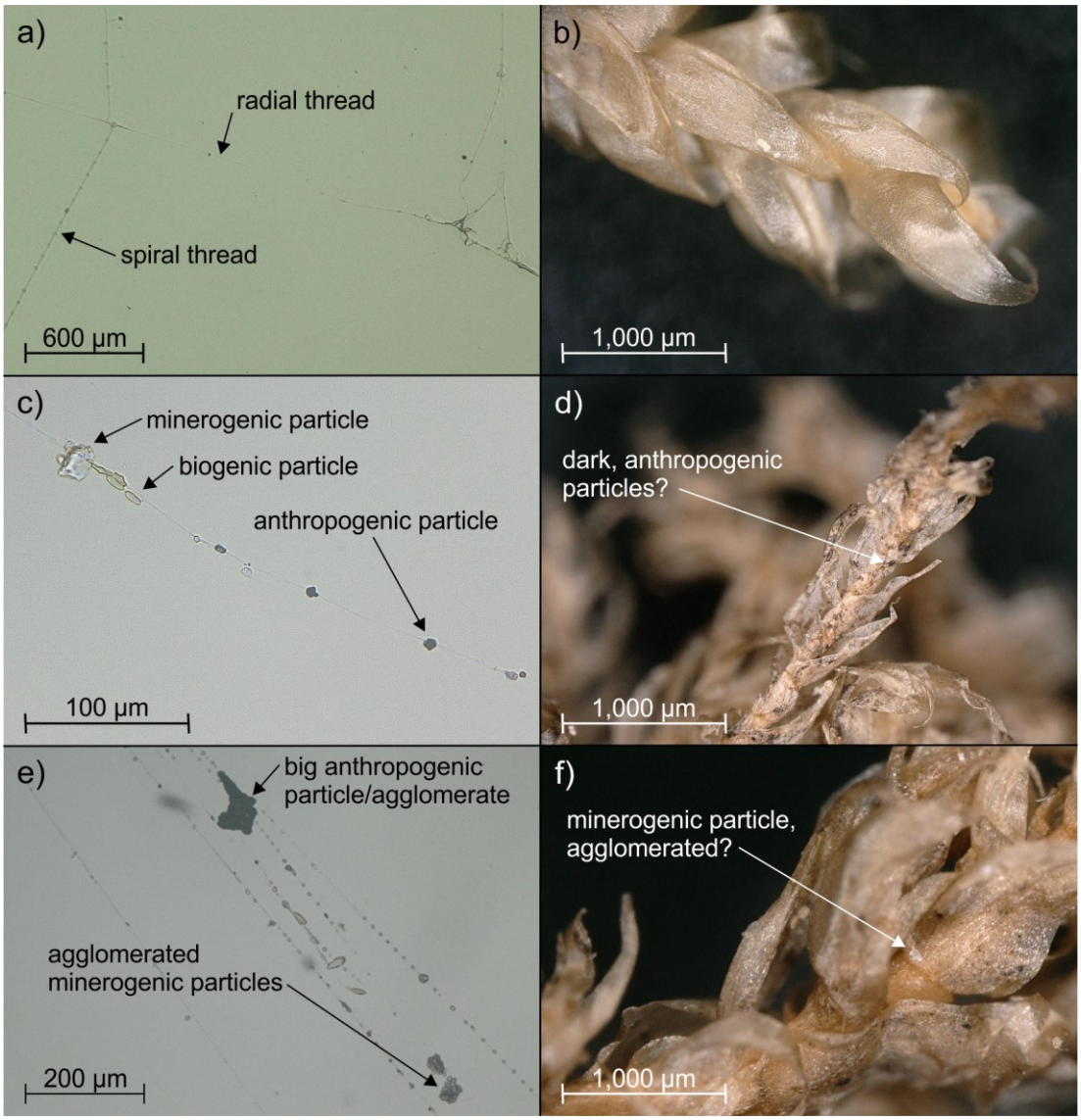

Fig. A-1: Images of selected spider web (a, c, e) and moss bag (b, d, f) samples taken with the digital microscope. a) characteristic appearance of wheel webs with a strong radial thread and a spiral thread covered with sticky droplets to capture prey, b) washed moss prior to exposure, c) coarse particles attached to the droplets on a spiral thread, d) moss after exposure, containing dark, likely anthropogenic particles, e) several spiral threads close to each other, capturing larger objects, f) moss after exposure, containing also big, minerogenic particles.

Tab. A-12: Median content [µg/g] and interquartile range (IQR) of elements determined in different sample materials. The table aggregates all samples taken per sample material except for moss bags, for which only the two campaigns of ten weeks of exposure time are aggregated. "-" indicates that more than 5% of the values were below the limit of detection.

Element	Spider webs (n = 296)		Moss bags (n = 30) 10 weeks exposure		Dust from windows (n = 56)		Long-term deposit (n = 24)	
	Median	IQR	Median	IQR	Median	IQR	Median	IQR
Ag	-	-	0.043	0.017	-	-	0.190	0.170
Al	5,210	4,890	786	183	13,200	4,350	6,470	4,450
As	-	-	-	-	-	-	-	-
B	-	-	9.97	10.0	83.0	76.8	17.5	25.3
Ba	190	192	42.9	14.4	479	292	85.7	78.8
Ca	14,400	14,800	5,160	663	55,600	26,900	8,490	8,270
Cd	-	-	0.280	0.037	1.36	1.44	0.663	0.465
Co	3.10	2.78	0.412	0.119	11.1	9.46	1.82	1.29
Cr	37.7	41.0	2.34	1.51	74.2	53.4	15.8	13.8
Cs	1.19	1.31	0.115	0.033	-	-	0.689	0.692
Cu	83.8	143	9.70	5.30	243	264	50.2	66.6
Fe	10,700	11,000	796	151	22,000	14,600	6,190	4,520
Hf	-	-	0.025	0.007	-	-	0.222	0.210
K	9,990	4,070	1,860	853	8,520	6,790	3,800	1,970
La	4.50	4.61	0.669	0.180	13.0	4.77	4.96	4.65
Li	-	-	0.517	0.237	24.1	8.15	6.24	5.51
Mg	3,190	2,770	1,040	226	8,670	4,060	2,470	1,360
Mn	211	153	499	65.7	435	176	144	95.7
Mo	-	-	0.343	0.107	7.05	4.59	1.70	1.15
Na	3,510	2,560	181	1,350	24,600	26,900	302	292
Nb	-	-	0.134	0.039	3.05	0.993	1.20	1.30
Ni	17.8	17.8	3.05	1.15	49.0	30.6[1)]	9.24	7.18
P	9,380	5,810	497	198	-	-	4,150	1,910
Pb	14.7	12.8	9.25	2.61	160	412[1)]	23.1	25.1
Rb	14.7	7.19	3.48	1.62	27.2	9.60	9.76	9.61
S	7,150	3,030	1,060	217	11,800	8,980	3,820	850
Sb	8.43	14.3	0.475	0.377	16.6	9.06	1.94	3.43
Si	6,170	4,790	1,150	310	9,240	9,940	3,530	3,250
Sn	13.7	27.1	0.970	0.662	56.4	27.7	7.47	12.4
Sr	65.4	63.0	14.6	3.26	213	117	34.1	38.7
Th	1.16	1.29	0.171	0.057	3.38	1.53	1.50	1.36
Ti	363	434	29.7	9.37	836	335	319	245
U	-	-	0.052	0.017	1.26	0.493	0.408	0.329
V	-	-	1.51	0.333	30.8	10.5	12.5	7.99
W	-	-	0.091	0.027	2.46	2.33	0.655	0.721
Y	2.51	2.46	0.391	0.093	6.58	2.91	2.79	2.28
Zn	384	534	45.4	18.1	1,540	1,780	243	819
Zr	9.00	8.33	0.776	0.238	21.6	7.55	7.54	7.01

[1)] Upper quartile: higher in some samples than test values named in the German Bundes-Bodenschutz- und Altlastenverordnung (BBodSchV) for the exposure pathway soil-humans.

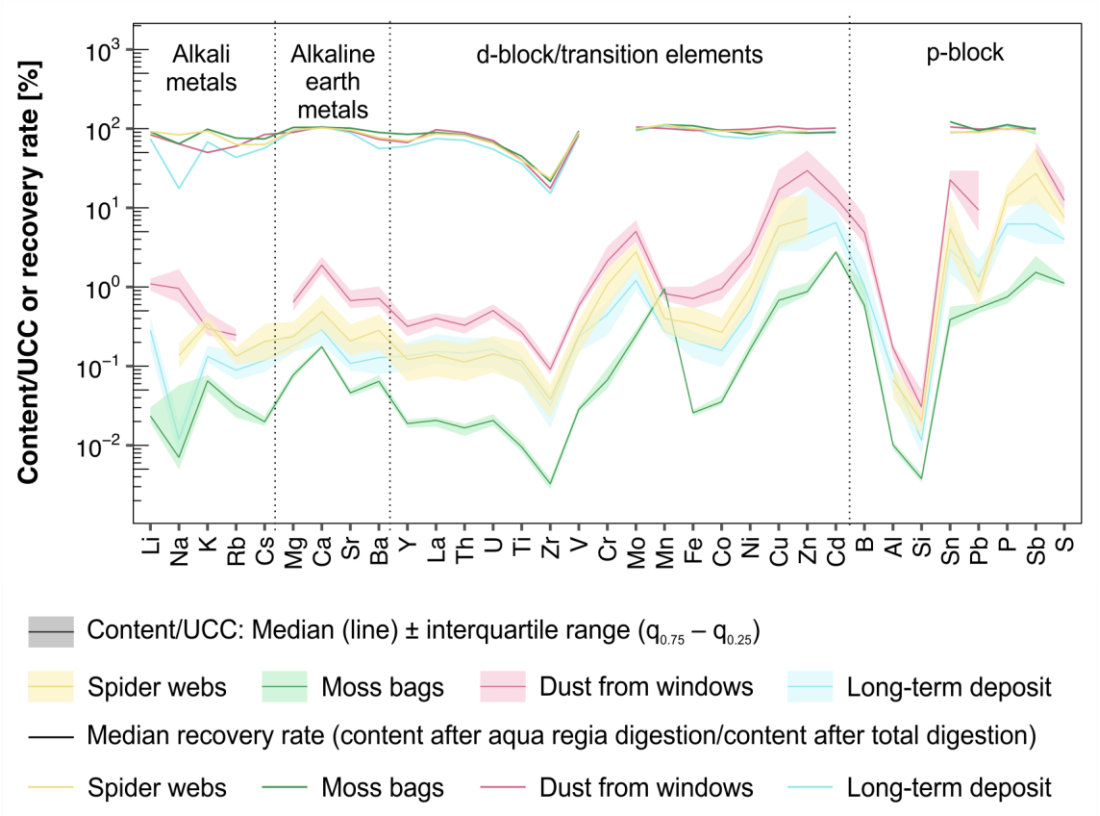

Fig. A-2: Contents of elements determined in different sample materials divided by contents in the upper continental crust (UCC) given by WEDEPOHL (1995) and recovery rates (content after aqua regia digestion divided by content after total digestion) in percent for each sample material.

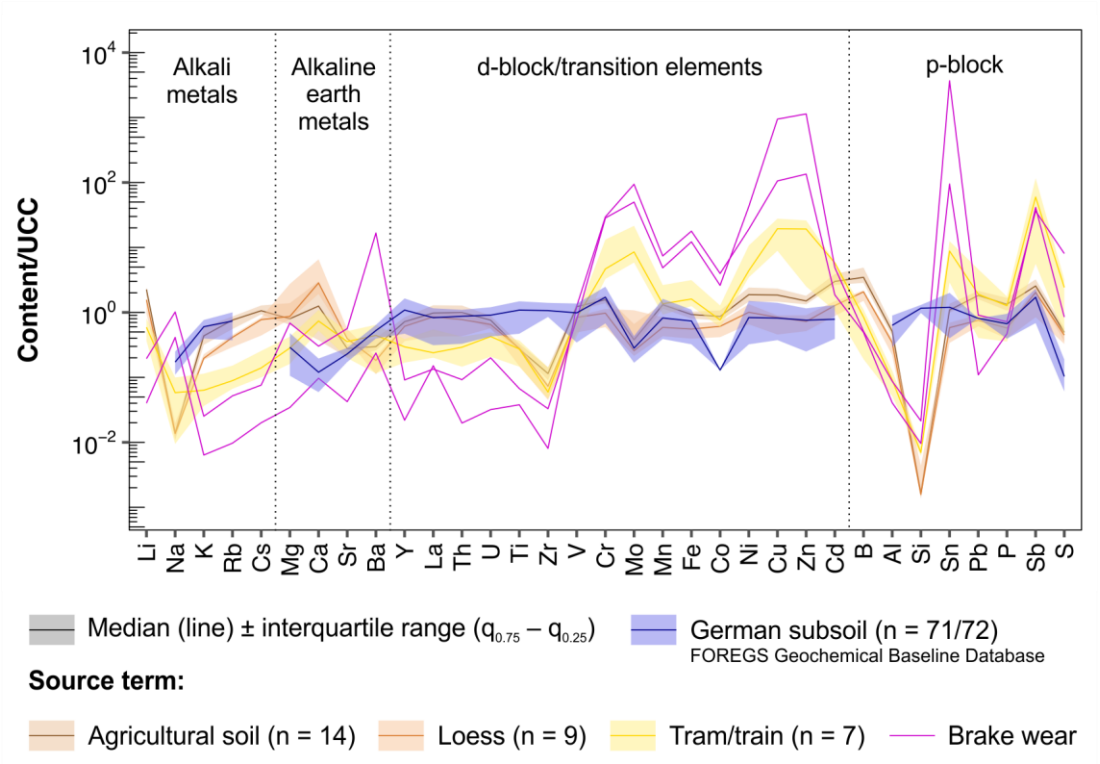

Fig. A-3: Contents determined in samples representing different source terms divided by contents in the upper continental crust (UCC) given by Wedepohl (1995). For comparison, total contents in German subsoil from FOREGS Geochemical Baseline Database (SALMINEN et al. 2005) were added.

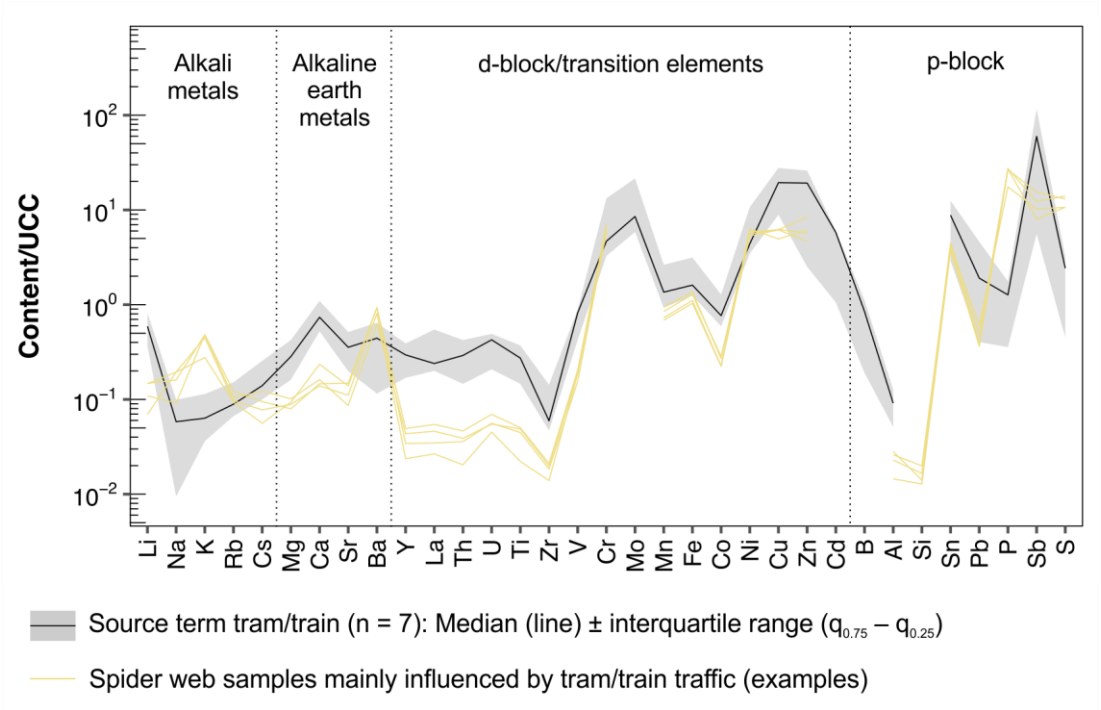

Fig. A-4: Comparison of contents determined in selected spider web samples from location TR-ARE, influenced by tram and train traffic, and in samples representing the source term tram/train, standardized to contents in the upper continental crust (UCC) given by WEDEPOHL (1995).

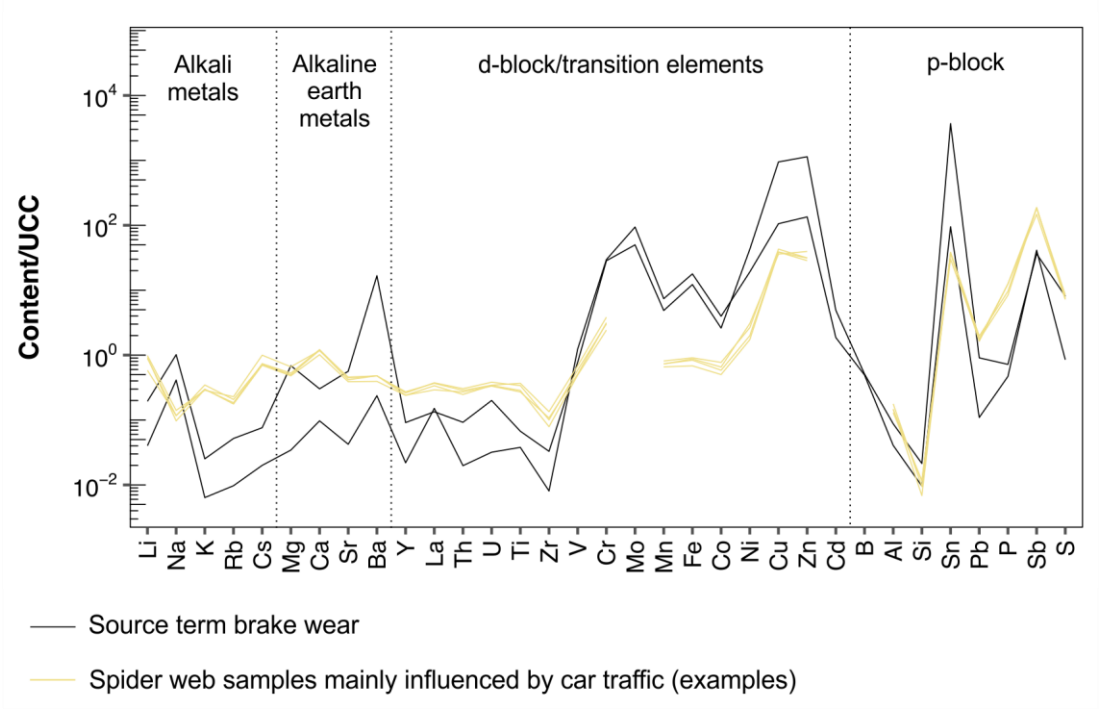

Fig. A-5: Comparison of contents determined in selected spider web samples from location CA-BUR_1, next to a busy road, and in samples representing the source term brake wear, standardized to contents in the upper continental crust (UCC) given by WEDEPOHL (1995).

Tab. A-13: Element contents in spider web samples (n = 265) from the city of Jena and the corresponding interquartile range (IQR). Outliers according to DIXON (P = 99%, 1951) were removed prior to the calcuations (n = 264) and normality was checked according to DAVID et al. (P = 99%, 1954).

Element	Median [µg/g]	Minimum [µg/g]	Maximum [µg/g]	IQR [µg/g] ($q_{0.75}$ - $q_{0.25}$)	IQR*100%/ Median [%]	Outlier removed?	Normal distribution?
Ca	14,600	2,330	63,500	15,200	104	yes	yes
Fe	11,300	572	42,000	11,400	101	no	yes
K	10,000	4,740	19,300	4,090	41	no	yes
P	9,330	2,650	20,900	5,790	62	no	no
S	7,150	2,770	13,300	3,050	43	yes	yes
Si	6,140	763	20,200	4,760	77	no	yes
Al	5,100	395	17,600	5,270	103	no	yes
Na	3,430	20.2	12,520	2,310	67	yes	yes
Mg	3,150	601	11,500	2,960	94	no	yes
Zn	379	47.0	2,600	503	133	yes	yes
Ti	338	26.2	1,450	449	133	no	yes
Mn	211	26.9	539	158	75	no	yes
Ba	194	10.4	1,630	202	104	yes	yes
Cu	82.5	6.60	613	146	176	yes	yes
Sr	66.2	10.7	355	63.9	97	yes	yes
Cr	38.0	2.31	238	43.1	113	yes	yes
Ni	18.0	1.20	109	18.5	103	yes	yes
Rb	14.6	6.00	37.1	7.08	49	yes	yes
Pb	14.0	1.16	156	11.8	84	yes	no
Sn	13.4	0.980	101	27.9	209	yes	no
Zr	8.50	0.080	31.9	8.21	97	yes	yes
Sb	8.10	0.289	58.3	14.4	178	no	no
Li	7.60	0.012	22.8	8.60	113	no	no
La	4.30	0.367	15.4	4.82	112	yes	no
Co	3.00	0.390	18.8	2.81	94	yes	no
Y	2.42	0.221	8.87	2.52	104	yes	yes
Cs	1.22	0.006	4.60	1.39	114	yes	no
Th	1.14	0.098	5.10	1.32	116	no	yes

Tab. A-14: Median enrichment factors (EF_{Al}) for spider webs from 22 locations in Jena. An asterisk indicates a large variation with ($q0_{.84} - q_{0.16}$) / 2 > SD. Petrol: $EF_{Al} < 1$, blank: $1 \leq EF_{Al} < 5$, yellow: $5 \leq EF_{Al} \leq 10$, purple: $EF_{Al} > 10$.

Location	Li	Na	K	Rb	Cs	Mg	Ca	Sr	Ba	Y	La	Th	Ti	Zr	Cr	Mn	Fe	Co	Ni	Cu	Zn	Si	Sn	Pb	P	Sb	S
CA/TR-CAM	6	3*	6	2	4	4	8*	3	4	2	2	2	2	1	19	6	6	4	15	152	123	0	180	12	220*	700*	126*
CA/TR-GOE_1	5	2	5	2	4	4	7	3	7*	2	2	2*	2	1	12	5	5	4	14	85	199	0	68	11*	196	485	102
CA/TR-GOE_2	4	3	4	2	4	4	7	3	8*	2	2	1	2*	1	13	5	5	4	12	98*	223*	0	114	11*	175*	574	81
CA-BUR_1	5*	1	2	1	5	4	8	3	3	2	2	2	2	1	19	5	5	4	13	207*	180	0*	208	12	91	1005	58
CA-BUR_2	5	1	4	1	4	4	8	3	3	2*	2	2	2*	1	14	5	5*	4	12	134	151	0	154	10	140	579	72
CA-JOH	5	1	3	1	4	3	8	3	3	2	2*	2	2	1	16	5	5	4	13	199	160	0*	216	13	95*	923*	55
CA-KUN	5	1	2	1	2	4	9*	3*	3	2	2	2	2	0	7	5	3*	4	10	28	42	0	22	9	54	98	33
CA-MAU	5	1*	6	2	3*	4	9*	4	3	2	2*	2	2	0	8	5	3	3	10*	51*	179	0	61	11	211	175	130
CA-PAR	5	3	5	2	4*	3	8	3	4	2	2	2	2	1	20	5*	5	4	14	195*	171*	0*	245	11	196	1049*	108
CA-WIE	5	1	3	1	3	3	9	4	5	2	2	2	2	1	11	4	4	3*	10	110	144*	0*	144	11	112	585	69
PD-BUR	5	8	14	4	3	4*	11	4	3	2*	2	2*	1	0*	10	6	3	3	10	72*	101*	0	71	13	762*	346*	336
PD-GRI	6	4	6	2	3	4	8	3	2	2	2	2	2	1	11	5	4	9	10	88	87	0	84	14	255	380	123
PD-IGW	6	2	8	2	2	4	10	4	4	2	2*	1*	1*	1	8	4	3	3	8	53*	69	0	46	12	454	236	161
PD-KUN	5	4	8	2	3	3	9	4	2	2	2*	2	1	0	7	5	3	3	9	41	46	0	31*	10	327	174*	132
PD-LOB	4*	3	9	2	3	4	9	4	3	2	2	2	1	1	9	5	3	3	7	56	100	0	51*	15	417	356	194
PD-SAA	6	1	6	2	3*	3	6	3	2	2	2	1	1*	1	18	5	5	4	12	80	130	0	71	13	341	483*	176
PD-STA	6	2	6	2	2	3	6	3	8	2	2	2	1	0*	8*	4	3	4	9	37	46	0	27	8	217	148*	103
PD-USV	6	2	5	2	3	3	7	3	3	2	2*	2	1	1*	9*	5	3	3	9*	50	85	0	48	30	175	247	88
RS-PAR	6	2	7	2	4	4	10	4	3*	2*	2	2*	1*	1	24	9	10*	5	19	128	119*	0	109	17	280	653*	118
TR-ARE	6	6	17	5	4	4	8	5	28	2	2*	2	2	1	131	24	35	7	126	228*	213	1	126	16	876	354*	435
TR-BUR	5	3	7	2	3	4	8	4	10	2	2	2	2	1	17	8	8	4	18	92	128	0	101	14	316*	289	153
TR-PAR	5	6	12	3	4	4	8	4	25*	2	2	2*	2*	1	57	11	12	5*	55	155*	164	1	115*	18	596	591	303

Tab. A-15: Significant (P = 99%) Spearman rank correlation coefficients (r_s) for elements determined in spider webs. Grey: r_s > median($|r_s|$), yellow: r_s > $q_{0.75}$ ($|r_s|$).

	Rb	K	S	P	Si	Al	Ca	Li	Sr	Y	Cs	Mg	Ti	La	Th	Zr	Pb	Co	Ba	Mn	Fe	Cr	Ni	Cu	Sb	Sn	Zn	Na
Rb	1.00					0.62	0.54	0.60	0.52	0.62	0.54	0.56	0.54	0.59	0.62	0.56	0.51	0.52	0.25	0.50	0.33	0.26	0.29	0.33	0.35	0.37	0.40	
K		1.00	0.64	0.76		-0.18	-0.27		-0.28	-0.21		-0.23	-0.27	-0.19			-0.18	-0.20						-0.20	-0.17			0.28
S			1.00	0.78															0.31	0.17	0.26	0.23	0.21					0.54
P				1.00		-0.31	-0.37	-0.29	-0.36	-0.35	-0-32	-0.37	-0.39	-0.33	-0.30	-0.27	-0.25	-0.29						-0.25	-0.24	-0.22	-0.21	0.39
Si					1.00	0.47	0.42	0.45	0.42	0.45	0.47	0.42	0.46	0.40	0.40	0.48	0.41	0.39	0.17	0.27	0.20	0.17		0.26	0.32	0.28	0.28	
Al						1.00	0.94	0.93	0.93	0.99	0.92	0.96	0.95	0.96	0.96	0.93	0.87	0.90	0.45	0.71	0.53	0.47	0.47	0.69	0.76	0.73	0.74	0.17
Ca							1.00	0.89	0.97	0.95	0.88	0.96	0.92	0.93	0.91	0.87	0.86	0.86	0.38	0.66	0.49	0.44	0.43	0.69	0.78	0.74	0.74	
Li								1.00	0.89	0.92	0.85	0.91	0.88	0.91	0.89	0.88	0.82	0.86	0.43	0.68	0.52	0.47	0.47	0.66	0.71	0.69	0.69	0.21
Sr									1.00	0.93	0.86	0.94	0.91	0.91	0.90	0.87	0.83	0.86	0.49	0.69	0.54	0.49	0.50	0.70	0.75	0.74	0.74	
Y										1.00	0.92	0.96	0.96	0.96	0.96	0.91	0.85	0.89	0.42	0.70	0.51	0.45	0.46	0.68	0.75	0.72	0.73	
Cs											1.00	0.91	0.95	0.90	0.88	0.94	0.81	0.84	0.42	0.69	0.57	0.55	0.51	0.81	0.86	0.83	0.83	
Mg												1.00	0.96	0.95	0.93	0.90	0.83	0.88	0.41	0.67	0.50	0.44	0.45	0.70	0.79	0.76	0.77	
Ti													1.00	0.92	0.90	0.91	0.81	0.88	0.44	0.68	0.54	0.50	0.50	0.76	0.81	0.79	0.81	
La														1.00	0.96	0.89	0.85	0.87	0.43	0.69	0.51	0.44	0.45	0.67	0.75	0.71	0.73	0.17
Th															1.00	0.88	0.85	0.86	0.42	0.69	0.49	0.42	0.43	0.63	0.72	0.69	0.70	
Zr																1.00	0.83	0.87	0.48	0.72	0.61	0.57	0.53	0.80	0.85	0.83	0.80	0.17
Pb																	1.00	0.81	0.42	0.65	0.50	0.44	0.42	0.63	0.72	0.68	0.73	
Co																		1.00	0.51	0.78	0.65	0.60	0.61	0.73	0.75	0.75	0.73	0.23
Ba																			1.00	0.68	0.72	0.66	0.73	0.50	0.37	0.45	0.52	0.20
Mn																				1.00	0.93	0.85	0.87	0.70	0,59	0.65	0.66	0.20
Fe																					1.00	0.95	0.93	0.74	0.57	0.64	0.63	0.23
Cr																						1.00	0.94	0.76	0.57	0.65	0.63	0.21
Ni																							1.00	0.66	0.46	0.55	0.57	0.21
Cu																								1.00	0.92	0.96	0.89	0.18
Sb																									1.00	0.96	0.89	0.17
Sn																										1.00	0.91	0.18
Zn																											1.00	
Na																												1.00

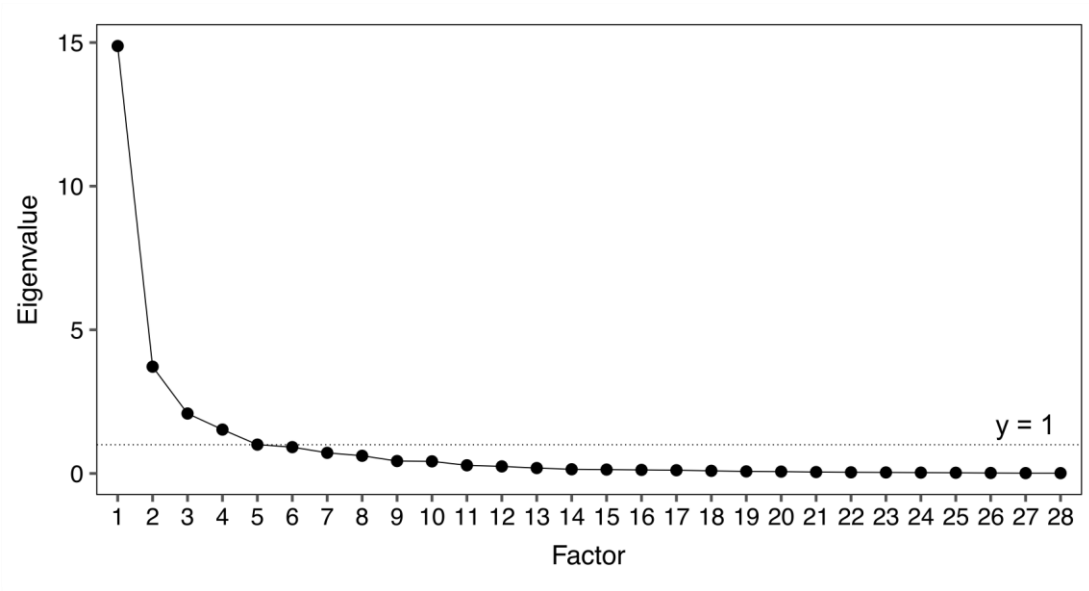

Fig. A-6: Screeplot of the factor analysis of 260 spider web samples from Jena. A horizontal line is drawn at an eigenvalue of 1 to show which eigenvalues meet the Guttman-Kaiser criterion.

Tab. A-16: Rates of correct classification of different classification models calculated with 260 spider web samples from Jena classified according to the five different types of nearby traffic. LDA: linear discriminant analysis, kNN: k-nearest neighbours classification, PLS-DA: partial least squares-discriminant analysis, SIMCA: soft independent method of class analogy.

	LDA	**kNN (1 neighbour)**	**kNN (3 neighbours)**	**PLS-DA (6 latent variables)**	**SIMCA**
Correct classification (reclassification)	88%	73%	76%	82%	58%
Correct classification (cross-validation)	83%	72%	78%	78%	-

Tab. A-17: Means of classes (autoscaled values) in the linear discriminant analysis for every element included in the discriminant model. Underlined: absolute mean bigger than 0.70.

Element	Classes				
	Car	**Car & tram/train**	**Pedestrian**	**Railroad station**	**Tram/train**
Al	0.71	0.02	-0.47	-0.43	-0.87
Ba	-0.07	0.21	-0.51	-0.58	1.08
Ca	0.73	-0.06	-0.51	-0.21	-0.85
Co	0.42	0.00	-0.27	-0.31	-0.52
Cr	0.18	-0.21	-0.76	-0.04	1.05
Cs	0.75	0.19	-0.64	-0.28	-0.78
Cu	0.75	-0.09	-0.73	-0.24	-0.47
Fe	0.23	-0.13	-0.89	0.48	1.01
K	-0.42	0.19	0.28	0.32	0.36
La	0.69	0.05	-0.47	-0.30	-0.85
Li	0.62	-0.01	-0.39	-0.23	-0.81
Mg	0.75	0.19	-0.56	-0.40	-0.91
Mn	0.44	-0.12	-0.83	0.27	0.42
Na	-0.23	0.46	0.13	-0.34	0.14
Ni	0.09	-0.15	-0.73	-0.18	1.24
P	-0.57	0.12	0.41	-0.17	0.66
Pb	0.46	-0.16	-0.24	-0.07	-0.62
Rb	0.38	0.04	-0.30	0.21	-0.48
S	-0.33	0.30	0.04	-0.24	0.62
Sb	0.74	0.01	-0.64	-0.17	-0.69
Si	0.16	0.20	-0.07	0.15	-0.45
Sn	0.81	-0.08	-0.72	-0.43	-0.60
Sr	0.72	-0.17	-0.52	-0.41	-0.68
Th	0.72	-0.06	-0.50	-0.41	-0.80
Ti	0.76	0.33	-0.65	-0.57	-0.82
Y	0.72	0.11	-0.51	-0.49	-0.87
Zn	0.68	0.43	-0.74	-0.43	-0.56
Zr	0.68	-0.04	-0.55	-0.22	-0.64

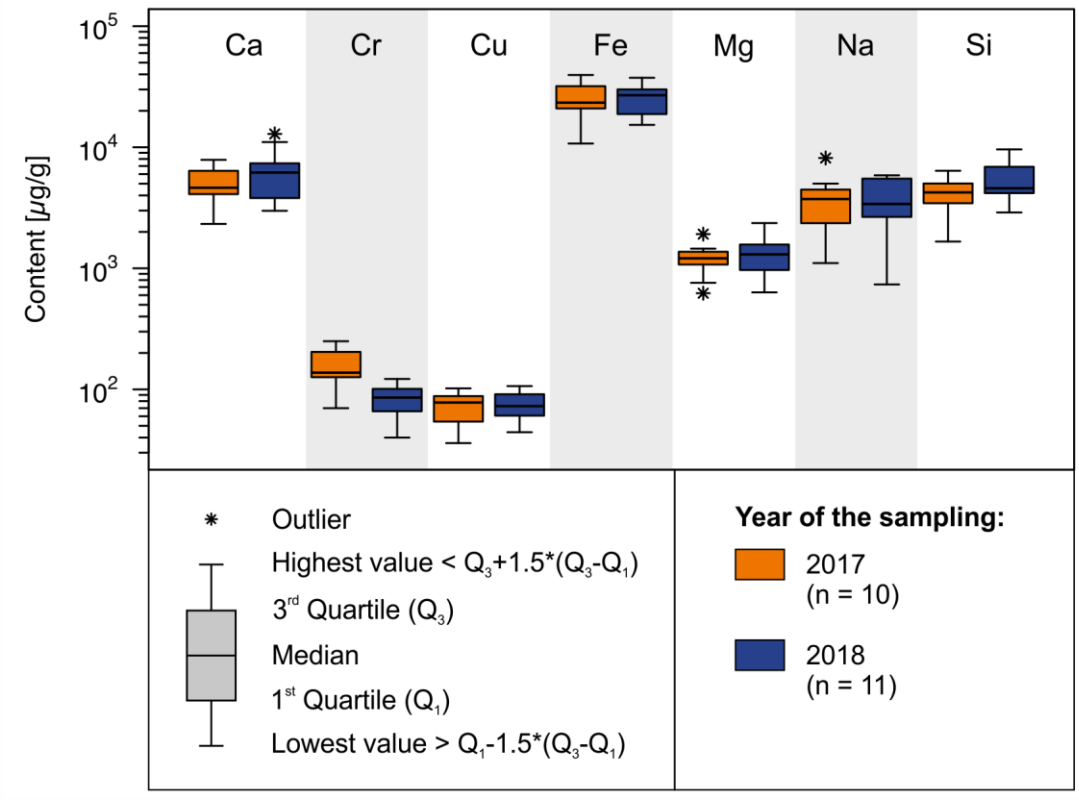

Fig. A-7: Comparison of contents of selected elements in spider webs collected at the location TR-ARE in 2017 and 2018. For some elements noticeable differences between the years can be found (e.g. Cr, Si) while for others boxplots look similar for the two years (e.g. Cu, Fe).

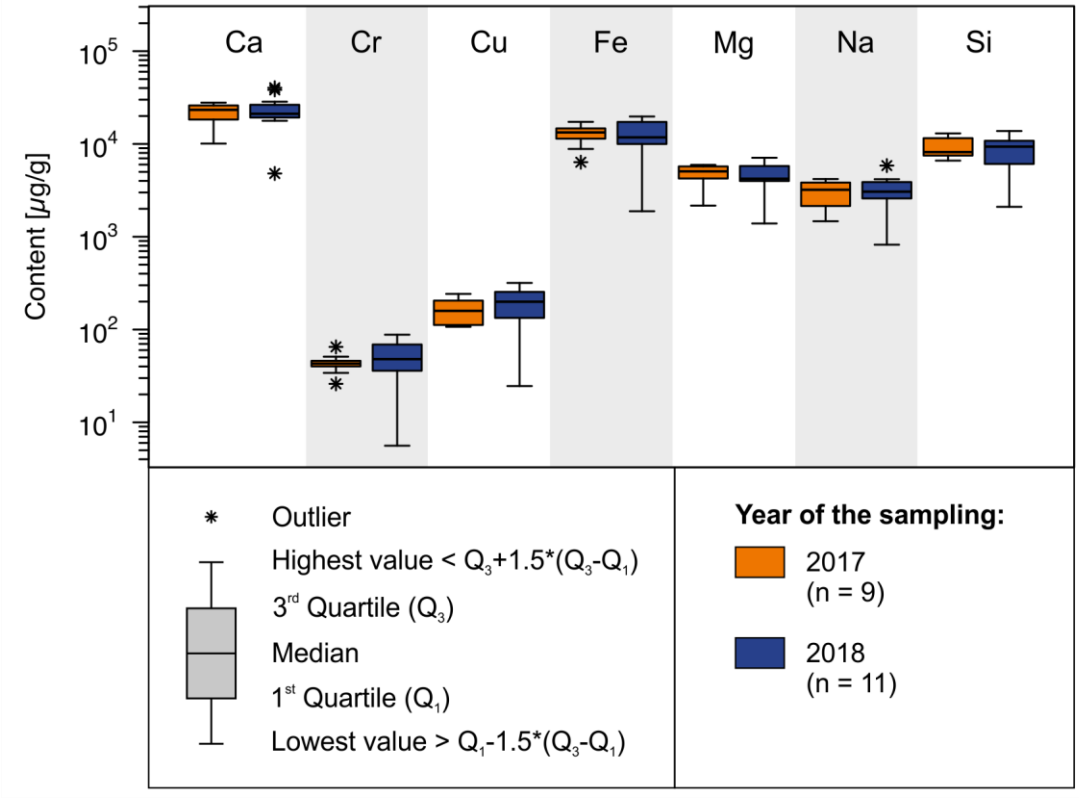

Fig. A-8: Comparison of contents of selected elements in spider webs collected at the location CA-BUR_2 in 2017 and 2018. While median contents for each element are similar for the two years, a greater variation can be observed for the samples from 2018 than for the ones from 2017.

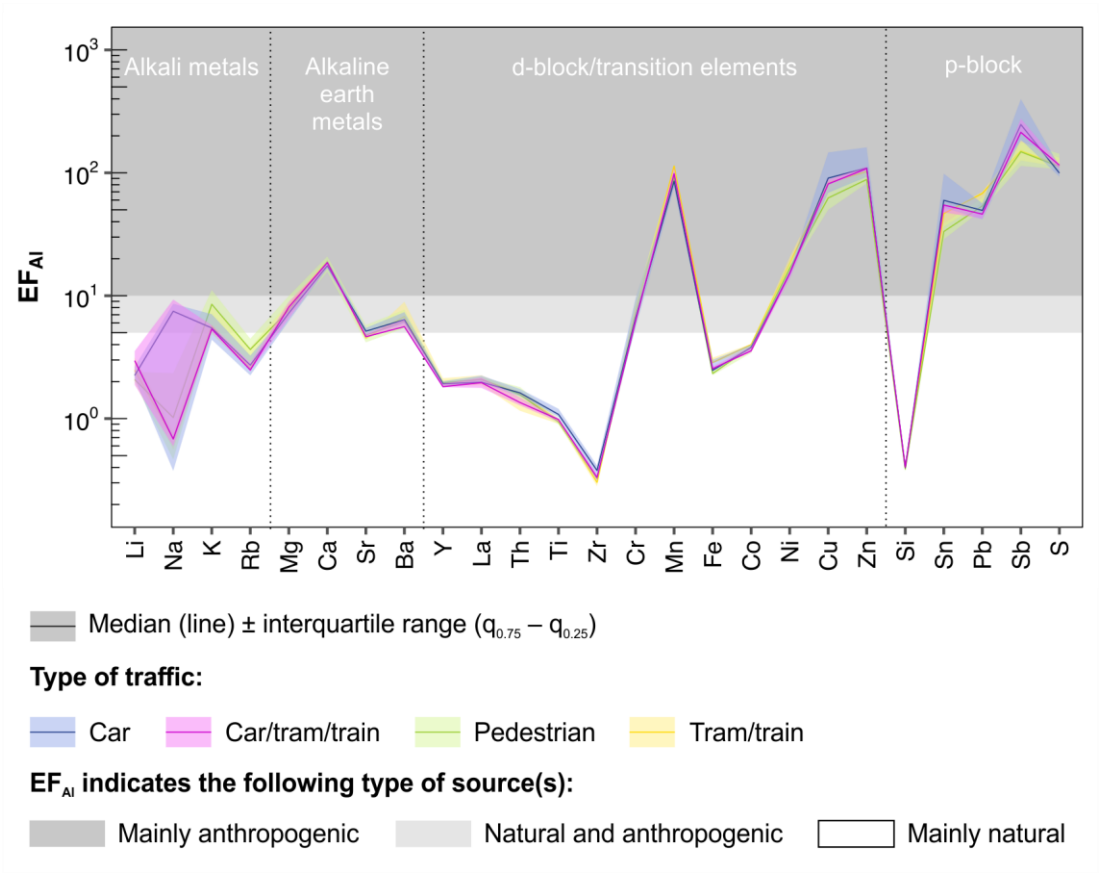

Fig. A-9: Enrichment factors of elements in moss bag samples from locations with different types of traffic: car (n = 8), car/tram/train (n = 5), pedestrian (n = 12) and tram/train (n = 5). Al has been used as internal normalizing element and contents in the upper continental crust given by WEDEPOHL (1995) were used as geogenic reference.

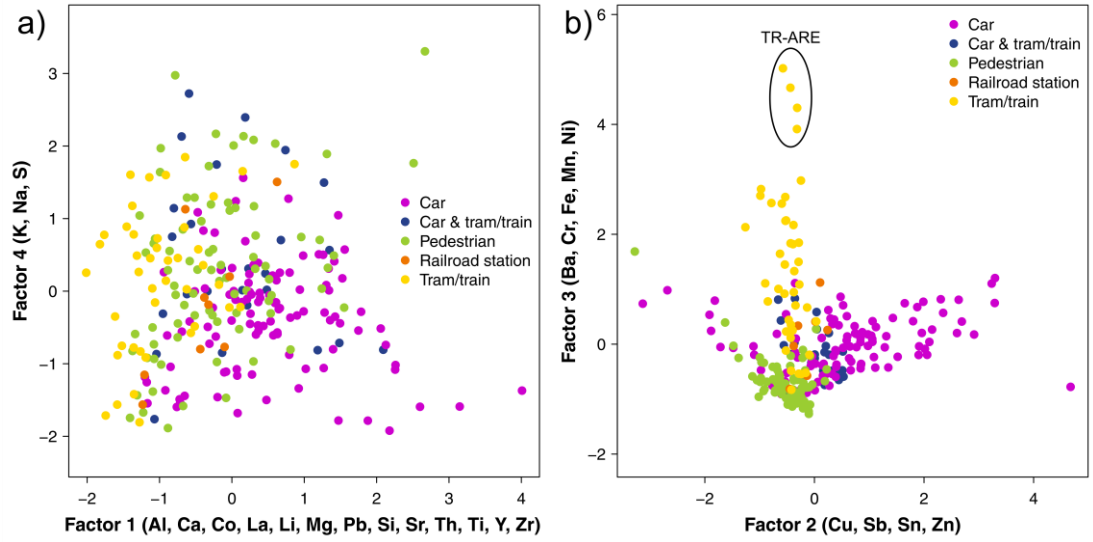

Fig. A-10: Plot of selected factor scores (a) factors 1 and 4, b) factors 2 and 3, factor analysis with varimax rotation) of 265 spider web samples from Jena and contents of 26 elements.

Tab. A-18: Factors loadings, communalities (h_i^2) and variance explained resulting from the factor analysis (varimax rotation) of 265 spider web samples from 22 locations in Jena. Only the highest loading for each element is shown.

Element	Factor 1	Factor 2	Factor 3	Factor 4	Factor 5	h_i^2
Al	0.92					0.97
Ba			0.51			0.40
Ca	0.86					0.88
Co	0.71					0.61
Cr			0.92			0.93
Cu		0.85				0.89
Fe			0.89			0.93
K				0.75		0.88
La	0.88					0.87
Li	0.86					0.85
Mg	0.90					0.94
Mn			0.72			0.92
Na				0.74		0.63
Ni			0.95			0.92
Pb	0.50					0.38
Rb					0.73	0.76
S				0.86		0.82
Sb		0.82				0.91
Si	0.44					0.21
Sn		0.87				0.94
Sr	0.82					0.79
Th	0.90					0.90
Ti	0.84					0.89
Y	0.90					0.88
Zn		0.66				0.75
Zr	0.70					0.83
Variance explained [%]	38	15	14	8	4	-

Tab. A-19: Factors loadings, communalities (h_i^2) and variance explained resulting from the factor analysis (varimax rotation) of 30 moss bag samples from Jena. Only the highest loading for each element is shown.

Element	Factor 1	Factor 2	Factor 3	Factor 4	Factor 5	h_i^2
Al	0.68					0.93
Ba				0.86		0.86
Ca	0.86					0.88
Co	0.71					0.87
Cr					0.60	0.73
Cu	0.96					0.94
Fe	0.87					0.92
K		0.82				0.88
La			0.53			0.92
Li			0.85			0.76
Mg		-0.68				0.89
Mn			0.85			0.78
Na		0.65				0.68
Ni					0.81	0.76
Pb				0.85		0.82
Rb		0.89				0.93
S		0.87				0.83
Sb	0.95					0.92
Si	0.70					0.87
Sn	0.95					0.95
Sr	0.83					0.86
Th		0.50				0.81
Ti	0.80					0.90
Y	0.67					0.97
Zn	0.67					0.50
Zr	0.91					0.96
Variance explained [%]	39	15	13	10	8	-

Tab. A-20: Factors loadings, communalities (h_i^2) and variance explained resulting from the factor analysis (varimax rotation) of 56 dust samples collected from windows in Jena. Only the highest loading for each element is shown.

Element	Factor 1	Factor 2	Factor 3	Factor 4	Factor 5	h_i^2
Al	0.91					0.91
Ba		0.87				0.84
Ca		0.74				0.71
Co				0.84		0.78
Cr			0.64			0.75
Cu			0.68			0.52
Fe			0.75			0.84
K				0.82		0.87
La	0.89					0.89
Li	0.42					0.24
Mg	0.80					0.68
Mn	0.62					0.78
Na	-0.46					0.58
Ni				0.63		0.70
Pb		0.83				0.71
Rb					0.65	0.61
S		0.60				0.60
Sb			0.74			0.64
Si					-0.54	0.39
Sn					0.75	0.64
Sr		0.80				0.73
Th	0.89					0.91
Ti	0.82					0.76
Y	0.91					0.93
Zn		0.51				0.30
Zr			0.48			0.33
Variance explained [%]	25	16	10	10	8	-

Tab. A-21: Factors loadings, communalities (h_i^2) and variance explained resulting from the factor analysis (varimax rotation) of 21 long-term deposit samples from Central Germany. Only the highest loading for each element is shown.

Element	Factor 1	Factor 2	Factor 3	Factor 4	Factor 5	h_i^2
Al	0.96					0.97
Ba					0.62	0.70
Ca				0.71		0.88
Co	0.94					0.95
Cr	0.65					0.90
Cu		0.92				0.89
Fe	0.86					0.90
K			0.77			0.74
La	0.92					0.93
Li	0.94					0.95
Mg			0.87			0.88
Mn					0.64	0.69
Na				0.89		0.92
Ni	0.76					0.86
Pb		0.79				0.81
Rb	0.88					0.88
S				0.90		0.86
Sb		0.73				0.81
Si					-0.88	0.81
Sn		0.93				0.93
Sr			0.84			0.80
Th	0.93					0.94
Ti	0.95					0.95
Y	0.94					0.95
Zn		0.40				0.35
Zr	0.84					0.73
Variance explained [%]	39	15	13	10	8	-

Danksagung

Diese Arbeit gäbe es nicht in der vorliegenden Form, ohne die Unterstützung etlicher Personen und Institutionen, denen ich auf diesem Wege danken möchte.

Mein größter Dank geht an meinen Doktorvater PD Dr. Michael Pirrung der mich von den Themen Feinstaub und Biomonitoring begeistert hat und stets ein offenes Ohr für jede Frage hat. Lieber Michael, ich bin unglaublich dankbar für deine tolle Unterstützung, für die du manchmal sogar deine Freizeit geopfert hast, aber auch für die Freiräume und Entfaltungsmöglichkeiten, die du mir gleichzeitig gelassen hast. Du hast immer versucht, einer Chemikerin die Geologie näher zu bringen und das ist dir auch gelungen.

Ein weiter großer Dank geht an PD Dr. Wolf von Tümpling für das persönliche Interesse, die vielen Telefonate neben dem laufenden Arbeitsalltag und die Bereitschaft, zu Terminen nach Jena zu kommen. Lieber Wolf, dein analytisches und chemometrisches Wissen hat maßgeblich zu den Ergebnissen dieser Arbeit beigetragen und mich immer wieder im Nachgang von der Wahl meines Studienfachs überzeugt.

Prof. Dr. Thorsten Schäfer und Prof. Dr. Georg Büchel möchte ich für die Aufnahme in die Arbeitsgruppe, die Finanzierung insbesondere der vielen praktischen Arbeiten, Diskussionen und das Interessen an meinem persönlichen Fortkommen danken.

Ein weiterer Dank geht an Dr. Dirk Merten, der mich im Rahmen meiner Masterarbeit erst in die Arbeitsgruppe Angewandte Geologie gebracht hat. Vielen Dank Dirk, für die stets pragmatischen Einschätzungen, die Begleitung meiner Arbeit und die Organisation der Laborarbeiten.

Letztere wären nicht möglich gewesen ohne die Unterstützung von Ulrike Buhler, Ines Kamp und Gerit Weinzierl. Ihnen möchte ich danken für die Durchführung vieler Aufschlüsse, ein stets offenes Ohr bei Problemen im Labor und die Diskussionsbereitschaft bei der Auswertung der Analysenergebnisse.

Für administrative Unterstützung jedweder Art sowie Ratschläge und Anregungen zum Vorankommen möchte ich mich bei Regina Piechnick bedanken. Weiterhin gilt mein Dank Frank Buchwald, Volker Schwarz und Michael Ude für die technische und handwerkliche Unterstützung. Nicht vergessen werden dürfen natürlich meine weiteren Kollegen aus der Arbeitsgruppe Angewandte Geologie, Dietrich Berger, Marcus Böhm, Sarah Hupfer, Daniel Jara Heredia, Thomas Lange, Arno Märten, Daniel Mirgorodsky, Sarah Nettemann und Markus Riefenstahl, die mich während meiner Promotion begleitet haben. Danke für die tolle Arbeitsatmosphäre, insbesondere dir, Marcus, für die Zeit im gemeinsamen Büro.

Ein besonderer Abschnitt meiner Promotionszeit war der Forschungsaufenthalt an der Universität Kopenhagen. Hier möchte ich meinem Gastgeber Prof. Dr. Rasmus Bro danken für

die freundliche Aufnahme und die vielen neuen Anregungen, in erster Linie aber für die Leichtigkeit und die ansteckende Begeisterung für die Chemometrik.

Ich hatte das Glück, meine Promotion als Mitglied eines Graduiertenprogramms, der International Max Planck Research School for Global Biogeochemical Cycles, durchzuführen. Dieser bin ich verbunden für die finanzielle Unterstützung und das tolle Rahmenprogramm. In diesem Rahmen möchte ich auch PD Dr. Axel Kleidon danken für die Begleitung meiner Arbeit als Mitglied meines PhD Advisory Committees und seinen ungetrübten, offenen Blick von außen. Weiterhin danke ich Steffi Rothhardt und John Kula für die administrative Unterstützung und Beratung sowie meinen Mitstreiterinnen und Mitstreitern im Graduiertenprogramm für den gemeinsamen Weg und den Erfahrungsaustausch.

Einige Probennahmekampagnen waren auch Teil von Abschlussarbeiten von Studierenden. Bei Anna Bonrath, Lena Herrschuh, Klara Perchermeier, Jonas Rombach, Florian Scheuerer, Rebekka Sinz und Franz Sperhake möchte ich mich daher herzlich für die tolle Arbeit im Gelände bedanken.

Bei den Kolleginnen und Kollegen aus den Arbeitsgruppen Allgemeine und Historische Geologie sowie Hydrogeologie möchte ich mich bedanken für die Ermöglichung von mikroskopischen Aufnahmen und REM-Aufnahmen.

Ein Dank geht auch an weitere Personen und Institutionen, die einzelne Beprobungen oder Beprobungskampagnen erst ermöglicht haben, insbesondere an den Kommunalservice Jena, das Helmholtz-Zentrum für Umweltforschung UFZ, das Geodynamische Observatorium Moxa, René Apitzsch (Flughafen Leipzig/Halle), Dr. Eike Guenther (Thüringer Landessternwarte Tautenburg) und Uwe Prüfer (Thüringer Landesamt für Landwirtschaft und Ländlichen Raum).

Zu guter Letzt gilt mein Dank meiner Familie und meinen Freunden, die die Zeit meiner Promotion von außen begleitet haben und stets von mir überzeugt sind. Insbesondere mein Mann Marcel hat alle Höhen und Tiefen mitbekommen und war und ist immer da um sich mit mir zu freuen oder mich zu unterstützen. Tausend Dank euch!

Selbstständigkeitserklärung

Ich erkläre, dass ich die vorliegende Arbeit selbstständig und unter Verwendung der angegebenen Hilfsmittel, persönlichen Mitteilungen und Quellen angefertigt habe.

Jena, den 11.11.2019

Neele Birte van Laaten